

Dissertation zur Erlangung des Doktorgrades  
der Fakultät für Chemie und Pharmazie  
der Ludwig-Maximilians-Universität München

# Subcutaneous suspensions of therapeutic proteins formulated as protein-coated microcrystals

Kristine Berkenhoff

geb. Macheleidt

aus

Herdecke, Deutschland

2013



## **Erklärung**

Diese Dissertation wurde im Sinne von § 7 der Promotionsordnung vom 28. November 2011 von Herrn Prof. Dr. Wolfgang Frieß betreut.

## **Eidesstattliche Versicherung**

Diese Dissertation wurde eigenständig und ohne unerlaubte Hilfe erarbeitet.

München, 22.02.2013

Kristine Berkenhoff

Dissertation eingereicht am: 22.02.2013

1. Gutachter: Prof. Dr. Wolfgang Frieß

2. Gutachter: Prof. Dr. Gerhard Winter

Mündliche Prüfung am: 16.04.2013



## **Acknowledgments**

This thesis has been prepared as cooperation between the Department of Pharmacy, Pharmaceutical Technology and Biopharmaceutics at the Ludwig-Maximilians-University in Munich and the Department Process Science Germany / Protein Science II at Boehringer Ingelheim Pharma GmbH & Co. KG in Biberach/Riss under the supervision of Prof. Dr. Wolfgang Frieß and Dr. Stefan Bassarab.

First and foremost, I want to express my deepest gratitude to my supervisor Prof. Dr. Wolfgang Frieß for his scientific guidance and his ongoing interest in the progress of my work. I am especially thankful for his encouragement and his personal advice. Moreover, I appreciate very much that he offered me the opportunities to present the work at numerous congresses worldwide.

I also would like to thank Prof. Dr. Gerhard Winter for his dedicated leadership of the chair and the profound discussions in Thursdays` seminars. Thank you a lot for taking over the co-referee of this thesis.

I am deeply grateful to Dr. Stefan Bassarab for giving me the chance of working on this interesting project and being the second scientific advisor in the last two years. Thank you very much for your continuous support and advice as well as our regular scientific discussions in an inspiring atmosphere.

Furthermore, I want to thank Dr. Karoline Bechtold-Peters for her committed supervision throughout my first year as Ph.D. student, her scientific enthusiasm and overall support.

I want to acknowledge Boehringer Ingelheim Pharma GmbH & Co. KG for providing the materials, financial support and the opportunity to work on this promising technology.

Many thanks to all my colleagues at Boehringer Ingelheim Pharma GmbH & Co KG. for their analytical and scientific support in the lab, many fruitful discussions and enjoyable breakfast and lunch breaks. Thank you very much for the pleasant working climate. Particularly, I want to thank Verena Christ for her technical advice and general mental encouragement. I really appreciate our friendship that has grown within the last years. I am grateful to Dr. Corinna

König for having established the pilot-scale PCMC manufacturing process during her time as PhD student. Manfred Kasper, Beater Leger, Maria-Theresia Trinz and Denise Sadlers are acknowledged for taking SEM pictures, Ralf Dukeck for x-ray powder diffraction, Birgit John for the bioassay, Susanne Marquart for performing the ELISA, Sandra Felk for CLSFM support, Claudia Ackermann and Heidrun Schott for their assistance in FT-IR measurements and Tina Rist, Maren Müller as well as Andreas Saumweber for their support in GC and HPLC analysis.

Thanks also to the students Verena, Stefan and Aurore for the excellent job they did in their internships.

Moreover, I would like to thank all members of the research groups of Prof. Dr. Wolfgang Frieß and Prof. Dr. Gerhard Winter. Sarah C. is kindly acknowledged for assisting me with the cascade impactor. Especially, I am grateful to Kerstin and Eva for our friendship and their frequent visits to Biberach. Kerstin, thank you very much for all the nice Wednesday`s evenings in Munich we spent together.

I also want to thank my parents and my brother Clemens for their encouragement and their love.

Finally, I sincerely thank my husband Johannes for his ongoing support and patience over the last years. Thank you for always being there for me and for your love. I am especially grateful to our little son Leopold for all the joy he brings into our life. We are glad that you are there.

For Leopold



## Table of Contents

Acknowledgments .....	V
Table of Contents.....	IX
<b>Chapter 1</b>	
<b>Introduction and objectives of the thesis.....</b>	<b>1</b>
1 Introduction .....	1
1.1 Challenges of protein drug formulation .....	1
1.2 The protein-coated microcrystals technology.....	2
1.2.1 Definition of protein-coated microcrystals .....	2
1.2.2 Development and application of the PCMC technology .....	3
1.2.3 PCMC production at Boehringer Ingelheim .....	5
2 Objectives of the thesis.....	8
3 References.....	9
<b>Chapter 2</b>	
<b>HSA-free formulation of a hydrophobic cytokine as protein-coated microcrystals.....</b>	<b>15</b>
Abstract.....	15
1 Introduction .....	16
2 Materials and methods.....	17
2.1 Materials .....	17
2.2 Methods.....	18
2.2.1 PCMC production process.....	18
2.2.2 Storage stability study.....	20
2.2.3 Analysis of PCMCs .....	20
2.2.3.1 Reconstitution of PCMC powder .....	20
2.2.3.2 Turbidity .....	21
2.2.3.3 Theoretical protein recovery .....	21
2.2.3.4 Protein integrity.....	22
2.2.3.5 Particle size .....	22
2.2.3.6 Particle morphology .....	23
2.2.3.7 Bioactivity .....	23
2.2.3.8 Oxidized species .....	23
2.2.3.9 Protein structure .....	24
2.2.3.10 X-ray powder diffraction.....	25
3 Results.....	25
3.1 Formulation screening.....	25
3.1.1 Particle formation and characterization .....	25
3.1.2 Protein process stability.....	27
3.2 Long-term stability study.....	29
4 Discussion.....	34
4.1 Particle formation and characterization.....	35

4.2 Influence of carrier combination on protein process stability .....	37
4.3 Long-term storage stability.....	41
4.3.1 Protein stability .....	41
4.3.2 Carrier and morphology stability .....	43
4.3.3 Comparison to lyophilized cytokine formulations .....	44
5 Conclusion.....	45
6 References.....	46
7 Appendix: supplementary material .....	51

## Chapter 3

<b>Formulation of a therapeutic monoclonal antibody via PCMC technology.....</b>	<b>53</b>
Abstract.....	53
1 Introduction .....	54
2 Materials and methods.....	55
2.1 Materials .....	55
2.2 Methods.....	56
2.2.1 Preparation of protein solutions.....	56
2.2.2 PCMC production process.....	56
2.2.3 Accelerated short-term storage stability study of PCMC powder .....	58
2.2.4 Accelerated short-term storage stability study of liquid mAb2 formulations .....	59
2.2.5 Analysis of PCMCs .....	59
2.2.5.1 Turbidimetry .....	59
2.2.5.2 Protein concentration and protein recovery via UV measurement .....	59
2.2.5.3 Protein aggregation and fragmentation via high performance size exclusion chromatography (HP-SEC) .....	60
2.2.5.4 Protein aggregation and fragmentation via SDS-PAGE .....	60
2.2.5.5 Protein structure via intrinsic fluorescence spectroscopy .....	60
2.2.5.6 Protein structure via 2 <sup>nd</sup> -derivative UV spectroscopy .....	61
2.2.5.7 Quantification of trehalose by high performance liquid chromatography (HPLC).....	61
2.2.5.8 Particle size via laser diffractometry (LD) .....	61
2.2.5.9 Particle morphology via scanning electron microscopy (SEM).....	62
2.2.5.10 Crystallinity via x-ray powder diffraction (XRD).....	62
2.2.5.11 Zeta potential measurement .....	62
3 Results and discussion .....	62
3.1 Formulation screening.....	62
3.1.1 Characterization of PCMC powder .....	62
3.1.2 Protein process stability.....	67
3.1.3 Selection of the lead formulation via accelerated short-term storage stability study .....	71
3.2 Optimization of protein load via accelerated short-term storage stability study.....	72
3.2.1 Characterization of powder properties and morphology stability.....	72
3.2.2 Protein storage stability .....	74
3.2.3 Considerations on protein process stability.....	81
3.3 Comparison to liquid mAb2 formulations .....	82
4 Conclusion.....	86
5 References.....	88

## Chapter 4

<b>Evaluation of organic water-miscible solvents as suspension media for PCMCs.....</b>	<b>93</b>
Abstract.....	93
1 Introduction .....	94
2 Materials and methods.....	95
2.1 Materials .....	95
2.2 Methods.....	95
2.2.1 PCMC production process.....	95
2.2.2 Incubation of PCMC powder with organic water-miscible solvents .....	97
2.2.3 Macroscopic appearance after solvent incubation.....	97
2.2.4 Analysis of protein integrity .....	97
2.2.4.1 Dissolution behavior .....	97
2.2.4.2 Turbidimetry .....	97
2.2.4.3 High pressure size exclusion chromatography (HP-SEC) .....	97
2.2.4.4 Analysis of protein structure .....	98
2.2.4.5 Binding assay .....	99
3 Results and discussion .....	99
3.1 Macroscopic appearance after solvent incubation .....	99
3.2 Protein integrity after solvent incubation .....	102
4 Conclusion.....	114
5 References.....	117

## Chapter 5

<b>Development of oily mAb1 PCMC suspensions for subcutaneous administration .....</b>	<b>123</b>
Abstract.....	123
1 Introduction .....	124
2 Materials and methods.....	125
2.1 Materials .....	125
2.2 Methods.....	126
2.2.1 PCMC production process.....	126
2.2.2 Development of an in vitro release model for oily PCMC suspensions .....	127
2.2.3 Compatibility between mAb1 PCMCs and oily solvents .....	128
2.2.3.1 MAb1 release from oily PCMC suspensions .....	128
2.2.3.2 Turbidimetry .....	129
2.2.3.3 Microflow-imaging (MFI) .....	129
2.2.3.4 Light microscopy .....	129
2.2.3.5 Protein recovery .....	129
2.2.3.6 High pressure size exclusion chromatography (HP-SEC) .....	129
2.2.3.7 Fourier transform infrared spectroscopy .....	130
2.2.3.8 Intrinsic fluorescence spectroscopy .....	130
2.2.3.9 2 <sup>nd</sup> -derivative UV spectroscopy .....	131
2.2.3.10 Binding assay .....	131
2.2.4 Characterization of oleaginous solvents and oily suspensions .....	131
2.2.4.1 Viscosity .....	131
2.2.4.2 Preparation of oily mAb1 suspensions .....	131
2.2.4.3 Syringe filling .....	131

2.2.4.4	Injectability .....	132
2.2.4.5	Light microscopy .....	132
2.2.4.6	X-ray powder diffraction.....	132
2.2.4.7	Swelling of stoppers and tip caps .....	132
2.2.4.8	Storage of prefilled syringes .....	133
2.2.4.9	Concentration of liquid mAb1 formulation .....	133
3	Results and discussion .....	133
3.1	Development of an in vitro release model for oily PCMC suspensions .....	133
3.2	Compatibility between mAb1 PCMCs and oily solvents.....	137
3.3	Injectability of oily solvents and compatibility with primary packaging material... 141	
3.3.1	Viscosity and injectability of oily solvents.....	141
3.3.2	Compatibility between oily solvents and primary packaging material .....	144
3.4	Characterization of oily mAb1 PCMC suspensions .....	146
3.4.1	Appearance and rheology of oily mAb1 PCMC suspensions.....	146
3.4.2	Injectability of oily mAb1 PCMC suspensions .....	149
3.4.3	Comparison of mAb1 formulated as oily PCMC suspension and liquid formulation .....	151
3.4.4	Sedimentation behavior of oily mAb1 PCMC suspensions .....	152
4	Conclusion.....	153
5	References.....	154
6	Appendix: supplementary material .....	159
6.1	Determination of inner needle diameter via SEM.....	159
6.2	Sedimentation behavior of S:B 70:30 and S:B 30:70 (v/v) mAb1 PCMC suspensions.....	160

## Chapter 6

<b>Mechanistic insights into the PCMC formation process.....</b>	<b>161</b>
Abstract.....	161
1 Introduction .....	162
2 Materials and methods.....	163
2.1 Materials .....	163
2.2 Methods.....	164
2.2.1 Preparation of protein solutions.....	164
2.2.2 PCMC production process.....	165
2.2.2.1 Preparation of protein-carrier solutions.....	165
2.2.2.2 Continuous precipitation of mAb1 and cytokine PCMCs.....	166
2.2.2.3 Batch mode preparation of cytokine and mAb1 PCMCs via one-step and two-step precipitation .....	167
2.2.2.4 Concentration/solvent exchange .....	167
2.2.2.5 Supercritical drying.....	168
2.2.3 Binding of Alexa <sup>®</sup> 488 dye to mAb1.....	168
2.2.4 Accelerated short-term storage stability study .....	169
2.2.5 Powder fractionation via cascade impactor.....	169
2.2.6 X-ray powder diffraction (XRD) .....	170
2.2.7 Protein content via UV measurement .....	170
2.2.8 Turbidimetry .....	170
2.2.9 High performance size exclusion chromatography (HP-SEC).....	170
2.2.10 Sodium dodecyl sulfate polyacrylamide gel electrophoresis (SDS-PAGE) .....	171

2.2.11	Particle morphology via scanning electron microscopy (SEM) .....	171
2.2.12	Water content via Karl-Fischer titration .....	171
2.2.13	Confocal laser scanning fluorescence microscopy (CLSM).....	172
2.2.14	Quantification of the cytokine by reverse-phase high performance liquid chromatography (RP-HPLC).....	172
2.2.15	Quantification of valine by gas chromatography (GC) .....	172
2.2.16	Quantification of trehalose by high performance liquid chromatography (HPLC) .....	173
2.2.17	Bioactivity assay .....	173
3	Results and discussion .....	174
3.1	Investigation of mAb1 PCMCs with varying protein load and trehalose content... 174	
3.1.1	Crystallinity of mAb1 PCMCs in dependence of protein load and trehalose content.....	174
3.1.2	Accelerated short-term stability study .....	176
3.1.3	Confocal laser scanning fluorescence microscopy of mAb1 PCMC powders.....	185
3.2	Fractionation of cytokine PCMCs and mAb1 PCMCs via cascade impactor.....	189
3.3	Preparation of cytokine and mAb1 PCMCs via one-step and two-step precipitation in batch mode .....	193
3.3.1	Precipitation of protein-free carrier solutions .....	193
3.3.2	Precipitation of cytokine on separately prepared carrier crystals in comparison to standard one-step precipitation .....	197
3.3.3	Precipitation of cytokine in the absence of carrier material.....	199
4	Conclusion.....	200
5	References.....	201
<b>Chapter 7</b>		
<b>Final summary .....</b>		<b>207</b>
<b>Appendix</b>		
List of abbreviations.....		i
Presentations and publications associated with this thesis .....		iv



## Chapter 1

# Introduction and objectives of the thesis

## 1 Introduction

### 1.1 Challenges of protein drug formulation

The chemical and physical properties of protein drugs result in unique challenges in the separation, purification, formulation, storage and delivery of these macromolecules, deviating from the difficulties typically occurring during the development of small organic molecule therapeutics [1, 2]. Based on the underlying mechanism, protein degradation can be separated into two pathways, namely chemical and physical instability [1-3]. Chemical instability describes any process that comprises covalent protein modification via bond formation or cleavage generating a new chemical entity [1, 2]. In contrast, physical instability involves changes in the secondary, tertiary or quaternary protein structure in the absence of covalent modifications [1, 2]. These include denaturation, aggregation, precipitation and adsorption to surfaces, whereas processes such as deamidation, racemization, hydrolysis, oxidation, disulfide exchange and  $\beta$ -elimination are examples of chemical instability [1-3]. Protein stabilization against both chemical and physical degradation can be addressed by various formulation strategies, including e.g. chemical modification of the protein and choice of appropriate additives, excipients and formulation pH [1-6]. Specifically the formulation development of high concentration protein injectables is frequently associated with enhanced protein aggregation due to increased molecular interaction and specific hurdles such as high viscosity [7, 8].

The susceptibility of proteins to degradation is generally lower in the dried state than in aqueous solution [2, 9]. The protein's mobility is reduced, impeding protein-protein interactions that are especially prerequisite for aggregation [10, 11]. Besides the conventional application by injection after reconstitution, the development of solid protein formulations allows for additional routes of administration, such as inhalation, modification of the release profile due to embedding in matrices as well as incorporation of proteins into tissue

engineering scaffolds and medical devices [12]. Lyophilization represents the process of choice for the preparation of dry protein powders [5, 6, 13]. However, the interest towards the development of alternative drying methods has steadily increased in recent years because freeze-drying, although successful for many proteins, has certain disadvantages, such as long processing times, batch operation and high capital equipment costs [14-16]. Other drying techniques for proteins, currently being evaluated, comprise spray-drying [17, 18], spray-freeze drying [17], supercritical fluid drying [19-23] and vacuum drying [14, 24, 25]. Furthermore, particle generating techniques, such as crystallization [8, 26-28] and precipitation [29], in combination with subsequent drying are suitable for manufacturing of dry protein powder.

The protein-coated microcrystals (PCMC) technology represents an alternative technique to stabilize the protein in the solid state and also allows for the development of nonstandard dosage forms, for example protein suspensions for subcutaneous application. This therapeutic dosage form could for instance be beneficial when high concentration protein solutions are not feasible due to reduced protein solubility, poor stability or high viscosity. Moreover, PCMC powder may be used for the development of drug delivery systems e.g. in the case of sustained release matrix material employed as co-precipitating excipients.

## **1.2 The protein-coated microcrystals technology**

### **1.2.1 Definition of protein-coated microcrystals**

The protein-coated microcrystals technology represents an alternative method of protein stabilization in the solid state. It is based on the coprecipitation of an aqueous solution of protein and carrier material induced by a rapid addition of a surplus of organic water-miscible solvent in which the PCMC components are not or hardly soluble, e.g. isopropanol or isobutanol. The immediate dehydration of the protein and the carrier components, comprising physiological acceptable substances such as buffer species, amino acids, sugars and inorganic salts, results in the formation of a suspension that is concentrated and subsequently dried via supercritical fluid extraction with carbon dioxide. The powder harvested consists of water-soluble particles in the lower micrometer range, typically less than 50  $\mu\text{m}$ .

### 1.2.2 Development and application of the PCMC technology

The PCMC technology, mainly as a batch process, was foremost described in the patent 'WO 00/69887 – Rapid dehydration of proteins' by Moore et al. [30]. Herein, the authors pointed out that biomolecules keep a native-like conformation after particle formation due to the rapid dehydration step. The term 'biomolecule' comprised not only proteins, peptides or polypeptides, but nucleic acids such as DNA and RNA as well. Figures attached to the patent application demonstrate the formation of crystals with planar surfaces covered by amorphous protein, a structure that was confirmed in several subsequent studies [31, 32]. The process leading to this type of particles was termed crystal lattice mediated self-assembly (CLAMS) by a group of chemists from the University of Strathclyde [33]. Additionally, it was shown that precipitated PCMCs can be stored in the organic solvent and that the protein retains its activity and stability throughout the process [30]. The patent described that applications of this technology include preparation of enzymes for biocatalysis, formulation of pharmaceutical drug products and purification processes.

Early applications of this technology mainly focused on enzyme PCMC suspensions for biocatalysis in organic solvents. Kreiner et al. were the first to prove that the preparation of subtilisin Carlsberg protease PCMCs and several lipase PCMCs with potassium sulfate as co-precipitant results in particles with higher catalytic activities than lyophilized enzyme products [31]. They further showed that storage of the PCMC suspension in propan-1-ol for up to 14 months leads to only negligible loss in activity [34]. The superiority of lipase  $K_2SO_4$  PCMCs over the free enzyme concerning bioactivity rates in non-aqueous media is acknowledged by several authors [32, 35, 36]. Raita et al. investigated the applicability and operational stability of lipase PCMCs during biodiesel production [37]. Kreiner et al. extended the idea of PCMCs as biocatalysts to oxidoreductases [38].

However, not only enzymes for biocatalysis can be addressed with the PCMC technology. Vos successfully co-precipitated proteins like trypsin, pepsin, adenosine deaminase and myoglobin with several carrier materials during his studies on the formation mechanism of PCMCs [39]. The PCMC technology also allows for co-immobilization of two proteins onto the same carrier crystals [40].

Khosravani et al. used the PCMC technology for the formulation of adenylate cyclase toxin (CyaA) of *Bordetella pertussis*, a potential candidate for vaccination against pertussis [41], which is usually stored in highly concentrated urea solutions for stability reasons. The authors showed that urea could be removed during the PCMC co-precipitation process with DL-valine as carrier due to its high solubility in the precipitating solvent ethanol. Furthermore, CyaA PCMCs that included calmodulin alone or in combination with bovine serum albumin (BSA) elicited full adenylate cyclase and cell invasive activities when reconstituted in aqueous buffer. Murdan et al. found that PCMCs of diphtheria toxoid stabilized the vaccine even at elevated temperatures [42]. Partridge et al. as well as König extended the PCMC technology to antibody (IgG) coated microcrystals [43, 44]. The pharmaceutical PCMC powders may be applied to the patient parenterally after reconstitution in aqueous media or as a suspension. Furthermore, as the resulting powders are usually very fine and free-flowing due to the supercritical fluid drying process, they can be used for pulmonary drug delivery if their particle size is between 0.5 and 5  $\mu\text{m}$ .

For the production of PCMCs, essentially, only one carrier component and a biomolecule are required, as shown in early studies [31, 35, 36, 38, 45]. According to WO 2004/062560, carriers can be nearly any compound that crystallizes rapidly and that can be used as a saturated solution. Most commonly an inorganic salt, an amino acid or a sugar was employed [46]. Potassium sulfate was the carrier of choice. Amongst the amino acids, especially DL-valine [41, 47], glycine [44] and L-glutamine [39, 48] proved to be suitable carrier components. Mannitol has been utilized as carrier by Vos [39]. Kreiner et al. extended the choice of immobilization matrix to both inorganic and zwitterionic compounds acting as solid-state buffers [45]. These substances, e.g. Na-AMPSO (3-((1,1-dimethyl-2-hydroxyethyl)amino)-2-hydroxypropanesulfonic acid),  $\text{Na}_2\text{CO}_3$  and  $\text{NaHCO}_3$ , can provide in situ ionization-state control which has been shown to be beneficial for the catalytic activities of two serine proteases [28]. It was pointed out by Moore et al. that certain biomolecules, like antibodies, need further stabilization during the PCMC production since exposure to polar solvent and immobilization on a surface means serious stress to the protein [49]. The authors recommended using a neutral co-precipitant, e.g. glycine, in combination with a basic and/or an acidic additive, especially the amino acids L-arginine and L-glutamic acid, and optionally further excipients like a neutral non-polymeric

additive, for instance sugars like trehalose, polysorbates and inorganic salts, such as NaCl. These precipitation-protective additives were suggested to form associates with the protein on the surface of the crystalline PCMC core [29]. The necessity of a rather complex carrier composition for sufficient stabilization was recently acknowledged during PCMC formulation development of an IgG at Boehringer Ingelheim [48].

These exemplary PCMC applications especially in the pharmaceutical field indicate that the PCMC technology represents a promising new method of stabilization of therapeutic biomolecules as dry powders. Therefore, this technology was introduced and further investigated at Boehringer Ingelheim in Biberach/Riss (D), initially in cooperation with XStalBio Limited (Glasgow, UK).

### **1.2.3 PCMC production at Boehringer Ingelheim**

The first PCMC-related patent WO 00/69887 and most of the published work described the production of PCMCs in a batch mode where an aqueous solution of the protein and the carrier (protein-carrier solution) was added dropwise to the anti-solvent under stirring [30]. In 'WO 2004/062560 - Pharmaceutical composition', however, the idea of producing PCMCs with a two-line continuous process for large-scale batches was introduced [46]. The authors stated that the use of a flow-co-precipitator could not only lead to PCMCs with higher uniformity, but also with increased bioactivity and stability compared to samples prepared by the batch process. These advantages were ascribed to the reduction of stress induced by the air-solvent interface or shear forces during mixing. Considering these aspects, a continuous PCMC production process was implemented at Boehringer Ingelheim [48].

In general, after preparation of the aqueous protein-carrier solution, the PCMC production at Boehringer Ingelheim encompasses the following three steps which are visualized in Figure 1-1:

#### **A. Mixing / PCMC precipitation**

A pre-blended aqueous solution of protein and carrier material (protein-carrier solution) is rapidly mixed with an excess of a water-miscible organic solvent saturated with all carrier excipients. Hence, the PCMCs co-precipitate immediately. The modular mixing platform (Figure 1-1A), established by König, comprised a static double or quadruple jet impingement

mixing module as well as pressure sensors, temperature sensors and mass flow meters to monitor and control the precipitation step [48]. In the double jet impingement mixer, usually chosen for the manufacturing of PCMCs, two independent anti-solvent streams delivered by micro gear pumps are merged with the protein-carrier solution. According to fluid dynamic computations [44], the design of the mixer as well as an appropriate pumping speed ensures homogenous mixing of the different phases. The resulting PCMC suspension is collected in an external vessel.

#### B. Concentration of the PCMC suspension / solvent exchange

The concentration step of the PCMC suspension is necessary in order to avoid excessive drying times and costs. For this purpose, a modified pressure filtration unit has been developed [44]. In the context of this thesis, the products were concentrated simply by sedimentation and subsequent decantation of the supernatant to avoid shear stress inevitable during pressure filtration. In order to reduce the water content, the sediment was resuspended in fresh, saturated solvent and allowed to settle again (Figure 1-1B).

#### C. Drying of the concentrated PCMC suspension

Supercritical fluid (SCF) drying with carbon dioxide (CO<sub>2</sub>) was chosen as a very effective and gentle way of removing the anti-solvent from PCMC suspensions [19]. CO<sub>2</sub> exists as a SCF above its critical point at 31.0 °C and 73.8 bar [50]. SCFs have diffusive and viscosity properties similar to gases and can dissolve other compounds due to liquid-like densities [51]. The nonpolar supercritical CO<sub>2</sub> is conducted through the PCMC suspension and dissolves the anti-solvent which is then carried out of the drying chamber and collected in a separator (Figure 1-1C). Polar water molecules show insufficient solubility in supercritical CO<sub>2</sub> and are not removed effectively. Consequently, the initial water content of the suspension has to be minimal to obtain powders of acceptable residual moisture. The PCMCs are left behind as a powder with low bulk density, low residual solvent content and increased fine particle fraction [46]. To further decrease the residual water content, a vacuum drying step follows SCF drying.

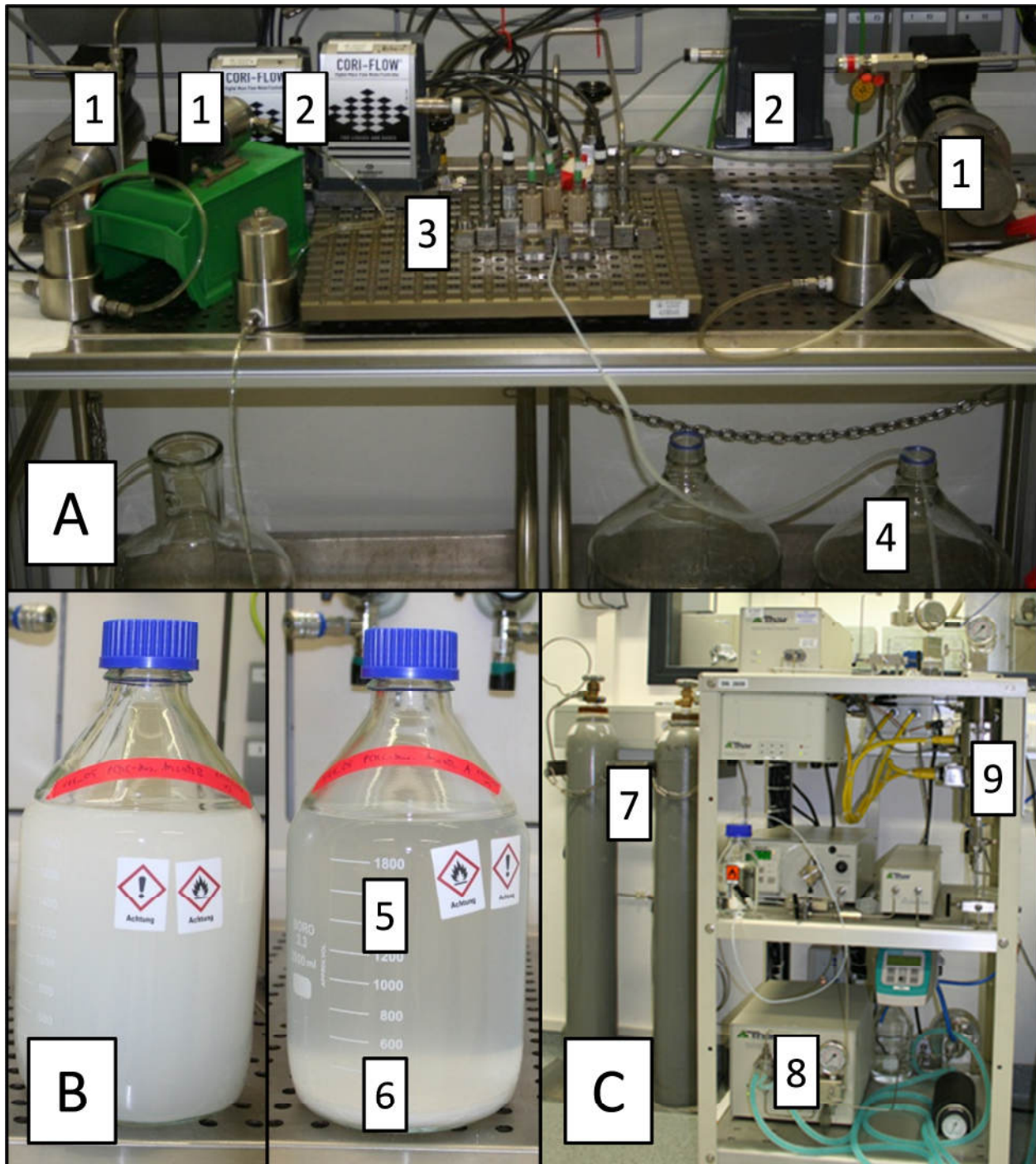


Figure 1-1: Visualization of the PCMC production process at Boehringer Ingelheim; (A): precipitation step; (1) three micro gear pumps for the delivery of solvent and protein-carrier solution, (2) mass flow meters, (3) Ehrfeld platform equipped with the double jet impingement mixer, pressure and temperature sensors, (4) glass bottles for harvesting of the PCMC suspension; (B) concentrating and solvent exchange step; left: freshly precipitated PCMC suspension, right: PCMC suspension 18 h after precipitation with (5) supernatant and (6) sediment; (C) supercritical drying with CO<sub>2</sub> which dissolves and removes the anti-solvent leaving behind the dry PCMC powder; (7) gas bottles with CO<sub>2</sub>, (8) pump for CO<sub>2</sub> delivery, (9) stainless steel basket filled with PCMC suspension and powder, respectively.

Production parameters like mixing speed and water-to-solvent ratio are known to significantly influence PCMC properties. Therefore, optimized values for these parameters were kept constant for reasons of comparability. A mixing speed of 1000 mL/min for pure isobutanol and 1:1 (v/v) isopropanol/2-methyl-2,4-pentanediol mixtures ensured turbulent (Reynolds number  $\geq 2300$ ) and efficient mixing. According to König et al., the mixing intensity not only affects the PCMC particle size and its distribution, but also the binding strength of the protein on the carrier material [44, 48].

In agreement with previous studies, the water-to-solvent ratio was set to 5:95 (v/v) [44]. On the one hand, an excess of solvent is crucial for rapid precipitation of PCMCs, on the other hand, a certain water content seems to be important for protein stability. Studying trypsin PCMCs, Vos found that the bioactivity of the enzyme decreased with declining water content [39], being consistent with the observations made on subtilisin Carlsberg by Partridge et al. [52]. The authors stated that water was essential for maintaining the enzymatic activity of trypsin as all proteins typically need key structural water molecules for stability [39].

## **2 Objectives of the thesis**

This thesis aimed to evaluate pharmaceutical applications of the protein-coated microcrystals technology. Besides formulation considerations, the focus was on the development of a potential final dosage form for PCMC powder as high concentration suspension allowing for subcutaneous administration as well as on mechanistic questions.

The first objective of the thesis was to apply the PCMC technology that has successfully been used for the formulation of various protein drugs, including mAbs [43, 44], adenylate cyclase toxin of *Bordetella pertussis* [41] and diphtheria toxin [42], to a non-glycosylated cytokine. This hydrophobic protein is commercially formulated as lyophilisate with a large amount of human serum albumin (HSA), but the PCMC formulation may allow for stabilizing the cytokine in the absence of this excipient. Therefore, a formulation screening had to be conducted, aiming at developing an optimal carrier composition that provided high process stability to the cytokine. The most promising formulation should subsequently be studied during a long-term stability study over 52 weeks and analyzed in detailed for biological activity.

In the following study, a previously developed mAb PCMC formulation was intended to be applied to another IgG (mAb2). Furthermore, the formulation screening aimed to reduce the number of carrier components and thus the overall complexity of the protein-coated microcrystals. Thus, the influence of each carrier component on the PCMC powder properties had to be investigated. The optimized formulation should further be studied during an accelerated short-term stability study to identify the maximal protein load enabling high antibody storage stability, additionally in comparison to a corresponding liquid formulation.

Apart from formulation development, the second major objective of this thesis was to develop PCMC suspensions for subcutaneous administration as alternative dosage form to protein solutions because specifically for mAbs high concentration s.c. formulations are of high practical relevance. This requires physiologically acceptable solvents as dispersing agent which are compatible with both the protein itself and the protein carrier powder particles. Organic water-miscible solvents selected for the according study comprised glycerol, N-methylpyrrolidone (NMP), propylene glycol and PEG 400, whereas sesame oil, benzyl benzoate and medium-chain triglycerides (MCT) were chosen as oily resuspension media. As opposed to the organic water-miscible vehicles, the evaluation of the oils additionally had to include detailed investigations of the release process of the protein from the oily PCMC suspensions. Furthermore, injectability of the formulations was to be demonstrated.

Despite widespread studies on the PCMC technology, the mechanism underlying the particles' formation and the protein stabilization are still not fully understood. Therefore, mechanistic questions, such as the characterization of the crystallinity/amorphicity and the morphology of the particles in dependence of the formulation composition, should finally be addressed to gain insights in the assembly of protein-coated microcrystals taking place during the rapid dehydration. Moreover, precipitation of protein on separately prepared carrier crystals was planned to advance the understanding of the PCMC formation process.

### 3 References

1. Manning, M., et al., *Stability of protein pharmaceuticals: An update*. Pharmaceutical Research, 2010. **27**(4): p.544-575.

2. Manning, M.C., Patel, K., and Borchardt, R.T., *Stability of protein pharmaceuticals*. Pharmaceutical Research, 1989. **6**(11): p.903-918.
3. Wang, W., et al., *Antibody structure, instability, and formulation*. Journal of Pharmaceutical Sciences, 2007. **96**(1): p.1-26.
4. Wang, W., *Instability, stabilization, and formulation of liquid protein pharmaceuticals*. International Journal of Pharmaceutics, 1999. **185**(2): p.129-188.
5. Wang, W., *Lyophilization and development of solid protein pharmaceuticals*. International Journal of Pharmaceutics, 2000. **203**(1-2): p.1-60.
6. Wang, W., *Protein aggregation and its inhibition in biopharmaceutics*. International Journal of Pharmaceutics, 2005. **289**(1-2): p.1-30.
7. Shire, S.J., Shahrokh, Z., and Liu, J., *Challenges in the development of high protein concentration formulations*. Journal of Pharmaceutical Sciences, 2004. **93**(6): p.1390-1402.
8. Yang, M.X., et al., *Crystalline monoclonal antibodies for subcutaneous delivery*. Proceedings of the National Academy of Sciences of the United States of America, 2003. **100**(12): p.6934-6939.
9. Maa, Y.-F. and Prestrelski, S.J., *Biopharmaceutical powders: Particle formation and formulation considerations*. Current Pharmaceutical Biotechnology, 2000. **1**(3): p.283-302.
10. Chang, L. and Pikal, M.J., *Mechanisms of protein stabilization in the solid state*. Journal of Pharmaceutical Sciences, 2009. **98**(9): p.2886-2908.
11. Yu, L., *Amorphous pharmaceutical solids: preparation, characterization and stabilization*. Advanced Drug Delivery Reviews, 2001. **48**(1): p.27-42.
12. Yang, S., Yuan, W., and Jin, T., *Formulating protein therapeutics into particulate forms*. Expert Opinion on Drug Delivery, 2009. **6**(10): p.1123-1133.
13. Pikal, M.J., *Freeze-drying of proteins: process, formulation, and stability*, in *Formulation and delivery of proteins and peptides*, Cleland, J.L. and Langer, R., editors. 1994. Washington: American Chemical Society. p.120-33.
14. Kumar, V., Sharma, V.K., and Kalonia, D.S., *In situ precipitation and vacuum drying of interferon alpha-2a: Development of a single-step process for obtaining dry, stable protein formulation*. International Journal of Pharmaceutics, 2009. **366**(1-2): p.88-98.
15. Rovero, G., Ghio, S., and Barresi, A.A., *Development of a prototype capacitive balance for freeze-drying studies*. Chemical Engineering Science, 2001. **56**(11): p.3575-3584.
16. Johnson, J.A.C. and Etzel, M.R., *Properties of lactobacillus helveticus CNRZ-32 attenuated by spray-drying, freeze-drying, or freezing*. Journal of Dairy Science, 1995. **78**(4): p.761-768.

17. Maa, Y.-F., et al., *Protein inhalation powders: Spray drying vs spray freeze drying*. *Pharmaceutical Research*, 1999. **16**(2): p.249-254.
18. Schüle, S., et al., *Stabilization of IgG1 in spray-dried powders for inhalation*. *European Journal of Pharmaceutics and Biopharmaceutics*, 2008. **69**(3): p.793-807.
19. Jovanović, N., et al., *Distinct effects of sucrose and trehalose on protein stability during supercritical fluid drying and freeze-drying*. *European Journal of Pharmaceutical Sciences*, 2006. **27**(4): p.336-345.
20. Jovanović, N., et al., *Stabilization of IgG by supercritical fluid drying: Optimization of formulation and process parameters*. *European Journal of Pharmaceutics and Biopharmaceutics*, 2008. **68**(2): p.183-190.
21. Jovanović, N., et al., *Stable sugar-based protein formulations by supercritical fluid drying*. *International Journal of Pharmaceutics*, 2008. **346**(1-2): p.102-108.
22. Moshashaée, S., et al., *Supercritical fluid processing of proteins: I: Lysozyme precipitation from organic solution*. *European Journal of Pharmaceutical Sciences*, 2000. **11**(3): p.239-245.
23. Moshashaée, S., et al., *Supercritical fluid processing of proteins: lysozyme precipitation from aqueous solution*. *Journal of Pharmacy and Pharmacology*, 2003. **55**: p.185-192.
24. Mattern, M. and Winter, G., *Method and preparations for stabilizing biological materials by drying methods without freezing*. US7172999, 2007.
25. Mattern, M., et al., *Formulation of proteins in vacuum-dried glasses. II. Process and storage stability in sugar-free amino acid systems*. *Pharmaceutical Development and Technology*, 1999. **4**(2): p.199-208.
26. Jen, A. and Merkle, H.P., *Diamonds in the rough: Protein crystals from a formulation perspective*. *Pharmaceutical Research*, 2001. **18**(11): p.1483-1488.
27. Shenoy, B., et al., *Stability of crystalline proteins*. *Biotechnology and Bioengineering*, 2001. **73**(5): p.358-369.
28. Shi, K., et al., *Progress in the development of crystallized proteins as drug delivery system*. *Acta Pharmaceutica Sinica*, 2009. **44**(8): p.845-851.
29. Matheus, S., et al., *Liquid high concentration IgG1 antibody formulations by precipitation*. *Journal of Pharmaceutical Sciences*, 2009. **98**(9): p.3043-3057.
30. Moore, B.D., et al., *Rapid dehydration of proteins*. WO00/69887, 2000.
31. Kreiner, M.M., Moore, B.D., and Parker, M.C., *Enzyme-coated micro-crystals: A 1-step method for high activity biocatalyst preparation*. *Chemical Communications*, 2001: p.1096-1097.

32. Shah, S. and Gupta, M.N., *Kinetic resolution of ( $\pm$ )-1-phenylethanol in [Bmim][PF6] using high activity preparations of lipases*. *Bioorganic & Medicinal Chemistry Letters*, 2007. **17**(4): p.921-924.
33. Murugesan, M., et al., *Nanoparticle-coated microcrystals*. *Chemical Communications*, 2005. **2005**(21): p.2677-2679.
34. Kreiner, M.M., et al., *Stability of protein-coated microcrystals in organic solvents*. *Journal of Molecular Catalysis B: Enzymatic*, 2005. **33**: p.65-72.
35. Gaur, R., et al., *Protein-coated microcrystals of pseudomonas aeruginosa PseA lipase*. *Applied Biochemistry and Biotechnology*, 2008. **151**(2-3): p.160-166.
36. Wu, J.C., et al., *Activity, stability and enantioselectivity of lipase-coated microcrystals of inorganic salts in organic solvents*. *Biocatalysis and Biotransformation*, 2009. **27**(5/6): p.283-289.
37. Raita, M., Champreda, V., and Laosiripojana, N., *Biocatalytic ethanolysis of palm oil for biodiesel production using microcrystalline lipase in tert-butanol system*. *Process Biochemistry*, 2010. **45**(6): p.829-834.
38. Kreiner, M. and Parker, M.C., *Protein-coated microcrystals for use in organic solvents: Application to oxidoreductases*. *Biotechnology Letters*, 2005. **27**(20): p.1571-1577.
39. Vos, J., *Understanding the formation mechanism of protein coated microcrystals* [dissertation]. Glasgow: University of Strathclyde, 2006.
40. Partridge, J., et al., *Dry powder formulations: payloads from 30 to 0.1% w/w*. *AAPS National Biotechnology Conference*. 2007. San Diego, CA, USA.
41. Khosravani, A., et al., *Formulation of the adenylate cyclase toxin of Bordetella pertussis as protein-coated microcrystals*. *Vaccine*, 2007. **25**(22): p.4361-4367.
42. Murdan, S., et al., *Immobilisation of vaccines onto micro-crystals for enhanced thermal stability*. *International Journal of Pharmaceutics*, 2005. **296**(1-2): p.117-121.
43. Partridge, J., et al., *Antibody-coated Microcrystals*. *AAPS National Biotechnology Conference*. 2005. Nashville, TN, USA.
44. König, C., et al., *Development of a pilot-scale manufacturing process for protein-coated microcrystals (PCMC): Mixing and precipitation – Part I*. *European Journal of Pharmaceutics and Biopharmaceutics*, 2012. **80**(3): p.490-498.
45. Kreiner, M. and Parker, M.C., *High-activity biocatalysts in organic media: solid-state buffers as the immobilisation matrix for protein-coated microcrystals*. *Biotechnology and Bioengineering*, 2004. **87**(1): p.24-33.
46. Moore, B.D., et al., *Pharmaceutical composition*. US2006/0292224, 2006.

47. Kreiner, M., et al., *DNA-coated microcrystals*. Chemical Communications, 2005(21): p.2675-2676.
48. König, C., *Entwicklung eines Prozesses in Pilotgröße zur Herstellung von Protein-coated Microcrystals* [dissertation]. Bonn: Universität Bonn, 2010.
49. Moore, B.D., Vos, J., and Partridge, J., *Precipitation stabilising compositions*. WO2008/132439, 2008.
50. *GESTIS-Stoffdatenbank*. IFA - Institut für Arbeitsschutz der Deutschen Gesetzlichen Unfallversicherung, accessed September 25, 2012. Available from: <http://www.dguv.de/ifa/de/gestis/stoffdb/index.jsp>.
51. Maltesen, M.J. and van de Weert, M., *Drying methods for protein pharmaceuticals*. Drug Discovery Today, 2008. 5(2–3): p.e81-e88.
52. Partridge, J., et al., *Stabilization of proteins in dry state without sugars*. AAPS National Biotechnology Conference. 2005. Nashville, TN, USA.



## Chapter 2

# HSA-free formulation of a hydrophobic cytokine as protein-coated microcrystals

This chapter is intended for publication:

K. Berkenhoff, K. Bechtold-Peters, V. Christ, S. Bassarab, W. Friess, HSA-free formulation of a hydrophobic cytokine as protein-coated microcrystals; *in preparation*.

### Abstract

The development of liquid injectables for hydrophobic cytokines bears particular challenges because the proteins' hydrophobicity may result in low solubility, a high aggregation tendency and marked adsorption phenomena. Therefore, various formulations contain HSA as stabilizing agent. Our study aimed to develop a stable HSA-free formulation of a hydrophobic cytokine as protein-coated microcrystals (PCMCs). Based on coprecipitation, the PCMC technology offers the possibility to stabilize protein in the solid state. For the optimization of the PCMC composition with respect to amino acid, sugar and salt, we performed a formulation screening that focused on protein process stability as well as on PCMC formation and particle structure. The investigation revealed only minor differences in protein process stability between the excipient combinations selected. One promising formulation based on valine and sucrose was chosen for further detailed investigation of protein bioactivity and long-term stability over one year at  $5 \pm 3$  °C and  $22 \pm 3$  °C. Bioactivity was completely preserved during the PCMC production process. Moreover, the level of aggregation detected via HP-SEC and SDS-PAGE as well as the amount of oxidized species increased only slightly over storage time depending on the storage temperature. Storage at  $5 \pm 3$  °C provided good stability of the cytokine coated microcrystals over one year. Compared to long-term stability studies with commercialized lyophilized cytokine formulations, the overall stability as PCMCs turned out to be improved.

Therefore, the PCMCs represent a very encouraging technology for the formulation of the hydrophobic cytokine as well as potentially various other protein drugs.

## 1 Introduction

Research is progressing fast in the area of cytokines that are widely used in the treatment of cancer, autoimmune disorders and related diseases [1]. In the formulation development of a number of cytokines, some specific challenges have to be overcome, originating from the hydrophobicity of these proteins [2]. Cytokines frequently are of a limited solubility [3, 4] and can show pronounced aggregation and adsorption tendencies [5, 6]. Therefore, in various cases human serum albumin (HSA) is added, e.g. to beta-interferons, because it provides stabilizing effects, increases solubility and reduces the unspecific adsorption to surfaces [7]. Extavia<sup>®</sup>, Betaferon<sup>®</sup>/Betaseron<sup>®</sup>, and Avonex<sup>®</sup> (lyophilisate) represent some marketed products that contain a large surplus of HSA (e.g. for Betaferon<sup>®</sup> 50-fold by weight) [8]. Nevertheless, the use of HSA in the formulation development of proteins gives rise to various concerns. First, HSA used in these formulations is generally obtained from human plasma and thus is tainted with the peril of blood derived pathogens. This problem would be cured by the use of recombinant HSA which has become available at larger quantities [9]. Furthermore, it can be speculated about the potential risk of mixed HSA/cytokine aggregates which may lead to severe immune responses [10]. Finally, the presence of the large HSA excess precludes or at least complicates the various analytics which would allow to demonstrate the cytokine's integrity in the formulation [2]. In consequence of these disadvantages, significant efforts are made to avoid the use of HSA in the development of cytokines as exemplarily realized in Avonex<sup>®</sup> (liquid) and Rebif<sup>®</sup> [8] or studied by Hawe and Friess [5]. These HSA-free formulations are classical liquid or lyophilized dosage forms.

The protein-coated microcrystals technology represents an alternative method of protein stabilization in the solid state. It is based on the coprecipitation of an aqueous solution of protein and carrier material which is induced by a rapid addition of a surplus of organic water-miscible solvent, e.g. isopropanol or isobutanol [11]. The immediate dehydration of the protein and the carrier components, comprising physiological acceptable substances such as buffer species, amino acids, sugars and inorganic salts [12], results in the formation of a

suspension that is concentrated and subsequently dried via supercritical fluid extraction with carbon dioxide. The powder harvested consists of water-soluble particles in the lower micrometer range. The idea of the PCMC technology goes back to a patent of Moore et al. [11]. The applications described by various researchers include not only proteins, peptides and polypeptides, such as e.g. subtilisin Carlsberg protease [13], lipase [14, 15], trypsin [16, 17], BSA [16, 18], IgGs [16, 19], but also DNA and RNA [20]. König established a pilot-scale production process for PCMCs that enables a continuous production of up to 120 L suspension per hour [16]. Thus, this technology has become an attractive method in protein formulation e.g. as highly concentrated suspension for subcutaneous injection or powder for pulmonary delivery.

The objective of our study was to develop a HSA-free formulation of a hydrophobic cytokine as PCMCs. Therefore, a formulation screening had to be conducted to optimize the carrier composition. The focus of the protein analytics was on monomer content, turbidity, protein recovery and bioactivity upon reconstitution of the powder. Subsequently, one promising formulation was to be chosen to investigate the bioactivity in comparison to a marketed lyophilized product of the cytokine. Moreover, a long-term stability study over 52 weeks was carried out considering the integrity (HP-SEC, RP-HPLC, SDS-PAGE) and the structure (2<sup>nd</sup>-derivative UV, intrinsic fluorescence, FT-IR spectroscopy) of the cytokine as well as the PCMC morphology (x-ray diffractometry, SEM).

## **2 Materials and methods**

### **2.1 Materials**

L-Phenylalanine, L-aspartic acid, DL-dithiothreitol, acetonitrile, Water CHROMASOLV® for HPLC and trifluoroacetic acid were purchased from Sigma-Aldrich, Steinheim, D, L-2-methyl-2,4-pentanediol and disodium EDTA dihydrate from Merck, Darmstadt, D. Sodium dodecyl sulfate was procured from Serva, Heidelberg, D, L-glutamic acid and D/L-valine were from Fluka, Buchs, CH. L-Arginine and glycine were obtained from Ajinomoto Omnicem, Louvain-la-Neuve, B, trisodium citrate dihydrate and citric acid monohydrate from Jungbunzlauer, Ladenburg, D. Sodium dihydrogen phosphate dihydrate was delivered by Dr. Paul Lohmann, Hungen, D, sodium chloride by Akzo Nobel, Hengelo, NL, and trehalose dihydrate by Ferro

Pfanstiehl, Waukegan, IL, USA. MOPS (3-(N-Morpholino)-1-propanesulfonic acid sodium salt) was acquired from Carl Roth, Karlsruhe, D, sucrose from Südzucker, Mannheim, D. SilverXpress® Silver Staining Kit originated from Invitrogen, Darmstadt, D, and isopropanol from Hedinger, Stuttgart, D. All chemicals were utilized without further purification.

The protein bulk drug substance provided by Boehringer Ingelheim was composed of 1.5 mg/mL hydrophobic cytokine, 50 mM sodium acetate trihydrate, 1 mM disodium EDTA dihydrate and 0.1 % sodium dodecyl sulfate (SDS). The buffer of the bulk drug substance was exchanged via ultra- and diafiltration resulting in a protein solution that consisted of 11-21 mg/mL protein, 22 mM citrate and 0 or 52 mM NaCl (crossflow buffer exchange and concentration unit, Boehringer Ingelheim, Biberach/Riss, D; membrane cassette Sartoclon Slice, Hydrosart, 5 kd, Sartorius, Göttingen, D; Quattroflow 150 S membrane pump, Quattroflow Fluid Systems, Hardeggen, D). Furthermore SDS was present in the protein solution because it cannot be removed via ultra- and diafiltration, as similarly reported by Mahler et al. for polysorbate 20 [21].

## **2.2 Methods**

### **2.2.1 PCMC production process**

The PCMC production process is divided into four main steps: preparation of protein-carrier solution, precipitation, concentration/solvent exchange, and drying. For the preparation of the protein-carrier solution the carrier material was dissolved in water and the solution pH value was adjusted to 5.5 (3.0 for formulation Asp3.0) prior to the addition of the protein solution. The composition of the protein-carrier solutions is presented in Table 2-1. Their solid content amounted to 45 mg/mL except for formulations Asp5.5 and Asp3.0 which had a solid content of 7 mg/mL due to the low solubility of aspartic acid of 4 g/L [22].

**Table 2-1: Composition of protein-carrier solutions [% w/w].**

Formulation	Val +NaCl	ValSuc +NaCl	ValSuc -NaCl	GlyPhe Tre	GlyGlu Arg	ValArg	Asp5.5	Asp3.0
Trisodium citrate dihydrate	8.6	8.6	8.6	8.6	8.6	8.6	8.6	8.6
Citric acid monohydrate	1.2	1.2	1.2	1.2	1.2	1.2	1.2	1.2
Sodium chloride	5.1	5.1	--	5.1	5.1	5.1	5.1	5.1
Cytokine	10.0	10.0	10.0	10.0	10.0	10.0	10.0	10.0
Glycine	--	--	--	40.0	46.2	--	--	--
L-Glutamic acid	--	--	--	--	4.6	--	--	--
L-Arginine	--	--	--	--	6.3	37.6	--	--
DL-Valine	75.1	74.1	79.2	--	--	37.6	--	--
Sucrose	--	1.0	1.0	--	--	--	--	--
L-Phenylalanine	--	--	--	5.7	--	--	--	--
L-Aspartic acid	--	--	--	--	--	--	57.1	57.1
MOPS	--	--	--	11.4	--	--	--	--
Trehalose dihydrate	--	--	--	18.0	18.0	--	18.0	18.0
Final pH	5.6	5.6	5.7	5.6	5.5	5.4	5.6	3.1
Solid content [mg/mL]	45	45	45	45	45	45	7	7

The precipitation was carried out as described in detail by König [23]. Briefly, two equal streams of precipitating agent were mixed with one stream of protein-carrier solution in a small double jet impingement mixer of an inner diameter of 1.5 mm (Boehringer Ingelheim Pharma GmbH Co. KG, Biberach/Riss, D). The precipitating agent was a 1:1 mixture of isopropanol and 2-methyl-2,4-pentanediol based on volume saturated with all carrier components. The mixing ratio of the precipitating agent and the protein-carrier solution was set to 95 : 5 (v/v). The modular mixing platform from Ehrfeld (Bayer Technology, Wendelsheim, D) encompassed three micro gear pumps (HNP pumps mzt 11507 and 7255, Hydraulik Nord Fluidtechnik, Parchim, D), pressure sensors and temperature sensors to monitor the precipitation step. The total flow rate of 1000 mL/min was controlled by the software LabView (National Instruments, Munich, D) and Coriflow mass flow meters (Bronkhorst, Kamen, D). The final suspension volume after precipitation was 1 L for the formulation screening (2 L for the formulations based on aspartic acid) and 5 L for the subsequent bioactivity and long-term stability study. Based on macroscopic

evaluation the precipitation behavior was ranked into three groups: (1) significantly decelerated, (2) slightly decelerated, (3) rapid.

For the formulation screening the PCMCs were gained by vacuum filtration of the suspension through a 0.45  $\mu\text{m}$  membrane filter (Durapore Membrane Filter 0.45  $\mu\text{m}$  HV 47 mm, Millipore, Schwalbach, D) and drying in the glove box flushed with dry air. For the bioactivity and long-term stability study this simplified procedure was replaced by the detailed PCMC production process as described by König et al. [23]. For concentration of the PCMC suspension the supernatant was decanted 18 h after the precipitating step and the concentrated suspension was filtered through a 0.45  $\mu\text{m}$  membrane filter (Stericup 47 mm, Sartorius, Göttingen, D). After two washing steps with isopropanol saturated with the excipients the filter cake was resuspended in this solvent. For the final supercritical drying process (Thar SFE-500, Thar Technologies, Pittsburgh, PA, USA) carbon dioxide at 100 bar and a flow rate of 25 g/min was utilized at 45 °C, after drying for 130 min the pressure was decreased by 3 bar/min.

### **2.2.2 Storage stability study**

For the stability study 10, 50 (analysis of protein structure), or 100 mg (x-ray diffractometry) of the PCMC powder based on formulation ValSuc-NaCl was filled into 2 R glass vials (Fiolax®, Schott, Mülheim, D). Half of the vials was stoppered (Gusto C 1503 6720 GC grau 6 TP, Stelmi, Roissy Charles De Gaulle Cedex, F) under lab atmosphere in the glove box, the other half in a freeze-dryer flooded with nitrogen (Epsilon 2-12 D, Martin Christ, Osterode, D) at 20 °C, 760 mbar. Samples were stored at  $5 \pm 3$  °C or  $22 \pm 3$  °C. Analysis of the PCMC powder was performed directly after PCMC production ( $t_0$ ), after two ( $t_{2\text{wk}}$ ), four ( $t_{4\text{wk}}$ ), eight ( $t_{8\text{wk}}$ ) and 52 weeks ( $t_{52\text{wk}}$ ) of storage. Investigations by x-ray diffractometry, scanning electron microscopy, SDS-PAGE as well as spectroscopic methods were limited to  $t_0$ ,  $t_{8\text{wk}}$  and  $t_{52\text{wk}}$ .

### **2.2.3 Analysis of PCMCs**

#### **2.2.3.1 Reconstitution of PCMC powder**

During the formulation screening 22 mM citrate buffer with 52 mM sodium chloride pH 2.0 was used to dissolve the powder. For formulation ValSuc-NaCl this buffer was prepared without sodium chloride. For the stability study samples were reconstituted with 11.5 mM NaCl, pH 2.0.

### 2.2.3.2 Turbidity

Turbidity was measured at a protein concentration of 1 mg/mL except for the formulations Asp5.5 and Asp3.0 which required double the volume of reconstitution medium due to low solubility of aspartic acid and which were thus analyzed at 0.5 mg/mL. During the formulation screening, turbidity was investigated by 90 ° light scattering at  $\lambda = 400\text{-}600$  nm (Turbidimeter 2100 AN, Hach Lange, Düsseldorf, D) expressed in formazine nephelometric units (FNU) 30 min after reconstitution (n=3). For the stability study, turbidity was determined by 90 ° light scattering at  $\lambda = 633$  nm 90 min after the addition of the reconstitution medium.

The turbidity values were compared to the reference solutions I-IV of the Ph. Eur. (method 2.2.1 clarity and degree of opalescence of liquids) [24], as shown in Table 2-2. According to the Ph.Eur., FNUs are equivalent to NTUs (Nephelometric Turbidity Unit) in regions up to 40 NTUs.

**Table 2-2: Turbidity of the opalescence reference solutions according to Ph. Eur..**

Reference solution	Turbidity [NTU]	Degree of opalescence
I	3	Clear ( $\leq$ Ref. I)
II	6	Slightly opalescent ( $\leq$ Ref. II)
III	18	Opalescent ( $\leq$ Ref. III)
IV	30	Very opalescent ( $\leq$ Ref. IV)

### 2.2.3.3 Theoretical protein recovery

For the evaluation of protein recovery 30 mg of PCMC powder were dissolved and filtered through a 0.45  $\mu\text{m}$  syringe filter (Rotilabo-Spritzenfilter steril 0.45  $\mu\text{m}$  PVDF, Carl Roth, Karlsruhe, D) 30 min after reconstitution. UV measurement (UV/VIS Spectrometer Lambda 20, PerkinElmer, Rodgau-Jügesheim, D) in Halfmicro Plastibrand® cuvettes (Brand, Wertheim, D) was carried out at 280 nm, corrected against buffer, based on an extinction coefficient of 1.70 (n=3) [5, 25]. Theoretical protein recovery was calculated as the quotient of the cytokine fraction in the PCMCs to the cytokine fraction in the total solid mass of the protein-carrier solution.

#### **2.2.3.4 Protein integrity**

##### **2.2.3.4.1 HP-SEC**

For HP-SEC method A a TSKgel G3000SW column (7.8 mm ID x 60.0 cm L) and a TSKgel SWXL Guardcol precolumn (Tosoh Bioscience, Stuttgart, D) were used on an Äkta micro (GE Healthcare, Uppsala, Sweden) with 200 mM sodium dihydrogen phosphate and 0.1 % SDS. 25 µl samples of 0.6 mg/mL protein were injected in duplicate and protein elution was monitored via UV-detection at 210 nm. Aggregation in percent was calculated based on the ratio of the area under the curve (AUC) of soluble aggregates to the total AUC of aggregates and monomer (n=2). Method A was used in the formulation screening as well as in the stability study, representing the standard HP-SEC method for the cytokine [5].

Additionally, method B, as developed by BI, was used as orthogonal method in the stability study to assess cytokine aggregation. It was performed on a TSKgel G3000SWXL column (7.8 mm ID x 30.0 cm L) and a TSKgel SWXL Guardcol precolumn (Tosoh Bioscience, Stuttgart, D). The mobile phase was composed of 60 % acetonitrile, 40 % water and 0.1 % TFA. Peaks were detected via UV at 214 nm.

##### **2.2.3.4.2 SDS-PAGE**

SDS-PAGE was conducted at 200 V with Power Ease 500 and XCell Sure Lock in combination with 12 % Bis-Tris gels (NuPAGE®, 1 mm, 10 wells, Invitrogen, Darmstadt, D) and NuPAGE® MOPS SDS running buffer. Samples were mixed 8:2 with NuPAGE® LDS sample buffer, and 7:2:1 with NuPAGE® LDS sample buffer and 0.5 M dithiothreitol for the reducing SDS-PAGE. After heating up to 95 °C for 5 min, 5 µl of the samples and the marker (Precision Plus Protein Standard), representing 1 µg protein, were loaded to each well. Furthermore, 2 ng BSA were loaded to one well for the purpose of sensitivity control. The gels were stained with SilverXpress® Silver Staining Kit.

##### **2.2.3.5 Particle size**

The particle size was determined in suspension by laser diffractometry (OASIS equipped with HELOS/BF, CUVETTE CUV-50ML/US, SUCELL/M, SVA, Sympatec, Clausthal-Zellerfeld, D). Suspension was added until an optical concentration of about 5 % was reached in the cuvette that contained 50 mL of the precipitating solvent at a stirring speed of 500 rpm. Based on

Fraunhofer model the particle size distribution was calculated and expressed as volume distribution ( $Q_3$ ). The mean value and the span 90 as  $(x_{90}-x_{10})/x_{50}$  were used for powder characterization (n=3).

### 2.2.3.6 Particle morphology

Particle morphology of PCMC suspensions was analyzed by the use of a light optical microscope (Olympus BX50 F4, Olympus, Tokyo, Japan) equipped with a digital camera (HVC 20, Hitachi, Maidenhead, GB). Additionally, for scanning electron microscopy (Zeiss SUPRA 55 VP, Zeiss, Oberkochen, D), powder samples on an aluminum stub and coated with gold/palladium (SCD 500, BAL-TEC, Witten, D) were prepared.

### 2.2.3.7 Bioactivity

The bioassay was based on lung cancer indicator cells A549 [26]. Briefly, preincubated with different concentrations of the cytokine, the cells were infected with encephalomyocarditis virus and thus a cytopathic effect was evoked leading to cell lysis. The number of viable cells was analyzed by an MTT (3-(4,5-Dimethylthiazol-2-yl)-2,5-diphenyltetrazolium bromide) assay. The concentration of the cytokine that led to the lysis of 50 % of the cells ( $ED_{50}$ ) was referred to cytokine standard. The biological activity of the samples was determined based on three independent batches of each sample. Each batch consisted of two plates with the sample in triplicates.

### 2.2.3.8 Oxidized species

The amount of oxidized cytokine was analyzed by RP-HPLC (Alliance 2695, Waters, Milford, MA, USA) with a Zorbax 300SB-CN column (4.6 x 150 mm, Agilent, Böblingen, D) as stationary phase. The mobile phase was composed of phase A (100 % water with 0.1 % trifluoroacetic acid (TFA)) and phase B (84 % acetonitrile, 16 % water, 0.084 % TFA). The volume fraction of phase B was increased from 40 % to 55 % (9 min), 60 % (15 min) and 80 % (20 min) and finally reduced back to 40 % (21 min). A duplicate of 50  $\mu$ l samples with 0.25 mg/mL protein was injected at a flow rate of 0.7 mL/min and detected at 214 nm (UV). The fraction of oxidized protein was calculated as percentage of the AUC of the peak caused by oxidized cytokine to the total AUC (n=2).

### 2.2.3.9 Protein structure

Conformational changes of the protein were analyzed via intrinsic fluorescence spectroscopy, UV spectroscopy and Fourier transform infrared spectroscopy. As valine which was used as main carrier component interferes with the FT-IR analysis, a special form of sample preparation was required prior to measurement [27, 28]. For the separation of protein from the carrier components in the PCMC powder, differences in solubility of the constituents were utilized. 50 mg of PCMC powder was suspended in 10 mL Water For Injection (WFI), stirred for 10 min and centrifuged at 3000 g for 10 min. The supernatant containing the water soluble components, including valine, was removed and fresh WFI was added. After four repetitions the lasting sediment that only consisted of protein was finally dissolved in 1.5 mL 0.25 % SDS solution and the solution was filtered through a 0.45  $\mu\text{m}$  syringe filter for further analysis. The absence of valine in the solution was controlled via thin layer chromatography based on ninhydrine detection.

#### 2.2.3.9.1 Intrinsic fluorescence spectroscopy

Samples of 0.1 mg/mL protein in SUPRASIL® 114-QS precision cuvettes (10 mm, Hellma, Mühlheim, D) were excited at 295 nm and 25 °C and the emission was scanned from 305 nm to 400 nm with a step size of 1 nm and 1 s integration time (Fluorimeter QM-4-CW, PTI, Birmingham, NJ, USA). The evaluation was based on normalized spectra.

#### 2.2.3.9.2 UV spectroscopy

Samples of 0.3 mg/mL protein were scanned from 240 to 350 nm (UV/VIS Spectrometer Lambda 20, PerkinElmer, Rodgau-Jügesheim, D). The second derivative of the absorption was used.

#### 2.2.3.9.3 Fourier transform infrared spectroscopy

FT-IR spectroscopy was performed using a Tensor 37 and a Confocheck measuring cell (Bruker, Ettlingen, D). Spectra were recorded from 4000 to 900  $\text{cm}^{-1}$  with 120 scans and a resolution of 2  $\text{cm}^{-1}$  at 25° C. Atmospheric compensation was done and buffer spectrum served as reference. Spectra were processed by vector normalization prior to calculating the average spectrum based on three measurements. Second derivative was built applying 17 smoothing points

(Savitzky-Golay algorithm). The protein concentration of the samples ranged from 3 to 8 mg/mL.

### **2.2.3.10 X-ray powder diffraction**

The crystallinity of cytokine PCMCs was analyzed with XRD in transmission mode from  $3^{\circ}$ - $40^{\circ}$   $2\theta$ ,  $0.5^{\circ}$  steps and 20 s/step based on  $1.5406 \text{ \AA}$   $\text{CuK}\alpha$ -radiation at 40 kV and 40 mA (Stoe, Darmstadt, D). Samples were fixed in the sample holder between two Ultraphan foils (cellulose diacetate) with a thickness of 0.014 mm (Stoe, Darmstadt, D).

## **3 Results**

### **3.1 Formulation screening**

#### **3.1.1 Particle formation and characterization**

Based on their precipitation behavior, the formulations were divided into three groups (Table 2-3). The formulations GlyPheTre, GlyGluArg and ValArg precipitated rapidly. The product that left the mixing unit already represented a white suspension. All formulations that contained valine as main carrier component (Val+NaCl, ValSuc+NaCl, ValSuc-NaCl) as well as the sample Asp5.5 showed a slightly decelerated precipitation behavior and the product was not yet turbid at the outlet of the mixer, but turbidity immediately built up in the container used for harvesting. In contrast, formulation Asp3.0 became turbid after 1 h.

The formulations clearly differed in their particle size that was analyzed via laser diffractometry (Table 2-3). ValArg, GlyGluArg and Asp5.5 formed rather small particles with  $x_{50}$  values ranging from  $4 \mu\text{m}$  to  $16 \mu\text{m}$ . Precipitation of the formulations Asp3.0, ValSuc-NaCl and Val+NaCl resulted in considerably larger particles in suspension with  $x_{50}$  values of 35, 37 and  $58 \mu\text{m}$ , respectively. GlyPheTre and ValSuc+NaCl particles were of medium size ( $x_{50}$  values of 22 and  $27 \mu\text{m}$ ). As the algorithm is based on spherical shaped particles, the  $x_{50}$  values do not represent an absolute particle size, but can serve for comparison. As exemplarily presented in Figure 2-1, the particle morphology was not spherical for any formulation. The formulations which were based on valine as only main carrier component (Val+NaCl, ValSuc+NaCl, ValSuc-NaCl) were characterized by a platelet-like shape (Figure 2-1a). A similar shape was found for the

formulation Asp5.5. The presence of arginine as additional carrier component apart from valine resulted in a fine and less defined particle morphology (Figure 2-1e). Needle-shaped PCMCs were found in the formulations that were based on glycine (Figure 2-1b, d) as well as for the sample Asp3.0 (Figure 2-1c). Additionally, as it can be seen in Figure 2-1a, b, d, smaller and more transparent particles were present besides the crystalline structures. This observation is underlined by the particle size distributions that were found to be bimodal (Table 2-3) except for the formulations GlyGluArg, Asp5.5 and Asp3.0, whose distributions were left-skewed monomodal. In the majority of cases, the bimodality of the particle size distributions was reflected by a higher span 90 value.

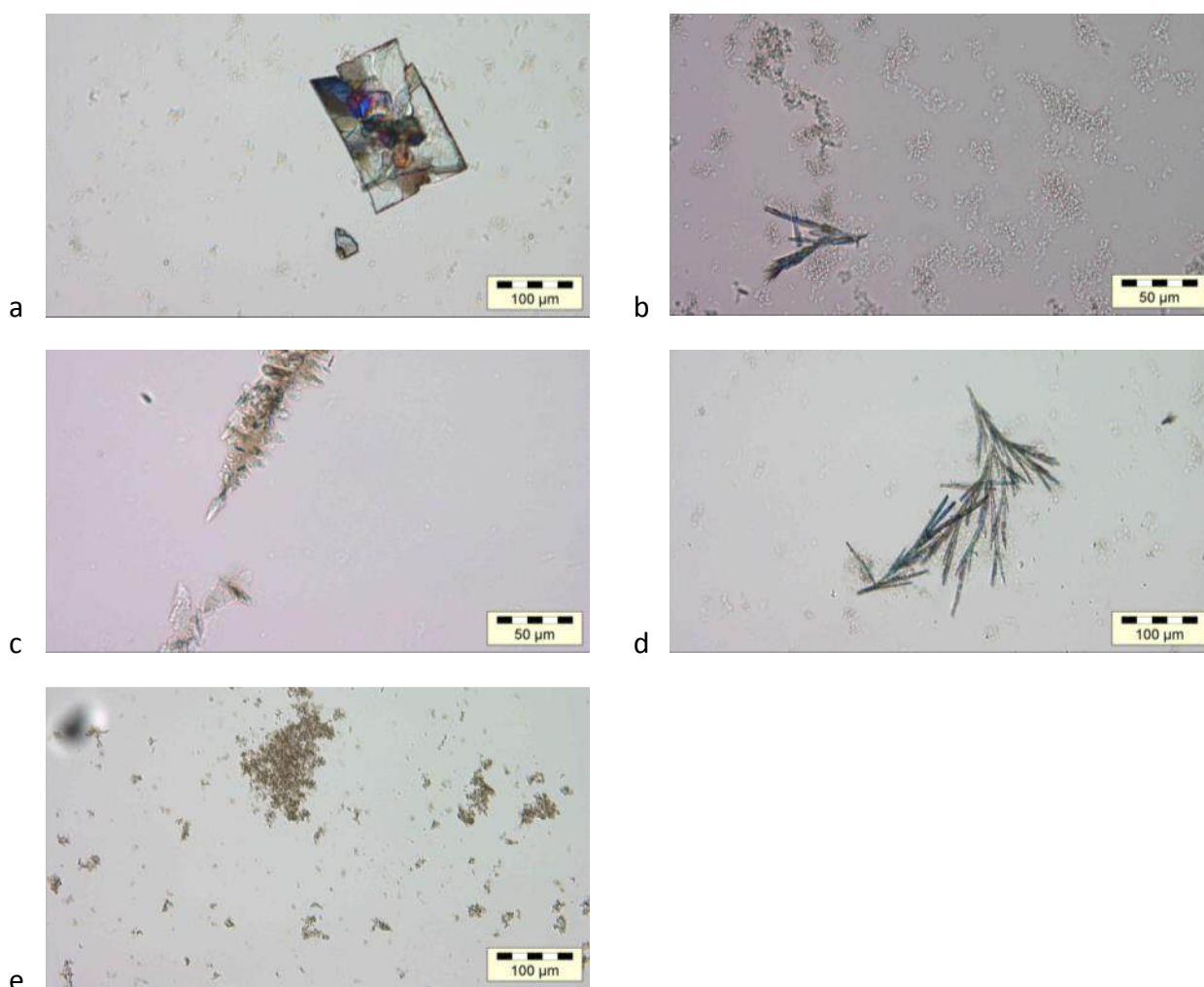


**Figure 2-1: Particle morphology of cytokine PCMCs in suspension (light microscopy): a: ValSuc+NaCl, b: GlyGluArg, c: Asp3.0 d: GlyPheTre, e: ValArg.**

### 3.1.2 Protein process stability

After dissolution of the PCMCs the turbidity of most of the samples did not significantly differ (Table 2-3), except for the formulations GlyPheTre and ValArg which showed higher turbidity values than reference sample II of the Ph. Eur. (6 NTU) [24]. For formulation GlyPheTre a slightly increased turbidity of 7.9 FNU was detected, whereas the sample ValArg could not be successfully dissolved and consequently was not analyzed further.

With respect to theoretical protein recovery calculated as the quotient of the cytokine fraction in the PCMCs to the cytokine fraction in the total solid mass of the starting solution, the samples differed significantly and could be classified into three groups. In the samples ValSuc-NaCl and GlyGluArg a 100 % protein recovery was found (Table 2-3). The formulations ValSuc+NaCl, GlyPheTre and Asp3.0 showed a protein recovery of about 130 %, whereas for Val+NaCl, ValArg and Asp5.5 recovery was considerably decreased to approx. 70-90 %.

The analysis of soluble aggregates via HP-SEC method A revealed some minor differences between the samples. The formulations ValSuc+NaCl, ValSuc-NaCl, GlyPheTre and GlyGluArg contained approx. 4 % of soluble aggregates (Table 2-3). The aggregate content of the formulations Val+NaCl, ValArg, Asp5.5 and Asp3.0 was 5-6 %. Only marginal amounts (< 0.3 %) of soluble fragments were found in some samples.

In the bioactivity test, the sample ValSuc-NaCl achieved the highest relative activity and was set as 1.00 for comparison and ranking of the formulations. The typically used bioactivity reference sample was not taken into consideration due to impact of the complex dissolution and sampling procedure at this stage. ValArg and Asp 5.5 revealed a bioactivity of > 0.90, whereas all other formulations exhibited significantly reduced values between 0.45 and 0.70.

**Table 2-3: Results of the formulation screening; precipitation behavior: (1) significantly decelerated, (2) slightly decelerated, (3) rapid; turbidity: n.m. = not measurable; theoretical protein recovery; HP-SEC: bulk drug substance: 2.0 %  $\pm$  < 0.1 aggregates, 97.9 %  $\pm$  < 0.1 monomers, 0.1 %  $\pm$  < 0.02 fragments; particle-size distribution (PSD): location of maxima, main peak printed in bold [ $\mu$ m]; bioactivity: related to bioactivity of sample ValSuc-NaCl = 1.**

Formulation	Precipitation behavior	Turbidity [FNU]	Theoretical protein recovery [%]	HP-SEC [%] (method A)		Laser diffractometry			Bioactivity
				Aggregates	Monomers	$x_{50}$ [ $\mu$ m]	Span 90	PSD	
Val+NaCl	2	2.8 $\pm$ < 0.1	91.7 $\pm$ 3.2	4.5 $\pm$ 0.3	95.4 $\pm$ 0.4	57.9 $\pm$ 6.0	1.4 $\pm$ 0.1	Bimodal (12; <b>80</b> )	0.66 $\pm$ 0.24
ValSuc+NaCl	2	3.5 $\pm$ 0.4	135.2 $\pm$ 0.4	3.7 $\pm$ 0.1	96.0 $\pm$ 0.3	26.5 $\pm$ 1.8	2.3 $\pm$ 0.1	Broad bimodal (20; 60)	0.47 $\pm$ 0.01
ValSuc-NaCl	2	1.7 $\pm$ 0.1	101.9 $\pm$ 1.1	3.9 $\pm$ 0.2	96.0 $\pm$ 0.2	37.1 $\pm$ 3.1	1.9 $\pm$ 0.1	Bimodal (15; <b>70</b> )	1.00 $\pm$ 0.16
GlyPheTre	3	7.9 $\pm$ 3.4	127.5 $\pm$ 0.5	3.7 $\pm$ 0.1	96.2 $\pm$ 0.1	22.4 $\pm$ 0.8	2.7 $\pm$ 0.1	Very broad bimodal (19; 60)	0.45 $\pm$ 0.08
GlyGluArg	3	3.8 $\pm$ 0.3	101.5 $\pm$ 1.7	4.1 $\pm$ 0.1	95.9 $\pm$ 0.1	9.1 $\pm$ 0.1	1.2 $\pm$ < 0.1	Left-skewed monomodal (12)	0.53 $\pm$ 0.11
ValArg	3	n.m.	69.3 $\pm$ 3.5	5.3 $\pm$ 0.1	94.6 $\pm$ < 0.1	15.8 $\pm$ 0.4	3.4 $\pm$ 0.3	Broad bimodal ( <b>18</b> ; 80)	0.92 $\pm$ 0.01
Asp5.5	2	1.6 $\pm$ 0.1	68.8 $\pm$ 3.9	5.7 $\pm$ < 0.1	94.2 $\pm$ < 0.1	4.3 $\pm$ < 0.1	1.2 $\pm$ 0.1	Left-skewed monomodal (5)	0.94 $\pm$ 0.10
Asp3.0	1	2.2 $\pm$ 0.3	126.6 $\pm$ 2.2	5.2 $\pm$ 0.1	94.8 $\pm$ 0.1	34.9 $\pm$ 1.0	1.2 $\pm$ 0.1	Left-skewed monomodal (48)	0.70 $\pm$ 0.01

### 3.2 Long-term stability study

Based on the results of the formulation screening, the formulation ValSuc-NaCl was selected for a storage stability study. Its bioactivity was 103 % referred to the standard lyophilized formulation of the hydrophobic cytokine. The biological activity did not significantly differ among the intermediate products of the PCMC process (powder harvested from the suspension after precipitation, powder harvested from the suspension after solvent exchange and concentration, powder harvested after supercritical drying). Samples were stored up to 52 weeks at  $5 \pm 3$  °C and  $22 \pm 3$  °C with air or nitrogen headspace.

Turbidity values for all samples investigated were in general low, between 0.2 and 1.7 FNU (Figure 2-2). Thus, turbidity was significantly lower than that of reference suspension I of the European Pharmacopoeia which exhibits a value of 3 NTU [24]. No significant increase or trend with storage could be detected for any storage conditions.

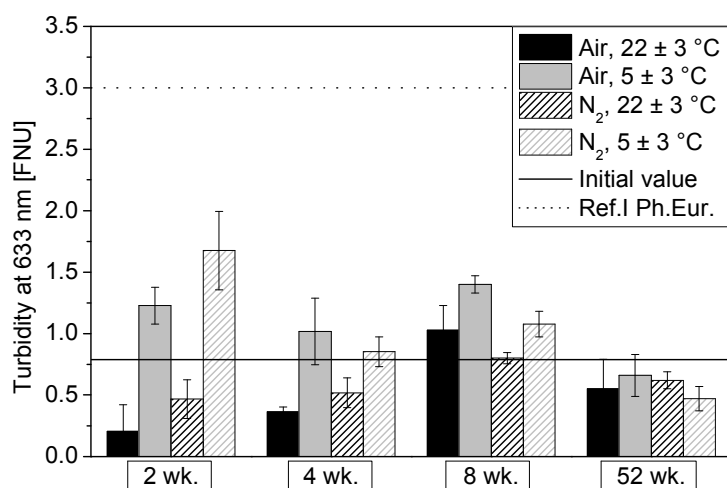


**Figure 2-2: Turbidity of ValSuc-NaCl PCMCs in long-term stability study.**

HP-SEC analysis via method A did not reveal significant changes in the amount of soluble aggregates within eight weeks and the monomer content of all samples was the same as for the initial material (Figure 2-3) ( $p > 0.05$ ). After 52 weeks the monomer content was reduced by approx. 1 % for the samples stored at  $22 \pm 3$  °C. A slight but significant decrease of monomer was also detected upon 52 week storage in the refrigerator ( $p < 0.05$ ), with air in the headspace as opposed to nitrogen. The HP-SEC results obtained by method A were confirmed by the

orthogonal method B which essentially rendered the same monomer content for all samples ( $\pm 0.2\%$ ).

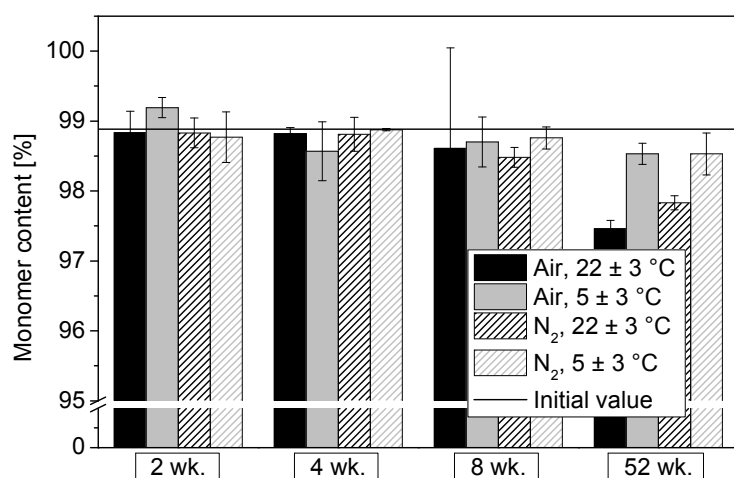


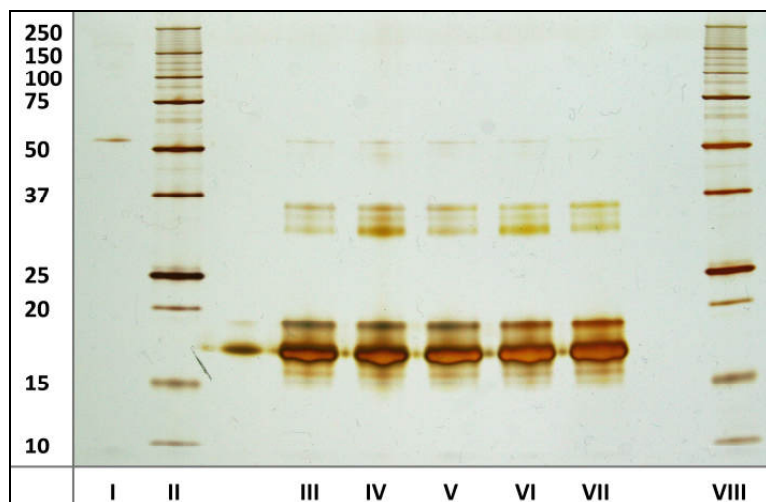
**Figure 2-3: Monomer content (HP-SEC, method A) of ValSuc-NaCl PCMCs in long-term stability study.**

In SDS-PAGE the main bands occurred in the range between 17 and 19 (monomer), and 30 and 36 kDa (dimer), respectively. Furthermore, minimal bands were seen at about the BSA band for the non-reduced gel and around 70 kDa and 15 kDa for the reduced gel. Evaluating the band patterns of all samples, SDS-PAGE gels both reduced and non-reduced showed slightly more intense covalent dimer bands for the samples stored at room temperature for 52 weeks in comparison to the initial material and PCMCs stored in the refrigerator (Figure 2-4). This minor increase in soluble aggregates was in line with the results obtained by HP-SEC analysis. Due to silver stain no quantification was feasible, but the SDS-PAGE indicated the covalent nature of some of the dimers. At least some of the covalent dimers were likely not linked via disulfide bridge because the corresponding band persisted under reducing conditions.

In RP-HPLC analysis no significant increase ( $p > 0.05$ ) in the amount of oxidized cytokine was observed for the samples stored under different conditions for 2 and 4 weeks (Figure 2-5). A slight, but not yet significant trend to more oxidized species was found after 8 weeks. After 52 weeks a significantly higher percentage of oxidized protein was detected for all samples. The change depended on the storage conditions as PCMCs stored at room temperature showed an

increase in oxidation level by 2.1 % (air) and 1.6 % (N<sub>2</sub>), whereas the amount of oxidized cytokine increased by 0.9 % (air) and 0.8 % (N<sub>2</sub>) in the refrigerator.

(a)



(b)

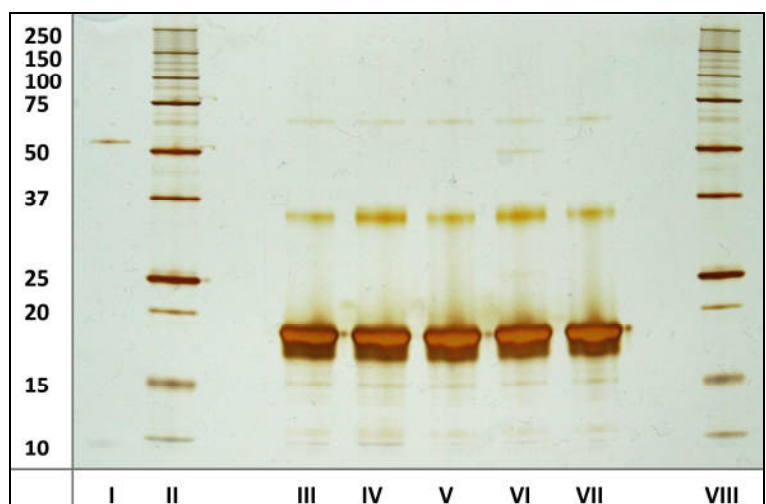


**Figure 2-4: SDS-PAGE of ValSuc-NaCl PCMCs in long-term stability study: (a) non-reduced samples; (b) reduced samples; lane assignment: I: BSA control; II: Precision Plus Protein Standard [kDa]; III: t<sub>0</sub> sample; IV: 52 wk. air, 22 ± 3 °C; V: 52 wk. air, 5 ± 3 °C; VI: 52 wk. N<sub>2</sub>, 22 ± 3 °C; VII: 52 wk. N<sub>2</sub>, 5 ± 3 °C; VIII: Precision Plus Protein Standard.**

Analysis of cytokine's secondary structure via FT-IR measurement did not reveal any significant differences between the initial PCMCs at t<sub>0</sub> and the samples stored under various conditions for 52 weeks (Figure 2-6). The spectra showed a distinctive band at approx. 1650 cm<sup>-1</sup> indicating the dominance of an  $\alpha$ -helical structure for the cytokine. No signs occurred at approx.

1620  $\text{cm}^{-1}$  or 1685  $\text{cm}^{-1}$ , typical of intermolecular  $\beta$ -sheet often appearing in aggregated material due to unfolding [29]. Hence, protein secondary structure did not change over storage time independent of the headspace and the temperature. This outcome was underlined by intrinsic fluorescence spectroscopy and 2<sup>nd</sup>-derivative UV spectroscopy of PCMCs stored for 52 weeks (Figure 2-9 and Figure 2-10 supplementary material). All samples rendered identical spectra independent of storage.

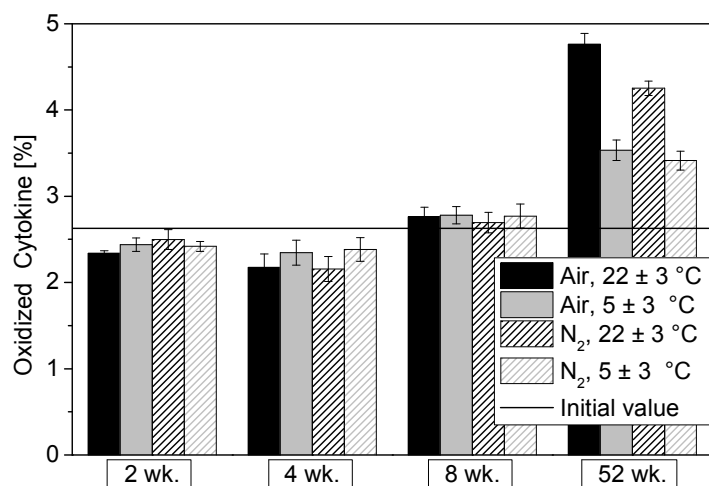


**Figure 2-5: Oxidized cytokine of ValSuc-NaCl PCMCs analyzed by RP-HPLC in long-term stability study.**

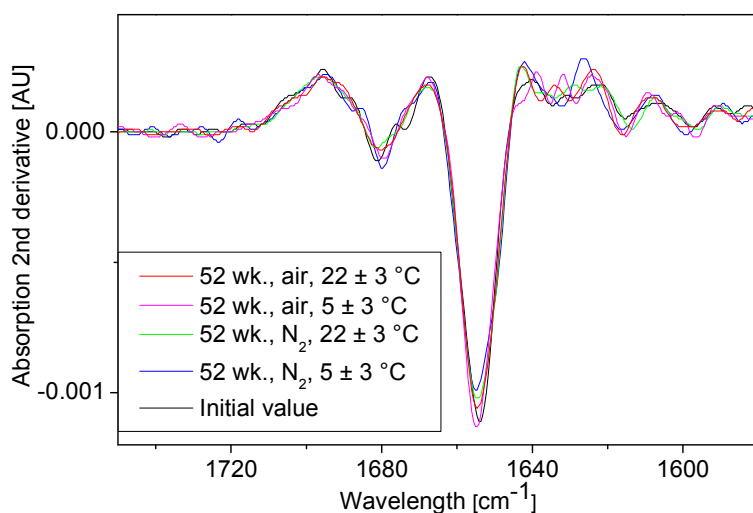


**Figure 2-6: FT-IR spectra of ValSuc-NaCl PCMCs after separation from carrier components in long-term stability study.**

The pattern recorded by x-ray diffractometry demonstrated that cytokine coated microcrystals were of crystalline character (Figure 2-7). A comparison to the spectra of the raw materials indicated that the ValSuc-NaCl PCMC spectrum was dominated by the signals originating from the main carrier valine. Important peaks of the other carrier components, sodium citrate, citric acid and sucrose, were not detected in the PCMC spectrum. The absence of those signal patterns was most evident at 2 theta of 8-17 ° because the PCMC spectrum did not show any significant signal in this range. Moreover, no spectral differences of the cytokine PCMCs were detected independent of the storage conditions as well as of the duration of the stability study.

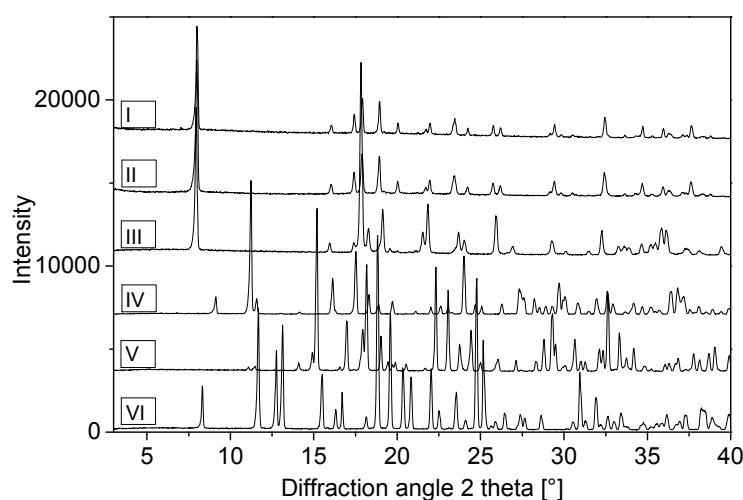


**Figure 2-7: X-ray analysis of ValSuc-NaCl PCMCs in long-term stability study; spectrum assignment: I: 52 wk. air, 22 ± 3 °C; II: PCMCs t<sub>0</sub>; III: D/L-valine; IV: trisodium citrate dihydrate; V: citric acid monohydrate; VI: sucrose; arbitrary offset for better comparison.**

In SEM, most PCMCs showed a more or less spherical shape with a crystalline core coated with crumbly material (Figure 2-8a, b) and particles of the small, crumbly, less compact coating were found separated from the large spherical particles. Placebo particles without protein were rosette shaped and of crystalline appearance (Figure 2-8c). In contrast to the cytokine PCMCs, this powder lacked of the less compact, smaller particles. No changes in particle morphology were seen in stored samples at all storage temperatures, storage time points and independent of the headspace (Figure 8d).

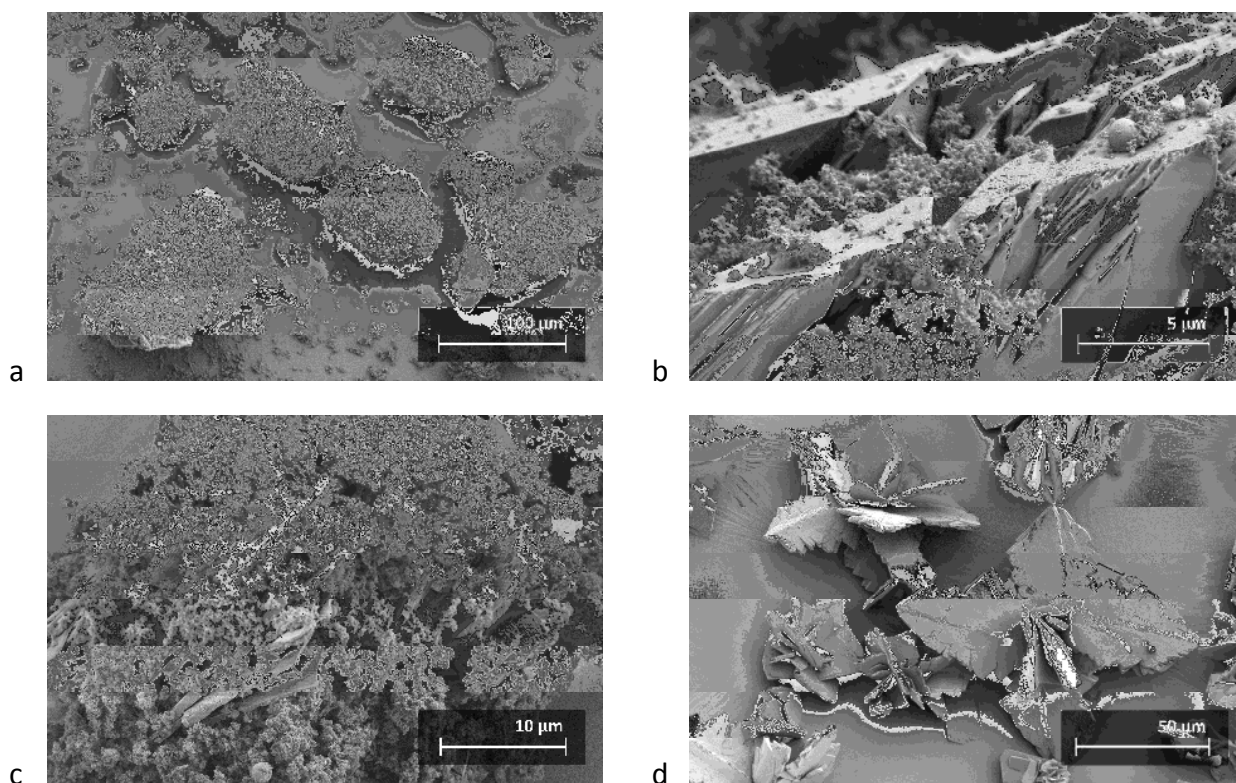


**Figure 2-8: SEM of ValSuc-NaCl PCMCs: a, b, c: cytokine coated ValSuc-NaCl PCMCs at  $t_0$  (a and b) and stored for 52 weeks at  $22 \pm 3$  °C with ambient air headspace (c); d: placebo ValSuc-NaCl PCMCs (i.e. precipitated from an aqueous carrier solution without cytokine).**

## 4 Discussion

The idea of the PCMC technology is to stabilize protein in the solid state. The particle formation is based on a coprecipitation of protein and water-soluble carrier components which is realized by the addition of an excess of organic water-miscible solvent. The focus of the paper was on the applicability of the PCMC technology to formulate a hydrophobic cytokine with respect to process and storage stability of the protein. In the formulation screening, different carrier components were combined including amino acids (arginine, aspartic acid, glycine, glutamic acid, phenylalanine, valine), sugars (sucrose, trehalose) and the inorganic salt NaCl. Particle formation and morphology were investigated as well as protein stability in terms of turbidity, protein recovery, monomer content and bioactivity. The most promising formulation ValSuc-NaCl was subsequently chosen for a long-term stability study over 52 weeks. Protein activity, integrity (HP-SEC, RP-HPLC, SDS-PAGE) and structure ( $2^{\text{nd}}$ -derivative UV, intrinsic

fluorescence, FT-IR spectroscopy) as well as PCMC morphology (x-ray diffractometry, SEM) were analyzed in detail.

#### **4.1 Particle formation and characterization**

According to their precipitation behavior, being rapid, slightly or significantly decelerated, the PCMC formulations of the screening were classified into three groups. The precipitation of the formulations that contained valine as main carrier component, Val+NaCl, ValSuc+NaCl, ValSuc-NaCl, was slightly decelerated. The presence or absence of NaCl and sucrose did not influence the precipitation rate. Replacing 50 % of valine by arginine, however, significantly accelerated the precipitation process. As arginine is considerably more hydrophilic than valine at the precipitation pH of 5.5, it is assumed to exhibit a reduced solubility in the hydrophobic solvent leading to the formation of crystallization nuclei that trigger the PCMC precipitation. The formulations with glycine as main carrier, GlyPheTre and GlyGluArg, precipitated rapidly. The dominance of highly water soluble components, such as glycine and trehalose, acting as nucleation starter in a rather hydrophobic surrounding probably enhanced the precipitation tendency. For two formulations which only differed in the exchange of glycine against valine, fast crystallization of glycine PCMCs compared to slow precipitation of valine containing carriers was observed [23]. With respect to the formulations Asp5.5 and Asp 3.0 that were based on aspartic acid, the precipitation behavior was slightly and significantly decelerated, respectively. This could be attributed to the reduced solid content of 7 mg/mL in the protein-carrier solutions as opposed to 45 mg/mL for all other formulations.

Furthermore, the particle morphology in the suspensions harvested after the precipitation step depended on the carrier composition of the formulations. The particles of glycine containing formulations (GlyPheTre and GlyGluArg) were needle-shaped, as previously described [16]. The use of valine as main carrier component resulted in platelet-like shaped particles as detected for Val+NaCl, ValSuc+NaCl and ValSuc-NaCl PCMCs via light microscopy. Platelet-like PCMCs were also found by Kreiner et al. who investigated DNA-coated microcrystals made of valine as well as by König for valine PCMCs coated with trypsin or trypsinogen [16, 20]. Moreover, Lahav and Leiserowitz reported on a plate-like shape of valine grown from aqueous solution [30]. They further argue that the platelet-like shape is caused by the hydrophobic side chains

providing increased layer energy and reduced water binding concentration at the sides of the bilayers, compared to  $\alpha$ -glycine. The formulation ValArg that contained valine and arginine in equal parts resulted in fine and less defined particles. In dependence of the precipitation pH, aspartic acid PCMCs were needle-shaped (pH 3) and platelet-shaped (pH 5.5).

Apart from larger crystalline structures, smaller and more transparent particles were found in the suspensions. This observation was in line with the bimodal particle size distributions and the consequently higher span 90 values that were detected for most of the formulations. SEM analysis of ValSuc-NaCl PCMCs confirmed the coexistence of two different particle fractions, namely larger crystalline particles and smaller, less compact material, in the powder. Parts of the less compact material were coated onto the larger crystals and a second fraction did exist separately. In contrast, ValSuc-NaCl placebo PCMCs were of a rosette-like crystalline structure composed of numerous platelets, but the smaller, crumbly particles, which were found in the cytokine PCMCs, were missing. Consequently, the crystalline core of the spherical particles can be assumed to consist of carrier components, primarily of valine. The less compact structure was likely made of protein and amorphous carrier of unknown ratio. The x-ray diffractogram of ValSuc-NaCl PCMCs showed the main signals of crystalline valine which corresponds to König who proposed a crystalline state for PCMCs with a protein load of  $\leq 10\%$  [23]. However, typical peaks of trisodium citrate, sucrose and citric acid did not appear in the PCMC diffractogram. This finding could be ascribed to the low amount of sucrose and citric acid (1.0 and 1.2 % w/w) present in the PCMCs, being below the detection limit of the method, or to an amorphous state as found for sodium citrate (8.6 % w/w). Assuming a fully crystalline state of valine and an amorphous state of sodium citrate/citric acid and sucrose, the latter two can stabilize the protein via formation of a glassy amorphous matrix as described in the literature. Izutsu et al. found that sodium citrate formed a glassy state after lyophilization, which prevented BSA and bovine IgG from alterations in secondary structure induced by freeze-drying [31]. The stabilization of proteins by sucrose, via amorphous matrix and/or hydrogen bonding, is frequently described for the manufacturing of solid protein formulations, such as lyophilization [32], spray drying [33, 34] and supercritical fluid drying [35].

With respect to the composition of the precipitated particles, the theoretical protein recovery reflects the ratio of protein to carrier. A value of 100 % indicated that the ratio of protein to carrier in the PCMC powder, initially originating from the composition of the protein-carrier solutions, did not change during the manufacturing process. A value of more than 100 % as detected for the formulations ValSuc+NaCl (135 %), GlyPheTre (128 %) and Asp3.0 (127 %) represented an augmented loss of carrier material. With respect to Asp3.0, the incomplete crystallization of aspartic acid was linked to a significantly reduced precipitation behavior. For ValSuc+NaCl and GlyPheTre, however, the high values must be attributed to incomplete precipitation of main carrier components, namely valine and glycine and/or trehalose, but could not further be explained. On the contrary, the samples ValArg and Asp5.5 contained less protein than theoretically expected (69 %). For ValArg PCMCs, the presence of the basic amino acid arginine resulted in an increased pH of the reconstituted PCMC powder. As the solubility of the cytokine is known to be reduced with increasing pH, the theoretical recovery does not reflect a protein loss during the manufacturing process, but the protein was not completely dissolved as indicated by a sediment formed in the sample [5]. In contrast, the reduced amount of protein in Asp5.5 PCMCs, which completely dissolved upon reconstitution, can be referred to an incomplete coprecipitation of the cytokine with the carrier component at pH 5.5.

## **4.2 Influence of carrier combination on protein process stability**

The influence of the carrier combination on protein process stability was studied via turbidity measurement, bioassay and HP-SEC. Quantitatively, amino acids are the most important excipient for the formulation of proteins as PCMCs. The present study included formulations that were based on a single amino acid, such as valine or glycine, as well as formulations made up of up to three amino acids (GlyGluArg). Glycine and valine were the main amino acids in the formulations because they had successfully been used for the PCMC stabilization of various molecules, such as albumin, lysozyme and trypsin, as well as during the development of the continuous PCMC manufacturing process [14, 17, 23, 36]. Amongst other things, the influence of NaCl and sucrose on the protein process stability of valine PCMCs was investigated. With respect to NaCl, a striking difference in turbidity was seen between the formulations ValSuc+NaCl and ValSuc-NaCl. NaCl did not influence the aggregation tendency of the cytokine formulated as PCMCs as the aggregation level in HP-SEC was 3.7 % (ValSuc+NaCl) and 3.9 %

(ValSuc-NaCl), but the absence of NaCl reduced the turbidity upon reconstitution of the PCMCs by about 50 % (3.5 FNU  $\rightarrow$  1.7 FNU). According to Hawe and Friess an increasing NaCl concentration and consequently growing ionic strength was found to result in a turbidity increase of the cytokine, independent of the pH value [5]. This finding was explained by a poor and strongly pH and ionic strength depended solubility of the cytokine. NaCl was subsequently assumed not to be a suitable excipient for isotonicity adjustment. The negative effect of NaCl on the solubility of the cytokine formulation was also seen in the bioactivity assay. ValSuc-NaCl PCMCs provided the highest cytokine activity, whereas ValSuc+NaCl showed significantly reduced bioactivity (0.47). In contrast, NaCl had previously been considered as indispensable for the precipitation of PCMCs [16]. Consequently, the stabilizing or destabilizing impact of NaCl depends on the protein formulation and cannot be generalized. Hawe and Friess, for example, described that, in contrast to the HSA-free cytokine formulation, the presence of HSA required the addition of NaCl to create a stable protein solution [5, 62]. This might be the reason, besides isotonicity adjustment, why some marketed HSA containing lyophilisates of the cytokine are reconstituted with NaCl solution, such as Betaferon<sup>®</sup> and Extavia<sup>®</sup> [8]. Also according to Zhang et al. NaCl decreased the aggregation rate of recombinant keratinocyte growth factor upon reconstitution of the lyophilisate [37].

Moreover, the formulations Val+NaCl and ValSuc+NaCl were selected to investigate the impact of sucrose on cytokine process stability. In comparison to Val+NaCl, the addition of sucrose slightly reduced the aggregate level in HP-SEC (4.5  $\rightarrow$  3.7 %), whereas turbidity marginally increased (2.8  $\rightarrow$  3.5 FNU). A stabilizing effect of sucrose against aggregation was also reported by Hawe and Friess for a liquid cytokine formulation [5]. Several patents claim sucrose as stabilizer in aqueous interferon formulations as well as diluent for the reconstitution of corresponding lyophilisates [38-41]. The stabilization of proteins by sucrose in solid protein formulations, as discussed above, is ascribed to the formation of a glassy state, hydrogen bonds or a combination thereof.

In formulation ValArg 50 % of valine was replaced by arginine whose properties to suppress protein unfolding and aggregation are particularly discussed in literature [27, 42-45]. The presence of arginine in the PCMC formulation of the cytokine resulted in an increase of

aggregates detected via HP-SEC (4.5 → 5.3 %). The turbidity of the formulation could not be measured due to incomplete dissolution and consequently sedimentation of the PCMC powder. Thus, the effect of arginine did not correspond with the solubility and stability enhancing effect as described by Shirley et al. as well as by Samaritani and Del Rio for liquid interferon formulations [46, 47]. However, the authors neither specified the concentration of arginine nor the pH value of the formulations and did not postulate any stabilizing mechanism that is apparently not yet sufficiently understood [42]. In the case of cytokine PCMCs, incomplete dissolution behavior was associated with reduced cytokine solubility in the presence of the basic amino acid arginine shifting the pH to a higher value.

Apart from valine, two formulations (GlyPheTre, GlyGluArg) were based on glycine as main carrier component. The bioactivity of the glycine based PCMCs was clearly reduced (0.47 and 0.53). Despite the typically high standard deviations and wide acceptance levels of cell-based bioactivity assays, this result at least reflects a clear trend. The turbidity values of the formulation GlyPheTre (7.8 FNU) were slightly higher compared to the values of the other samples (1.6-3.8 FNU), but the aggregate level was low (3.7 %). Thus, this carrier combination provided good cytokine process stability with respect to aggregate formation, but the overall cytokine solubility was decreased. Compared to GlyPheTre, phenylalanine and MOPS were replaced by glutamic acid and arginine in the formulation GlyGluArg. Turbidity (3.8 FNU) as well as aggregate level (4.1 %) was in an acceptable range. Thus, although widely applied as stabilizer in cytokine formulations, glycine was less effective in stabilizing the cytokine formulated as PCMCs compared to valine. Hawe and Friess developed stable liquid and lyophilized formulations for a hydrophobic cytokine that were based on a 20 mM glycine buffer [5]. Various patents claim glycine as stabilizing agent in liquid as well as in lyophilized interferon formulations [38-41, 46, 48-50]. However, a long-term stability study of IgG coated microcrystals showed that glycine may even result in destabilization depending on the storage conditions due to a change in glycine modification [23].

In comparison to glycine, the protein stabilizing effect of phenylalanine and glutamic acid has rarely been investigated [51-53]. Though, some patents include the stabilizing ability of glutamic as well as aspartic acid in interferon formulations [39, 46, 47]. The latter was used as

carrier component in two formulations precipitated at pH 5.5 (Asp5.5) and 3.0 (Asp 3.0). As turbidity generally depends on the protein concentration and the low solubility of aspartic acid required a reduction in protein concentration to 0.5 mg/mL instead of 1.0 mg/mL, the turbidity values could not be compared to the other formulations [54]. The monomer level of the two formulations was lower and the aggregate level higher (5.7 and 5.2 % aggregates) than detected for the majority of the other samples, whereas the biological activity was rather high (0.94 and 0.70). Thus, the presence of an increased amount of soluble aggregates was not reflected in the bioactivity of the formulations. The lower pH of 3.0 prior to precipitation reduced the amount of aggregates in HP-SEC, but resulted in an increased turbidity. Consequently, a decreased precipitation pH value did not improve the overall PCMC process stability of the cytokine and the preference of an acidic over a neutral pH value, as reported by Hawe and Friess for a hydrophobic cytokine as well as claimed in several patents on interferon formulations, could not be transferred to the manufacturing of cytokine PCMCs [5, 38, 40, 46-48].

Overall, PCMCs represent a complex mixture of various carrier components and protein. Therefore, stabilizing or destabilizing effects observed in the current study could not easily be attributed to single excipients. As the PCMC formation mechanism is not understood in detail yet, explanations derived from other protein technologies, such as lyophilization, are not readily transferrable to the challenging PCMC manufacturing process. Altogether, all cytokine formulations provided rather good protein process stability considering the formation of soluble and insoluble aggregates as well as the preservation of the biological activity. In comparison to the other samples, the formulation ValSuc-NaCl provided slightly superior stability. Besides, the bioactivity of ValSuc-NaCl PCMCs was equivalent to the standard lyophilized product of the cytokine and was not affected by the manufacturing process which includes three potentially rather stressful steps, namely precipitation, concentration and supercritical drying. This formulation was thus chosen for a long-term stability study.

### 4.3 Long-term storage stability

#### 4.3.1 Protein stability

The formulation ValSuc-NaCl, selected for the storage stability study, was tested for both protein and carrier stability. As reported by Mahler et al. as well as by Bondos and Bicknell, turbidimetry represents an appropriate tool for the detection of insoluble protein aggregates [55, 56]. The turbidity values of the samples ranged between 0.2 and 1.7 FNU and, consequently, were very moderate and significantly lower than the value of the reference suspension I of the Ph.Eur.. Thus, supported by the absence of large particles visible by the naked eye, the formulations were considered as clear for all analytical time points, essentially free from large aggregates and unchanged over 52 weeks.

The minimal increase of aggregates (dimers to oligomers) by 0.4 % within 52 weeks at  $5 \pm 3$  °C, as detected by HP-SEC, additionally proved the high stability of the PCMC formulation. As typically seen for protein formulations, less aggregates were detected in the samples stored at  $5 \pm 3$  °C, 1.5 % for both air and N<sub>2</sub> in the headspace, compared to PCMCs stored at  $22 \pm 3$  °C with 2.6 % (air) and 2.2 % (N<sub>2</sub>) aggregates, respectively. It has to be taken into consideration that SDS was present in the exclusively aqueous mobile phase of HP-SEC method A, which is the standard SEC method for the hydrophobic cytokine [5]. As the adsorption tendency of hydrophobic proteins is well known [5], the addition of SDS aims to reduce the adsorption of the protein to the column matrix. However, SDS denatures proteins depending on the concentration used and is discussed to dissociate non-covalently linked protein aggregates [57, 58]. Therefore, a second HP-SEC method based on a SDS-free, but acetonitrile containing eluent, method B, was developed and applied. Both methods gave the same results. Nevertheless, one has to bear in mind that acetonitrile is reported to dissociate insulin hexamers and hence may have similar dissociation properties on cytokine aggregates as SDS [59].

The evaluation of protein aggregation within a particular formulation requires the application of orthogonal methods because of the great variability of the nature of aggregates [57, 60]. Mahler et al. listed sedimentation velocity analytical ultracentrifugation (SV-AUC), flow field flow fractionation (FFFF) as well as light scattering (e.g. dynamic light scattering (DLS)) as

possible additional methods to accurately and reproducibly quantify the level of aggregates [54]. Hawe and Friess used DLS in addition to HP-SEC for the characterization of the aggregate level in formulations of a hydrophobic cytokine. The intensity of a second peak in the DLS-size distribution with a maximum of 13.5 nm was assigned to aggregated protein. An intensity of about 1 % was correlated to 2.5 % aggregates detected via HP-SEC. As the aggregation level revealed during our stability study was significantly lower than 2.5 %, with exception to the samples stored at room temperature for 52 weeks, DLS did not represent an appropriate orthogonal method in this case.

SDS-PAGE was additionally applied for the detection of soluble covalently linked aggregates. The bands between 30 and 36 kDa, which were present in the initial PCMC powder as well as in the samples stored for 52 weeks, originated from dimer formation. These aggregate bands were slightly more pronounced in samples stored at room temperature, compared to the initial value and to the samples stored at  $5 \pm 3$  °C, indicating a marginal formation of covalently linked aggregates. One of the dimer bands persisted under reducing conditions and thus indicated that some of these aggregates were caused by non-disulfide bridging. The evaluation of the gels was based on silver staining and hence only the detection of supplementary bands can be evaluated as significant differences between the samples [54]. Nevertheless, SDS-PAGE underlined the result of the HP-SEC that only slight dimer formation took place at  $22 \pm 3$  °C. It further specified that at least some of the soluble dimeric species were covalently linked, not exclusively via intermolecular disulfide bridging.

Related to their positioning within the native conformation of the cytokine, three out of four methionine residues are sensitive towards oxidation, as detected in previous studies (unpublished data) and described by Orru et al. [61]. Within 52 weeks, the amount of oxidized cytokine detected via RP-HPLC increased by 2.1 % (air) and 1.6 % (N<sub>2</sub>) for the samples stored at  $22 \pm 3$  °C. Upon storage at  $5 \pm 3$  °C the level of oxidized protein augmented by 0.9 % for the samples with air headspace and by 0.8 % for those with N<sub>2</sub>. Thus, the use of nitrogen in the headspace decreased the oxidation rate of the cytokine at room temperature, but did not affect the more slowly progressing oxidation at  $5 \pm 3$  °C.

The secondary and tertiary structure of the reconstituted cytokine was analyzed by several spectroscopic methods, including FT-IR, intrinsic protein fluorescence and 2<sup>nd</sup>-derivative UV spectroscopy, as recommended by Baudys and Kim [62]. Besides the wide application of FT-IR techniques to protein solutions, e.g. high-concentration liquid formulations [63], the method is used to investigate changes in the native secondary structure during various manufacturing processes of solid protein formulations, such as lyophilization [29], spray drying [64] or incorporation in particulate delivery systems [65], as reviewed by van de Weert and Joergesen [66]. Intrinsic fluorescence spectroscopy and 2<sup>nd</sup>-derivative UV spectroscopy enables the monitoring of conformational changes in the tertiary protein structure. None of these spectroscopic techniques revealed changes in secondary or tertiary structure of the reconstituted cytokine in our long-term stability study. Hence, independent of the conditions, storage over 52 weeks did not impact the conformational structure of the cytokine formulated as PCMCs. Moreover, the spectroscopic methods were not sensitive enough to be affected by the low cytokine aggregation level of 0.8-2.5 % identified via HP-SEC. In contrast, a dimer/oligomer content of 19-76 % resulted in conformational changes of recombinant human interferon beta recorded via 2<sup>nd</sup>-derivative UV spectroscopy [67].

In summary, the cytokine PCMCs provided high physicochemical protein stability over 52 weeks. Storage at  $5 \pm 3$  °C as opposed to  $22 \pm 3$  °C reduced the aggregation and oxidation rate of the cytokine, but both conditions appear suitable from commercial product perspective. The use of nitrogen headspace, compared to ambient air, is not required for room temperature storage.

#### **4.3.2 Carrier and morphology stability**

Besides protein stability, the carrier and morphology stability of PCMC formulations need to be addressed during long-term storage studies because they are often associated with each other. For example, a polymorphic transformation of glycine incorporated in mAb PCMCs at 25 °C/60 % RH which was detected via XRD and by structural changes in SEM, resulted in increased mAb aggregation [23]. Referring to the cytokine coated microcrystals, x-ray spectra of all samples recorded after 52 weeks of storage did not differ from the initial pattern. This indicated the absence of recrystallization processes of sucrose and citrate that were considered to be at least partially amorphous after the precipitation step. SEM pictures did not provide any

indication of excipient recrystallization or collapse either, proving high excipient and morphology stability of the PCMCs. However, it has to be taken into consideration that the cytokine PCMCs were not exposed to high moisture levels during storage.

#### **4.3.3 Comparison to lyophilized cytokine formulations**

The objective evaluation of the PCMC results requires stability data of other solid cytokine formulations for comparison. However, many formulations contain a multiple surplus of HSA that impedes the determination of the aggregation and oxidation level of the cytokine. Moreover, there are often differences in the design of the stability studies, e.g. storage time and conditions or analytical techniques applied, which make a direct comparison difficult.

The stability study conducted by Hawe and Friess on a hydrophobic cytokine included at least in parts comparable storage conditions and analytical methods [5]. Based on a low pH glycine buffer, they stored five liquid and five lyophilized HSA-free cytokine formulations. Within 6 months of storage the level of dimers and trimers in the lyophilisates, analyzed via HP-SEC, increased by about 0.3-0.7 % at 2-8 °C and up to 6.5 % at 25 °C/60 % RH, respectively, depending on the formulation. Formulated as PCMCs, the aggregation level of the cytokine augmented by 1.1-1.4 % at 22 ± 3 °C and by only about 0.4 % at 5 ± 3 °C within 52 weeks. According to Hawe and Friess, Met-oxidized cytokine formed as a function of storage temperature and time. In lyophilized samples stored at 2-8 °C the amount of oxidized protein, detected in RP-HPLC, enlarged by 1.4-2.4 %. Storage at 25 °C/60 % RH increased the oxidation level by 2.0-4.5 %. Consequently, storage at 2-8 °C was recommended. The cytokine coated microcrystals showed the same oxidation tendency as the lyophilisates studied by Hawe and Friess, but the increase in met-oxidized cytokine, 1.6-2.1 % at 22 ± 3 °C and 0.8-0.9 % at 5 ± 3 °C, was clearly lower for the PCMCs than for the lyophilized formulations, despite a twofold longer storage period. Thus, the PCMCs represent a good alternative towards those lyophilized cytokine formulations, with an improved long-term stability and the potential for storage at room temperature.

Several patents that claim cytokine lyophilisates also provide information on the stability of the formulations [38, 40, 41, 46, 49, 50]. In most cases a comparison between the stability of the PCMCs and the stability of the lyophilisates could not easily be drawn. WO 2012/071366 claims

that less than 10 % of the interferon-beta formulation is aggregated, fragmented or oxidized over an extended period of time, such as 12, 24 or 36 months or longer [38]. Furthermore, the biological activity is postulated to be within 10 % of the bioactivity exhibited at the time of preparation. The cytokine PCMC formulation met the first requirement, as only 4.9-7.4 % of the cytokine was aggregated, oxidized or fragmented after 52 weeks. The bioactivity of the cytokine PCMCs was not monitored over the storage time because, according to Geigert et al., it does not enable to accurately assess subtle changes of the protein as opposed to physicochemical analytical methods [68].

## 5 Conclusion

The basic mechanism of protein stabilization via PCMC technology is still unknown. Based on the high complexity of PCMC formulations in combination with the sophisticated manufacturing process, which can be divided into the three steps precipitation, concentration and supercritical drying, stabilizing effects can hardly be correlated to the presence of single carrier components. Nevertheless, the PCMC process was found to be very robust because all formulations showed good overall cytokine stability. Apart from the precipitation behavior and the morphology of the precipitates, only minor differences in protein process stability resulted between the eight cytokine PCMC formulations tested. Compared to glycine, the use of valine as main carrier component provided higher cytokine process stability. As the absence of NaCl in valine PCMCs increased the solubility of the cytokine, it further resulted in a decreased turbidity and an increased bioactivity of the formulation. Sucrose was found to reduce the aggregation level of cytokine valine PCMCs. The carrier combination of valine and sucrose in absence of NaCl (ValSuc-NaCl) also showed high bioactivity, equivalent to the biological activity of the standard lyophilized formulation. Thus, ValSuc-NaCl PCMCs were selected to investigate the storage stability over 52 weeks. The long-term stability study revealed a small increase in dimers (approx. 0.4 % at  $5 \pm 3$  °C and 1 % at  $22 \pm 3$  °C) as well as a slightly augmented level of oxidized species (approx. 1 % at  $5 \pm 3$  °C and 2 % at  $22 \pm 3$  °C). Irrespective of the storage conditions, the secondary and tertiary structure of the cytokine as well as the particle morphology was not altered. SEM analysis revealed the presence of larger rosette-shaped crystals beside smaller less compact material, assumed to be composed of protein and amorphous sucrose and citrate.

Compared to lyophilized formulations of the cytokine, the PCMC technology provided overall very good protein stabilization and therefore represents a promising alternative to lyophilization for the manufacturing of stable HSA-free formulations of the hydrophobic cytokine.

## 6 References

1. Tayal, V. and Kalra, B.S., *Cytokines and anti-cytokines as therapeutics - An update*. European Journal of Pharmacology, 2008. **579**(1-3): p.1-12.
2. Hawe, A. and Friess, W., *Formulation development for hydrophobic therapeutic proteins*. Pharmaceutical Development and Technology, 2007. **12**(3): p.223-237.
3. Lin, L.S., Kunitani, M.G., and Hora, M.S., *Interferon- $\beta$ -1b (Betaseron®): A model for hydrophobic therapeutic proteins*, in *Formulation, Characterization, and Stability of Protein Drugs*, Pearlman, R. and Wang, J.Y., editors. 1996. New York: Plenum Press. p.275-301.
4. Shire, S.J., Shahrokh, Z., and Liu, J., *Challenges in the development of high protein concentration formulations*. Journal of Pharmaceutical Sciences, 2004. **93**(6): p.1390-1402.
5. Hawe, A. and Friess, W., *Development of HSA-free formulations for a hydrophobic cytokine with improved stability*. European Journal of Pharmaceutics and Biopharmaceutics, 2008. **68**(2): p.169-182.
6. Ruiz, L., et al., *Influence of packaging material on the liquid stability of interferon- $\alpha$ 2b*. Journal of Pharmacy and Pharmaceutical Sciences, 2005. **8**(2): p.207-216.
7. Wang, W., *Lyophilization and development of solid protein pharmaceuticals*. International Journal of Pharmaceutics, 2000. **203**(1-2): p.1-60.
8. *Rote Liste® Online*. Bundesverband der Pharmazeutischen Industrie (BPI), Verband Forschender Arzneimittelhersteller (VFA), accessed June 22, 2012. Available from: [www.rote-liste.de/online](http://www.rote-liste.de/online).
9. Mead, D., Pearson, D., and Devine, M., *Recombinant human albumin: applications as a biopharmaceutical excipient*. Innovations in Pharmaceutical Technology, 2007(22): p.42-44.
10. van Beers, M.M.C., Jiskoot, W., and Schellekens, H., *On the role of aggregates in the immunogenicity of recombinant human interferon beta in patients with multiple sclerosis*. Journal of Interferon & Cytokine Research, 2010. **30**(10): p.767-775.
11. Moore, B.D., et al., *Rapid dehydration of proteins*. WO00/69887, 2000.

12. Moore, B.D., et al., *Pharmaceutical composition*. US2006/0292224, 2006.
13. Kreiner, M.M., Moore, B.D., and Parker, M.C., *Enzyme-coated micro-crystals: A 1-step method for high activity biocatalyst preparation*. Chemical Communications, 2001: p.1096-1097.
14. Kreiner, M. and Parker, M.C., *Protein-coated microcrystals for use in organic solvents: Application to oxidoreductases*. Biotechnology Letters, 2005. **27**(20): p.1571-1577.
15. Kreiner, M.M., et al., *Stability of protein-coated microcrystals in organic solvents*. Journal of Molecular Catalysis B: Enzymatic, 2005. **33**: p.65-72.
16. König, C., *Entwicklung eines Prozesses in Pilotgröße zur Herstellung von Protein-coated Microcrystals* [dissertation]. Bonn: Universität Bonn, 2010.
17. Vos, J., *Understanding the formation mechanism of protein coated microcrystals* [dissertation]. Glasgow: University of Strathclyde, 2006.
18. Partridge, J., Lyle, C., and Moore, B.D., *Protein coated microcrystals dry powder formulations with payloads of 30 % w/w to 0.01 % w/w*. AAPS National Biotechnology Conference. 2007. San Diego, CA, USA.
19. Partridge, J., et al., *Stabilization of proteins in dry state without sugars*. AAPS National Biotechnology Conference. 2005. Nashville, TN, USA.
20. Kreiner, M., et al., *DNA-coated microcrystals*. Chemical Communications, 2005(21): p.2675-2676.
21. Mahler, H.C., et al., *Behaviour of polysorbate 20 during dialysis, concentration and filtration using membrane separation techniques*. Journal of Pharmaceutical Sciences, 2008. **97**(2): p.764-774.
22. *(S)-(+)-Asparaginsäure zur Synthese*. Merck KGaA, accessed June 28, 2012. Available from: [http://www.merckmillipore.com/germany/chemicals/s-plus-asparaginsaeure/MDA\\_CHEM-816003/p\\_w6b.s1LNvwAAAEWioEfVhTI?attachments=MSDS](http://www.merckmillipore.com/germany/chemicals/s-plus-asparaginsaeure/MDA_CHEM-816003/p_w6b.s1LNvwAAAEWioEfVhTI?attachments=MSDS).
23. König, C., et al., *Development of a pilot-scale manufacturing process for protein-coated microcrystals (PCMC): Mixing and precipitation – Part I*. European Journal of Pharmaceutics and Biopharmaceutics, 2012. **80**(3): p.490-498.
24. *Clarity and degree of opalescence of liquids*, in *European Pharmacopoeia*. 2005. Stuttgart: Deutscher Apotheker Verlag. p.27-29.
25. Meager, A. and Das, R.G., *Biological standardization of human interferon beta: Establishment of a replacement world health organization international biological standard for human glycosylated interferon beta*. Journal of Immunological Methods, 2005. **306**(1–2): p.1-15.

26. Runkel, L., et al., *Structural and functional differences between glycosylated and non-glycosylated forms of human interferon- $\beta$  (IFN- $\beta$ )*. *Pharmaceutical Research*, 1998. **15**(4): p.641-649.
27. Tian, F., et al., *Spectroscopic evaluation of the stabilization of humanized monoclonal antibodies in amino acid formulations*. *International Journal of Pharmaceutics*, 2007. **335**(1-2): p.20-31.
28. Meyer, J.D., et al., *Infrared spectroscopic studies of protein formulations containing glycine*. *Journal of Pharmaceutical Sciences*, 2004. **93**(5): p.1359-1366.
29. Dong, A., et al., *Infrared spectroscopic studies of lyophilization- and temperature-induced protein aggregation*. *Journal of Pharmaceutical Sciences*, 1995. **84**(4): p.415-424.
30. Lahav, M. and Leiserowitz, L., *The effect of solvent on crystal growth and morphology*. *Chemical Engineering Science*, 2001. **56**(7): p.2245-2253.
31. Izutsu, K.-i., et al., *Stabilization of protein structure in freeze-dried amorphous organic acid buffer salts*. *Chemical and Pharmaceutical Bulletin*, 2009. **57**(11): p.1231-1236.
32. Lueckel, B., et al., *Effects of formulation and process variables on the aggregation of freeze-dried interleukin-6 (IL-6) after lyophilization and on storage*. *Pharmaceutical Development and Technology*, 1998. **3**(3): p.337-346.
33. Dani, B., Platz, R., and Tzannis, S.T., *High concentration formulation feasibility of human immunoglobulin G for subcutaneous administration*. *Journal of Pharmaceutical Sciences*, 2007. **96**(6): p.1504-1517.
34. Schüle, S., et al., *Stabilization of IgG1 in spray-dried powders for inhalation*. *European Journal of Pharmaceutics and Biopharmaceutics*, 2008. **69**(3): p.793-807.
35. Jovanović, N., et al., *Stable sugar-based protein formulations by supercritical fluid drying*. *International Journal of Pharmaceutics*, 2008. **346**(1-2): p.102-108.
36. Davidson, K.A., *Protein refolding via immobilisation on crystal surfaces* [dissertation]. Glasgow: University of Glasgow, 2008.
37. Zhang, M.Z., et al., *A new strategy for enhancing the stability of lyophilized protein: The effect of the reconstitution medium on keratinocyte growth factor*. *Pharmaceutical Research*, 1995. **12**(10): p.1447-1452.
38. Brader, M. and Vaidya, A., *Stable preserved compositions of interferon-beta comprising phenol and a stabilizer*. WO2012/071366, 2012.
39. Akagi, Y., Miura, Y., and Hoshino, T., *Stable  $\gamma$ -interferon composition*. EP0168008, 1986.
40. McCaman, M., Ottoboni, S., and Pungor, E., *Human interferon- $\beta$  formulations*. WO03/006053, 2003.

41. Wang, W., Nayar, R., and Shearer, M.A., *Stabilized formulations of interleukin 2*. WO02/00243, 2002.
42. Arakawa, T., et al., *Biotechnology applications of amino acids in protein purification and formulations*. *Amino Acids*, 2007. **33**(4): p.587-605.
43. Lange, C. and Rudolph, R., *Suppression of protein aggregation by L-arginine*. *Current Pharmaceutical Biotechnology*, 2009. **10**(4): p.408-414.
44. Shikari, K., et al., *Biophysical effect of amino acids on the prevention of protein aggregation*. *Journal of Biochemistry*, 2002. **132**(4): p.591-595.
45. Tsumoto, K., et al., *Review: Why is Arginine Effective in Suppressing Aggregation?* *Protein and Peptide Letters*, 2005. **12**(7): p.613-619.
46. Shirley, B.A., et al., *HSA-free formulations of interferon-beta*. US2008/0193415, 2002.
47. Samaritani, F. and Del Rio, A., *Stabilized interferon liquid formulations*. WO2005/117949, 2005.
48. Dibiasi, M.D., et al., *Stable liquid interferon formulations containing an amino acid as stabilizing agent*. WO98/28007, 1998.
49. Kwan, H.K.H., *Stabilized interferon formulations*. EP0082481, 1983.
50. Kwan, H.K. and Summit, N.J., *Biologically stable alpha-interferon formulations*. US4496537, 1985.
51. Mattern, M., et al., *Formulation of proteins in vacuum-dried glasses. II. Process and storage stability in sugar-free amino acid systems*. *Pharmaceutical Development and Technology*, 1999. **4**(2): p.199-208.
52. Zhao, H. and Topp, E.M., *Recent U.S. patents on protein drug formulation: 2000-2007*. *Recent Patents on Drug Delivery and Formulation*, 2008. **2**(3): p.200-208.
53. Mattern, M. and Winter, G., *Method and preparations for stabilizing biological materials by drying methods without freezing*. US7172999, 2007.
54. Mahler, H.C., et al., *Protein aggregation: Pathways, induction factors and analysis*. *Journal of Pharmaceutical Sciences*, 2009. **98**(9): p.2909-2934.
55. Bondos, S.E. and Bicknell, A., *Detection and prevention of protein aggregation before, during, and after purification*. *Analytical Biochemistry*, 2003. **316**(2): p.223-231.
56. Mahler, H.-C., et al., *Induction and analysis of aggregates in a liquid IgG1-antibody formulation*. *European Journal of Pharmaceutics and Biopharmaceutics*, 2005. **59**(3): p.407-417.
57. Carpenter, J.F., et al., *Potential inaccurate quantitation and sizing of protein aggregates by size exclusion chromatography: Essential need to use orthogonal methods to assure*

- the quality of therapeutic protein products*. Journal of Pharmaceutical Sciences, 2010. **99**(5): p.2200-2208.
58. Arakawa, T., et al., *The critical role of mobile phase composition in size exclusion chromatography of protein pharmaceuticals*. Journal of Pharmaceutical Sciences, 2010. **99**(4): p.1674-1692.
  59. Bocian, W., et al., *Structure of human insulin monomer in water/acetonitrile solution*. Journal of Biomolecular NMR, 2008. **40**(1): p.55-64.
  60. Philo, J., *Is any measurement method optimal for all aggregate sizes and types?* AAPS Journal, 2006. **8**(3): p.E564-E571.
  61. Orru, S., et al., *Structural analysis of modified forms of recombinant IFN- $\beta$  produced under stress-simulating conditions*. Biological Chemistry, 2000. **381**(1): p.7-17.
  62. Baudys, M. and Kim, S.W., *Peptide and protein characterization*, in *Pharmaceutical formulation development of peptides and proteins*, Frokjaer, S. and Hovgaard, L., editors. 2000. London: Taylor & Francis. p.41-69.
  63. Matheus, S., Friess, W., and Mahler, H.-C., *FTIR and nDSC as analytical tools for high-concentration protein formulations*. Pharmaceutical Research, 2006. **23**(6): p.1350-1363.
  64. Schüle, S., et al., *Conformational analysis of protein secondary structure during spray-drying of antibody/mannitol formulations*. European Journal of Pharmaceutics and Biopharmaceutics, 2007. **65**(1): p.1-9.
  65. Fu, K., et al., *FTIR characterization of the secondary structure of proteins encapsulated within PLGA microspheres*. Journal of Controlled Release, 1999. **58**(3): p.357-366.
  66. van de Weert, M. and Joergensen, L., *Infrared spectroscopy to characterize protein aggregates*, in *Analysis of Aggregates and Particles in Protein Pharmaceuticals*, Mahler, H.C. and Jiskoot, W., editors. 2012. Hoboken: John Wiley & Sons. p.227-248.
  67. van Beers, M.M.C., et al., *Oxidized and aggregated recombinant human interferon beta is immunogenic in human interferon beta transgenic mice*. Pharmaceutical Research, 2011. **28**(10): p.2393-2402.
  68. Geigert, J., et al., *The long-term stability of recombinant (serine-17) human interferon- $\beta$* . Journal of Interferon Research, 1988. **8**(4): p.539-47.

## 7 Appendix: supplementary material

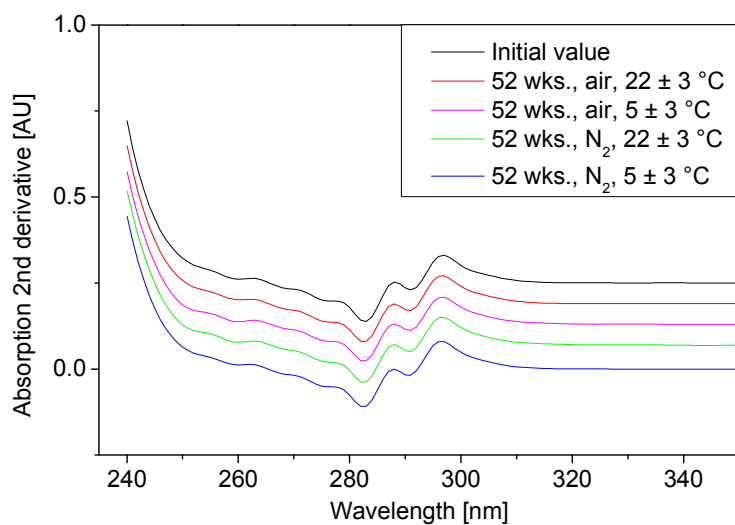


**Figure 2-9: 2<sup>nd</sup>-Derivative UV spectra of ValSuc-NaCl PCMCs after separation from carrier components in long-term stability study; arbitrary offset for better comparison.**

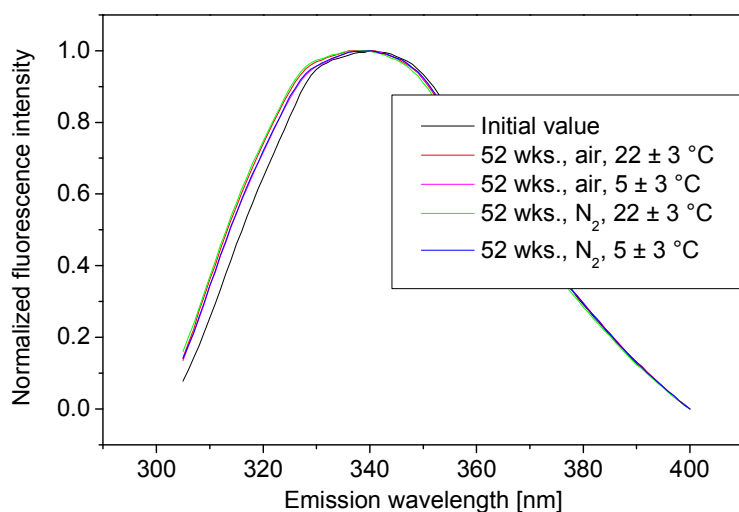


**Figure 2-10: Intrinsic fluorescence spectra of ValSuc-NaCl PCMCs after separation from carrier components in long-term stability study.**



## Chapter 3

# Formulation of a therapeutic monoclonal antibody via PCMC technology

This chapter is intended for publication:

K. Berkenhoff, V. Saller, V. Christ, S. Bassarab, K. Bechtold-Peters, W. Friess, Formulation of a therapeutic monoclonal antibody via PCMC technology; *in preparation*.

### Abstract

Protein-coated microcrystals (PCMCs) are formed upon rapid co-precipitation of a protein with carrier components after addition of an excess of organic anti-solvent. After concentration and supercritical drying of the resulting suspension the PCMCs provide protein stabilization in the solid state. In the current study, we applied the PCMC technology to a therapeutic monoclonal antibody (mAb2) and investigated the influence of each formulation component, including sodium chloride, glycine, histidine, phenylalanine and trehalose, on PCMC powder properties. Sodium chloride had positive effects on the manufacturability of PCMCs and prevented the antibody from the formation of insoluble protein particles. Glycine, histidine and trehalose elicited positive effects on the monomer content. Trehalose was further necessary to inhibit glycine crystallization and thus to achieve a homogenous and amorphous product. As no further benefits regarding PCMC product quality could be ascribed to the excipient phenylalanine, this component was excluded in the lead formulation to reduce the complexity of the system. The optimum protein loading of the lead formulation of around 50-62.5 % was derived from an accelerated short-term stability study conducted at 40 °C over 4-8 weeks. Higher protein load resulted in increased amounts of soluble aggregates detected via HP-SEC and SDS-PAGE. Alterations of the tertiary protein structure were not observed in 2<sup>nd</sup>-derivative UV and intrinsic fluorescence spectra. Overall, the mAb2 formulated as PCMCs provided good storage stability especially in comparison to corresponding liquid formulations. Besides

aggregation phenomena, these antibody solutions were prone to fragmentation that was successfully inhibited in PCMCs representing an effective way of protein stabilization in the solid state.

## 1 Introduction

The increasing importance of biopharmaceuticals on the pharmaceutical market is evident. According to VFA (Verband Forschender Arzneimittelhersteller e.V.) data, sales volume of biopharmaceuticals on the German market reached nearly 5.4 billion Euros in 2011 [1]. Nearly every fourth new licensed drug is currently a therapeutic protein [2]. Especially the class of monoclonal antibodies (mAbs) as therapeutics is of high interest because they are considered to be safe drugs due to their specific interactions with the body's own toolkit of proteins [3].

The major aspect addressed during formulation development of a new biological entity is the stabilization of the protein's structure and its monomeric state during storage to ensure drug efficacy and safety. It is known that proteins are more stable in the solid state than in aqueous solution [4]. The overall idea is that in the solid state the protein molecules' mobility is reduced [5, 6] and through the addition of excipients physical dilution and separation of protein molecules is achieved [7]. Thus, protein-protein interactions which are a prerequisite especially for aggregation are reduced. Nevertheless, chemical and physical instabilities can occur in the solid state as well [5, 8] and need to be studied during formulation development. To date, the most widely used technique to obtain solid-state biopharmaceuticals is freeze-drying [8]. Lyophilization results in elegant cakes that are reconstituted with aqueous media prior to parenteral application. With biopharmaceutical powders alternative delivery routes, e.g. pulmonary or intradermal delivery, can be addressed. Such powders can be obtained by methods like spray-drying, spray freeze-drying, pulverization, supercritical fluid drying or precipitation [4].

Benefits of the most commonly used techniques like freeze-drying and spray-drying are compromised by e.g. high acquisition costs and long process times. Therefore new methods for obtaining solid dosage forms of proteins are of interest. In this study, the innovative PCMC technology was employed to achieve pharmaceutically relevant powders. These so-called

protein-coated microcrystals are formed upon mixing an aqueous solution of protein and carrier with organic solvent in which the protein and carrier components co-precipitate due to low solubility [9]. An initial PCMC formulation development study for another monoclonal antibody (mAb1) resulted in a rather complex formulation containing several amino acids, a sugar and an inorganic salt component for mAb stabilization [10]. For future mAb product development, especially at early stages of development, a simplified platform technology would be of great benefit.

Therefore, in our study we transferred this initial PCMC formulation to another mAb (mAb2) and aimed at reducing the complexity of the system. By subsequent elimination of single excipients the influence of each formulation component on mAb2 process stability was to be elucidated. Protein content, aggregation (turbidity, HP-SEC) and potential changes in tertiary protein structure (2<sup>nd</sup>-derivative UV and intrinsic fluorescence spectroscopy) were monitored. Furthermore, the protein load of the optimal formulation was to be maximized in an accelerated short-term storage stability study because often high doses (several mg/kg) in low volumes are required in the treatment with antibody therapeutics [11]. High concentration liquid protein formulations are associated with challenges such as pronounced aggregation tendencies, high viscosity and poor overall stability [11]. The comparison between the optimized mAb2 PCMC formulation and liquid formulations of the antibody should reveal possible stability advantages and disadvantages of the PCMC technology.

## 2 Materials and methods

### 2.1 Materials

Chemicals employed during this study included glycine, L-histidine hydrochloride monohydrate, L-histidine, L-arginine (Ajinomoto OmniChem, Louvain-la-Neuve, B), disodium EDTA dihydrate, acetic acid 100 % (Merck, Darmstadt, D), trehalose dihydrate (Ferro Pfanstiehl, Waukegan, IL, USA), sodium chloride (Akzo Nobel, Hengelo, NL), polysorbate 20 (Croda, Nettetal, D), ammonium sulfate, sodium hydroxide, L-phenylalanine from non-animal source, isopropyl alcohol Chromasolv<sup>®</sup> for HPLC (Sigma-Aldrich, Steinheim, D), sodium dodecyl sulfate (Serva, Heidelberg, D), methanol (Avantor, Deventer, NL), dithiothreitol (Biomol, Hamburg, D) and

MOPS (3-(N-morpholino)-1-propanesulfonic acid) (Carl Roth, Karlsruhe, D). For pH adjustments, Titrisol® Hydrochloric acid 0.1 M (Merck, Darmstadt, D) and 85 % ortho phosphoric acid (Fluka, Buchs, CH) were used. The anti-solvent isobutanol (Emplura® quality) was purchased from Merck (Darmstadt, D). Carbon dioxide was procured from Sauerstoffwerk Friedrichshafen (Friedrichshafen, D). All chemicals were utilized without further purification.

The protein bulk drug substance composed of 10.1 mg/mL mAb2 in 25 mM citrate buffer pH 6.0 containing 115 mM sodium chloride and 0.2 mg/mL polysorbate 20 was provided by Boehringer Ingelheim.

## **2.2 Methods**

### **2.2.1 Preparation of protein solutions**

For the manufacturing of PCMCs, the buffer of the bulk drug substance was exchanged during ultra- and diafiltration resulting in a solution of 30-40 mg/mL mAb2, 40 mM histidine (formulation D no histidine), 20 mM trehalose dihydrate (formulation C no trehalose), 0.2 mg/mL Di-Na-EDTA dihydrate and approx. 0.7 mg/ml polysorbate 20 (crossflow buffer exchange and concentration unit, Boehringer Ingelheim, Biberach/Riss, D; membrane cassette PESU Sartocoon Slice, 30 kd, 0.1 m<sup>2</sup>, Sartorius, Göttingen, D; Quattroflow 150 S membrane pump, Quattroflow Fluid Systems, Hardegsen, D).

The preparation of liquid antibody formulations included 300fold buffer exchange (Slide-A-Lyzer® 20 K Dialysis Cassettes, Thermo Scientific, Rockford, IL, USA) of the protein bulk drug substance against 40 mM histidine buffer pH 5.5 containing 20 mM trehalose dihydrate and 0.2 mg/mL Di-Na-EDTA dihydrate at 22 ± 3 °C within 18 h, followed by concentration via centrifugation (Heraeus® Biofuge® primo, Carl Roth, Karlsruhe, D) in filtration units (Amicon® Ultra-15 Ultracel-30k, Millipore, Schwalbach, D) to 10, 50, 75 and 100 mg/mL protein. Samples were filtered through a 0.22 µm filter (73 mm, PES membrane, Millipore, Billerica, MA, USA).

### **2.2.2 PCMC production process**

The PCMC production process is divided into four main steps: preparation of protein-carrier solution, precipitation, concentration/solvent exchange, and drying. For the preparation of the protein-carrier solution, the carrier material was dissolved in water and the solution pH value

was adjusted to 5.5 prior to the addition of the protein solution. The composition of the protein-carrier solutions for the formulation screening with a consistent protein content of 43.6 % and approx. 0.2 mg/mL polysorbate 20 is presented in Table 3-1. Elimination of one or several components led to an increase of the relative amount of the remaining carrier components (glycine, phenylalanine, sodium chloride, trehalose dihydrate) to ensure a constant solid content of the protein-carrier solutions of 25.7 mg/mL. For the accelerated short-term stability study, the protein content of the formulations with a solid content of 51.4 mg/mL was in the range from 25 to 75 % resulting in varying amounts of carrier components and polysorbate 20 concentration of approx. 0.3-0.8 mg/mL (Table 3-2).

**Table 3-1: Composition of protein-carrier solutions in the formulation screening [% w/w].**

Excipient	Initial formulation	A (no phe)	B (no NaCl)	C (no tre)	D (no his)	E (no gly)	F (no gly/phe/NaCl)	G (no gly/phe)
mAb2	43.6	43.6	43.6	43.6	43.6	43.6	43.6	43.6
L-Histidine HCl monohydrate	2.6	2.6	2.6	2.6	--	2.6	2.6	2.6
L-Histidine	0.5	0.5	0.5	0.5	--	0.5	0.5	0.5
NaCl	5.2	5.4	--	12.2	5.5	7.4	--	7.8
Glycine	15.8	16.3	17.5	36.9	16.7	--	--	--
L-Phenylalanine	1.7	--	1.9	4.1	1.9	2.5	--	--
Trehalose dihydrate	30.5	31.5	33.8	--	32.3	43.3	53.2	45.4
Di-Na-EDTA dihydrate	0.1	0.1	0.1	0.1	0.1	0.1	0.1	0.1

**Table 3-2: Composition of protein-carrier solutions in the accelerated short-term storage stability study for optimization of protein load (PL) [% w/w].**

Excipient	25 % PL	37.5 % PL	50 % PL	62.5 % PL	75 % PL
mAb2	25.0	37.5	50.0	62.5	75.0
L-Histidine HCl monohydrate	2.6	2.6	2.6	2.6	2.6
L-Histidine	0.5	0.5	0.5	0.5	0.5
NaCl	7.3	6.0	4.8	3.5	2.2
Glycine	22.0	18.2	14.3	10.5	6.7
Trehalose dihydrate	42.5	35.1	27.7	20.3	12.9
Di-Na-EDTA dihydrate	0.1	0.1	0.1	0.1	0.1

The precipitation was carried out as described in detail by König [12]. Briefly, two equal streams of precipitating agent were mixed with one stream of protein-carrier solution in a small double jet impingement mixer of an inner diameter of 1.5 mm (Boehringer Ingelheim, Biberach/Riss, D). The mixing ratio of the precipitating agent, isobutanol saturated with all carrier components, and the protein-carrier solution was set to 95 : 5 (v/v). The modular mixing platform from Ehrfeld (Bayer Technology, Wendelsheim, D) encompassed three micro gear pumps (HNP pumps mzt 11507 and 7255, Hydraulik Nord Fluidtechnik, Parchim, D), pressure sensors and temperature sensors to monitor the precipitation step. The total flow rate of 1000 mL/min was controlled by the software LabView (National Instruments, Munich, D) and Coriflow mass flow meters (Bronkhorst, Kamen, D). The final suspension volume after precipitation was 2 L for the formulation screening and 4 L for the accelerated short-term storage stability study.

Solvent exchange was achieved by decanting the supernatant of the PCMC suspension 18 h after the precipitating step. The supernatant was replaced with fresh saturated isobutanol. After 24 h of sedimentation the sediment, i.e. the concentrated suspension, was used for the supercritical drying process (Thar SFE-500, Thar Technologies, Pittsburgh, PA, USA) with carbon dioxide at 100 bar and a flow rate of 25 g/min. After drying of 240 mL concentrated suspension within 90 min at 45 °C the pressure was decreased by 3 bar/min. Subsequently, vacuum drying of the PCMC powder was performed at 30 mbar and 40 °C for 2 h (APT.line™ VDL, Binder, Tuttlingen, D; diaphragm membrane pump MZ 2C, Vacuubrand, Wertheim, D).

### **2.2.3 Accelerated short-term storage stability study of PCMC powder**

Vials were filled with 120 mg PCMC powder with protein loading rates of 25 %, 37.5 %, 50 %, 62.5 % and 75 %, stoppered under lab atmosphere in the glove box, crimped and subsequently stored at 40 °C for eight (25 %, 50 % and 75 %) or four (37.5 % and 62.5 %) weeks (2 R Fiolax® vials, Schott, Mühlheim, D; Gusto C 1503 6720 GC grey 6 TP, Stelmi, Roissy Charles De Gaulle Cedex, France). PCMCs were analyzed for protein content, turbidity and monomer content directly after PCMC production ( $t_0$ ), after 7 ( $t_{7d}$ ), 14 ( $t_{14d}$ ), 28 ( $t_{28d}$ ) and 56 days ( $t_{56d}$ ). For formulations with loading rates of 25 %, 50 % and 75 % protein structure integrity was additionally monitored via 2<sup>nd</sup>-derivative UV scans, intrinsic fluorescence spectroscopy and SDS-PAGE analysis at  $t_0$  and after 28 and 56 days.

## 2.2.4 Accelerated short-term storage stability study of liquid mAb2 formulations

Under a laminar flow cabinet 2.0 mL of filtered mAb2 solutions with protein concentrations of 10, 50, 75 and 100 mg/mL were filled into autoclaved 2R vials which were subsequently closed with 13 mm stoppers and crimped for storage at 40 °C (2 R Fiolax® vials, Schott, Mühlheim, D; Gusto C 1503 6720 GC grey 6 TP, Stelmi, Roissy Charles De Gaulle Cedex, France). Analysis of protein concentration, turbidity and monomer content was performed at  $t_0$ ,  $t_{7d}$ ,  $t_{14d}$ , and  $t_{28d}$ . 2<sup>nd</sup>-derivative UV scans, intrinsic fluorescence spectroscopy and SDS-PAGE analysis were carried out at  $t_0$  and after 28 days.

## 2.2.5 Analysis of PCMCs

### 2.2.5.1 Turbidimetry

60 min after dissolution of PCMC powder with deionized water, turbidity was measured at a protein concentration of 1 mg/mL by 90° light scattering at  $\lambda = 633$  nm (UH turbidimeter, Boehringer Ingelheim, self-construction) and expressed in formazine nephelometric units (FNU). For turbidity measurement of liquid antibody formulations, undiluted protein solutions were employed. Mean values and standard deviations from three duplicates per formulation were calculated.

### 2.2.5.2 Protein concentration and protein recovery via UV measurement

PCMC powder was dissolved in deionized water to give a concentration of approx. 0.4 mg/mL to ensure absorption within the linear range of the spectrometer (0.3 to 0.8 AU). 60 min after reconstitution, the solution was filtered through a 0.45  $\mu$ m syringe filter (Rotilabo-Spritzenfilter steril 0.45  $\mu$ m PVDF, Carl Roth, Karlsruhe, D) to provide a particle-free sample. Liquid mAb2 formulations were diluted in deionized water resulting in a protein concentration of approx. 0.4 mg/mL. Absorption in Halfmicro Plastibrand® cuvettes (Brand, Wertheim, D) was measured at 279 nm based on an extinction coefficient of 1.72 with a Lambda 20 spectrometer (PerkinElmer, Rodgau-Jügesheim, D) and deionized water serving as blank. Protein recovery was calculated as the quotient of the antibody concentration in the sample to the theoretical protein concentration based on the antibody fraction in the total solid mass of the protein-carrier solution. Mean values and standard deviations from three triplicates per formulation were calculated.

### **2.2.5.3 Protein aggregation and fragmentation via high performance size exclusion chromatography (HP-SEC)**

60 min after reconstitution of PCMC powder in deionized water, the solution was filtered through a 0.45 µm syringe filter (Rotilabo-Spritzenfilter steril 0.45 µm PVDF, Carl Roth, Karlsruhe, D) and 50 µl samples of 2.0 mg/mL protein were injected in duplicate. Liquid mAb2 formulations were diluted with histidine buffer to give a final protein concentration of 10 mg/mL, filtered (0.45 µm) and injected (10 µl) in duplicate. Soluble protein aggregates, monomers and fragments were separated on an Äkta micro (GE Healthcare, Uppsala, S) with a TSKGel G3000 SWXL column (7.8 mm ID x 30.0 cm L, Tosoh, Stuttgart, D), equipped with a 40 x 6.0 mm TSKgel SWXL Guardcol precolumn. Filtered (0.22 µm) and degassed mobile phase with a pH of 7.3 consisted of 200 mM L-arginine, 120 mM ammonium sulfate and 10 % isopropanol in deionized water. At a flow rate of 0.5 mL/min UV detection was performed at 280 nm. Aggregation and fragmentation in percent was calculated based on the ratio of the area under the curve (AUC) of soluble aggregates and fragments to the total AUC of aggregates, monomer and fragments (n=2). Relative monomer content in % was defined in reference to the monomer content of the protein-carrier solution prior to precipitation which was set to 100 %.

### **2.2.5.4 Protein aggregation and fragmentation via SDS-PAGE**

SDS-PAGE was conducted at 200 V with Power Ease 500 and XCell Sure Lock in combination with 12 % Bis-Tris gels (NuPAGE®, 1 mm, 10 wells, Invitrogen, Darmstadt, D) and NuPAGE® MOPS SDS running buffer. Samples were mixed 8:2 with NuPAGE® LDS sample buffer, and 7:2:1 with NuPAGE® LDS sample buffer and 0.5 M dithiothreitol for the reducing SDS-PAGE. After heating up to 95 °C for 5 min, 5 µl of the samples and the marker (Precision Plus Protein Standard, Bio-Rad, Hercules, CA, USA), representing 1 µg protein, were loaded to each well. Furthermore, 2 ng BSA were loaded to one well for the purpose of sensitivity control. The gels were stained with SilverXpress® Silver Staining Kit. All equipment was from Invitrogen (Darmstadt, D).

### **2.2.5.5 Protein structure via intrinsic fluorescence spectroscopy**

Samples of 0.1 mg/mL protein in SUPRASIL® 114-QS precision cuvettes (10 mm, Hellma, Mühlheim, D) were excited at 295 nm and 25 °C and the emission was scanned from 305 nm

to 400 nm with a step size of 1 nm and 1 s integration time (Fluorimeter QM-4-CW, PTI, Birmingham, NJ, USA). The evaluation was based on normalized spectra (n=3).

#### **2.2.5.6 Protein structure via 2<sup>nd</sup>-derivative UV spectroscopy**

Samples, diluted to 0.3 mg/mL protein with deionized water, were scanned from 240 to 350 nm against deionized water as blank (UV/VIS Spectrometer Lambda 20, PerkinElmer, Rodgau-Jügesheim, D). The second derivative of the absorption was used (n=3).

#### **2.2.5.7 Quantification of trehalose by high performance liquid chromatography (HPLC)**

Lower molecular weight substances, such as trehalose and the amino acids, were separated from protein via centrifugation (Heraeus® Biofuge® primo, Carl Roth, Karlsruhe, D). The filtration units (Amicon® Ultra-0.5 Ultracel-10k, Millipore, Schwalbach, D) were rinsed with 0.5 mL 0.1 N NaOH and subsequently equilibrated with dissolved PCMCs containing 2 mg/mL mAb2 in deionized water at 12000 g for 10 min. 0.5 mL samples of dissolved PCMCs with 2 mg/mL protein were subsequently separated at 12000 g for 10 min. The filtrate was checked for protein residues via UV absorption and analyzed (2 x 40 µl) by HPLC using a Rezex RCM Monosaccharide Ca<sup>2+</sup> 300 x 7.80 mm column with guard column (SecurityGuard Cartridges Carbo-Ca 4 x 3.0 mm, Phenomenex, Torrance, CA, USA) at 85 °C. Filtered HPLC-water (Chromasolv® plus, Sigma-Aldrich, Steinheim, D) was used for elution at a flow rate of 0.6 mL/min. Detection was performed via changes in refractive index (RI). The trehalose RI signal between 5.5 and 6.9 mL was integrated and the trehalose content was calculated using the linear calibration curve for concentrations up to 4 mg/mL (n=3).

#### **2.2.5.8 Particle size via laser diffractometry (LD)**

The particle size was determined in suspension by laser diffractometry (OASIS equipped with HELOS/BF, CUVETTE CUV-50ML/US, SUCELL/M, SVA, Sympatec, Clausthal-Zellerfeld, D). PCMC powder or suspension was added until an optical concentration of about 5 % was reached in the cuvette that contained 50 mL of saturated isobutanol at a stirring intensity of 60 %. Based on Fraunhofer model the particle size distribution was calculated and expressed as volume distribution (Q<sub>3</sub>). The mean value was ciphered (n=3).

### **2.2.5.9 Particle morphology via scanning electron microscopy (SEM)**

Particle morphology of PCMC powder was analyzed by the use of a scanning electron microscope (Model Tescan Vega II SBH, Tescan, Brno, CZ). Samples were prepared on an aluminum stub and coated with gold/palladium (Model Cressington 108auto/SE Cool Sputter Coater, Cressington, Watford, GB).

### **2.2.5.10 Crystallinity via x-ray powder diffraction (XRD)**

The crystallinity of mAb2 PCMCs was analyzed with XRD in transmission mode from  $3^{\circ}$ - $40^{\circ}$   $2\theta$ ,  $0.5^{\circ}$  steps and 20 s/step based on  $1.5406 \text{ \AA}$  CuK $\alpha$ -radiation at 40 kV and 40 mA (Stoe, Darmstadt, D). Samples were fixed in the sample holder between two Ultraphan foils (cellulose diacetate) with a thickness of 0.014 mm (Stoe, Darmstadt, D).

### **2.2.5.11 Zeta potential measurement**

$\zeta$ -potentials of protein-carrier solutions of the initial formulation and formulation B (no NaCl) were measured with a Malvern Zetasizer nano ZS (Malvern Instruments, Malvern, UK). Measurements in folded capillary cell DTS 1060 cuvettes were performed in triplicates with a total of 100 single measurements per run at 20 °C.

## **3 Results and discussion**

### **3.1 Formulation screening**

Based on the initial formulation, the influence of each excipient on PCMC powder properties and mAb2 process stability was tested by elimination of single components as well as carrier combinations. The aim was to minimize the number of carrier components in order to reduce the complexity of the system while obtaining PCMC powders of high quality at the same time. PCMC powder was analyzed for particle size and morphology. Quality features with respect to protein process stability encompassed low turbidity values, high monomer contents, limited aggregate formation and preservation of tertiary mAb2 structure.

#### **3.1.1 Characterization of PCMC powder**

Based on their macroscopic appearance, mAb2 PCMC powders were subdivided into three groups (Table 3-3). Formulations that included both sodium chloride and trehalose (group 1)

resulted in smooth and voluminous, but agglomerated powders of poor flowability. As described by Chew and Chan, agglomerates are formed due to inherently strong cohesive forces between micro- or nanometer-sized particles [13]. Variations concerning the other components resulted in only minor changes concerning powder performance. Formulation D (no his) appeared slightly more compact and clumpy, whereas formulations E (no gly) and G (no gly/phe) revealed extremely poor flowability due to electrostatic particle interactions and adhesion to vial walls. Formulations B (no NaCl), F (no gly/phe/NaCl) and C (no tre), without sodium chloride or trehalose, differed from these PCMC powders. MAb2 PCMC powders lacking sodium chloride (group 2) were of granulous character with enhanced flowability. Formulation C (no tre) formed smooth, shiny needle-like crystals of poor flowability.

**Table 3-3: Macroscopic appearance of mAb2 PCMC powder in the formulation screening.**

Group	1	2	3
<b>Formulations</b>	Initial formulation, A (no phe), D (no his), E (no gly), G (no gly/phe)	B (no NaCl), F (no gly/phe/NaCl)	C (no tre)
<b>Macroscopic appearance</b>			
<b>Description</b>	smooth, voluminous, poor flowability, forms agglomerates	granulous, enhanced flowability	smooth, shiny, needle-like crystals, poor flowability

Visually detected differences between these three groups were also observed microscopically. Figure 3-1a shows a SEM image of formulation A representing all other formulations of group 1 which contained trehalose and sodium chloride. Spherical particles with an appearance similar to spray-dried products [4, 14, 15] were found. The surface of mAb2 PCMCs without sodium chloride appeared less crisp and rather molten (Figure 3-1b). The SEM image of the formulation without trehalose clearly showed large and crystalline saw-like structures (> 100  $\mu\text{m}$ ) next to smaller spherical particles (Figure 3-1c).

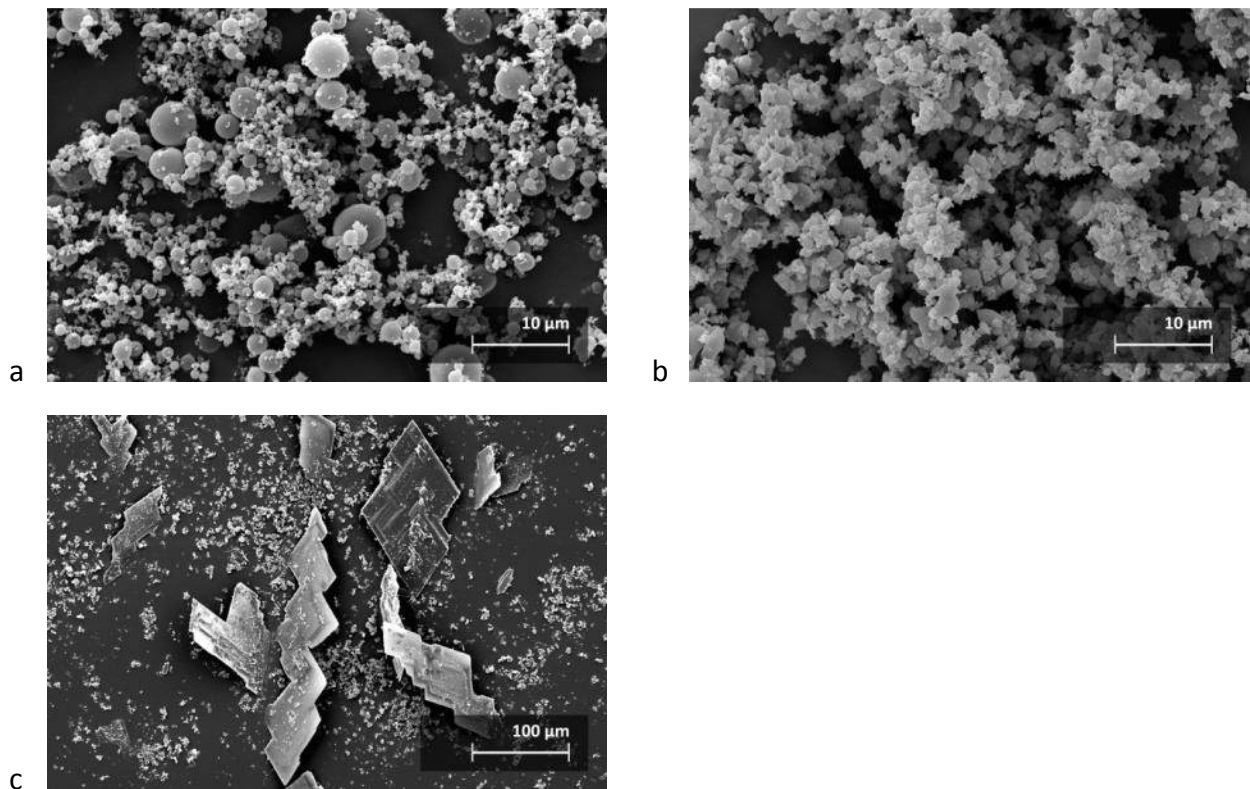


**Figure 3-1: SEM images of mAb2 PCMC powders of (a) formulation A (representing powders of group 1), (b) formulation B (representing powders of group 2) and (c) formulation C (group 3) in the formulation screening.**

The particle size of mAb2 PCMC powders containing trehalose and sodium chloride (group 1), determined via laser diffractometry, was smaller than that of group 2 and 3 (Figure 3-2). Moreover,  $x_{50}$  values gained from suspensions and PCMC powders of group 1 did not correlate because the particle size in suspension was bigger (3.7-5.8 µm) than in the final powder (1.9-2.0 µm). This effect was associated with the presence of particle agglomerates in the suspensions that were dispersed during the supercritical drying process.

Elimination of sodium chloride resulted in very small suspension particles of about 1 µm for formulation B (no NaCl) and F (no gly/phe/NaCl). These particles showed very poor sedimentation/concentrating behavior and, consequently, solvent exchange could not be performed before drying. The higher  $x_{50}$  values for the corresponding PCMC powders (B: 7.0 µm, F: 30.0 µm) were consistent with the granulous macroscopic appearance and were caused by compaction of the small suspended particles during the drying process. The assumption that sodium chloride may lead to an increase in particle size in suspension due to

shielding of repulsive electrostatic charges [16] could not be confirmed. Protein-carrier solutions of both the initial formulation and formulation B without sodium chloride had similar  $\zeta$ -potentials of 7 to 8 mV. Therefore, it is more likely that sodium chloride somehow acted as a nucleation enhancer during the PCMC formation process. Nucleation and growth as well as spinodal decomposition are possible particle formation mechanisms [16]. In short, the favored spinodal decomposition mechanism can be understood as a phase separation and partitioning process which is followed by crystallization. Vos also stated that salts enhanced binding of protein to PCMCs and should be of great benefit for the formulation of proteins with this technology [16].

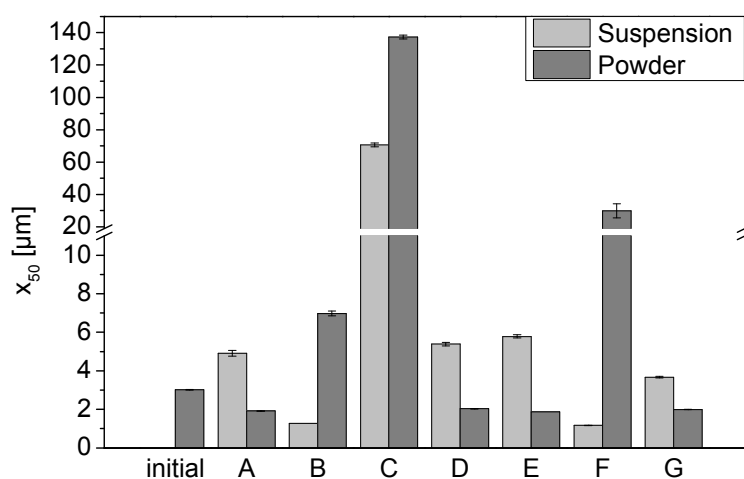


**Figure 3-2: Particle sizes of mAb2 PCMCs in suspension and powder as determined by LD measurements: A (no phe), B (no NaCl), C (no tre), D (no his), E (no gly), F (no gly/phe/NaCl), G (no gly/phe); particle size of PCMC suspensions was determined before solvent exchange.**

In accordance with macroscopic and microscopic observations, LD data confirmed the presence of large particles in formulation C that was prepared without trehalose. The continuous increase in particle size from approx. 71  $\mu\text{m}$  in suspension before the concentration/solvent exchange step to 103  $\mu\text{m}$  after concentration/solvent exchange and to 137  $\mu\text{m}$  after drying pointed to secondary particle growth during PCMC manufacturing (Figure 3-2). X-ray diffractometry of the PCMC powder revealed that the large crystals were made of  $\alpha$ -glycine (Figure 3-3). Glycine is a rapidly crystallizing amino acid [12] and poor glass former [6], but its crystallization could be inhibited by the addition of trehalose. Glycine usually precipitates as the kinetically controlled  $\beta$ -polymorph during the PCMC production process, but transition into  $\alpha$ -

glycine and finally the most stable  $\gamma$ -form occurs upon exposition to moisture [10]. With respect to mAb PCMCs, König reported that this transformation was accompanied by a loss of protein integrity [12]. Inhibition of glycine crystallization during lyophilization in the presence of trehalose was also reported by Chatterjee et al. [17]. In that case, the prevention of glycine crystallization required a weight ratio of glycine to trehalose dihydrate ratio of  $> 1$ . For mAb2 PCMCs, however, a weight ratio of glycine to trehalose dihydrate of 0.5 was sufficient to inhibit crystallization of the disaccharide.

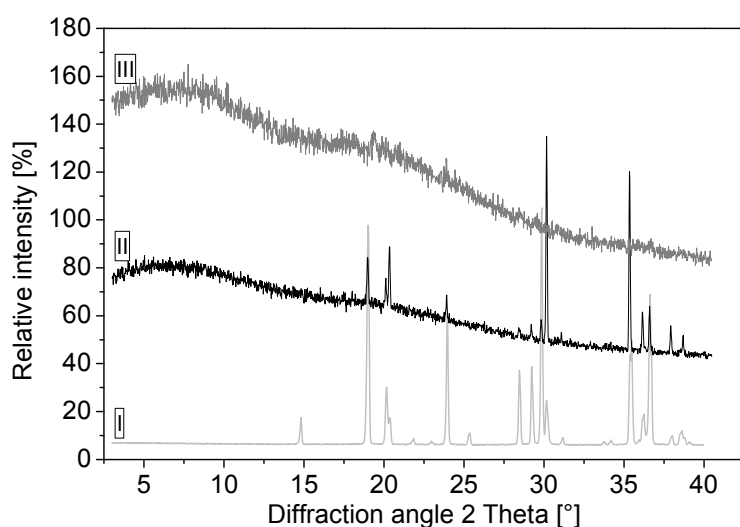


**Figure 3-3: XRD spectra of mAb2 PCMCs; spectrum assignment: I:  $\alpha$ -glycine; II: formulation C (no tre); III: initial formulation; arbitrary offset for better comparison.**

Rapid precipitation by anti-solvent addition is discussed as familiar route towards the amorphous state [6]. Although no traces of crystallinity were detected for the initial formulation in XRD analysis (Figure 3-3) and SEM images were similar to those of amorphous spray-dried products, not only an amorphous but also a microcrystalline state could be hypothesized for these PCMC powders. Attempts to determine glass transition temperatures with DSC and thus to confirm the amorphous state [18] for the initial formulation as well as formulations A (no phe), B (no NaCl) and F (no gly/phe/NaCl) failed. On the other hand, strong glass formers like proteins often show only very small changes in heat capacity at  $T_g$  and complex mixtures can lead to a broadening of the glass transition event due to nonidealities, so that detecting  $T_g$  can be difficult [19]. In any case, truly crystalline protein-coated microcrystals

as defined by the inventors of this technology [9] were not achieved with the present mAb2 formulation.

### 3.1.2 Protein process stability

Surfactants, such as polysorbate 20 and 80, frequently used in antibody formulation, are known to influence protein stability [20, 21]. With respect to mAb2 PCMCs, it has to be considered that these surfactants were assumed to be removed by the PCMC precipitation step due to their solubility in aliphatic alcohols [22], such as isopropanol, and that they were most likely not included in the final mAb2 powders.

The observation that PCMCs lacking trehalose or sodium chloride (formulations C, B, F) differed from all other formulations was confirmed by protein recovery, aggregation data and turbidity (Table 3-4). For formulation C (no tre), only 71.1 % of the theoretical mAb2 content based on complete precipitation was recovered in the PCMC powder, indicating incomplete precipitation of the antibody in the absence of trehalose. In HP-SEC, an increase of higher molecular weight species by 1.2 % to 1.6 % and of dimers by 2.6 % to 3.9 %, compared to the initial formulation of the antibody, was found when trehalose was omitted from the formulation. Moreover, the stabilizing effect of trehalose against protein aggregation was not limited to soluble protein species, as detected via turbidity measurement, which is frequently applied in formulation development and purification of therapeutic proteins to detect insoluble protein aggregates [23, 24]. A high turbidity value of 48.8 FNU was revealed in the absence of trehalose, opposed to 5.6 FNU for the initial formulation containing the disaccharide. Hence, trehalose prevented the antibody from the formation of insoluble protein particles during the PCMC manufacturing process. The augmented level of insoluble protein particles could also explain, at least partially, the reduced protein recovery because this protein fraction was assumed to be removed via filtration during sample preparation for UV measurement. Sugars in general, commonly used as stabilizers during lyophilization, are expected to physically stabilize the protein in the solid state either thermodynamically via formation of hydrogen bonds with the protein (water substitution hypothesis) or by a kinetic mechanism based on immobilization (glass dynamics hypothesis) [5]. Trehalose has successfully been introduced as stabilizing agent in a number of solid antibody dosage forms including lyophilisates [25, 26], spray-dried formulations [27, 28], spray freeze-dried particles [29] and protein powder generated via spray-drying in supercritical CO<sub>2</sub> [30].

Nevertheless, its superiority especially over sucrose is unproven, although addition of trehalose usually leads to higher  $T_g$  values which are considered to be beneficial for storage stability [6]. In the case of mAb2 PCMCs, the stabilizing effect of trehalose, representing an indispensable formulation component, was attributed to the formation of a glassy matrix discussed in section 3.1.1.

**Table 3-4: Protein recovery, monomers, dimers, higher molecular weight aggregates and turbidity of mAb2 PCMCs; \* PCMC powder B (no NaCl) and F (no gly/phe/NaCl) did not completely dissolve in deionized water, therefore turbidity could not be measured (n.m.) and the values of monomers, dimers and higher molecular weight aggregates refer to the soluble protein fraction.**

	Protein recovery [%]	Monomers [%]	Dimers [%]	Higher molecular weight aggregates [%]	Turbidity [FNU]
<b>Initial formulation</b>	129.2 ± 3.3	98.4 ± 0.1	1.3 ± < 0.1	0.4 ± < 0.1	5.6 ± 0.6
<b>A (no Phe)</b>	128.3 ± 3.4	99.0 ± < 0.1	1.0 ± < 0.1	< 0.1	13.5 ± 2.1
<b>B (no NaCl)*</b>	83.8 ± 2.6	98.8 ± 0.1	1.2 ± 0.1	< 0.1	n.m.
<b>C (no tre)</b>	71.1 ± 4.4	94.5 ± < 0.1	3.9 ± < 0.1	1.6 ± < 0.1	48.8 ± 2.5
<b>D (no his)</b>	132.9 ± 2.1	96.9 ± 0.1	2.2 ± 0.1	0.9 ± < 0.1	10.6 ± 2.0
<b>E (no gly)</b>	125.1 ± 3.0	97.3 ± 0.1	1.8 ± 0.1	0.9 ± < 0.1	5.5 ± 1.0
<b>F (no gly/phe/NaCl)*</b>	95.1 ± 3.0	98.7 ± 0.4	1.3 ± 0.4	< 0.1	n.m.
<b>G (no gly/phe)</b>	135.0 ± 1.0	96.3 ± < 0.1	2.1 ± < 0.1	1.6 ± < 0.1	4.5 ± 0.5

The absence of NaCl did not only affect the particle size and morphology of PCMCs, as discussed in section 3.1.1, but also mAb2 process stability (Table 3-4). The reduced protein recovery of 83.8 % (formulation B: no NaCl) and 95.1 % (formulation F: no gly/phe/NaCl) was caused by incomplete dissolution behavior of the powder in deionized water indicating the formation of insoluble protein particles. These particles were eliminated via filtration during sample preparation for UV measurement. Due to sedimentation of the particles, the aqueous suspension was not stable and thus turbidity could not be measured reliably. The level of soluble protein particles assessed via HP-SEC, however, was not influenced by the elimination of NaCl as the aggregate levels of both formulation B (no NaCl) and F (no gly/phe/NaCl) were not increased compared to the initial formulation. The AUC normalized to the protein concentration of the samples did not differ from the data of the initial formulation either.

Hence, NaCl was suggested to play a key role in the formulation of PCMCs because it prevented the antibody from forming substantial amounts of insoluble aggregates. Thus, NaCl could not be eliminated from the mAb2 formulation. Due to multiple mechanisms of interacting with protein molecules and of affecting protein-protein interactions, including preferential binding and charge-shielding effects, the use of salts can result in both stabilization and destabilization of protein formulations [31-33]. NaCl is included in many marketed antibody formulations representing either liquid or lyophilized dosage forms, as listed by Wang et al. and Daugherty and Mrsny [21, 34].

Amino acids are the excipients with the highest weight fraction in PCMCs. All formulations that lacked one (A, D, E) or two amino acids (G) showed a protein recovery ranging from 125.1 % to 135.0 % (Table 3-4), comparable to the initial formulation (129.2 %). These high values above 100 % indicated that the loss of carrier material during the PCMC production process was relatively more pronounced than a potential protein loss. HPLC analysis of the carrier fraction revealed that the high protein recovery was associated with significantly reduced trehalose contents. Exemplarily, trehalose recoveries were 87.4 and 84.5 %, respectively, for the initial formulation and formulation A (no phe). Incomplete precipitation was attributed to the trehalose concentration (8.1-13.7 mg/mL) in the protein-carrier solutions that was far below the solubility limit (50 g/L) of the disaccharide due to low total solid content of the solutions [35]. The level of both higher molecular weight aggregated species and dimers increased by 0.5-1.2 % and 0.5-0.9 % at the expense of monomers, when histidine, glycine or the combination of phenylalanine and glycine were omitted from the formulation. On the contrary, the elimination of only phenylalanine slightly reduced both the higher molecular weight aggregated species and the dimer amount. The turbidity of the formulations A (no phe) and D (no his), was slightly higher, with values of 13.5 FNU and 10.6 FNU, whereas for the formulations E (no gly) and G (no phe/gly) turbidity values (5.5 FNU and 4.5 FNU) similar to the initial carrier formulation were detected. Furthermore, the absence of histidine, acting as buffering agent, significantly increased the pH of reconstituted mAb2 PCMCs. Dissolving formulation D PCMCs (no his) in deionized water resulted in a pH value of 7.4, as opposed to pH 6.4-6.6 detected for all other completely soluble formulations (initial formulation, A, C, E, G). Thus, the pH of histidine-free formulations was governed by the pI of the antibody, being 7.8-8.4. Therefore, histidine buffer

was considered to be essential in the formulation of mAb2 PCMCs. This amino acid is reported to protect antibodies against aggregation and structural perturbation during lyophilization [36, 37]. Amongst the amino acid formulations investigated in their FTIR studies of a lyophilized monoclonal antibody, Tian et al. found histidine to be an effective amino acid in inhibiting changes in protein secondary structure [38]. Arakawa et al. speculated that the stabilizing effect of histidine during protein lyophilization is attributed to its tendency to become amorphous in combination with the ability of protein binding [39]. With respect to mAb PCMCs, histidine was also assumed to be amorphous after precipitation and subsequent supercritical drying because crystals were not seen in SEM nor did XRD analysis show any peaks.

Glycine is routinely used as co-freeze-drying excipient in protein formulations due to its ability to form a strong, porous and elegant cake structure in the final lyophilized product [25, 40]. As discussed in section 3.1.1, it exists in several polymorphous forms. During lyophilization, glycine had protective effects on antibody stability only if retained amorphous [37]. In the case of mAb2 PCMCs, glycine crystallized in the absence of trehalose resulting in significantly reduced monomer level, whereas amorphous glycine prevented the protein from aggregation and thus represented an obligatory component of the formulation.

Regarding the specific role of phenylalanine in protein formulations, Mattern et al. reported that arginine/phenylalanine glasses enhanced process and storage stability of vacuum-dried LDH and rhG-CSF and suggested that sugar-free amino acid formulations were potential stabilizers for proteins [41]. In the formulation development of mAb2 PCMCs, the elimination of phenylalanine resulted in a slightly higher absolute monomer content than in the initial formulation, but also in an increase in turbidity. For this reason, both formulations were further investigated in the course of an accelerated short-term stability study. The exclusion of phenylalanine would at least partially reduce the complexity of the mAb2 PCMCs. All other carrier components were needed to provide maximal protein process stability. Sodium chloride was necessary in terms of manufacturability and aggregation. The addition of trehalose as well as glycine and histidine were pivotal for protein stabilization towards aggregation, too.

### 3.1.3 Selection of the lead formulation via accelerated short-term storage stability study

A short-term stability study was conducted over eight weeks at 40 °C to identify potential differences between the initial formulation and formulation A (no phe) with a protein load of 50 % and a solid content of 51.4 mg/mL. Analysis of protein content, turbidity and monomer content was performed at  $t_0$ ,  $t_{7d}$ ,  $t_{14d}$ ,  $t_{28d}$  and  $t_{56d}$ . Moreover, tertiary protein structure was studied via 2<sup>nd</sup>-derivative UV and intrinsic fluorescence spectroscopy at  $t_0$  and after 28 and 56 days.

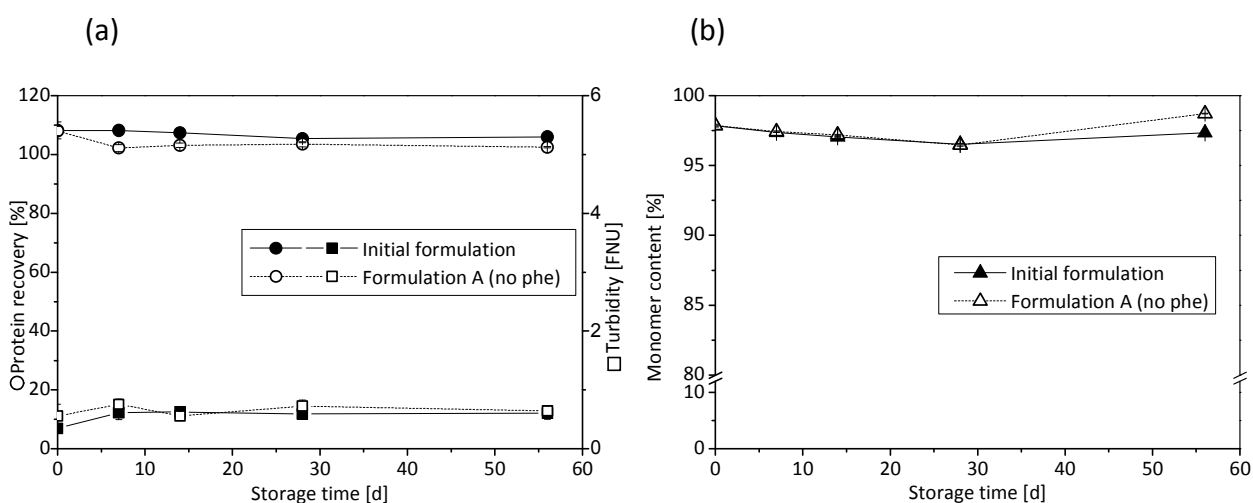


**Figure 3-4: (a) Protein recovery, turbidity and (b) monomer content of the initial formulation and formulation A (no phe) stored at 40 °C for 8 weeks.**

Protein content, turbidity values and monomer contents for both powders were comparable and constant during the course of the study (Figure 3-4). No differences in tertiary structure were detected at any time point. Thus, the elimination of phenylalanine did not have any detrimental effects on mAb2 PCMC powder storage stability, additionally to powder properties and protein process stability discussed in detail in sections 3.1.1 and 3.1.2. Based on these results, formulation A was subsequently chosen as lead formulation for further studies due to its reduced complexity.

## 3.2 Optimization of protein load via accelerated short-term storage stability study

Short-term stability studies are most commonly conducted at elevated temperatures as degradation rates usually increase with increasing temperature. The idea is that data analysis based on an Arrhenius' plot allows estimation of stability at ambient temperature [42]. Wang pointed out that such an extrapolation is generally problematic with antibodies due to the presence of complex and multiple degradation pathways which may have different degrees of temperature dependency [21]. Moreover, stability studies with amorphous solids should usually be carried out below the glass transition temperature of the formulation as degradation kinetics above  $T_g$  are not comparable to those below  $T_g$  [5, 43]. Based on standards defined by the World Health Organization (WHO), the aggregate level in commercial intravenous immunoglobulin products should not exceed 5 % upon administration [21]. This aggregate content must further be ensured over a shelf life of 18 months which is usually the minimum requirement for protein pharmaceutical products [7].

Accelerated short-term storage stability studies performed for mAb2 PCMCs were not intended to draw conclusions about room temperature stabilities, but aimed to identify the most stable PCMC composition more rapidly and clearly. To determine the optimal protein load, mAb2 PCMCs based on the lead formulation (section 3.1.3) with protein loadings of 25, 37.5, 50, 62.5 and 75 % were stored at 40 °C for either eight (25, 50 and 75 % protein load) or 4 weeks (37.5 and 62.5 %). PCMCs were analyzed for protein content, turbidity and monomer content at  $t_0$ ,  $t_{7d}$ ,  $t_{14d}$ ,  $t_{28d}$  and  $t_{56d}$ . For formulations with loading rates of 25, 50 and 75 %, protein structure and integrity were additionally monitored via 2<sup>nd</sup>-derivative UV scans, intrinsic fluorescence spectroscopy and SDS-PAGE analysis after 0, 28 and 56 days of storage. PCMC particle size and morphology were characterized directly after manufacturing. SEM pictures were additionally taken at  $t_0$  and after 4 weeks of storage to assess potential carrier and morphology instability.

### 3.2.1 Characterization of powder properties and morphology stability

Macroscopic evaluation of PCMC powders revealed that powders with low protein loadings (25 and 37.5 %) were very smooth and voluminous with relatively good flowability. With increasing protein content the powders were grainier and elicited worse flowability characteristics. At the

same time, in accordance with literature, laser diffractometry revealed decreasing particle size with increasing protein load (Figure 3-5a) [10, 16]. Furthermore, the bulk density of the powders increased as well (Figure 3-5b). This was consistent with the rather compact macroscopic appearance of the powder with a protein loading of 75 %. Usually, flowability correlates with particle size because with decreasing particle size interparticular attraction forces increase, causing agglomerate formation and reducing flowability [13].

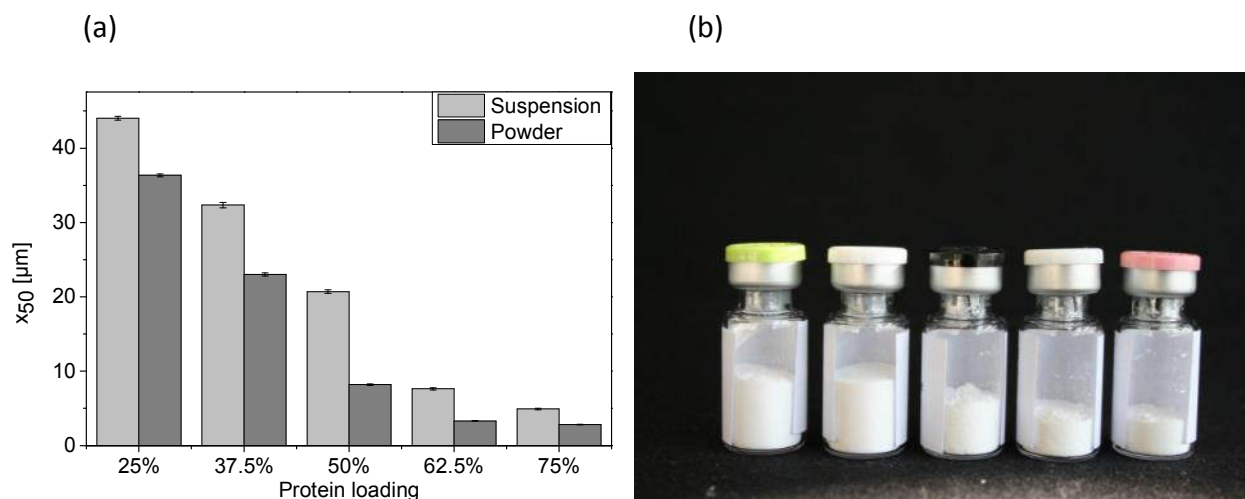


**Figure 3-5: MAb2 PCMCs (lead formulation) with varying protein load; (a) particle size via LD measurements; particle size of PCMC suspensions was determined after solvent exchange; (b) vials filled with 120 mg PCMC powder; from left to right: protein loading of 25 %, 37.5 %, 50 %, 62.5 % and 75 %.**

PCMCs with protein loadings of 25 %, 50 % and 75 % were further evaluated using scanning electron microscopy (Figure 3-6a-c). The samples with a protein loading of 25 % showed rather molten textures in comparison to the more crisp appearance of the samples with 50 % protein loading. As expected, the morphology of this latter sample was similar to the powders of group 1 during formulation screening (see section 3.1.1) because the lead formulation selected was allocated to this group and had a comparable protein load. Moreover, donut-shaped particles, also described for spray-dried antibody formulations [4, 15], were found within all samples, most pronounced in the powder with 75 % protein load (Figure 3-6c).

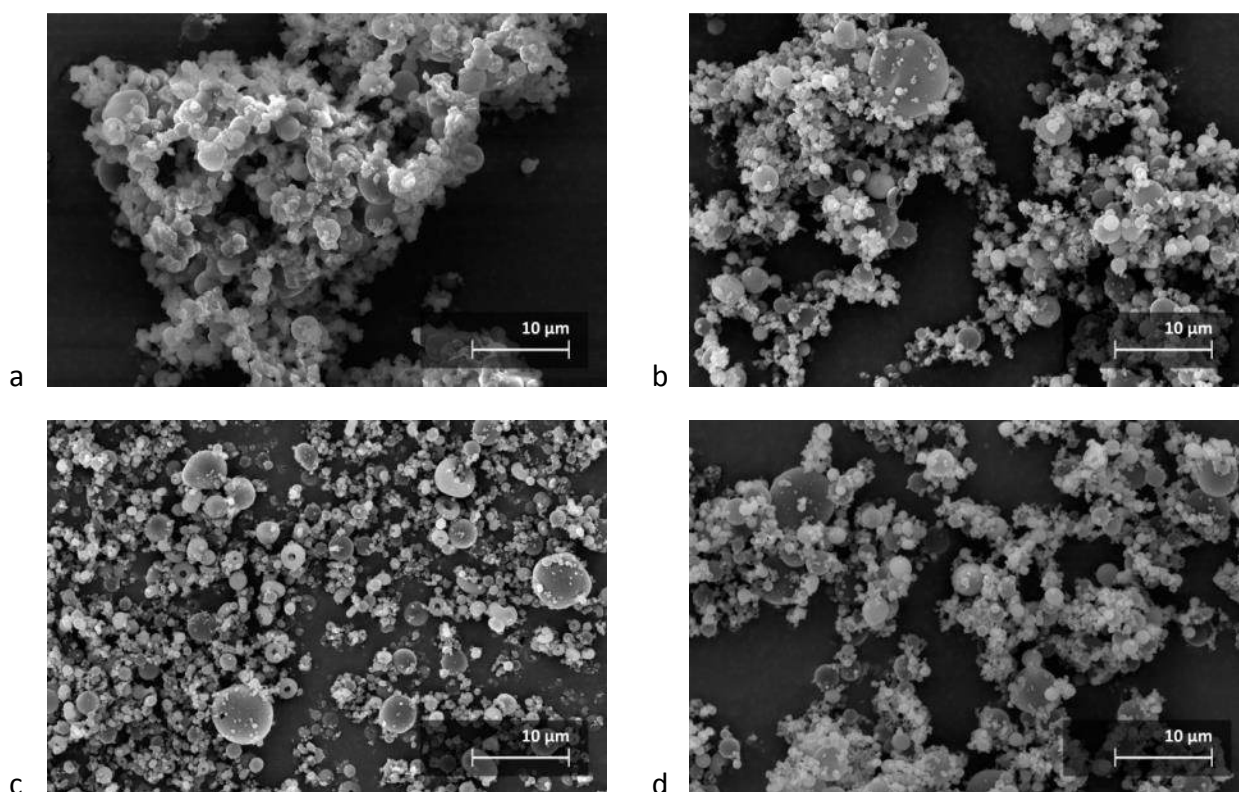


**Figure 3-6: SEM images of mAb2 PCMC powders (lead formulation) at (a-c)  $t_0$  with a protein loading of (a) 25 %, (b) 50 %, (c) 75 % and at (d)  $t_{28d}$  with a protein loading of 50 %.**

Besides protein stability, the carrier and morphology stability of PCMC formulations need to be addressed during accelerated short-term storage studies because they often correlate (see chapter 2 section 4.3.2). Referring to mAb2 coated microcrystals, SEM pictures taken after 4 week storage did not provide any indication of excipient recrystallization or collapse either, as exemplarily shown for the powder with 50 % protein load (Figure 3-6d).

### 3.2.2 Protein storage stability

As mentioned above, the most critical parameter that defines product shelf life of protein therapeutics is aggregation. Aggregation should be kept to a minimum as especially large, insoluble and irreversible aggregates are considered of being immunogenic [44, 45]. Turbidity measurements and visual inspection are the analytical methods of choice to detect large and insoluble particles, although they are not specific for protein aggregates [46]. The presence of detectable smaller and soluble aggregates in a formulation has to be seen as a warning for potential immunogenicity issues, too. Richard described such multimers as “the signature of aggregation-competent species” [45].

Apart from a slightly decreased protein recovery after seven days for protein loadings of 25 %, 50 % and 75 %, protein recovery was found to be consistent, irrespective of the protein content (Figure 3-7). A decrease in protein recovery might point to protein loss due to removal of large soluble and insoluble protein aggregates by sample filtration (0.45  $\mu\text{m}$ ) prior to UV measurements. However, aside from single fibers probably introduced during supercritical drying, the colorless samples were free from visible insoluble particles, as confirmed by turbidity measurement, and the AUC in HP-SEC was not impacted either (see below).

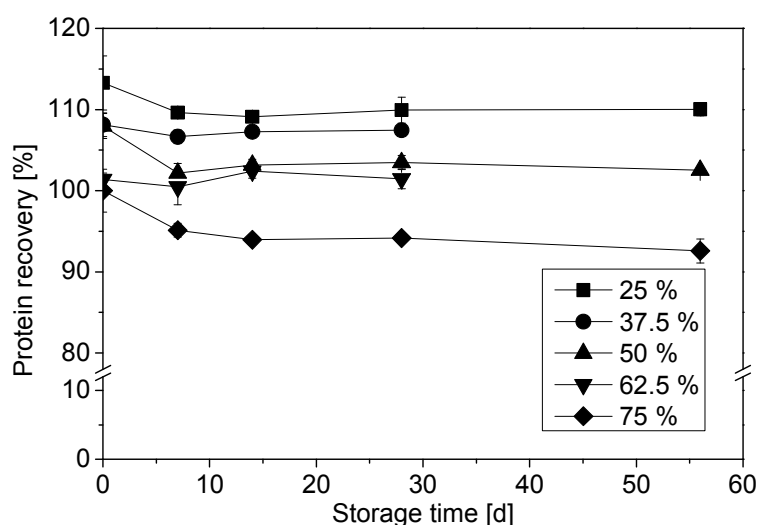


**Figure 3-7: Protein recovery of mAb2 PCMCs (lead formulation) with varying protein load stored at 40 °C.**

No significant increase in turbidity was detected after four and eight weeks of storage, respectively. Turbidity values for all samples were low, between 0.4 and 2.4 FNU (Figure 3-8). Thus, turbidity was significantly lower than that of reference suspension I of the European Pharmacopoeia which exhibits a value of 3 NTU and which indicates a clear solution [47]. Hence, independent of the protein load, all PCMC samples were free of larger amounts of insoluble protein aggregates.

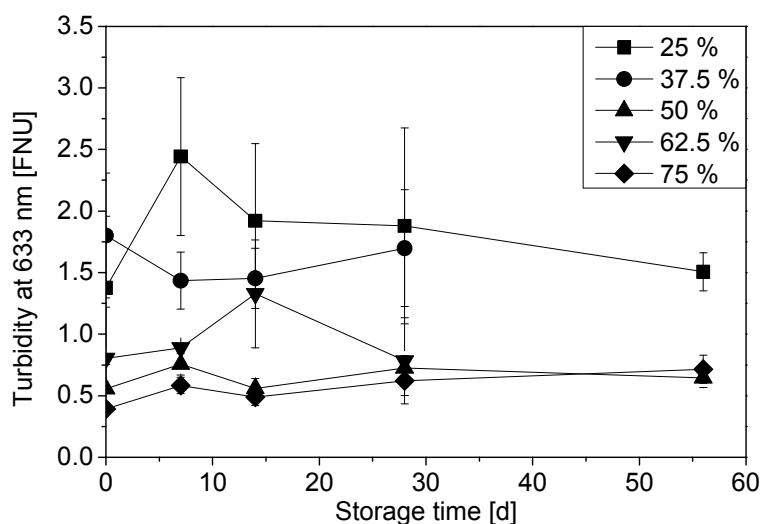


**Figure 3-8: Turbidity of mAb2 PCMCs (lead formulation) with varying protein load stored at 40 °C.**

Monomer content analysis via HP-SEC revealed significant differences in storage stability with respect to aggregation in dependence of protein loadings (Figure 3-9). Monomer degradation of samples with protein loadings of up to 62.5 % was minimal or not existent. Over 4 or 8 weeks storage, the monomer contents of these formulations varied only by maximal 1.3 %. Monomer loss was clearly more pronounced for PCMCs with a protein content of 75 %. A decrease by 3.7 % was detected within eight weeks. Thus, this formulation did not provide sufficient stability of the antibody with respect to the formation of soluble aggregates [48]. According to the HP-SEC results of the formulation screening (section 3.1.2), the decrease of the monomer content was associated with an increase in both higher molecular weight species and dimers for all samples investigated. Fragmentation of the antibody was not observed. The AUC normalized to the protein concentration of the samples was not affected, irrespective of protein load and storage time. Hence, all PCMC samples were free of significant amounts of larger soluble protein aggregates that are typically prone to be removed via filtration during sample preparation or to accumulate at the column top or precolumn [48].

Protein stability of other solid dosage forms, such as lyophilized products, was found to depend on the ratio between stabilizing excipient and protein [25, 26, 49]. For example, a specific molar ratio of sugar to protein of 360:1 was required to adequately stabilize rhuMab HER2 during lyophilization and storage against aggregation and deamidation [25]. Andya et al. reported that

the use of sucrose or trehalose prevented an IgG1 against aggregation during storage at 30 °C to a maximum degree when the ratio between sugar and protein was  $\geq 500$ . This number was approximately equivalent to the number of water-binding sites on the protein surface [26]. Based on the storage of an lyophilized IgG1 at 40 °C, Chang et al. even recommended a molar ratio of sucrose to protein of  $\geq 800:1$  to achieve a maximum of protection against chemical degradation and aggregation [49]. Relating to mAb2 PCMCs, the molar ratio between the main carrier component trehalose and protein varied from approx. 670:1 to 70:1. For a protein load of  $\geq 50\%$ , it was thus significantly smaller ( $\leq 220$ ) than the overall recommended ratio of  $\geq 360$ . However, reduced PCMC protein storage stability based on the formation of soluble aggregates was only revealed in the case of 75 % antibody load. This overall high protein stability against aggregation provided by the PCMC technology was attributed to the presence of additional carrier components acting as supplementary protein stabilizers, as discussed in section 3.1.

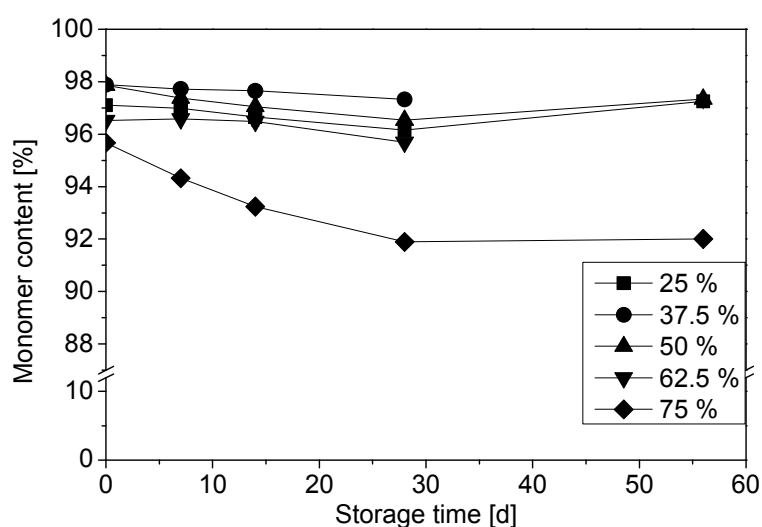


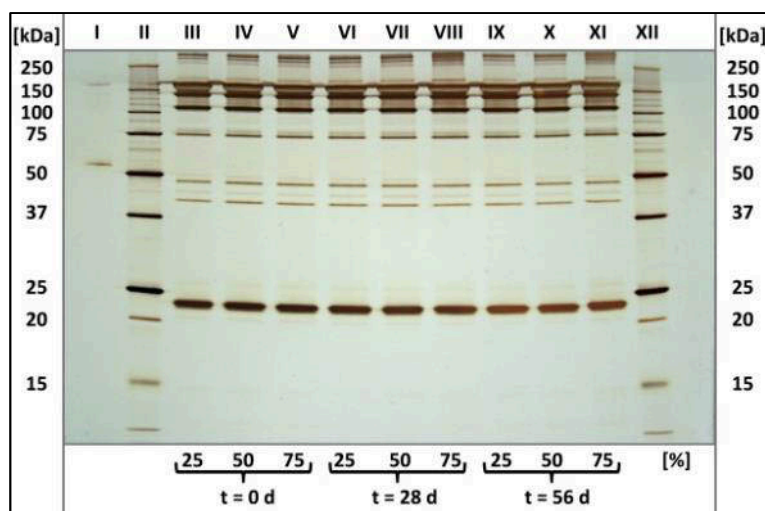
**Figure 3-9: Monomer content via HP-SEC of mAb2 PCMCs (lead formulation) with varying protein load stored at 40 °C.**

SDS-PAGE, representing an orthogonal method for the analysis of soluble protein aggregates [50], confirmed the HP-SEC results with a slight increase in aggregates for 75 % mAb2 loaded PCMCs (Figure 3-10). The aggregate band above 250 kDa under non-reducing conditions (gel a) in lanes VIII and XI was more pronounced than in all other lanes. Likewise, the band at about 100 kDa and 75 kDa under reducing conditions (gel b) was slightly darker in lanes VIII and XI. However, as silver stained bands cannot be quantified reliably, interpretation should mainly be

restricted to qualitative evaluation [50]. Extra bands indicating mAb2 degradation with prolonged storage time or increased protein loading were not detected. The band between 50 and 75 kDa in lane VI in gel (b) was attributed to some external contamination as it was not present in the eight-week sample or on the non-reduced gel and was not detected in SDS-PAGE analysis after four weeks either. No further differences between the samples with varying protein load were observed over 8 weeks storage. Under non-reducing conditions not only the intact antibody with a molecular weight of 150 kDa was detected, but aggregates (> 150 kDa) and fragments (< 150 kDa) were present as well. Fragments were not detected during HP-SEC analysis and therefore fragment levels were assumed to be very low. A closer look revealed that there was in fact more than one band at around 150 kDa. Similar observations have been ascribed to the heterogeneity of a purified antibody resulting from differences in glycosylation patterns, instability during production and terminal processing [21]. Bands in both gels with molecular weights of 100 kDa, 75 kDa, 50 kDa and 25 kDa were attributed to varying combinations of light and heavy chains. Light chains of IgGs have a molecular weight of 25 kDa and heavy chains are around 50 kDa [21]. The 25 kDa and 50 kDa bands were very strong under reducing conditions. Non-reducible aggregates were not detected because no aggregate band persisted under reducing conditions. Overall, all mAb2 PCMC samples were free of considerable amounts of soluble protein aggregates.

In 2<sup>nd</sup>-derivative UV spectroscopy the broad peak at  $\lambda = 240\text{-}300$  nm is composed of multiple overlapping spectra, including phenylalanine, tyrosine and tryptophan [51]. The calculation of a second derivative spectrum from UV scans is beneficial as it preserves and even highlights fine spectral differences initiated by vibrational transitions of the aromatic amino acid chains, but on the other side eliminates possible interferences related to the measuring system, the sample itself or external factors. Distinct spectral changes can be interpreted as conformational alterations of protein structure [52]. Similarly, in intrinsic fluorescence studies with an excitation wavelength of 295 nm tryptophan fluorescence emission, being very sensitive to conformational changes of a protein, can be selectively studied [53, 54]. Especially upon thermal denaturation the intensity of the fluorescence signal is evaluated [55].

(a)



(b)

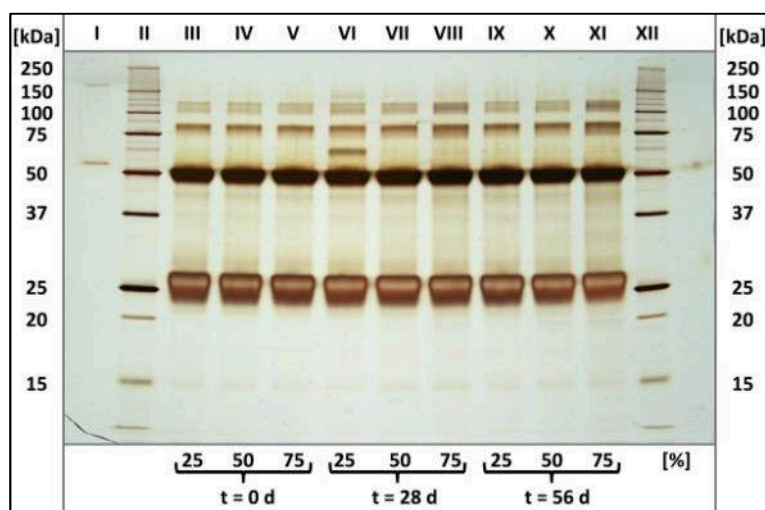


**Figure 3-10: SDS-PAGE of mAb2 PCMCs (lead formulation) with varying protein load stored at 40 °C for 28 and 56 days; (a) non-reducing and (b) reducing conditions; lane assignment: I: BSA control; II: Precision Plus Protein Standard; III-XI: reconstituted mAb2 PCMC samples with protein loading of 25 %, 50 % and 75 % ; XII: Precision Plus Protein Standard.**

For mAb2 PCMCs, no spectral differences in dependence of the protein load were found, as presented in Figure 3-11a and Figure 3-12a for  $t_0$ . Furthermore, 2<sup>nd</sup>-derivative UV scans and intrinsic fluorescence spectra did not reveal any conformational changes over time for any formulation (exemplarily shown for the lead formulation with a protein loading of 50 % in Figure 3-11b and Figure 3-12b). In general, it is believed that the formation of aggregates is accompanied by an alteration of protein structure due to unfolding. For mAb2 PCMCs with a

protein loading of 75 %, the small amount of soluble aggregates (3.7 %) determined via HP-SEC did not result in detectable changes of the tertiary protein structure probably because of limited sensitivity of the spectroscopic methods. The formation of non-denatured aggregate species has also been reported [56] as well as the formation of aggregates from protein molecules which only exhibited marginal local unfolding [7].

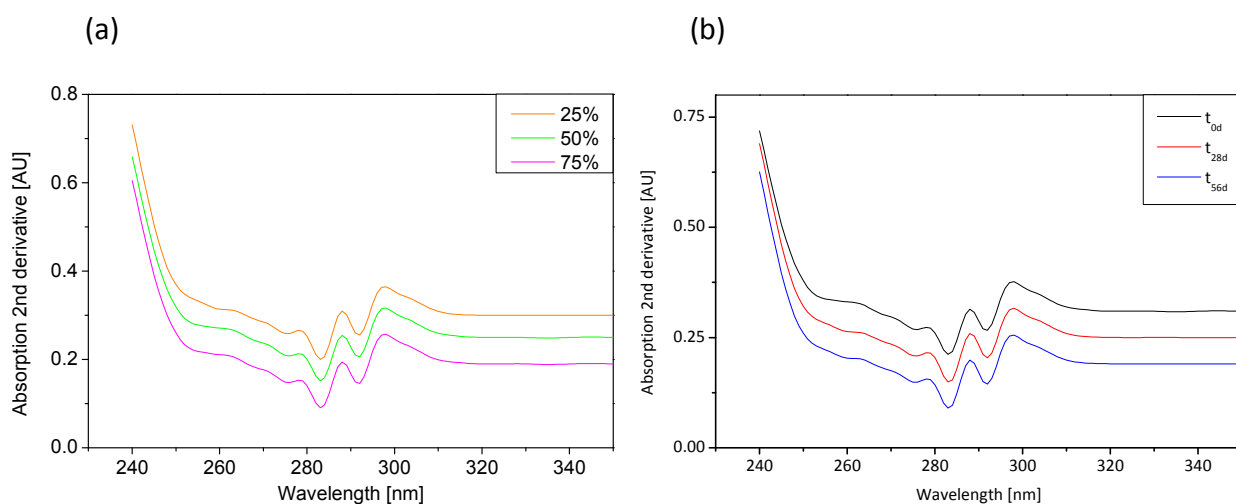


**Figure 3-11: 2<sup>nd</sup>-derivative UV analysis of mAb2 PCMCs (lead formulation) with (a) different protein loadings at  $t_0$  and (b) a protein loading of 50 % stored at 40 °C for 28 and 56 days; arbitrary offset for better comparison.**

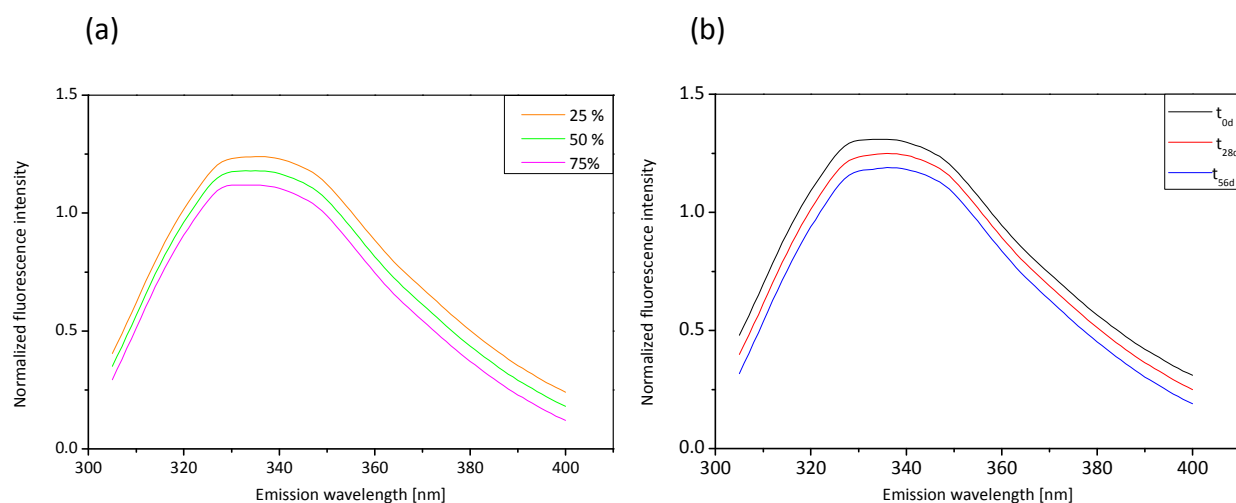


**Figure 3-12: Intrinsic fluorescence spectroscopic analysis of mAb PCMCs (lead formulation) with (a) different protein loadings at  $t_0$  and (b) a protein loading of 50 % stored at 40 °C for 28 and 56 days; arbitrary offset for better comparison.**

In summary, mAb2 PCMCs provided high physicochemical protein stability over 8 weeks at 40 °C. Apart from slightly increasing soluble aggregate levels at the highest protein loading, antibody degradation was not observed. No changes in protein tertiary structure or in powder morphology were detected. The augmented monomer loss for the formulation with a protein loading of 75 % indicated that a certain minimum proportion of excipients was necessary for effective stabilization of the protein during storage. Thus, the maximal protein load of this antibody formulation should not exceed 62.5 %, confirmed by considerations on protein process stability presented in section 3.2.3.

### 3.2.3 Considerations on protein process stability

Besides information on protein storage stability, some information on protein process stability could be derived from the data collected during the accelerated short-term storage stability study. Protein quantification revealed that protein recovery approached 100 % with increasing protein load (Figure 3-7). Relative loss of carrier decreased with increasing protein fraction although the amount of total carrier declined at the same time. Carrier solubility in the PCMC suspension medium was potentially reduced at higher protein concentrations and thus resulted in a more quantitative recovery of carrier components in the final PCMC powder. Furthermore, comparison of the initial relative monomer content related to the monomer content of the corresponding protein-carrier solution implied that the optimum process stability might be around 37.5-50 % protein load (Figure 3-13).

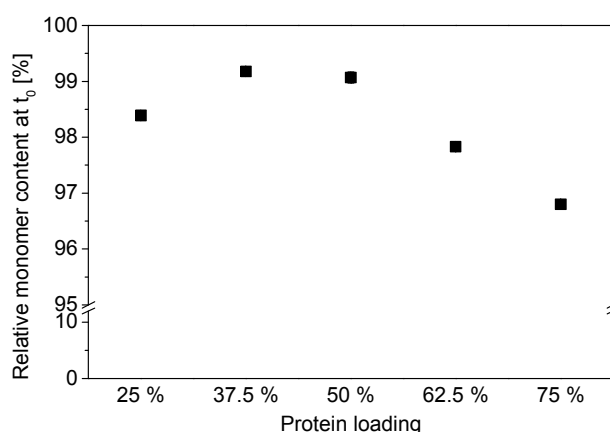


**Figure 3-13: Relative monomer content of mAb2 PCMCs (lead formulation) with varying protein loading at  $t_0$ .**

### 3.3 Comparison to liquid mAb2 formulations

An accelerated short-term storage stability study conducted at 40 °C over 4 weeks with four mAb2 solutions aimed to compare liquid formulation stability with the stability provided by the PCMC technology. The liquid formulations contained 10 mg/mL, 50 mg/mL, 75 mg/mL and 100 mg/mL protein in 40 mM histidine buffer pH 5.5 with 20 mM trehalose dihydrate and 0.2 mg/mL Di-Na-EDTA dihydrate. Analysis of protein concentration, turbidity and monomer content was performed at  $t_0$ ,  $t_{7d}$ ,  $t_{14d}$  and  $t_{28d}$ . Second derivative UV scans, intrinsic fluorescence spectroscopy and SDS-PAGE analysis were carried out at  $t_0$  and after 28 days.

Protein concentration of the different formulations was constant over time (Figure 3-14a). The slight turbidity increase by 6.2-10.1 FNU clearly indicated an increase in insoluble aggregates over time for protein solutions of 50 mg/mL, 75 mg/mL and 100 mg/mL (Figure 3-14b). This was in accordance to visual examinations. At  $t_0$  all formulations were clear and colorless. After 28 days at 40 °C all solutions stayed macroscopically clear, but only the formulation with 10 mg/mL remained colorless. The higher concentrated solutions had turned yellowish. This discoloration of liquid mAb formulations was confirmed by Stroop et al. who investigated fluorescent light photodegradation of a monoclonal antibody formulated in histidine buffer [57]. The exposure to yellowish photosensitizers extracted from photo-aged histidine buffer was further found to promote oxidation, fragmentation and aggregation of the antibody.

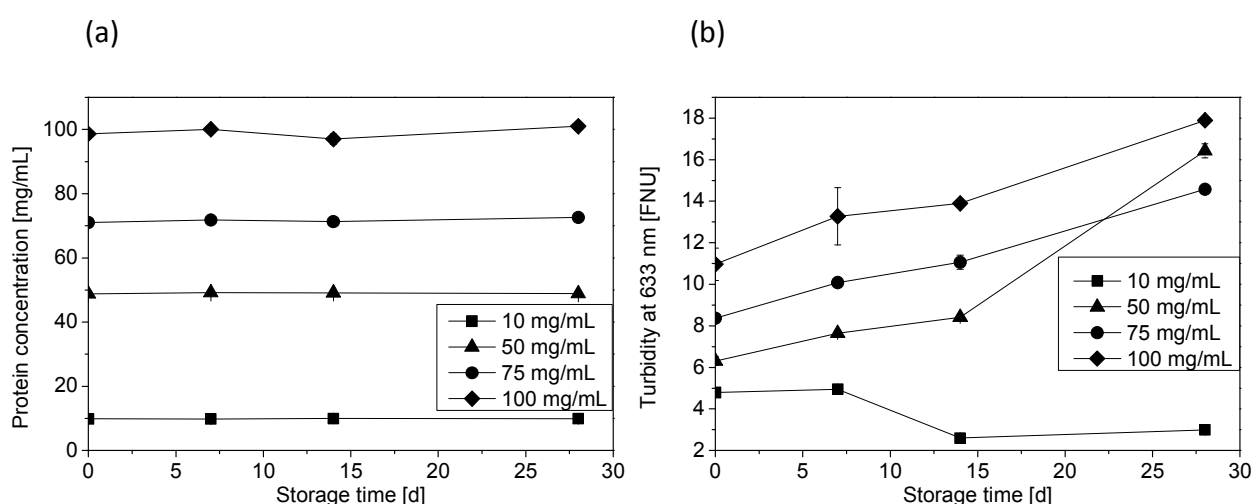


**Figure 3-14: Protein concentration (a) and turbidity (b) of liquid mAb2 formulations with 10, 50, 75 and 100 mg/mL protein stored at 40 °C for 4 weeks.**

Monomer loss depended on the protein concentration and was more pronounced for formulations with higher protein concentrations (Figure 3-15a). The monomer content of the formulation with 10 mg/mL protein decreased by less than 1 % from 98.7 % to 97.9 % within four weeks at 40 °C. The monomer content of the 100 mg/mL formulation was slightly lower at the beginning of the stability study and also decreased by 2.6 % from 98.5 % to 95.9 % over storage time. The monomer loss was mainly attributed to the formation of soluble protein dimers, as opposed to mAb2 PCMCs that additionally contained higher molecular weight aggregated species (Figure 3-16). Moreover, independent of the protein concentration, fragments were detected in the chromatograms of all liquid formulations after 7-28 days of storage (Figure 3-15b). The formation of fragments observed in liquid formulations was successfully inhibited by the stabilization of the antibody in the solid state.

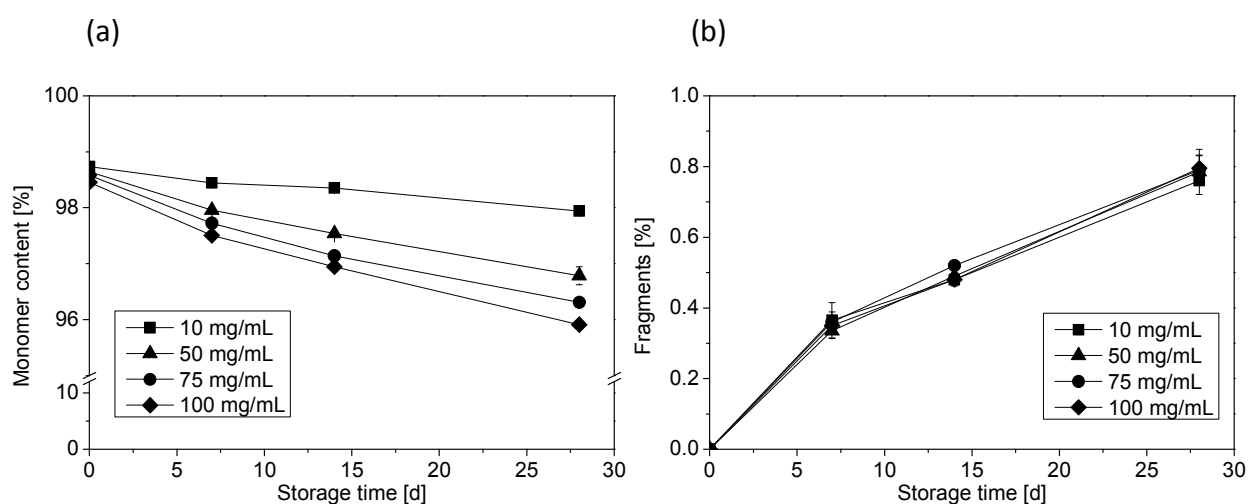


**Figure 3-15: Monomer content (a) and fragment content (b) detected via HP-SEC of liquid mAb2 formulations with 10, 50, 75 and 100 mg/mL protein stored at 40 °C for 4 weeks.**

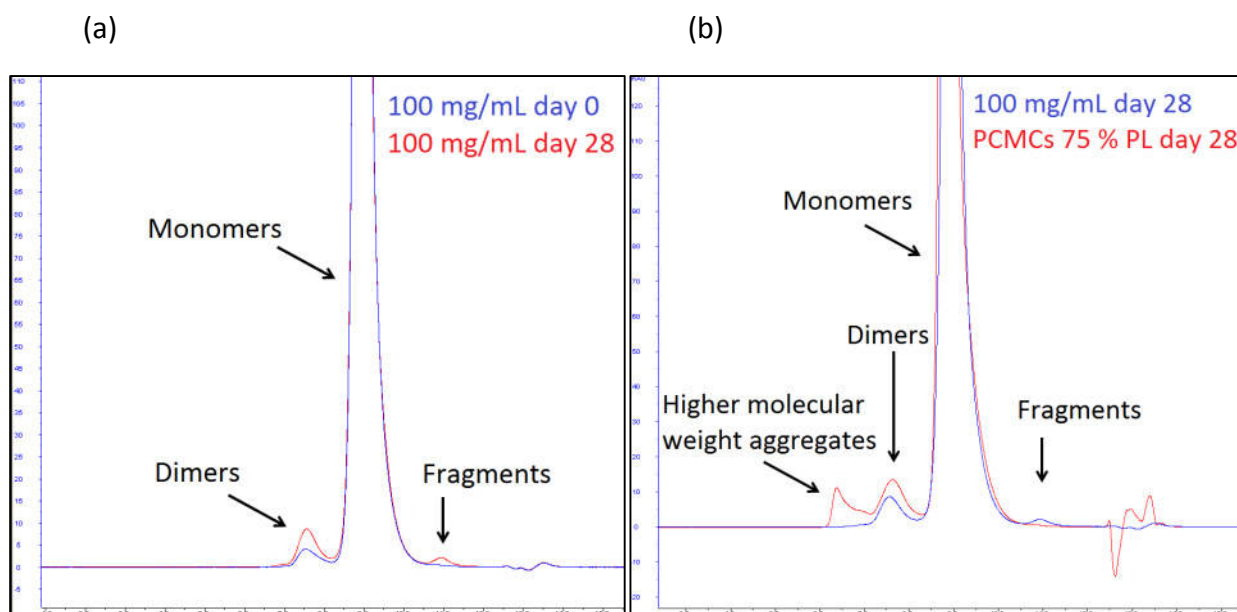
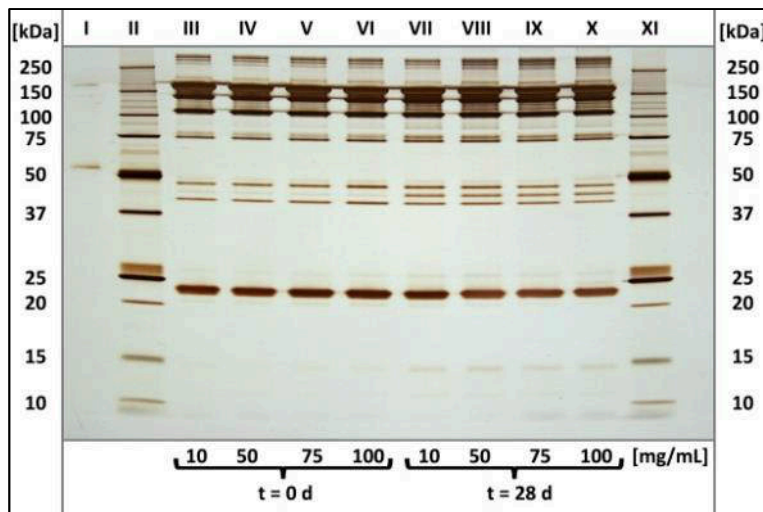


**Figure 3-16: (a) Overlay of chromatograms of the liquid formulation with 100 mg/mL protein after 0 (blue) and 28 (red) days at 40 °C; (b) comparison of chromatograms obtained from mAb2 PCMCs with 75 % protein load (red) and the liquid formulation with 100 mg/mL protein (blue) after 28 days at 40 °C; x-axis: elution volume [mL], y-axis: UV signal at 280 nm [mAU]; signals between 12 and 14 mL were caused by the elution of buffer components.**

SDS-PAGE analysis under non-reducing conditions revealed an additional band at below 50 kDa for all protein solutions that were stored at 40 °C for four weeks (Figure 3-17a). Moreover, a faint extra band at 15 kDa was identified and attributed to fragmentation within these samples. These observations were consistent with the fragments detected in HP-SEC. Furthermore, the aggregate band above the 250 kDa marker band was darker for formulations of 50 mg/mL, 75 mg/mL and 100 mg/mL protein after thermal stress, being in accordance with HP-SEC and turbidity data. Under reducing conditions (Figure 3-17b) no extra bands were detected, but faint bands for  $t_0$  samples at 37 kDa, around 30 kDa and 15 kDa were more pronounced after 28 days at 40 °C. Bands at 15 kDa indicating fragmentation as well as bands between 25 and 37 kDa under reducing conditions were not detected in SDS-PAGE analysis of reconstituted mAb2 PCMCs.

(a)



(b)

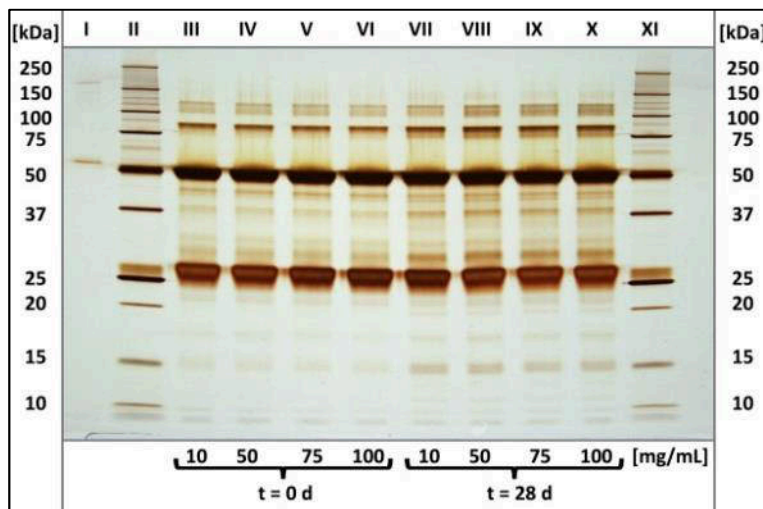


**Figure 3-17: SDS-PAGE of liquid mAb2 formulations stored at 40 °C for 28 days; (a) non-reducing and (b) reducing conditions; lane assignment: I: BSA control; II: Precision Plus Protein Standard; III-X: liquid mAb2 formulations with 10, 50, 75 and 100 mg/mL protein; XI: Precision Plus Protein Standard.**

Analysis of tertiary structure did not reveal any conformational perturbations, irrespective of the initial protein concentration and storage time (Figure 3-18).

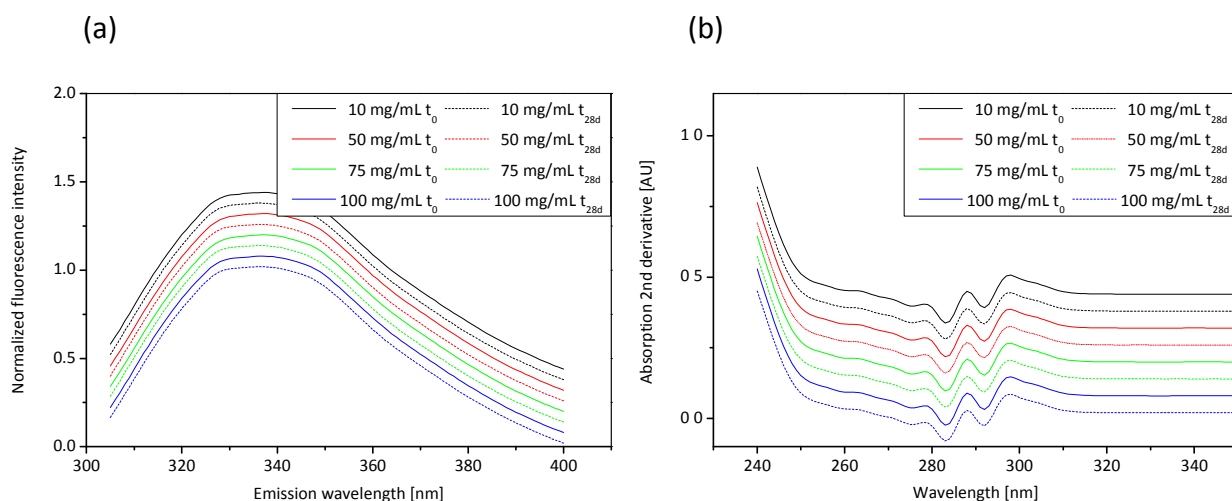


**Figure 3-18: Tertiary protein structure of liquid mAb2 formulations with 10, 50, 75 and 100 mg/mL protein stored at 40 °C for 4 weeks and investigated via (a) intrinsic fluorescence spectroscopy and (b) 2<sup>nd</sup>-derivative UV spectroscopy.**

Summing up, the data indicated that the mAb2 under investigation could be effectively stabilized as PCMC powder at certain protein loading rates, whereas aqueous formulations especially of higher concentrations were significantly impacted by the formation of aggregates and fragments over storage time. The aggregates were both of soluble and insoluble nature as detected via HP-SEC, SDS-PAGE analysis and turbidity measurement. The tendency of partially hydrophobic proteins, such as mAb2, towards aggregation is well known [7]. Comprising histidine buffer, trehalose and EDTA, the composition of the formulation, apart from optionally lacking salt additives, was comparable to commercially available therapeutic mAb formulations. The buffering agent histidine and the disaccharide trehalose are not only effective in stabilizing proteins in the solid state as described above, but are also frequently used in liquid antibody formulations [21]. The chelating agent EDTA reduces oxidation stress due to the complexation of metal ions [58].

## 4 Conclusion

The current study revealed the effects of single carrier components on the overall process stability of mAb2 formulated as PCMCs. Sodium chloride influenced the manufacturability of PCMCs because its absence resulted in slow sedimentation and consequently concentration of the precipitated suspension. Furthermore, without sodium chloride the PCMC powder did not

completely dissolve in water indicating the formation of insoluble protein particles. The amino acids glycine and histidine had positive effects on protein monomer recovery as detected via HP-SEC. Trehalose was not only most effective in the protection against aggregation, but had a significant impact on the overall appearance of the PCMC particles because it inhibited glycine crystallization. The resulting amorphous state of the formulation provided high protein process stability. However, literally, the term 'protein-coated microcrystals' did not apply for these PCMCs. Detrimental effects upon elimination of phenylalanine were not observed, even after storage at 40 °C for eight weeks.

Based on a lead formulation containing sodium chloride, glycine, histidine and trehalose, the influence of the protein load on storage stability of mAb2 PCMCs was assessed at 40 °C for 4-8 weeks. Overall, the storage stability of the mAb2 PCMCs was very good. Conformational changes in tertiary protein structure were not observed for any formulation. A maximal increase in soluble aggregates of 3.7 % was detected for a protein load of 75 % after 8 week storage at 40 °C. 50 % to 62.5 % protein load was optimal for retaining high monomer content. In accordance with reports on the stabilization of lyophilized protein formulations, a specific protein to excipient ratio was necessary to successfully stabilize the protein as PCMC powder. The storage stability of the PCMC powder was superior to liquid mAb2 formulations with 10 mg/mL, 50 mg/mL, 75 mg/mL and 100 mg/mL protein. Although alterations of protein conformation in the liquid formulations were not detected, increased aggregation rates and fragmentation were observed via HP-SEC and SDS-PAGE analysis. Therefore, the PCMC technology provided an efficient and beneficial way of formulating this mAb as an example of therapeutic proteins of which high doses are required.

The basic mechanism of protein stabilization via PCMC technology is still unclear because this technology combines a challenging manufacturing process, based on precipitation, concentration and supercritical drying, with complex formulations. Therefore, questions concerning the stabilization mechanism need to be addressed in subsequent studies to contribute to a better understanding of essential formulation and production parameters. Especially solid state analytics of protein structure should be performed because analysis of reconstituted PCMCs does not reflect the actual situation in the dry powder.

## 5 References

1. *Biopharmazeutika: Wirtschaftsdaten und neue Anwendungsgebiete zum Nutzen für die Patienten*. Verband Forschender Arzneimittelhersteller e.V., accessed August 16, 2012. Available from: <http://www.vfa-bio.de/vb-de/aktuelle-themen/branche/wirtschaftsdaten-und-neue-anwendungsgebiete-zum-nutzen-fuer-die-patienten.html>.
2. *Zugelassene gentechnische Arzneimittel in Deutschland*. Verband Forschender Arzneimittelhersteller e.V., accessed August 16, 2012. Available from: <http://www.vfa.de/de/arzneimittel-forschung/datenbanken-zu-arzneimitteln/amzulassungen-gentec.html>.
3. Nelson, A.L., Dhimolea, E., and Reichert, J.M., *Development trends for human monoclonal antibody therapeutics*. *Nature Reviews Drug Discovery*, 2010. **9**(10): p.767-774.
4. Maa, Y.-F. and Prestrelski, S.J., *Biopharmaceutical powders: Particle formation and formulation considerations*. *Current Pharmaceutical Biotechnology*, 2000. **1**(3): p.283-302.
5. Chang, L. and Pikal, M.J., *Mechanisms of protein stabilization in the solid state*. *Journal of Pharmaceutical Sciences*, 2009. **98**(9): p.2886-2908.
6. Yu, L., *Amorphous pharmaceutical solids: preparation, characterization and stabilization*. *Advanced Drug Delivery Reviews*, 2001. **48**(1): p.27-42.
7. Wang, W., *Protein aggregation and its inhibition in biopharmaceutics*. *International Journal of Pharmaceutics*, 2005. **289**(1–2): p.1-30.
8. Lai, M.C. and Topp, E.M., *Solid-state chemical stability of proteins and peptides*. *Journal of Pharmaceutical Sciences*, 1999. **88**(5): p.489-500.
9. Moore, B.D., et al., *Rapid dehydration of proteins*. WO00/69887, 2000.
10. König, C., *Entwicklung eines Prozesses in Pilotgröße zur Herstellung von Protein-coated Microcrystals* [dissertation]. Bonn: Universität Bonn, 2010.
11. Shire, S.J., Shahrokh, Z., and Liu, J., *Challenges in the development of high protein concentration formulations*. *Journal of Pharmaceutical Sciences*, 2004. **93**(6): p.1390-1402.
12. König, C., et al., *Development of a pilot-scale manufacturing process for protein-coated microcrystals (PCMC): Mixing and precipitation – Part I*. *European Journal of Pharmaceutics and Biopharmaceutics*, 2012. **80**(3): p.490-498.
13. Chew, N.Y.K. and Chan, H.-K., *The role of particle properties in pharmaceutical powder inhalation formulations*. *Journal of Aerosol Medicine*, 2002. **15**(3): p.325-330.

14. Ógáin, O.N., et al., *Particle engineering of materials for oral inhalation by dry powder inhalers. I—Particles of sugar excipients (trehalose and raffinose) for protein delivery*. International Journal of Pharmaceutics, 2011. **405**(1–2): p.23-35.
15. Schüle, S., et al., *Stabilization of IgG1 in spray-dried powders for inhalation*. European Journal of Pharmaceutics and Biopharmaceutics, 2008. **69**(3): p.793-807.
16. Vos, J., *Understanding the formation mechanism of protein coated microcrystals* [dissertation]. Glasgow: University of Strathclyde, 2006.
17. Chatterjee, K., Shalae, E.Y., and Suryanarayanan, R., *Partially crystalline systems in lyophilization: I. Use of ternary state diagrams to determine extent of crystallization of bulking agent*. Journal of Pharmaceutical Sciences, 2005. **94**(4): p.798-808.
18. Johari, G.P., et al., *Characterizing amorphous and microcrystalline solids by calorimetry*. Journal of Non-Crystalline Solids, 1990. **116**(2–3): p.282-285.
19. Hancock, B.C. and Zografi, G., *Characteristics and significance of the amorphous state in pharmaceutical systems*. Journal of Pharmaceutical Sciences, 1997. **86**(1): p.1-12.
20. Manning, M., et al., *Stability of protein pharmaceuticals: An update*. Pharmaceutical Research, 2010. **27**(4): p.544-575.
21. Wang, W., et al., *Antibody structure, instability, and formulation*. Journal of Pharmaceutical Sciences, 2007. **96**(1): p.1-26.
22. *Polysorbate 20*. ScienceLab.com, accessed December 04, 2012. Available from: <http://www.sciencelab.com/msds.php?msdsId=9926640>.
23. Bondos, S.E. and Bicknell, A., *Detection and prevention of protein aggregation before, during, and after purification*. Analytical Biochemistry, 2003. **316**(2): p.223-231.
24. Mahler, H.-C., et al., *Induction and analysis of aggregates in a liquid IgG1-antibody formulation*. European Journal of Pharmaceutics and Biopharmaceutics, 2005. **59**(3): p.407-417.
25. Cleland, J.L., et al., *A specific molar ratio of stabilizer to protein is required for storage stability of a lyophilized monoclonal antibody*. Journal of Pharmaceutical Sciences, 2001. **90**(3): p.310-321.
26. Andya, J., Hsu, C., and Shire, S., *Mechanisms of aggregate formation and carbohydrate excipient stabilization of lyophilized humanized monoclonal antibody formulations*. AAPS Journal, 2003. **5**(2): p.21-31.
27. Maury, M., et al., *Spray-drying of proteins: Effects of sorbitol and trehalose on aggregation and FT-IR amide I spectrum of an immunoglobulin G*. European Journal of Pharmaceutics and Biopharmaceutics, 2005. **59**(2): p.251-261.

28. Andya, J.D., et al., *The effect of formulation excipients on protein stability and aerosol performance of spray-dried powders of a recombinant humanized anti-IgE monoclonal antibody*. *Pharmaceutical Research*, 1999. **16**(3): p.350-358.
29. Maa, Y.-F., et al., *Protein inhalation powders: Spray drying vs spray freeze drying*. *Pharmaceutical Research*, 1999. **16**(2): p.249-254.
30. Jovanović, N., et al., *Stabilization of IgG by supercritical fluid drying: Optimization of formulation and process parameters*. *European Journal of Pharmaceutics and Biopharmaceutics*, 2008. **68**(2): p.183-190.
31. Chi, E.Y., et al., *Physical stability of proteins in aqueous solution: Mechanism and driving forces in nonnative protein aggregation*. *Pharmaceutical Research*, 2003. **20**(9): p.1325-1336.
32. Kamerzell, T.J., et al., *Protein–excipient interactions: Mechanisms and biophysical characterization applied to protein formulation development*. *Advanced Drug Delivery Reviews*, 2011. **63**(13): p.1118-1159.
33. Sarciaux, J.-M., et al., *Effects of buffer composition and processing conditions on aggregation of bovine IgG during freeze-drying*. *Journal of Pharmaceutical Sciences*, 1999. **88**(12): p.1354-1361.
34. Daugherty, A.L. and Mrsny, R.J., *Formulation and delivery issues for monoclonal antibody therapeutics*. *Advanced Drug Delivery Reviews*, 2006. **58**(5–6): p.686-706.
35. *D(+)-Trehalose Dihydrat*. Sigma-Aldrich Chemie GmbH, accessed August 11, 2012. Available from: <http://www.sigmaaldrich.com/MSDS/MSDS/DisplayMSDSPage.do?country=DE&language=de&productNumber=90208&brand=FLUKA&PageToGoToURL=http%3A%2F%2Fwww.sigmaaldrich.com%2Fcatalog%2Fproduct%2Ffluka%2F90208%3Flanguage%3Dde>.
36. Chen, B., et al., *Influence of histidine on the stability and physical properties of a fully human antibody in aqueous and solid forms*. *Pharmaceutical Research*, 2003. **20**(12): p.1952-1960.
37. Sane, S.U., Wong, R., and Hsu, C.C., *Raman spectroscopic characterization of drying-induced structural changes in a therapeutic antibody: Correlating structural changes with long-term stability*. *Journal of Pharmaceutical Sciences*, 2004. **93**(4): p.1005-1018.
38. Tian, F., et al., *Spectroscopic evaluation of the stabilization of humanized monoclonal antibodies in amino acid formulations*. *International Journal of Pharmaceutics*, 2007. **335**(1-2): p.20-31.
39. Arakawa, T., et al., *Biotechnology applications of amino acids in protein purification and formulations*. *Amino Acids*, 2007. **33**(4): p.587-605.

40. Liu, W., Wang, D.Q., and Nail Steven, L., *Freeze-drying of proteins from a sucrose-glycine excipient system: effect of formulation composition on the initial recovery of protein activity*. AAPS PharmSciTech, 2005. **6**(2): p.E150-7.
41. Mattern, M., et al., *Formulation of proteins in vacuum-dried glasses. II. Process and storage stability in sugar-free amino acid systems*. Pharmaceutical Development and Technology, 1999. **4**(2): p.199-208.
42. Waterman, K.C. and Adami, R.C., *Accelerated aging: Prediction of chemical stability of pharmaceuticals*. International Journal of Pharmaceutics, 2005. **293**(1–2): p.101-125.
43. Franks, F., *Accelerated stability testing of bioproducts: Attractions and pitfalls*. Trends in Biotechnology, 1994. **12**(4): p.114-117.
44. Wang, W., et al., *Immunogenicity of protein aggregates - Concerns and realities*. International Journal of Pharmaceutics, 2012. **431**(1–2): p.1-11.
45. Richard, J. and Prang, N., *The formulation and immunogenicity of therapeutic proteins: product quality as a key factor*. IDrugs, 2010. **13**(8): p.550-558.
46. Li, B., Flores, J., and Corvari, V., *A simple method for the detection of insoluble aggregates in protein formulations*. Journal of Pharmaceutical Sciences, 2007. **96**(7): p.1840-1843.
47. *Clarity and degree of opalescence of liquids*, in *European Pharmacopoeia*. 2005. Stuttgart: Deutscher Apotheker Verlag. p.27-29.
48. Zölls, S., et al., *Particles in therapeutic protein formulations, Part 1: Overview of analytical methods*. Journal of Pharmaceutical Sciences, 2012. **101**(3): p.914-935.
49. Chang, L., et al., *Mechanism of protein stabilization by sugars during freeze-drying and storage: Native structure preservation, specific interaction, and/or immobilization in a glassy matrix?* Journal of Pharmaceutical Sciences, 2005. **94**(7): p.1427-1444.
50. Mahler, H.C., et al., *Protein aggregation: Pathways, induction factors and analysis*. Journal of Pharmaceutical Sciences, 2009. **98**(9): p.2909-2934.
51. Kueltzo, L.A., et al., *Derivative absorbance spectroscopy and protein phase diagrams as tools for comprehensive protein characterization: A bGCSF case study*. Journal of Pharmaceutical Sciences, 2003. **92**(9): p.1805-1820.
52. Mach, H., et al., *Examination of phenylalanine microenvironments in proteins by second-derivative absorption spectroscopy*. Archives of Biochemistry and Biophysics, 1991. **287**(1): p.33-40.
53. Hawe, A., et al., *Forced degradation of therapeutic proteins*. Journal of Pharmaceutical Sciences, 2012. **101**(3): p.895-913.
54. Weichel, M., Bassarab, S., and Garidel, P., *Probing thermal stability of mAbs by intrinsic tryptophan fluorescence*. BioProcess International, 2008: p.42-52.

55. Garidel, P., et al., *A rapid, sensitive and economical assessment of monoclonal antibody conformational stability by intrinsic tryptophan fluorescence spectroscopy*. Biotechnology Journal, 2008. **3**(9-10): p.1201-1211.
56. Rosenberg, A.S., *Effects of protein aggregates: An immunologic perspective*. AAPS Journal, 2006. **8**(3): p.E501-E507.
57. Stroop, S.D., et al., *Photosensitizers form in histidine buffer and mediate the photodegradation of a monoclonal antibody*. Journal of Pharmaceutical Sciences, 2011. **100**(12): p.5142-5155.
58. Wang, W., *Instability, stabilization, and formulation of liquid protein pharmaceuticals*. International Journal of Pharmaceutics, 1999. **185**(2): p.129-188.

## Chapter 4

# Evaluation of organic water-miscible solvents as suspension media for PCMCs

### Abstract

For the development of PCMC suspensions for subcutaneous administration physiologically acceptable solvents are required that show good protein compatibility and that do not, at least substantially, dissolve the PCMC powder prior to application. This study aimed to screen glycerol, NMP, propylene glycol and PEG 400, pure as well as mixed with 10 to 90 % water (v/v), as potential organic water-miscible solvents for the resuspension of mAb1 PCMC powder. The focus was on macroscopic appearance of the suspensions as well as on protein aggregation (turbidimetry, HP-SEC) and protein structure (FT-IR, intrinsic fluorescence and 2<sup>nd</sup>-derivative UV spectroscopy). Glycerol and PEG 400 were found to be overall compatible with mAb1 PCMCs. Irrespective of the solvent content, the protein integrity was not affected, including the specific antigen binding capacity of the antibody. Furthermore, suspensions were formed in the presence of  $\geq 50\%$  solvent. With respect to propylene glycol, at least 90 % solvent was necessary for the formation of a suspension. However, these high propylene glycol concentrations resulted in considerable levels of insoluble and soluble aggregates and perturbation of secondary and tertiary protein structure. For NMP, a PCMC suspension was formed in the presence of the pure solvent, but the antibody was found to be aggregated to a significant extend. Reduction of the solvent concentration either resulted in complete dissolution of the PCMC powder (90 and 70 % NMP) or protein instability in terms of aggregate formation or/and conformational changes ( $\leq 50\%$  NMP). Consequently, the use of glycerol and PEG 400 is recommended for further development of non-aqueous PCMC suspensions in water-miscible organic solvents for subcutaneous delivery.

## 1 Introduction

The formulation development of subcutaneous high concentration protein injectables bears particular challenges. The most significant restrictions for subcutaneous formulations are the low injection volume of 0.5-2 mL administered via 0.5-1 inch 23-gauge (or smaller) needle, a need for isotonicity and low viscosity and a pH range of 2.7-9.0 [1-4]. High concentration protein, specifically mAb, solutions are frequently associated with problems including high viscosity, protein aggregation, and poor overall stability [5, 6]. Thus, high concentration suspensions, e.g. formulated as PCMCs, represent a promising alternative. The development of PCMC suspensions for subcutaneous delivery requires the evaluation of appropriate suspension media that do not dissolve the PCMC powder and that are physiologically acceptable and compatible with the protein. Moreover, the ideal non-aqueous suspension medium should be miscible with water and body fluids, remain stable under normal conditions of pharmaceutical use, have a high boiling point for potential heat sterilization and a viscosity allowing for easy injection [7, 8]. Constant purity and degree of flammability are additional considerations. Obviously, the ideal solvent does not exist yet [7, 8]. Commonly used organic water-miscible cosolvents for parenteral administration that are numerous reviewed include ethanol, glycerol, polyethylene glycol (PEG) 300 and 400, N-methyl-pyrrolidone (NMP), propylene glycol, dimethylacetamide, dimethyl sulfoxide etc. [2-4, 7-16]. However, only a few of them are administered subcutaneously and their amount is limited to e.g. 6 % ethanol, 32 % glycerol and 10 % propylene glycol [2, 9].

The aim of this study was to evaluate organic water-miscible solvents, namely glycerol, NMP, propylene glycol and PEG 400, as resuspension media for mAb1 PCMC powder. Pure solvents as well as mixtures with water (90:10, 70:30, 50:50, 30:70 and 10:90 (v/v)) were screened. The study focused on the macroscopic appearance of the suspensions as well as on protein stability after dissolution of the PCMC powder with regard to aggregation (turbidimetry, HP-SEC) and changes in the structure of the monoclonal antibody (FT-IR, intrinsic fluorescence and 2<sup>nd</sup>-derivative UV spectroscopy). For glycerol and PEG 400, the binding activity of the antibody after solvent incubation and dissolution of residual PCMC powder was additionally analyzed.

## 2 Materials and methods

### 2.1 Materials

L-Phenylalanine and sodium hydroxide were purchased from Sigma-Aldrich, Steinheim, D, disodium EDTA dihydrate, hydrochloric acid (1 mol/L), water free glycerin (Emprove®) and isobutanol (Emplura®) from Merck, Darmstadt, D. Glycine, L-histidine and L-histidine hydrochloride monohydrate were procured from Ajinomoto Omnicem, Louvain-la-Neuve, B. Sodium dihydrogen phosphate dihydrate was delivered by Dr. Paul Lohmann, Hungen, D, sodium chloride by Akzo Nobel, Hengelo, NL, and trehalose dihydrate by Ferro Pfanstiehl, Waukegan, IL, USA. N-Methyl-pyrrolidone (Pharmasolve®) was obtained from ISP (Köln, D). Highly purified polyethylene glycol 400 (Super Refined PEG 400-LQ-/MH) was acquired from Croda (Nettetal, D), propylene glycol (1,2-propanediol Ph.Eur.) from Fluka, Buchs, CH.

The protein bulk drug substance provided by Boehringer Ingelheim was composed of 20 mg/mL mAb1, representing a human IgG2 monoclonal antibody, 0.68 mg/mL L-histidine, 3.27 mg/mL L-histidine hydrochloride monohydrate, 0.1 mg/mL disodium EDTA dihydrate, 84.0 mg/mL trehalose dihydrate and 0.02 % polysorbate 80. The buffer of the bulk drug substance was exchanged via ultra- and diafiltration resulting in a protein solution that consisted of 105.6 mg/mL protein, 0.68 mg/mL L-histidine, 3.27 mg/mL L-histidine hydrochloride monohydrate, 0.1 mg/mL disodium EDTA dihydrate and 56.0 mg/mL trehalose dihydrate (crossflow buffer exchange and concentration unit, Boehringer Ingelheim, Biberach/Riss, D; membrane cassette Sartocoon Slice, Hydrosart, 30 kd, Sartorius, Göttingen, D; Quattroflow 150 S membrane pump, Quattroflow Fluid Systems, Hardegsen, D). Furthermore, polysorbate 80 was present in the protein solution because it cannot be removed via ultra-/diafiltration, as reported by Mahler et al. for polysorbate 20 [17].

### 2.2 Methods

#### 2.2.1 PCMC production process

The PCMC production process is divided into four main steps: preparation of protein-carrier solution, precipitation, concentration/solvent exchange, and drying. For the preparation of the protein-carrier solution (Table 4-1) the carrier material was dissolved in deionized water and

the solution pH value was adjusted to 5.5 prior to the addition of the protein solution. The final solution was filtered through a 0.22  $\mu\text{m}$  membrane filter (Stericup-GV, 47mm, PVDF, Sartorius, Göttingen, D).

**Table 4-1: Composition of protein-carrier solution.**

Substance	Mass [mg] in 200.0 ml	Percent by weight [%]
mAb1	2239.8	43.6
L-Histidine	27.8	0.5
L-Histidine HCl monohydrate	133.7	2.6
Disodium EDTA dihydrate	4.1	0.1
Glycine	811.1	15.8
L-Phenylalanine	89.5	1.7
Sodium chloride	269.0	5.2
Trehalose dihydrate	1568.1	30.5
Sum	5143.1	100.0

The precipitation was carried out as described in detail by König [18]. Briefly, two equal streams of precipitating agent were mixed with one stream of protein-carrier solution in a small double jet impingement mixer of an inner diameter of 1.5 mm (Boehringer Ingelheim, Biberach/Riss, D). The precipitating agent was isobutanol saturated with all carrier components. The mixing ratio of the precipitating agent and the protein-carrier solution was set to 95 : 5 (v/v). The modular mixing platform from Ehrfeld (Bayer Technology, Wendelsheim, D) encompassed three micro gear pumps (HNP pumps mzt 11507 and 7255, Hydraulik Nord Fluidtechnik, Parchim, D), pressure sensors and temperature sensors to monitor the precipitation step. The total flow rate of 1000 mL/min was controlled by the software LabView (National Instruments, Munich, D) and Coriflow mass flow meters (Bronkhorst, Kamen, D). The final suspension volume after precipitation was 4 L. Solvent exchange was achieved by decanting the supernatant of the PCMC suspension 18 h after the precipitating step. The supernatant was replaced with fresh saturated isobutanol. After further 24 h of sedimentation the sediment, i.e. the concentrated suspension, was used for the supercritical drying process (Thar SFE-500, Thar Technologies, Pittsburgh, PA, USA) with carbon dioxide at 100 bar and a flow rate of 25 g/min. After drying of 240 mL concentrated suspension within 130 min at 45 °C the pressure was decreased by 3 bar/min.

### **2.2.2 Incubation of PCMC powder with organic water-miscible solvents**

NMP, PEG 400, glycerol and propylene glycol served as organic water-miscible solvents selected for the incubation of the PCMC powder. Apart from the pure solvents, mixtures with deionized water were prepared in ratios of 90:10, 70:30, 50:50, 30:70 and 10:90 (v/v). PCMC powder incubated with pure water was used as reference sample. 68.9 mg powder was incubated with 3.0 mL of the solvent or solvent water mixture in 20 R vials (CRP-NBB-20ml, type FC, Schott, Mühlheim, D) for 5 min on a horizontal shaker (Kombischüttler KL 2, Edmund Bühler, Hechingen, D) at a shaking speed of 250 rpm.

### **2.2.3 Macroscopic appearance after solvent incubation**

The macroscopic appearance of the suspensions after solvent incubation was evaluated with respect to agglomeration tendency, turbidity and coloration.

### **2.2.4 Analysis of protein integrity**

After solvent incubation 12.0 mL deionized water was added to achieve complete dissolution of the PCMC powder required for protein analysis. In that case, the final protein concentration in the solutions was 2 mg/mL and the solvent content ranged from 2 to 18 % (v/v).

#### **2.2.4.1 Dissolution behavior**

The dissolution behavior (agglomeration tendency, turbidity and coloration) of the suspensions was macroscopically investigated after the addition of water (see section 2.2.4).

#### **2.2.4.2 Turbidimetry**

Turbidity was measured at a protein concentration of 2 mg/mL by 90 ° light scattering at  $\lambda = 633$  nm (UH turbidimeter, Boehringer Ingelheim, self-construction) and expressed in formazine nephelometric units (FNU) (n=3).

#### **2.2.4.3 High pressure size exclusion chromatography (HP-SEC)**

HP-SEC was performed on an Äkta micro (GE Healthcare, Uppsala, Sweden) with a TSKgel G3000SWXL column (7.8 mm ID x 30.0 cm L) and a 40 x 6.0 mm TSKgel SWXL Guardcol precolumn (Tosoh Bioscience, Stuttgart, D) at a flow rate of 1 mL/min. The mobile phase was composed of 60 mM sodium chloride and 5 mM sodium dihydrogen phosphate with a pH adjusted to 7.0. After filtration through a 0.45  $\mu$ m membrane filter (Millex® HV, Cork, IRL), 25  $\mu$ l

samples of 2.0 mg/mL protein were injected in duplicate and protein elution was monitored via UV-detection at 280 nm. Aggregation in percent was calculated based on the ratio of the area under the curve (AUC) of soluble aggregates to the total AUC of aggregates and monomer (n=2). Furthermore, changes in the AUC were considered.

#### **2.2.4.4 Analysis of protein structure**

Conformational changes of the protein were analyzed via Fourier transform infrared spectroscopy (FT-IR), intrinsic fluorescence spectroscopy and 2<sup>nd</sup>-derivative UV spectroscopy. A special form of sample preparation was required prior to measurement, because amino acids that were used as carrier components may interfere with spectroscopic methods, such as FT-IR analysis [19, 20]. Therefore, diafiltration of 5.0 mL samples was performed against 500 mL water for injection (WFI) with stirring at room temperature (Spectra/Por® 7 Dialysis Membrane MWCO 25,000, Carl Roth, Karlsruhe, D). WFI was exchanged twice within 18 h of diafiltration.

##### **2.2.4.4.1 Fourier transform infrared spectroscopy**

As the precision of FT-IR depends on the protein concentration, dialyzed samples were concentrated in the centrifuge (Heraeus® Biofuge® primo, Carl Roth, Karlsruhe, D). The filtration units (Amicon® Ultra-4 Ultracel-30k, Millipore, Schwalbach, D) were rinsed with 4.0 mL 0.1 N NaOH and subsequently equilibrated with water at 7500 g for 10 min. Concentration of 4.0 mL samples at 7500 g for 10-20 min resulted in a final protein concentration of 5-20 mg/mL. Samples were filtered through a 0.2 µm syringe filter (Acrodisc® Syringe Filters with Supor® Membrane, Pall, Dreieich, D).

FT-IR spectroscopy was performed using a Tensor 37 and a Confocheck measuring cell (Bruker, Ettlingen, D). Spectra were recorded from 4000 to 900 cm<sup>-1</sup> with 120 scans and a resolution of 2 cm<sup>-1</sup> at 25° C. Atmospheric compensation was done and WFI served as reference. Spectra were processed by vector normalization prior to calculating the average spectrum based on three measurements. Second derivative was built applying 17 smoothing points (Savitzky-Golay algorithm).

##### **2.2.4.4.2 Intrinsic fluorescence spectroscopy**

Samples of 0.1 mg/mL protein in SUPRASIL® 114-QS precision cuvettes (10 mm, Hellma, Mühlheim, D) were excited at 295 nm and 25 °C. The emission was scanned from 305 nm

to 400 nm with a step size of 1 nm and 1 s integration time (Fluorimeter QM-4-CW, PTI, Birmingham, NJ, USA). The evaluation was based on normalized spectra (n=3).

#### 2.2.4.4.3 2<sup>nd</sup>-derivative UV spectroscopy

Samples of 0.3 mg/mL protein were scanned in Halfmicro Plastibrand® cuvettes (Brand, Wertheim, D) from 240 to 350 nm (UV/VIS Spectrometer Lambda 20, PerkinElmer, Rodgau-Jügesheim, D). The second derivative of the absorption was used (n=3).

#### 2.2.4.5 Binding assay

mAb1 prevents the target antigen from binding to a specific cell surface protein (CSP). Consequently, binding activity of the antibody to the target antigen was analyzed according to BI internal method using a competitive ELISA following typical protocols [21]. Briefly, mAb1 and the target antigen were added to CSP immobilized on a microtiter plate. Decreasing concentration of mAb1 resulted in decreasing inhibition of binding of target antigen to CSP. After the addition of goat anti-mouse-IgG horseradish peroxidase that bound to CSP and of tetramethylbenzidine dye, the amount of colored product, being inversely proportional to the binding activity of the antibody, was measured based on the absorption at 450 nm (n=2).

### 3 Results and discussion

Solvent incubation, carried out with glycerol, NMP, propylene glycol and PEG 400 on a horizontal shaker, was limited to 5 min because the PCMC powder and the suspension medium are intended to be marketed in a dual chamber syringe system. Thus, the suspension, representing the final dosage form, would be prepared immediately before subcutaneous injection. After solvent incubation the macroscopic appearance of the suspension was analyzed. Subsequent dissolution of residual PCMC powder allowed for analysis of protein integrity, including aggregation level and structural changes.

#### 3.1 Macroscopic appearance after solvent incubation

The incubation of mAb1 PCMC powder with pure glycerol resulted in a big powder nest located in the middle of the vial (Figure 4-1). Pure glycerol was too viscous to disperse the powder under the shaking conditions selected [22]. Down to a mixing ratio of glycerol to water of 50:50 suspensions with many powder particles were formed during shaking. Apart from the particles

detected by the naked eye, the suspensions were macroscopically turbid. In the samples incubated with smaller amounts of glycerol (30 % and 10 %) only few powder agglomerates were visible. Thus, 70 % of water was sufficient for the dissolution of mAb1 PCMC powder in the presence of glycerol. The sample that was incubated with pure water and hence served as reference sample was a clear solution. The good water solubility found in this study is typical of most of the PCMC powders [18, 23].



**Figure 4-1: Incubation of PCMC powder with glycerol and corresponding water mixtures; glycerol to water ratio (v/v): (1) 100:0, (2) 90:10, (3) 70:30, (4) 50:50, (5) 30:70, (6) 10:90, (7) 0:100 = pure water.**

The appearance of the samples incubated with NMP and NMP water mixtures strongly depended on the mixing ratio (Figure 4-2). Sample (8) with pure NMP represented a turbid suspension, whereas clear solutions were detected when 90 or 70 % NMP was used. In the presence of an increasing amount of water, namely 50 and 70 %, the PCMC powder was not completely dissolved. Powder agglomerates were detected in these samples. The sample that contained 10 % NMP and 90 % water represented a turbid suspension without any big agglomerate.

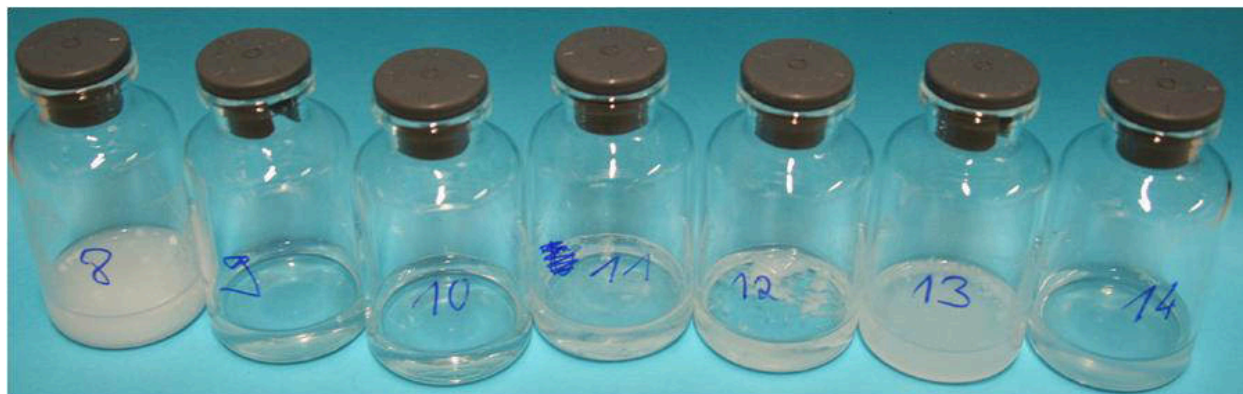


**Figure 4-2: Incubation of PCMC powder with NMP and corresponding water mixtures; NMP to water ratio (v/v): (8) 100:0, (9) 90:10, (10) 70:30, (11) 50:50, (12) 30:70, (13) 10:90, (14) 0:100 = pure water.**

In contrast to NMP, the solubility of PCMC powder in the presence of propylene glycol clearly increased with increasing amount of water. A turbid suspension with many powder agglomerates was formed after the incubation with pure propylene glycol (Figure 4-3). Still there were some powder agglomerates visible in the samples containing 90, 70 and 50 % propylene glycol, but the number decreased with rising water content. Clear solutions were detected when the amount of propylene glycol was reduced to 30 % or less.



**Figure 4-3: Incubation of PCMC powder with propylene glycol and corresponding water mixtures; propylene glycol to water ratio (v/v): (15) 100:0, (16) 90:10, (17) 70:30, (18) 50:50, (19) 30:70, (20) 10:90, (21) 0:100 = pure water.**

PCMC powder incubated with PEG 400 and PEG 400 water mixtures showed the same solubility tendency. The amount of powder agglomerates and the turbidity of the samples increased when the volume fraction of PEG 400 was augmented (Figure 4-4). In the presence of only 10 % PEG 400 the powder completely dissolved and no agglomerates were macroscopically visible.



**Figure 4-4: Incubation of PCMC powder with PEG 400 and corresponding water mixtures; PEG 400 to water ratio (v/v): (22) 100:0, (23) 90:10, (24) 70:30, (25) 50:50, (26) 30:70, (27) 10:90, (28) 0:100 = pure water.**

Overall, the solubility of mAb1 PCMCs in the presence of glycerol, propylene glycol and PEG 400 improved with increasing amount of water. In the case of NMP, a stronger turbidity in NMP/water mixtures was seen with higher water content. At least 50 % glycerol or PEG 400 and 90 % propylene glycol were required to form a suspension. Suspensions were also detected for 30:70 and 10:90 NMP water mixtures as well as for pure NMP.

### 3.2 Protein integrity after solvent incubation

After solvent incubation protein analysis, focusing on aggregation and structural alterations, required the addition of 12.0 mL water to achieve complete dissolution of residual PCMC powder. Consequently, the solvent content ranged from 2 to 18 % (v/v). The dissolution behavior may also provide information on the compatibility between the solvent and the monoclonal antibody. For example, high turbidity of protein solutions typically indicates the presence of insoluble aggregates [24].

In the samples incubated with glycerol or glycerol water mixtures the residual powder could be easily dissolved. Clear solutions were obtained independent of the initial glycerol content (Figure 4-5). Turbidity measurement underlined the macroscopic appearance of the samples with turbidity values ranging from 4.4 to 11.1 FNU (Figure 4-9). Thus, all samples were free of larger amounts of insoluble protein aggregates. Samples with an initial glycerol content of  $\geq 70$  % showed turbidity values of 4-5 FNU as opposed to 10-11 FNU detected for PCMC powder incubated with a lower amount of glycerol. The turbidity of those samples was even lower than

the one detected for PCMC powder reconstituted with pure water in the absence of glycerol (10.8 FNU). As reported by Chen et al., the refractive index of glycerol water mixtures augmented linearly with increasing volume percentage of glycerol [25]. Various studies in the field of micro-flow imaging and light obscuration on suspensions, either glass bead suspensions or high concentration protein solutions contaminated with insoluble proteinaceous particles, showed that increasing refractive indexes of the surrounding medium decreased the difference in refractive index between the particles and the medium resulting in reduced contrast and thus significant underestimation of particle number or undersizing [26, 27]. Pan et al. found that the turbidity of highly charged fluorinated monodisperse spherical particles suspended in ethylene glycol water mixtures decreased with increasing refractive index within a certain range [28]. Hence, the observation of reduced turbidity for PCMCs dissolved in glycerol water mixtures in the presence of increasing glycerol concentrations was attributed to a shift of the refractive index of the solvent.



**Figure 4-5: Dissolution behavior of PCMC suspensions, made of 68.9 mg mAb1 PCMC powder and 3.0 mL solvent, after addition of 12.0 mL water; initial glycerol to water ratio (v/v): (1) 100:0, (2) 90:10, (3) 70:30, (4) 50:50, (5) 30:70, (6) 10:90, (7) 0:100 = pure water.**

The samples initially incubated with 90 and 70 % NMP were macroscopically clear after the addition of water and showed low turbidity values of 7-8 FNU (Figure 4-6 and Figure 4-9). Turbidity measurement of the sample originally incubated with pure NMP also revealed a value of 7 FNU despite a few individual large flakes in the vial visible by the naked eye. Flake-shaped particles were also found after incubation with 50 and 30 % NMP. The turbidity of these samples was 20 and 24 FNU. Turbidity was particularly pronounced after the addition of water to the powder dispensed with 10 % NMP, reaching a value of 130 FNU. Hence, apart from the

samples initially containing 90 and 70% NMP, larger amounts of insoluble protein aggregates were apparently present in all formulations.



**Figure 4-6: Dissolution behavior of PCMC suspensions, made of 68.9 mg mAb1 PCMC powder and 3.0 mL solvent, after addition of 12.0 mL water; initial NMP to water ratio (v/v): (8) 100:0, (9) 90:10, (10) 70:30, (11) 50:50, (12) 30:70, (13) 10:90, (14) 0:100 = pure water.**



**Figure 4-7: Dissolution behavior of PCMC suspensions, made of 68.9 mg mAb1 PCMC powder and 3.0 mL solvent, after addition of 12.0 mL water; initial propylene glycol to water ratio (v/v): (15) 100:0, (16) 90:10, (17) 70:30, (18) 50:50, (19) 30:70, (20) 10:90, (21) 0:100 = pure water.**

With respect to propylene glycol, all samples initially incubated with  $\leq 70\%$  solvent were macroscopically clear. Their turbidity ranged from 3-12 FNU with lower values (3 and 5 FNU) for the samples incubated with 70% and 50% propylene glycol (Figure 4-9), as detected for glycerol water mixtures, too. Similarly, this observation was associated with an increasing refractive index of the solvent system with augmenting propylene glycol concentration, as likewise reported by Fogg et al. for ethylene glycol [29]. However, incubation with higher amounts of propylene glycol, namely 90% and 100%, resulted in turbidity values of 16 and

42 FNU indicating an increased amount of insoluble protein particles. Moreover, flakes were macroscopically detected in these samples.



**Figure 4-8: Dissolution behavior of PCMC suspensions, made of 68.9 mg mAb1 PCMC powder and 3.0 mL solvent, after addition of 12.0 mL water; initial PEG 400 to water ratio (v/v): (22) 100:0, (23) 90:10, (24) 70:30, (25) 50:50, (26) 30:70, (27) 10:90, (28) 0:100 = pure water.**

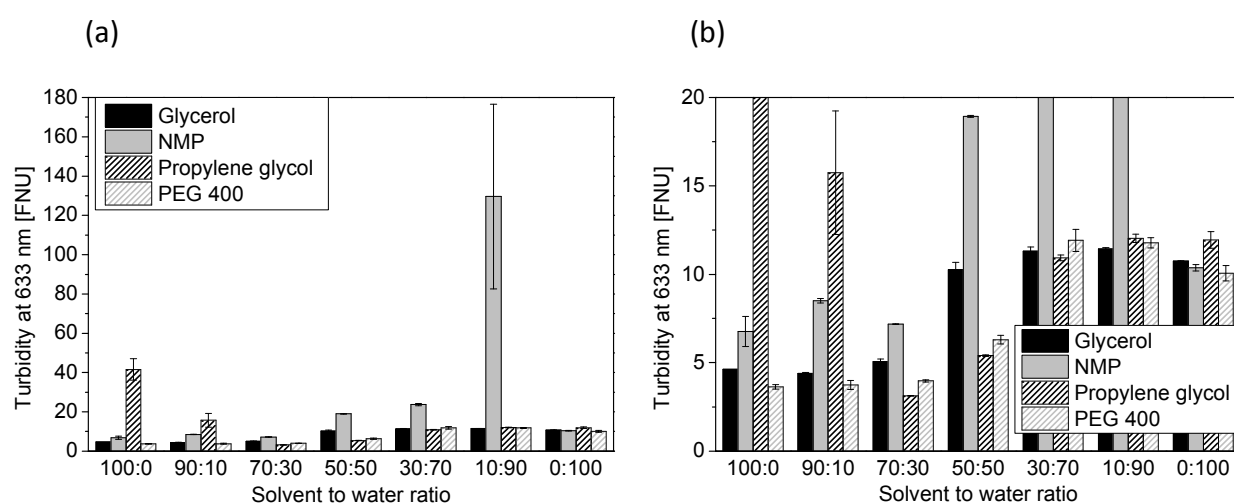


**Figure 4-9: Turbidity after incubation with 3.0 mL glycerol, NMP, propylene glycol and PEG 400 as well as solvent water mixtures (v/v) and subsequent dissolution of residual PCMC powder with 12.0 mL water (a); (b) zoomed in between 0 and 20 FNU.**

At first sight, all samples incubated with PEG 400 or mixtures made of PEG 400 and water appeared clear (Figure 4-8). The turbidity was low with values between 4-12 FNU (Figure 4-9), although single flake-shaped particles were detected in the formulations with 50 and 30 % PEG 400. Similar to glycerol and propylene glycol incubation, the turbidity values were lower for the samples containing a higher amount of PEG 400, very likely due to changes of the refractive

index (see above). An increase of the refractive index of mixtures made of PEG 300 and water with augmenting mole ratio of PEG 300 was detected by Rajulu and Sab [30].

Size exclusion chromatography is one of the most commonly used techniques for the analysis and quantification of soluble protein aggregates, oligomers, monomers and fragments [24, 31]. The presence of larger soluble aggregates and protein particles that accumulate in the precolumn or at the top of the column or that are removed via filtration during sample preparation can be assessed by a decrease in the AUC [32].

The monomer content in the samples incubated with glycerol and corresponding mixtures with water ranged from 98-100 % (Figure 4-10a). Compared to the reference sample incubated with pure water, the AUC of those samples was not decreased either. Thus, the incubation with glycerol and glycerol water mixtures did not induce considerable aggregation levels of the mAb formulated as PCMCs. The use of glycerol as stabilizer in protein formulations is widely described [33-36]. According to Gekko and Timasheff, glycerol is preferentially excluded from the protein surface in aqueous solution and hence favors the folded native state of the protein [37]. Vagenende et al. further specified that glycerol additionally tends to interact with hydrophobic surface regions of the protein, usually responsible for protein aggregation. The amphiphilic interface orientation of glycerol hence prevents the protein from aggregation processes [38].

Significant differences in the aggregation level were found after the incubation with NMP (Figure 4-10a). Samples initially incubated with 90 and 70 % NMP were free of soluble aggregates in HP-SEC. Incubation with pure NMP resulted in 6 % soluble protein aggregates. Significant larger amounts of aggregated species were detected in the samples with 50 and 30 % NMP, with residual monomer contents of 68 and 65 %. The soluble aggregate level resulting from incubation with 10 % NMP could not be assessed because the chromatogram did not show any protein peak indicating that the mAb was completely aggregated forming insoluble large particles. The AUC was also reduced for the samples incubated with pure NMP and 30 % NMP, by approx. 35 and 95 %, respectively (Figure 4-10b). NMP is used as solvent in the in situ hardening parenteral drug delivery formulation of leuprolide acetate, marketed as Eligard® [39]. The formulation is based on the Atrigel® technology, combining a biodegradable

polymer of D,L-lactide-co-glycolic acid (PLGA) and a biocompatible solvent, developed by Dunn et al. [40]. Protein aggregation after release from NMP containing drug delivery systems was reported by Tae et al. and Dong et al. [41, 42]. Figueiredo et al. further found that myoglobin was severely deteriorated, indicated by a color change and an increase in temperature, when it was dissolved in NMP [43]. In addition, rhGDF-5 underwent substantial oxidation upon incubation in NMP, which was induced by oxidizing species existing in the solvent [44].

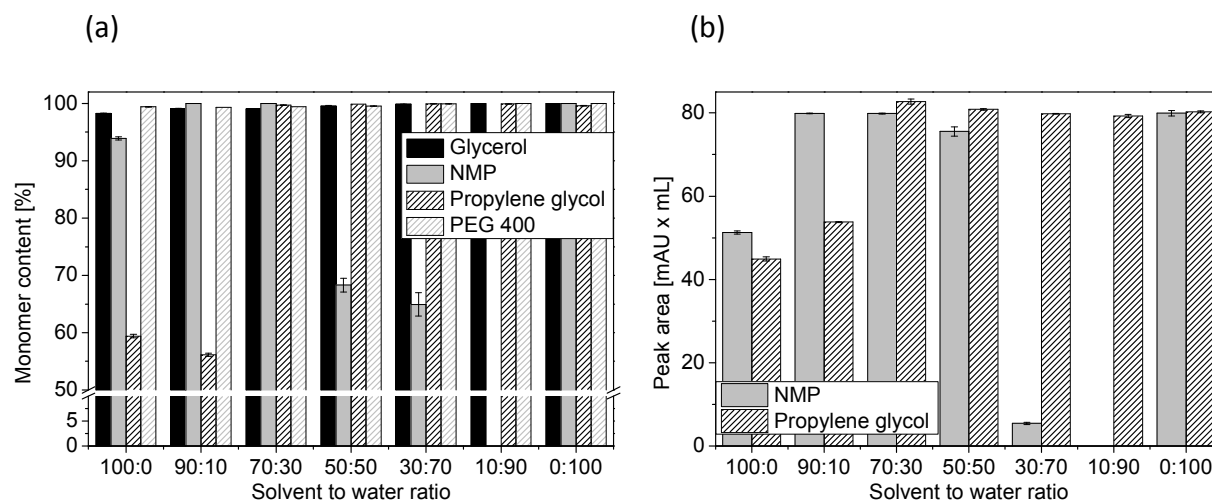


**Figure 4-10: Monomer content (a) and peak area (b) in HP-SEC after incubation with 3.0 mL glycerol, NMP, propylene glycol and PEG 400 as well as solvent water mixtures (v/v) and subsequent dissolution of residual PCMC powder with 12.0 mL water.**

Dispersing mAb1 PCMC powder in 90 and 100 % propylene glycol led to the formation of high amounts of soluble aggregates (Figure 4-10a). In these samples, 44 and 41 % aggregated species were found. Furthermore, the AUC was significantly decreased by approx. 33 and 44 %, respectively, indicating the formation of larger oligomers that could not be analyzed via HP-SEC (Figure 4-10b). This finding was in line with the macroscopic appearance after the addition of water because flake-shaped particles were present in both samples. For all the other samples, neither the monomer content nor the AUC was affected. Liu et al. who investigated the effects of polyols on the stability of whey proteins detected an increase in protein aggregation to almost 100 % at the three levels tested, including 33, 50 and 67 wt% propylene glycol [45].

Incubation with PEG 400 did not influence the monomer content in the samples, irrespective of the solvent concentration (Figure 4-10a). Changes in the AUC were not detected either. Not many data on protein aggregation caused by PEG 400 are available in literature. Knepp et al.

found that lyophilized plasma derived factor IX significantly aggregated within 1.5 week storage at 37 °C when it was suspended in PEG 400. They argued that protein instability might in part be caused by an oxidative attack arising from peroxides formed upon oxidation of the ether moieties [46]. The formation of peroxides in PEG upon light exposure and aging as well as subsequent protein degradation is well-known [47-49]. The absence of such degradation reactions in the recent study on mAb1 PCMCs might be attributed to the high quality of PEG 400 used for incubation in combination with the short incubation time.

As recommended by Baudys and Kim, several spectroscopic methods, namely FT-IR, intrinsic fluorescence and 2<sup>nd</sup>-derivative UV spectroscopy, were used to analyze potential conformational alterations of the secondary and tertiary structure of the reconstituted mAb [50] (see chapter 2 section 4.3.1). Independent of the solvent concentration, the incubation with glycerol did not change the secondary or tertiary conformational structure of the mAb as all spectra were identical to the one recorded after reconstitution of PCMCs with pure water (Figure 4-11a-Figure 4-13a). By comparison to previously published IgG FT-IR spectra, the bands can be assigned to protein structural elements [51, 52]. For example, typical intramolecular  $\beta$ -sheet bands occurred at 1692 and 1638  $\text{cm}^{-1}$  showing the predominance of  $\beta$ -sheets in IgGs. Well-resolved bands at frequencies of 1678 and 1662  $\text{cm}^{-1}$  represented turn structure and peaks at 1616  $\text{cm}^{-1}$  could be attributed either to more  $\beta$ -sheet structure or to side-chain effects. Monitoring of changes in protein tertiary structure via intrinsic fluorescence spectroscopy can for example be applied in forced degradation studies or to probe thermal stability of proteins in preformulation development [53, 54]. After incubation with glycerol or glycerol water mixtures the emission maximum was located at a wavelength of  $\lambda = 299 \text{ nm}$  for all samples (Figure 4-12a). In 2<sup>nd</sup>-derivative UV spectroscopy the broad peak at  $\lambda = 240\text{-}300 \text{ nm}$  is composed of multiple overlapping absorbance spectra, including phenylalanine, tyrosine and tryptophan [55]. Peaks between 245 nm and 270 nm are affected by phenylalanine, while peaks in the wavelength of 265-285 nm can be attributed mainly to tyrosine. Absorbance between 265 and 295 nm primarily arises from tryptophan. The 2<sup>nd</sup>-derivative UV spectrum of reconstituted PCMCs after incubation with glycerol and corresponding water mixtures was characterized by peak minima occurring at 277, 284 and 292 nm, while peak maxima were found at 265, 279, 288 and 297 nm (Figure 4-13a). Corresponding to the results for mAb1

PCMCs, Wakankar et al. found that the tertiary structure of a recombinant humanized monoclonal antibody was not affected by the addition of glycerol in a concentration of up to 80 % (v/v), analyzed via intrinsic fluorescence spectroscopy [56]. The structural protein stability in differential scanning calorimetry was even increased with increasing glycerol concentration. However, Figueiredo et al. reported that the secondary structure of myoglobin was retained in aqueous solution containing 50 % (v/v) glycerol, while the use of 96 % (v/v) glycerol caused turbidity of the system.

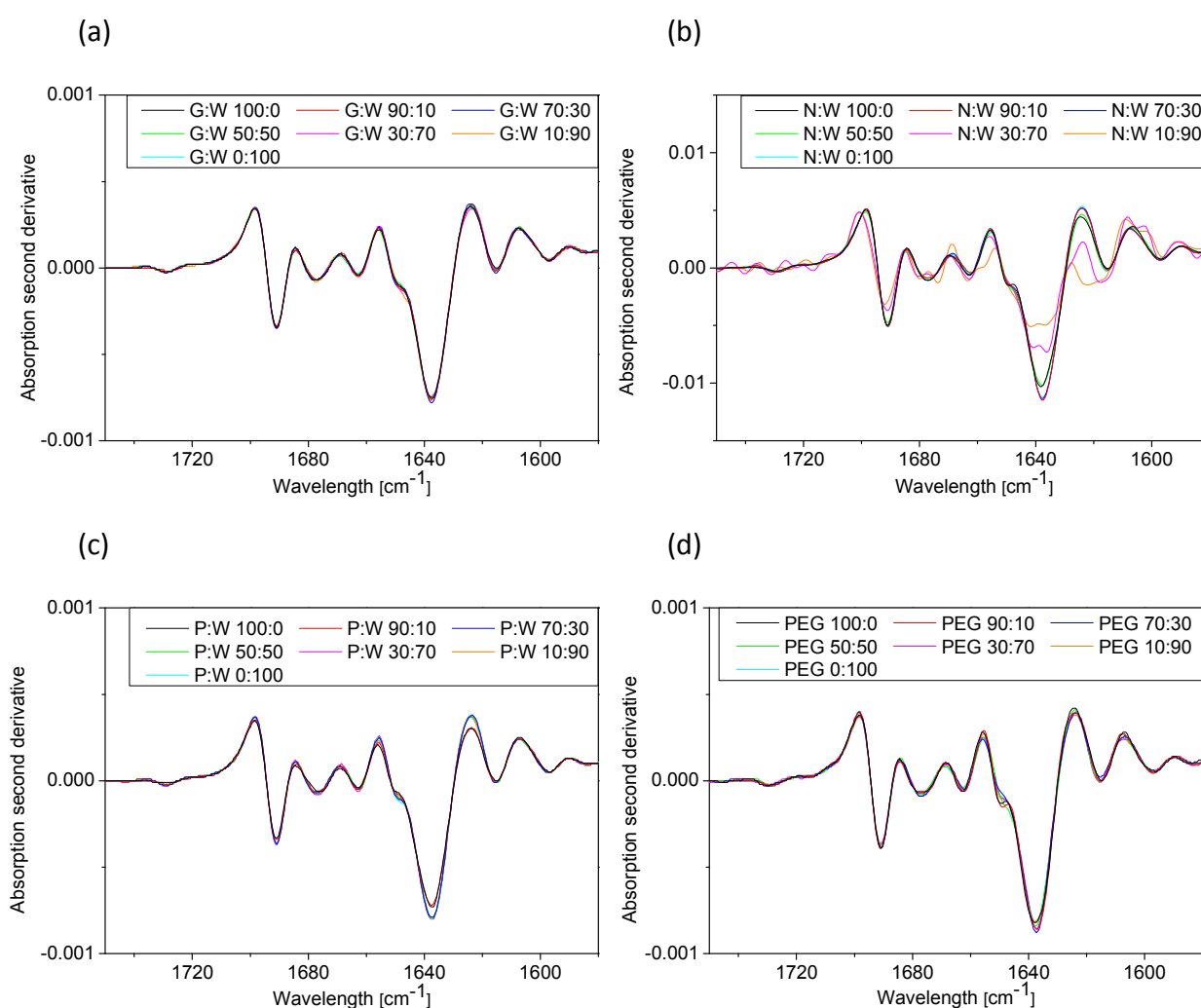


**Figure 4-11: FT-IR spectra after incubation with 3.0 mL (a) glycerol (G), (b) NMP (N), (c) propylene glycol (P) and (d) PEG 400 as well as solvent water (W) mixtures (v/v) and subsequent dissolution of residual PCMC powder with 12.0 mL water.**

Again for NMP, differences between the samples were seen in the overlay of the spectra. With respect to FT-IR spectroscopy, incubation of PCMC powder with 30 and 10 % NMP induced a

signal at 1618-1624  $\text{cm}^{-1}$  and a weak intensity peak at 1698  $\text{cm}^{-1}$  at the expense of signal intensity at 1692 and 1638  $\text{cm}^{-1}$  (Figure 4-11b). Equivalent changes in FT-IR spectra reported by Matheus et al. for high-concentration IgG formulations upon heating were associated with intermolecular hydrogen-bonded antiparallel  $\beta$ -sheet structure typical of aggregated protein [57, 58]. Referring to HP-SEC, the samples incubated with 30 and 10 % NMP revealed the highest loss of AUC indicating the presence of considerable amounts of either insoluble or larger soluble aggregates that cannot be assessed chromatographically (see above). The use of 50 % NMP, however, resulted in the formation of 32 % soluble aggregates in HP-SEC, but did neither affect the AUC nor the FT-IR spectrum. Thus, soluble aggregates detectable via HP-SEC had no impact on the FT-IR spectrum.

The spectra recorded via intrinsic fluorescence spectroscopy supported the structural changes detected in FT-IR spectroscopy after incubation with 30 and 10 % NMP. The maximum of both spectra was shifted from  $\lambda = 299 \text{ nm}$  to  $\lambda = 335 \text{ nm}$  and  $\lambda = 337 \text{ nm}$ , respectively, and both spectra contained a second maximum with a lower fluorescence intensity at  $\lambda = 383 \text{ nm}$  and  $\lambda = 381 \text{ nm}$  (Figure 4-12). Furthermore, the shape of the spectra was broader in both cases, as compared to the other samples. The shift of  $\lambda_{\text{max}}$  to a higher wavelength, referred to as red shift, generally indicates changes in the hydration of tryptophan residues and subsequently in protein structure [53]. Hence, structural changes of the monoclonal antibody after the incubation with NMP in concentrations of 30 and 10 % did not only involve the secondary but also the tertiary protein structure, as also reflected in 2<sup>nd</sup>-derivative UV spectroscopy (Figure 4-13b). The shape of the UV spectra was the same for all samples, but the amplitude was significantly decreased in all regions in the case of 30 and 10 % NMP. Van Beers et al. also observed reduced intensities of the positive and negative peaks in the 2<sup>nd</sup>-derivative UV spectra of metal-catalyzed oxidized interferon beta, demonstrating changes in the tertiary protein structure [59]. Apart from Figueiredo et al. who studied the structural stability of myoglobin in organic media via circular dichroism, including NMP, and who detected deterioration of the native protein folding, investigations of protein conformation in presence of NMP have not been reported in literature [43].

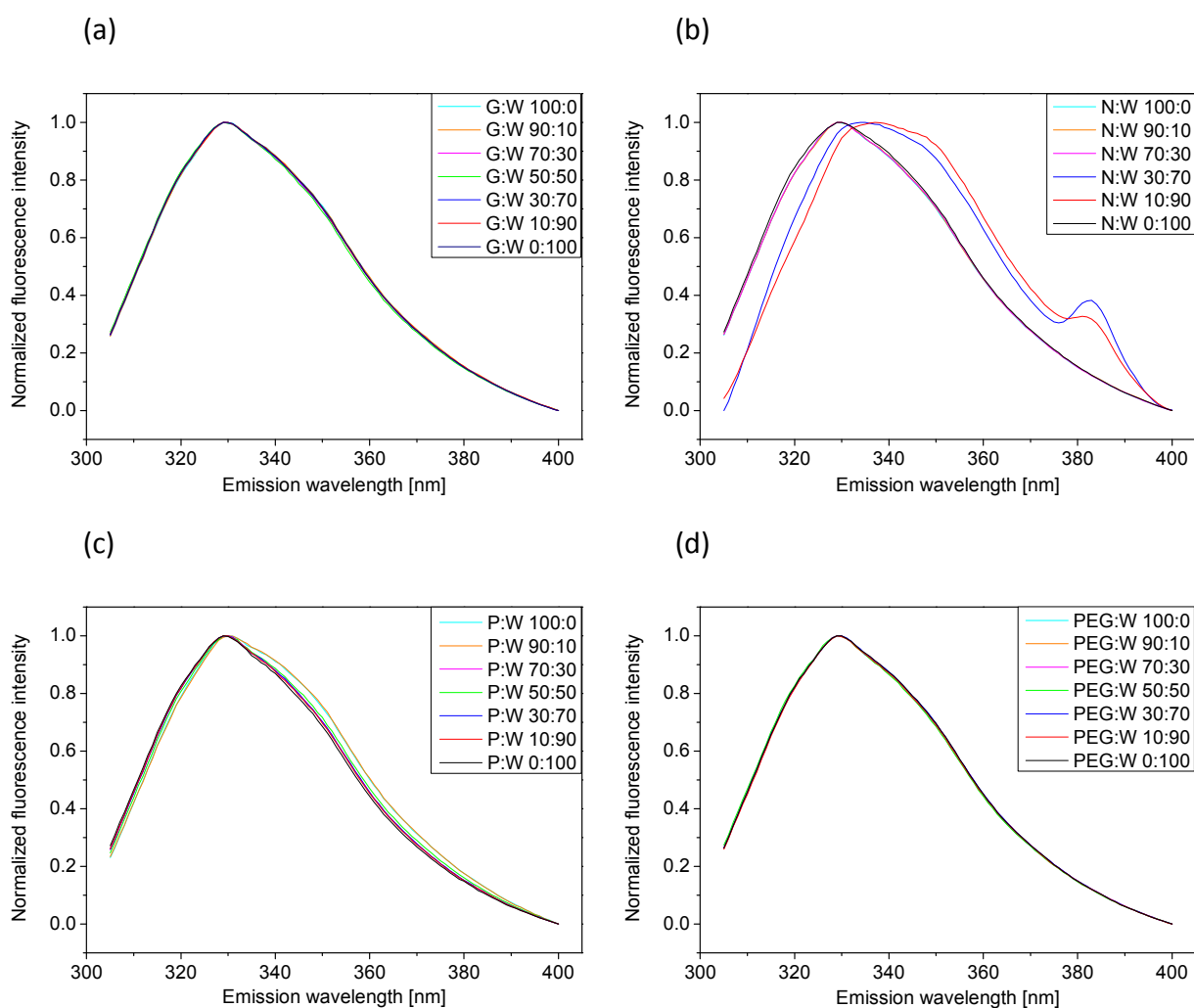


**Figure 4-12: Intrinsic fluorescence spectra after incubation with 3.0 mL (a) glycerol (G), (b) NMP (N), (c) propylene glycol (P) and (d) PEG 400 as well as solvent water (W) mixtures (v/v) and subsequent dissolution of residual PCMC powder with 12.0 mL water; normalized intensity for better comparison.**

Incubation with 100 and 90 % propylene glycol resulted in alterations of the secondary protein structure as analyzed by FT-IR. Peak intensities at  $\lambda = 1638 \text{ cm}^{-1}$  and  $\lambda = 1692 \text{ cm}^{-1}$  decreased, while bands at  $\lambda = 1624 \text{ cm}^{-1}$  and  $\lambda = 1698 \text{ cm}^{-1}$  increased (Figure 4-11c). However, these spectroscopic changes representing the formation of intermolecular at the expense of intramolecular  $\beta$ -sheets were significantly less pronounced than for the samples incubated with 30 and 10 % NMP. In accordance with those NMP samples, the level of soluble aggregates and the reduction of the AUC in HP-SEC were considerable for the PCMC powder incubated with 100 and 90 % propylene glycol. The amount of soluble aggregates was higher for the propylene glycol samples (41 and 44 %) than for the NMP samples (35 % and not measurable). The loss in

AUC amounted to 33 and 44 % for the incubation with propylene glycol, while a reduction by 95 and 100 % was detected in the case of NMP. This observation supported the hypothesis that mainly the presence of larger soluble aggregated species was related to alterations of the secondary structure of the monoclonal antibody. Initial propylene glycol concentrations of  $\leq 70$  % did not affect the secondary protein structure. In intrinsic fluorescence spectroscopy, the spectra recorded after incubation with 100 and 90 % propylene glycol also showed minor differences in comparison to the other samples. The emission maximum was not shifted to a higher wavelength, but the spectra were broader (Figure 4-12c). Changes were not visible in 2<sup>nd</sup>-derivative UV spectroscopy (Figure 4-13c), independent of the propylene glycol concentration, due to lower sensitivity of the latter method [55]. Thus, the clear changes in the secondary structure did come along with only marginal effects on the tertiary level of the mAb. Based on densitometric and CD investigations Gekko and Koga found that propylene glycol could induce weakening of the tertiary structure of bovine serum albumin via hydrophobic bonding and hence promotion of  $\alpha$ -helix formation [60]. The effect depended on the solvent concentration and the pH value, being more pronounced in the acidic range as opposed to neutral pH. Changes of secondary protein structure, namely a decrease of  $\beta$ -sheets and an increase of  $\alpha$ -helices, in the presence of at least 40 % propylene glycol were also described by Chobert et al. for  $\beta$ -lactoglobulin [61]. The promotion of  $\alpha$ -helical secondary structure in FT-IR by propylene glycol was confirmed by Liu et al. who studied the effects of polyols on the stability of whey proteins [45]. Furthermore, aggregation phenomena were explained by the induction of intermolecular  $\beta$ -sheets detected in FT-IR. DSC studies further revealed a loss of most of the tertiary structures in the presence of 50 wt% propylene glycol. Minor changes in the secondary and tertiary structure of the mAb formulated as PCMCs were also detected via FT-IR and intrinsic fluorescence spectroscopy after incubation with 100 and 90 % propylene glycol. Intramolecular  $\beta$ -sheets were replaced by intermolecular ones, but promotion of  $\alpha$ -helix was not observed. However, in the case of mAb1 PCMCs incubation with the initial solvent concentration was carried out for only 5 min at room temperature, as opposed to 7 days at 45 °C for whey proteins.

With respect to PEG 400, none of the three spectroscopic methods revealed any structural changes of mAb1 after incubation (Figure 4-11d-Figure 4-13d). The secondary and tertiary

protein structure was completely preserved independent of the solvent concentration. In contrast, Ahmad et al. reported that PEG 400 was capable of inducing a molten globule like state from acid-denatured stem bromelain and that small amounts of nonnative tertiary contacts were formed in the presence of 70 % (w/v) PEG 400 [62]. Moreover, far UV-CD spectroscopy conducted by Kumar et al. revealed a slight loss of secondary structural elements of bovine serum albumin in the presence of 10 % (w/v) PEG 400 [63].

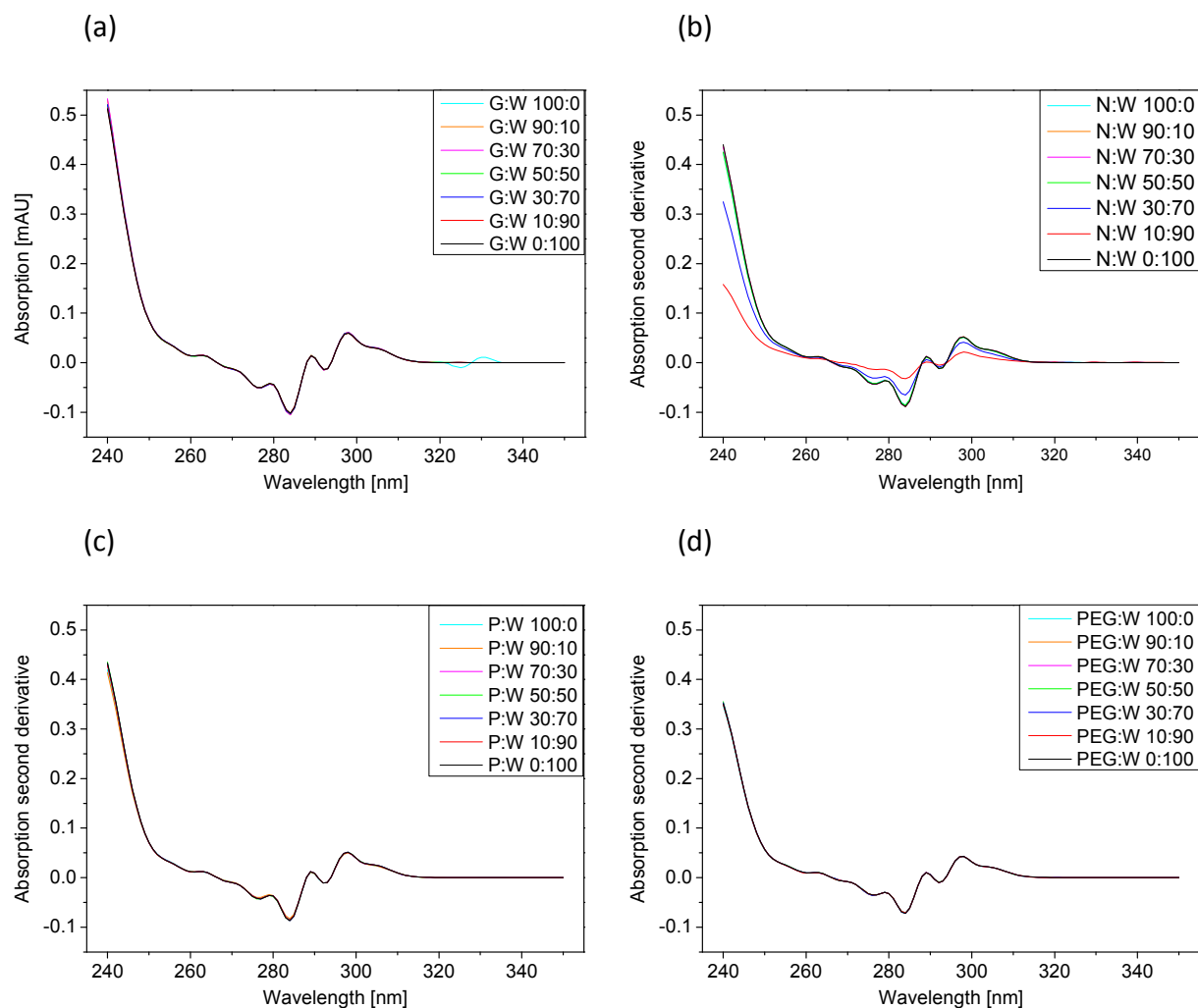


**Figure 4-13: 2<sup>nd</sup>-derivative UV spectra after incubation with 3.0 mL (a) glycerol (G), (b) NMP (N), (c) propylene glycol (P) and (d) PEG 400 as well as solvent water (W) mixtures (v/v) and subsequent dissolution of residual PCMC powder with 12.0 mL water.**

Additionally, a binding assay was conducted for the samples incubated with glycerol and PEG 400 to verify whether suspending mAb1 PCMCs in these solvents affected the specific antigen binding of the antibody. This investigation was limited to glycerol and PEG 400 because

these samples showed neither aggregation phenomena nor changes of the secondary or tertiary protein structure. Figure 4-14 visualizes that the binding activity of the antibody was completely retained for all glycerol and PEG 400 concentrations investigated as the values were within the specification limits of 65-130 % of the standard reference sample.

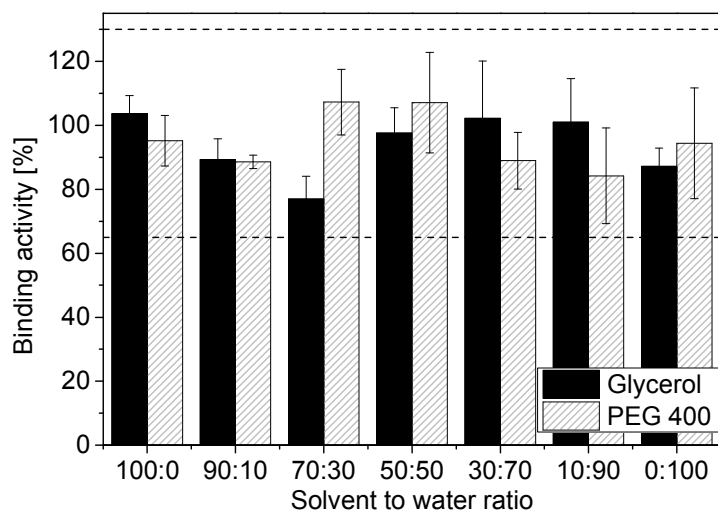


**Figure 4-14: Binding activity referred to standard reference sample after incubation with 3.0 mL glycerol or PEG 400 as well as solvent water mixtures (v/v) and subsequent dissolution of residual PCMC powder with 12.0 mL water; dotted lines indicate specification limits.**

## 4 Conclusion

The screening of glycerol, NMP, propylene glycol and PEG 400 as organic water-miscible resuspension media for mAb1 PCMCs focused on the macroscopic appearance after solvent incubation and on protein stability, including aggregation tendency and secondary and tertiary protein structure. An overview of the results is presented in the summary tables of Table 4-2.

At first sight, the tables for glycerol and PEG 400 show a good compatibility of these solvents with mAb1 PCMCs. In glycerol, attractive suspensions were formed in the presence of  $\leq 50\%$  water. Moreover, protein integrity, specific antigen binding and conformational structure were not disrupted in the presence of glycerol. Similar outcomes were found for the incubation with PEG 400. At least 50 % PEG 400 was required to form a PCMC suspension. Apart from single flake-shaped particles detected in 50:50 and 30:70 mixtures of PEG 400 and water, clear solutions were achieved by the addition of water. The protein stability, including the binding capacity of the antibody, was not affected by the solvent. With respect to NMP, appropriate

suspension quality was only found when pure NMP was used for dispensing the PCMC powder. However, incomplete dissolution behavior and the presence of soluble aggregates were observed after the addition of water. Protein stability was high when 90 and 70 % NMP was used, but these mixtures were capable of completely dissolving the PCMC powder. At higher amounts of water ( $\geq 50$  %) protein stability was severely reduced with substantial aggregation and a loss in protein structure. Similar to NMP, good suspending properties were provided by pure and 90 % propylene glycol, but the antibody was found to be aggregated to a significant extent and slight changes in the secondary and tertiary protein structure were revealed. At least 30 % water was required to prevent the monoclonal antibody from aggregation and structural alterations, but also resulted in complete dissolution of the PCMC powder. Hence, neither NMP nor propylene glycol was appropriate for PCMC resuspension, but glycerol and PEG 400 represented promising media for the manufacturing of subcutaneous PCMC suspensions.

**Table 4-2: Summary tables of PCMC stability results after incubation with 3.0 mL (a) glycerol, (b) NMP, (c) propylene glycol and (d) PEG 400 as well as solvent water mixtures (v/v); color assignment: suspension: green indicates the formation of a suspension, yellow the presence of single powder agglomerates, red complete dissolution of the PCMC powder after solvent incubation; dissolution: green designates the formation of a clear solution, yellow the presence of single powder agglomerates, red the presence of considerable amounts of insoluble material after dissolution of residual PCMC powder with 12.0 mL water; turbidity: green indicates turbidity values comparable to those of PCMC powder incubated with pure water of  $\leq 10$ -12 FNU, yellow slightly increased turbidity values of approx. 19-24 FNU, red significantly higher turbidity values of  $\geq 42$  FNU or the presence of many particle flakes; HP-SEC: green designates monomer levels comparable to those of PCMC powder incubated with pure water of  $\geq 98$  %, yellow a slightly reduced monomer level of approx. 94 %, red considerable decreased monomer contents of 56-68 % or the absence of any evaluable peak; FT-IR, IF and UV spectroscopy: green indicates spectra overlapping with those of PCMC powder incubated with pure water, red deviating curve shapes.**

(a)

Glycerol : water	100 : 0	90 : 10	70 : 30	50 : 50	30 : 70	10 : 90
Suspension	Green	Green	Green	Green	Yellow	Yellow
Dissolution	Green	Green	Green	Green	Green	Green
Turbidity	Green	Green	Green	Green	Green	Green
HP-SEC	Green	Green	Green	Green	Green	Green
FT-IR	Green	Green	Green	Green	Green	Green
IF	Green	Green	Green	Green	Green	Green
UV	Green	Green	Green	Green	Green	Green

(b)

NMP : water	100 : 0	90 : 10	70 : 30	50 : 50	30 : 70	10 : 90
Suspension	Green	Red	Red	Yellow	Yellow	Red
Dissolution	Yellow	Green	Green	Yellow	Red	Red
Turbidity	Green	Green	Green	Yellow	Yellow	Red
HP-SEC	Yellow	Green	Green	Red	Red	Red
FT-IR	Green	Green	Green	Green	Red	Red
IF	Green	Green	Green	Green	Red	Red
UV	Green	Green	Green	Green	Red	Red

(c)

Propyl. : water	100 : 0	90 : 10	70 : 30	50 : 50	30 : 70	10 : 90
Suspension	Green	Green	Yellow	Yellow	Red	Red
Dissolution	Red	Red	Green	Green	Green	Green
Turbidity	Red	Green	Green	Green	Green	Green
HP-SEC	Red	Red	Green	Green	Green	Green
FT-IR	Red	Red	Green	Green	Green	Green
IF	Red	Red	Green	Green	Green	Green
UV	Green	Green	Green	Green	Green	Green

(d)

PEG 400 : water	100 : 0	90 : 10	70 : 30	50 : 50	30 : 70	10 : 90
Suspension	Green	Green	Green	Green	Yellow	Red
Dissolution	Green	Green	Green	Yellow	Yellow	Green
Turbidity	Green	Green	Green	Green	Green	Green
HP-SEC	Green	Green	Green	Green	Green	Green
FT-IR	Green	Green	Green	Green	Green	Green
IF	Green	Green	Green	Green	Green	Green
UV	Green	Green	Green	Green	Green	Green

## 5 References

1. Boylan, J.C. and Nail, S.L., *Parenteral products*, in *Modern pharmaceuticals*, Banker, G.S. and Rhodes, C.T., editors. 2002: Informa Healthcare. p.381-414.
2. Strickley, R.G., *Parenteral formulations of small molecules therapeutics marketed in the United States (1999) - Part I*. PDA Journal of Pharmaceutical Science and Technology, 1999. **53**: p.324-349.
3. Strickley, R.G., *Parenteral formulations of small molecules therapeutics marketed in the United States (1999) - Part II*. PDA Journal of Pharmaceutical Science and Technology, 2000. **54**: p.69-96.
4. Strickley, R.G., *Parenteral formulations of small molecules therapeutics marketed in the United States (1999) - Part III*. PDA Journal of Pharmaceutical Science and Technology, 2000. **54**(2): p.152-169.
5. Shire, S.J., Shahrokh, Z., and Liu, J., *Challenges in the development of high protein concentration formulations*. Journal of Pharmaceutical Sciences, 2004. **93**(6): p.1390-1402.
6. Yang, M.X., et al., *Crystalline monoclonal antibodies for subcutaneous delivery*. Proceedings of the National Academy of Sciences of the United States of America, 2003. **100**(12): p.6934-6939.
7. Spiegel, A.J. and Noseworthy, M.M., *Use of nonaqueous solvents in parenteral products*. Journal of Pharmaceutical Sciences, 1963. **52**: p.917-927.
8. Mottu, F., et al., *Organic solvents for pharmaceutical parenterals and embolic liquids: A review of toxicity data*. PDA Journal of Pharmaceutical Science and Technology, 2000. **54**, No. 6: p.456-469.
9. Strickley, R., *Solubilizing excipients in oral and injectable formulations*. Pharmaceutical Research, 2004. **21**(2): p.201-230.
10. Akers, M.J., *Excipient-drug interactions in parenteral formulations*. Journal of Pharmaceutical Sciences, 2002. **91**: p.2283-2300.
11. Heintz, C. and Boymon, C., *Aspects pharmaco-toxicologiques et utilisation thérapeutique de quelques solvants injectables non aqueux miscibles à l'eau*. S.T.P. Pharma, 1989. **5** (8/9): p.548-560.
12. Sweetana, S. and Akers, M.J., *Solubility principles and practices for parenteral drug dosage form development*. Journal of Pharmaceutical Science and Technology, 1996. **50**(5): p.330-342.
13. Wang, Y.-C.J. and Kowal, R.R., *Review excipients pH's for parenteral products used in the United States*. PDA Journal of Pharmaceutical Science and Technology, 1980. **34**(6): p.452-462.

14. Kruss, B., *Toxikologie und Verträglichkeit von Lösungsmitteln zur parenteralen Anwendung*, in *Flüssige Arzneiformen schwerlöslicher Arzneistoffe*, Essig, D. and Stumpf, H., editors. 1990. p.42-61.
15. Bertholom, C., et al., *Critères de choix des solvants injectables non aqueux miscibles à l'eau*. S.T.P. Pharma Pratiques, 2000. **10**(3): p.137-143.
16. Nema, S., Washkuhn, R.J., and Brendel, R.J., *Excipients and their use in injectable products*. Journal of Pharmaceutical Science and Technology, 1997. **51**(4): p.166-171.
17. Mahler, H.C., et al., *Behaviour of polysorbate 20 during dialysis, concentration and filtration using membrane separation techniques*. Journal of Pharmaceutical Sciences, 2008. **97**(2): p.764-774.
18. König, C., et al., *Development of a pilot-scale manufacturing process for protein-coated microcrystals (PCMC): Mixing and precipitation – Part I*. European Journal of Pharmaceutics and Biopharmaceutics, 2012. **80**(3): p.490-498.
19. Tian, F., et al., *Spectroscopic evaluation of the stabilization of humanized monoclonal antibodies in amino acid formulations*. International Journal of Pharmaceutics, 2007. **335**(1-2): p.20-31.
20. Meyer, J.D., et al., *Infrared spectroscopic studies of protein formulations containing glycine*. Journal of Pharmaceutical Sciences, 2004. **93**(5): p.1359-1366.
21. Renneker, S., et al., *Development of a competitive ELISA for detection of theileria annulata infection*. Transboundary and Emerging Diseases, 2008. **55**(5/6): p.249-256.
22. *Glycerin wasserfrei*. Merck KGaA, accessed July 04, 2012. Available from: [http://www.merckmillipore.com/germany/chemicals/glycerin/MDA\\_CHEM-104093/p\\_L5qb.s1LozYAAAEWI.EfVhTI?attachments=MSDS](http://www.merckmillipore.com/germany/chemicals/glycerin/MDA_CHEM-104093/p_L5qb.s1LozYAAAEWI.EfVhTI?attachments=MSDS).
23. Bechtold-Peters, K., *Protein immobilization by crystallization and precipitation: An alternative to lyophilization*, in *Current trends in monoclonal antibody development and manufacturing*, Shire, S.J., et al., editors. 2010: Springer New York. p.149-175.
24. Zölls, S., et al., *Particles in therapeutic protein formulations, Part 1: Overview of analytical methods*. Journal of Pharmaceutical Sciences, 2012. **101**(3): p.914-935.
25. Chen, H., et al., *Shape- and size-dependent refractive index sensitivity of gold nanoparticles*. Langmuir, 2008. **24**(10): p.5233-5237.
26. Demeule, B., et al., *Characterization of particles in protein solutions: Reaching the limits of current technologies*. AAPS Journal, 2010. **12**(4): p.708-715.
27. Sharma, D.K., et al., *Micro-flow imaging: Flow microscopy applied to sub-visible particulate analysis in protein formulations*. AAPS Journal, 2010. **12**(3): p.455-464.

28. Pan, G., et al., *Synthesis of highly fluorinated monodisperse colloids for low refractive index crystalline colloidal arrays*. Journal of the American Chemical Society, 1998. **120**(26): p.6518-6524.
29. Fogg, E.T., Hixson, A.N., and Thompson, A.R., *Densities and refractive indexes for ethylene glycol-water solutions*. Analytical Chemistry, 1955. **27**(10): p.1609-1611.
30. Rajulu, A.V. and Sab, P.M., *Refractometric studies in water/polyethylene glycol-300 mixtures*. European Polymer Journal, 1998. **34**(1): p.31-32.
31. Mahler, H.C., et al., *Protein aggregation: Pathways, induction factors and analysis*. Journal of Pharmaceutical Sciences, 2009. **98**(9): p.2909-2934.
32. Hawe, A. and Friess, W., *Development of HSA-free formulations for a hydrophobic cytokine with improved stability*. European Journal of Pharmaceutics and Biopharmaceutics, 2008. **68**(2): p.169-182.
33. Chi, E.Y., et al., *Physical stability of proteins in aqueous solution: Mechanism and driving forces in nonnative protein aggregation*. Pharmaceutical Research, 2003. **20**(9): p.1325-1336.
34. Wang, W., *Instability, stabilization, and formulation of liquid protein pharmaceuticals*. International Journal of Pharmaceutics, 1999. **185**(2): p.129-188.
35. Wang, W., *Lyophilization and development of solid protein pharmaceuticals*. International Journal of Pharmaceutics, 2000. **203**(1-2): p.1-60.
36. Wang, W., *Protein aggregation and its inhibition in biopharmaceutics*. International Journal of Pharmaceutics, 2005. **289**(1-2): p.1-30.
37. Gekko, K. and Timasheff, S.N., *Mechanism of protein stabilization by glycerol: preferential hydration in glycerol-water mixtures*. Biochemistry, 1981. **20**(16): p.4667-4676.
38. Vagenende, V., Yap, M.G.S., and Trout, B.L., *Mechanisms of protein stabilization and prevention of protein aggregation by glycerol*. Biochemistry, 2009. **48**(46): p.11084-11096.
39. Packhaeuser, C.B., et al., *In situ forming parenteral drug delivery systems: An overview*. European Journal of Pharmaceutics and Biopharmaceutics, 2004. **58**(2): p.445-455.
40. Dunn, R.L., et al., *Biodegradable in-situ forming implants and methods of producing the same*. US4938763, 1990.
41. Dong, W.Y., et al., *Stability of poly(D,L-lactide-co-glycolide) and leuprolide acetate in in-situ forming drug delivery systems*. Journal of Controlled Release, 2006. **115**(2): p.158-167.

42. Tae, G., Kornfield, J.A., and Hubbell, J.A., *Sustained release of human growth hormone from in situ forming hydrogels using self-assembly of fluoroalkyl-ended poly(ethylene glycol)*. *Biomaterials*, 2005. **26**(25): p.5259-5266.
43. Figueiredo, K., et al., *Structural stability of myoglobin in organic media*. *The Protein Journal*, 2009. **28**(5): p.224-232.
44. Pompe, C., *Development of new in-situ hardening and bioactivated composite materials for orthopedic indications* [dissertation]. München: Ludwig-Maximilians-Universität München, 2008.
45. Liu, X., et al., *Effects of polyols on the stability of whey proteins in intermediate-moisture food model systems*. *Journal of Agricultural and Food Chemistry*, 2009. **57**(6): p.2339-2345.
46. Knepp, V.M., et al., *Stability of nonaqueous suspension formulations of plasma derived factor IX and recombinant human alpha interferon at elevated temperatures*. *Pharmaceutical Research*, 1998. **15**(7): p.1090-1095.
47. Wasylaschuk, W.R., et al., *Evaluation of hydroperoxides in common pharmaceutical excipients*. *Journal of Pharmaceutical Sciences*, 2007. **96**(1): p.106-116.
48. Singh, S., et al., *Effect of polysorbate 80 quality on photostability of a monoclonal antibody*. *AAPS PharmSciTech*, 2012. **13**(2): p.422-430.
49. Ha, E., Wang, W., and Wang, Y.J., *Peroxide formation in polysorbate 80 and protein stability*. *Journal of Pharmaceutical Sciences*, 2002. **91**(10): p.2252-2264.
50. Baudys, M. and Kim, S.W., *Peptide and protein characterization*, in *Pharmaceutical formulation development of peptides and proteins*, Frokjaer, S. and Hovgaard, L., editors. 2000. London: Taylor & Francis. p.41-69.
51. Andya, J., Hsu, C., and Shire, S., *Mechanisms of aggregate formation and carbohydrate excipient stabilization of lyophilized humanized monoclonal antibody formulations*. *AAPS Journal*, 2003. **5**(2): p.21-31.
52. Costantino, H.R., et al., *Fourier-transform infrared spectroscopic analysis of the secondary structure of recombinant humanized immunoglobulin G*. *Pharmaceutical Sciences*, 1997. **3**(3): p.121-128.
53. Weichel, M., Bassarab, S., and Garidel, P., *Probing thermal stability of mAbs by intrinsic tryptophan fluorescence*. *BioProcess International*, 2008: p.42-52.
54. Hawe, A., et al., *Forced degradation of therapeutic proteins*. *Journal of Pharmaceutical Sciences*, 2012. **101**(3): p.895-913.
55. Kueltzso, L.A., et al., *Derivative absorbance spectroscopy and protein phase diagrams as tools for comprehensive protein characterization: A bGCSF case study*. *Journal of Pharmaceutical Sciences*, 2003. **92**(9): p.1805-1820.

56. Wakankar, A.A., et al., *The effect of cosolutes on the isomerization of aspartic acid residues and conformational stability in a monoclonal antibody*. Journal of Pharmaceutical Sciences, 2007. **96**(7): p.1708-1718.
57. Dong, A., et al., *Infrared spectroscopic studies of lyophilization- and temperature-induced protein aggregation*. Journal of Pharmaceutical Sciences, 1995. **84**(4): p.415-424.
58. Matheus, S., Friess, W., and Mahler, H.-C., *FTIR and nDSC as analytical tools for high-concentration protein formulations*. Pharmaceutical Research, 2006. **23**(6): p.1350-1363.
59. van Beers, M.M.C., et al., *Oxidized and aggregated recombinant human interferon beta is immunogenic in human interferon beta transgenic mice*. Pharmaceutical Research, 2011. **28**(10): p.2393-2402.
60. Gekko, K. and Koga, S., *The stability of protein structure in aqueous propylene glycol: Amino acid solubility and preferential solvation of protein*. Biochimica et Biophysica Acta - Protein Structure and Molecular Enzymology, 1984. **786**(3): p.151-160.
61. Dib, R., et al., *Secondary structure changes and peptic hydrolysis of  $\beta$ -lactoglobulin induced by diols*. Biopolymers, 1996. **39**(1): p.23-30.
62. Ahmad, B., et al., *Low versus high molecular weight poly(ethylene glycol)-induced states of stem bromelain at low pH: Stabilization of molten globule and unfolded states*. Biopolymers, 2006. **81**(5): p.350-359.
63. Kumar, V., Sharma, V.K., and Kalonia, D.S., *Effect of polyols on polyethylene glycol (PEG)-induced precipitation of proteins: Impact on solubility, stability and conformation*. International Journal of Pharmaceutics, 2009. **366**(1–2): p.38-43.



## Chapter 5

# Development of oily mAb1 PCMC suspensions for subcutaneous administration

This chapter is intended for publication:

K. Berkenhoff, V. Christ, S. Bassarab, W. Friess, Development of oily mAb PCMC suspensions for subcutaneous administration; *in preparation*.

### Abstract

The protein-coated microcrystals (PCMC) technology that is based on coprecipitation offers the possibility to stabilize protein in the solid state. As PCMCs can be administered as subcutaneous suspension by injection appropriate suspensions media are required that are physiologically acceptable and compatible with the protein. The study aimed to develop biocompatible and injectable oily mAb1 PCMC suspensions based on sesame oil, benzyl benzoate and medium-chain triglycerides (MCT) and comprised the development of an appropriate *in vitro* release model, the investigation of protein integrity after release from oily suspensions, the compatibility between the oily solvents and primary packaging material as well as the characterization of rheology and injectability of the suspensions. 100 % recovery of the monoclonal antibody mAb1 was found after 24 h incubation at 40 °C in water with integrated short-term stirring and final centrifugation at 100 g for 30 min. After release from oily PCMC suspensions, the integrity of mAb1 was completely retained with respect to aggregation, secondary and tertiary protein structure and specific antigen binding affinity, irrespective of the choice of oily solvent. The injectability of the oily solvents depended on the siliconization process of the glass syringes and was not affected during 6 months storage at  $22 \pm 3$  °C indicating compatibility with the primary packaging material. Only swelling of the tip caps occurred due to oil uptake. Oily suspensions based on MCT and 70:30 and 30:70 (v/v) mixtures of sesame oil and benzyl benzoate were prepared up to a solid content of 316 mg/mL,

corresponding to 138 mg/mL protein. The viscosity of the suspensions that depended on the viscosity of the oily solvent augmented with increasing solid content and was characterized by shear thinning. A linear relationship between the viscosity and the injectability of the suspensions was revealed. Maximal injection forces were approx. 40 N for a 30:70 (v/v) sesame oil benzyl benzoate suspension with a solid content of 316 mg/mL, opposed to 50 N for the inverse mixture and MCT. Although it was not beneficial with respect to viscosity and injectability compared to a corresponding mAb1 solution, formulating mAb1 as oily PCMC suspension was feasible, including compatibility with the protein and injectability, and thus represents an alternative to high concentration liquid formulations typically associated with challenges such as low solubility, aggregation phenomena and poor overall stability.

## 1 Introduction

Apart from organic water-miscible solvents, analyzed in detail in chapter 4, oily liquids represent potential media for the development of subcutaneous mAb1 PCMC suspensions. Advantages of oily vehicles over organic water-miscible solvents generally include high chemical stability and low toxicity [1, 2]. However, vegetable oils containing large amounts of polyunsaturated fatty acids are prone to the formation of hydroperoxides that might lead to protein instability and increasing overall toxicity [3-6]. The use of highly purified oils that are mostly free of hydroperoxides and other impurities further improves their biocompatibility. As these solvents are not water-miscible, their application is discussed to provide a sustained release effect [1, 3, 7]. Consequently, the frequency of administration can be reduced resulting in higher patient convenience and compliance [3, 7]. Therefore, oily solvents, such as sesame oil or cottonseed oil, are often applied to lipophilic steroid hormones or psychotropic drugs for intramuscular administration providing a depot for sustained drug delivery over several weeks [8, 9]. Though, the general high viscosity of oily solvents is suspected of requiring high injection forces for parenteral administration [10]. The investigation of injectability and syringeability is thus indispensable in the development of oily parenteral formulations [11]. Injectability describes the performance of the formulation during injection, including force or pressure required for injection, evenness of flow and freedom from clogging, whereas syringeability is

defined as ability of an injectable therapeutic to pass easily through a hypodermic needle on transfer from a vial prior to an injection [11-14].

The purpose of the study was to evaluate the three oily solvents sesame oil (S), benzyl benzoate (B) and MCT (M) as resuspension media for mAb1 PCMC powder. Benzyl benzoate was screened as additive to reduce the viscosity of sesame oil based preparations allowing for easier injection because sesame oil has a significantly higher viscosity than MCT. The investigation of the compatibility between the oleaginous vehicles and mAb1 formulated as PCMCs required the development of a suitable in vitro release model ensuring 100 % protein recovery. Subsequently, the integrity (HP-SEC, binding assay) and structure (FT-IR, intrinsic fluorescence, 2<sup>nd</sup>-derivative UV spectroscopy) of the monoclonal antibody was analyzed after release from oily PCMC suspensions. To avoid administration problems arising from the high viscosity of the solvents, the pure oils were tested for injectability. A 6 months storage study of oily vehicles in glass syringes was additionally included to detect potential incompatibility with the primary packaging material suspected of complicating the injection due to swelling phenomena. Finally, the rheology and injectability of oily mAb1 PCMC suspensions was investigated and compared to a high concentration liquid formulation of the protein.

## **2 Materials and methods**

### **2.1 Materials**

L-Phenylalanine, sodium hydroxide, benzyl benzoate and phosphate buffered saline pH 7.4 were purchased from Sigma-Aldrich, Steinheim, D, disodium EDTA dihydrate, hydrochloric acid (1 mol/L), isobutanol (Emplura®) from Merck, Darmstadt, D. Glycine, L-histidine and L-histidine hydrochloride monohydrate were procured from Ajinomoto Omnicem, Louvain-la-Neuve, B. Sodium dihydrogen phosphate dihydrate was delivered by Dr. Paul Lohmann, Hungen, D, sodium chloride by Akzo Nobel, Hengelo, NL, and trehalose dihydrate by Ferro Pfanstiehl, Waukegan, IL, USA. Highly purified sesame oil (Super Refined Sesame NF-LQ-(MH)) was acquired from Croda (Nettetal, D), MCT (Miglyol® 812 N) from Sasol, Witten, D. All chemicals were utilized without further purification.

The protein bulk drug substance provided by Boehringer Ingelheim was composed of 20 mg/mL mAb1, representing a human IgG2 monoclonal antibody, 0.68 mg/mL L-histidine, 3.27 mg/mL L-histidine hydrochloride monohydrate, 0.1 mg/mL disodium EDTA dihydrate, 84.0 mg/mL trehalose dihydrate and 0.02 % polysorbate 80.

The buffer of the bulk drug substance was exchanged via ultra- and diafiltration resulting in a protein solution that consisted of 105.6 mg/mL protein, 0.68 mg/mL L-histidine, 3.27 mg/mL L-histidine hydrochloride monohydrate, 0.1 mg/mL disodium EDTA dihydrate and 56.0 mg/mL trehalose dihydrate (crossflow buffer exchange and concentration unit, Boehringer Ingelheim, Biberach/Riss, D; membrane cassette Sartocoon Slice, Hydrosart, 30 kd, Sartorius, Göttingen, D; Quattroflow 150 S membrane pump, Quattroflow Fluid Systems, Hardegsen, D). Furthermore, polysorbate 80 was present in the protein solution because it cannot be removed via ultra-/diafiltration, as reported by Mahler et al. for polysorbate 20 [15].

## 2.2 Methods

### 2.2.1 PCMC production process

The PCMC production process is divided into four main steps: preparation of protein-carrier solution, precipitation, concentration/solvent exchange, and drying. For the preparation of the protein-carrier solution (Table 4-1) the carrier material was dissolved in deionized water and the solution pH value was adjusted to 5.5 prior to the addition of the protein solution. The final solution was filtered through a 0.22 µm membrane filter (Stericup-GV, 47mm, PVDF, Sartorius, Göttingen, D).

**Table 5-1: Composition of protein-carrier solution.**

Substance	Mass [mg] in 200.0 ml	Percent by weight [%]
mAb1	2239.8	43.6
L-Histidine	27.8	0.5
L-Histidine HCl monohydrate	133.7	2.6
Disodium EDTA dihydrate	4.1	0.1
Glycine	811.1	15.8
L-Phenylalanine	89.5	1.7
Sodium chloride	269.0	5.2
Trehalose dihydrate	1568.1	30.5
Sum	5143.1	100.0

The precipitation was carried out as described in detail by König [16]. Briefly, two equal streams of precipitating agent were mixed with one stream of protein-carrier solution in a small double jet impingement mixer of an inner diameter of 1.5 mm (Boehringer Ingelheim, Biberach/Riss, D). The mixing ratio of the precipitating agent, isobutanol saturated with all carrier components, and the protein-carrier solution was set to 95 : 5 (v/v). The modular mixing platform from Ehrfeld (Bayer Technology, Wendelsheim, D) encompassed three micro gear pumps (HNP pumps mzt 11507 and 7255, Hydraulik Nord Fluidtechnik, Parchim, D), pressure sensors and temperature sensors to monitor the precipitation step. The total flow rate of 1000 mL/min was controlled by the software LabView (National Instruments, Munich, D) and Coriflow mass flow meters (Bronkhorst, Kamen, D). The final suspension volume after precipitation was 4 L.

Solvent exchange was achieved by decanting the supernatant of the PCMC suspension 18 h after the precipitating step. The supernatant was replaced with fresh saturated isobutanol. After 24 h of sedimentation the sediment, i.e. the concentrated suspension, was used for the supercritical drying process (Thar SFE-500, Thar Technologies, Pittsburgh, PA, USA) with carbon dioxide at 100 bar and a flow rate of 25 g/min. After drying of 240 mL concentrated suspension within 90 min at 45 °C the pressure was decreased by 3 bar/min. Subsequently, vacuum drying of the PCMC powder was performed at 125 mbar and 40 °C for 2 h (APT.line™ VDL, Binder, Tuttlingen, D; diaphragm membrane pump MZ 2C, Vacuubrand, Wertheim, D).

### **2.2.2 Development of an in vitro release model for oily PCMC suspensions**

The development of an in vitro release model was based on a mAb1 PCMC sesame oil suspension, prepared by dispersing 305 mg mAb1 PCMC powder in 14.0 mL sesame oil on a magnetic stirrer. 25.0 mL of the aqueous phase, either water for injection (WFI) or 10 mM phosphate buffered saline pH 7.4 (PBS), and 1.25 or 2.5 mL oily suspension were incubated in plastic syringes (Omnifix® 30 mL Luer lock, Braun, Melsungen, D) equipped with a magnetic stirring bar and a tip cap (7025/65 grey, West, Eschweiler, D) (Figure 5-1). The influence of incubation time (24 or 96 h), temperature (22 ± 3, 37.5 or 40 °C), agitation (2 min stirring or 24 h shaking) and centrifugation (10 min, 300 g; Heraeus® Biofuge® primo, Carl Roth, Karlsruhe, D) on protein recovery was analyzed via UV spectroscopy. Stirring in horizontally lying syringes was carried out via magnetic stirrer at 300 rpm (Modell RT 10 power IKAMAG®, IKA, Staufen,

D), while horizontal shaking was performed in a shaking water bath with a frequency of  $130 \text{ min}^{-1}$  (Modell 1086, GFL, Burgwedel, D). After incubation the aqueous phase was harvested through the tip of the syringe and UV measurement (UV/VIS Spectrometer Lambda 20, PerkinElmer, Rodgau-Jügesheim, D) was performed in Halfmicro Plastibrand® cuvettes (Brand, Wertheim, D) at 280 nm, corrected against WFI or PBS, based on an extinction coefficient of 1.43 ( $n=3$ ). Protein recovery was calculated as the quotient of the antibody concentration in the aqueous phase to the theoretical protein concentration of 0.5 or 1.0 mg/mL, based on the antibody fraction in the total solid mass of the protein-carrier solution. If necessary, samples were filtered through a  $0.45 \mu\text{m}$  syringe filter (Rotilabo® Spritzenfilter steril, 33 mm, PVDF, Carl Roth, Karlsruhe, D) prior to UV measurement. In this case, light microscopy (Axio Imager Z2m, Zeiss, Jena, D) was additionally performed to analyze the origin of turbidity.

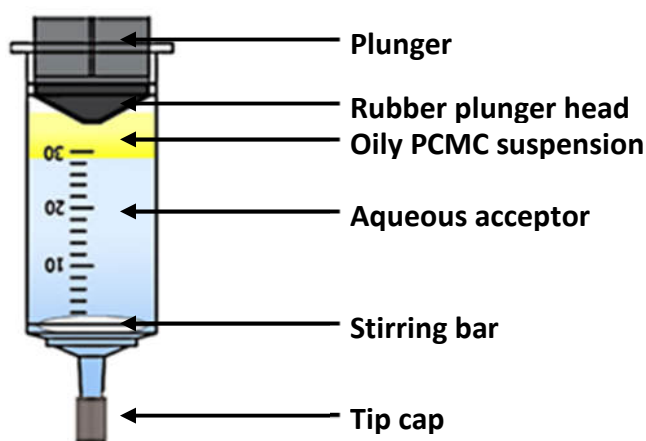


**Figure 5-1: In vitro release model for oily PCMC suspensions.**

### **2.2.3 Compatibility between mAb1 PCMCs and oily solvents**

#### **2.2.3.1 MAb1 release from oily PCMC suspensions**

For the release of mAb1 from oily PCMC suspensions, 25.0 mL WFI and 1.25 mL oily suspension, composed of 27.2 mg mAb1 PCMC powder dispersed into sesame oil, benzyl benzoate or MCT, were incubated in 30 mL plastic syringes for 24 h at  $40 \text{ }^\circ\text{C}$  with integrated 2 min horizontal stirring and final centrifugation for 30 min at 100 g (section 3.1). MAb1 PCMC powder dissolved into WFI, incubated in the same way as the oily suspensions, served as reference. After incubation the aqueous phase was harvested and analyzed for protein integrity.

### 2.2.3.2 Turbidimetry

Turbidity of the native aqueous phase and after 0.45  $\mu\text{m}$  filtration (Rotilabo® Spritzenfilter, 33 mm, PVDF, Carl Roth, Karlsruhe, D) was measured at a protein concentration of 0.5 mg/mL by 90 ° light scattering at  $\lambda = 633 \text{ nm}$  (UH turbidimeter, Boehringer Ingelheim, self-construction) and expressed in formazine nephelometric units (FNU) (n=3).

### 2.2.3.3 Microflow-imaging (MFI)

Microflow imaging analysis of the native aqueous acceptor was performed with a Brightwell DPA 4200 instrument equipped with a 470 nm LED laser and a 100  $\mu\text{m}$  flow cell (Brightwell, Ottawa, Canada) (n=2). Samples were drawn with a peristaltic pump (Masterflex® Plus P/S, Thermo Fisher, Waltham, MA, USA). Before each 0.5 mL sample run within 5 min, 0.22  $\mu\text{m}$  filtered (Steritop, 0.22  $\mu\text{m}$ , PVDF, Millipore, Schwalbach, D) deionized water was flushed through the system to optimize illumination and to achieve a clean baseline. Sesame oil and MCT samples with particle counts above the manufacturer's recommended limit were diluted in 0.22  $\mu\text{m}$  filtered deionized water 5-fold prior to analysis and results were multiplied by 5 to report final particle counts [17, 18].

### 2.2.3.4 Light microscopy

An optical light microscope was used to characterize the native aqueous phase (Axio Imager Z2m, Zeiss, Jena, D).

### 2.2.3.5 Protein recovery

UV measurements were conducted as described in section 2.2.2.

### 2.2.3.6 High pressure size exclusion chromatography (HP-SEC)

The aqueous acceptors were concentrated in the centrifuge prior to analysis (Heraeus® Biofuge® primo, Carl Roth, Karlsruhe, D). The filtration units (Amicon® Ultra-15 Ultracel-30k, Millipore, Schwalbach, D) were rinsed with 10.0 mL 0.1 N NaOH and subsequently equilibrated with water at 3500 g for 10 min. Samples were filtered through a 0.45  $\mu\text{m}$  filter (Rotilabo® Spritzenfilter steril, 33 mm, PVDF, Carl Roth, Karlsruhe, D). Concentration of 6.0 mL samples at 3500 g for 5-10 min resulted in a final protein concentration of approx. 2 mg/mL.

HP-SEC was performed on an Äkta micro (GE Healthcare, Uppsala, Sweden) with a TSKgel G3000SWXL column (7.8 mm ID x 30.0 cm L, Tosoh, Stuttgart, D) and a 40 x 6.0 mm TSKgel SWXL Guardcol precolumn (Tosoh Bioscience, Stuttgart, D) at a flow rate of 1 mL/min. The mobile phase was composed of 60 mM sodium chloride and 5 mM sodium dihydrogen phosphate with a pH adjusted to 7.0. Samples were injected in duplicate (2 x 40 µl) and protein elution was monitored via UV-detection at 280 nm. Aggregation in percent was calculated based on the ratio of the area under the curve (AUC) of soluble aggregates to the total AUC of aggregates and monomer (n=3). Furthermore, changes in AUC were considered.

### **2.2.3.7 Fourier transform infrared spectroscopy**

Sample concentration for FT-IR measurement was conducted in the centrifuge, described in detail in section 2.2.3.6. Concentrated samples were filtered through a 0.45 µm syringe filter (Rotilabo® Spritzenfilter steril, 33 mm, PVDF, Carl Roth, Karlsruhe, D). As amino acids that were used as carrier components of mAb1 PCMCs may interfere with FT-IR analysis [19, 20], diafiltration of 0.75 mL concentrated and filtered samples was performed against 500 mL WFI with stirring at room temperature (Slide-A-Lyzer® Dialysis Cassette G2 MWCO 20,000, Thermo Scientific, Rockford, IL, USA). WFI was exchanged twice within 18 h of diafiltration.

FT-IR spectroscopy was performed using a Tensor 37 and a Confocheck measuring cell (Bruker, Ettlingen, D). Spectra were recorded from 4000 to 900 cm<sup>-1</sup> with 120 scans and a resolution of 2 cm<sup>-1</sup> at 25° C (n=3). Atmospheric compensation was done and WFI served as reference. Spectra were processed by vector normalization prior to calculating the average spectrum based on three measurements. Second derivative was built applying 17 smoothing points (Savitzky-Golay algorithm).

### **2.2.3.8 Intrinsic fluorescence spectroscopy**

Samples of 0.1 mg/mL protein in SUPRASIL® 114-QS precision cuvettes (10 mm, Hellma, Mühlheim, D) were excited at 295 nm and 25 °C. The emission was scanned from 305 to 400 nm with a step size of 1 nm and 1 s integration time (Fluorimeter QM-4-CW, PTI, Birmingham, NJ, USA). The evaluation was based on normalized spectra (n=3).

### 2.2.3.9 2<sup>nd</sup>-derivative UV spectroscopy

Samples of 0.3 mg/mL protein were scanned from 240 to 350 nm (UV/VIS Spectrometer Lambda 20, PerkinElmer, Rodgau-Jügesheim, D). The second derivative of the absorption was used (n=3).

### 2.2.3.10 Binding assay

mAb1 prevents the target antigen from binding to a specific cell surface protein (CSP). Consequently, binding activity of the antibody to the target antigen was analyzed according to BI internal method using a competitive ELISA following typical protocols [21]. Briefly, mAb1 and the target antigen were added to CSP immobilized on a microtiter plate. Decreasing concentration of mAb1 resulted in decreasing inhibition of binding of target antigen to CSP. After the addition of goat anti-mouse-IgG horseradish peroxidase that bound to CSP and of tetramethylbenzidine dye, the amount of colored product, being inversely proportional to the binding activity of the antibody, was measured based on the absorption at 450 nm (n=2).

## 2.2.4 Characterization of oleaginous solvents and oily suspensions

### 2.2.4.1 Viscosity

Viscosity was determined by a cone-plate rheometer (Haake RheoStress 600, Thermo Electron, Karlsruhe, D) equipped with a 35 mm 1° angle cone (C35/1, Thermo Electron, Karlsruhe, D). Recorded in the range of  $\dot{\gamma}$ = 10-2000/s at 20 °C, viscosity was determined at  $\dot{\gamma}$ = 1000/s (n=3).

### 2.2.4.2 Preparation of oily mAb1 suspensions

Mixing of mAb1 PCMC powder and oily solvents was performed in 10 R or 20 R vials (Fiolax® clear, Schott, Mühlheim, D) via vortexer (MS2 Minishaker, IKA, Wilmington, NC, USA) at 1500 min<sup>-1</sup> until a visually even dispersion was observed. The solid content of the oily suspensions finally ranged from 133 to 316 mg/mL, corresponding to 58-138 mg/mL protein.

### 2.2.4.3 Syringe filling

With respect to the oily solvents, baked-on siliconized and spray siliconized 1 mL long syringes (RTF-syringe with luer cone, Gerresheimer, Düsseldorf, D) with tip caps (7025/65 grey, West, Eschweiler, D) were manually filled with 1 mL oil (sesame oil, benzyl benzoate or MCT) and closed with rubber stoppers. Manual closing was performed by the use of a 1 inch 18 G needle

(Becton Dickinson, Heidelberg, D), resulting in a headspace of approx. 2 mm. The rubber stoppers were either coated with a fluorocarbon film (FluroTec PH4023/50, grey, West, Eschweiler, D) or a fluorinated polymer (Omniflex FM257/2, Hoelvet, Karlsbad, D).

For injectability testing of the oily mAb1 suspensions, spray siliconized 1 mL long syringes (RTF-syringe with luer cone, Gerresheimer, Düsseldorf, D) equipped with tip caps (7025/65 grey, West, Eschweiler, D) and rubber stoppers (FluroTec PH4023/50, grey, West, Eschweiler, D) were manually filled with 1 mL suspension.

#### **2.2.4.4 Injectability**

Injectability testing was performed with a tensile compression testing machine (Zwicki-TN1S, Zwick, Ulm, D) at a crosshead speed of 100 mm/min and  $22 \pm 3$  °C (n=6). The syringes were vertically inserted with the tip downwards and injection of pure oils and oily PCMC suspensions was carried out into air. Force-displacement curves were recorded to calculate the mean force required to expel the oils from the syringe, in the range from 8 to 29 mm. For injectability testing of the oily solvents, 23 G 1 inch needles (BD Microlance™ 33 Nr. 16, Becton Dickinson, Heidelberg, D) were used. Thin wall 23 G 1 inch needles (Terumo Neolus, Leuven, B) served for the investigation of the injectability of oily PCMC suspensions. Furthermore, thin wall 20 G 1 inch and 25 G 1 inch needles (Terumo Neolus, Leuven, B) were utilized to analyze the influence of the inner needle diameter on injectability.

#### **2.2.4.5 Light microscopy**

Light microscopy was performed as presented in 2.2.3.4.

#### **2.2.4.6 X-ray powder diffraction**

The crystallinity of mAb1 PCMCs was analyzed with XRD in transmission mode from  $3^\circ$ -  $40^\circ$   $2\theta$ ,  $0.5^\circ$  steps and 20 s/step based on  $1.5406 \text{ \AA}$  CuK $\alpha$ -radiation at 40 kV and 40 mA (Stoe, Darmstadt, D). Samples were fixed in the sample holder between two Ultraphan foils (cellulose diacetate) with a thickness of 0.014 mm (Stoe, Darmstadt, D).

#### **2.2.4.7 Swelling of stoppers and tip caps**

The swelling of stoppers (FluroTec PH4023/50, grey, West, Eschweiler, D; Omniflex FM257/2, Hoelvet, Karlsbad, D) and tip caps (7025/65 grey, West, Eschweiler, D) was investigated after

incubation over 24, 48 and 98 h in a beaker with sesame oil, benzyl benzoate or MCT. The height of stoppers and the length of tip caps were measured with a caliper (n=3).

#### **2.2.4.8 Storage of prefilled syringes**

Storage of oily solvents was performed with baked-on siliconized and spray siliconized syringes (see section 2.2.4.3 for detailed preparation) equipped with West rubber stoppers (FluroTec PH4023/50, grey, West, Eschweiler, D) and tip caps (7025/65 grey, West, Eschweiler, D). The syringes were stored horizontally in the dark at  $22 \pm 3$  °C for 3 and 6 months (n=6).

#### **2.2.4.9 Concentration of liquid mAb1 formulation**

Concentration of mAb1 bulk, containing 3.27 mg/mL L-histidine HCl monohydrate, 0.68 mg/mL L-histidine, 84.0 mg/mL trehalose dihydrate and 0.1 mg/mL disodium EDTA dihydrate, was conducted via centrifugation, described in detail in section 2.2.3.6. Buffer, equivalent to the composition of the protein bulk, was used for equilibration of the filtration units. Solutions with final protein concentrations of 63, 83, 120, 127, 151, 172 and 193 mg/mL, measured via UV spectroscopy (section 2.2.3.5), were analyzed for viscosity and injectability.

### **3 Results and discussion**

#### **3.1 Development of an in vitro release model for oily PCMC suspensions**

The aim of this investigation was to optimize the incubation conditions for mAb1 PCMC sesame oil suspensions to achieve 100 % protein recovery, prerequisite for assessing the entire mAb population in subsequent analysis of protein stability. The release process, performed in 30 mL plastic syringes, encompassed three steps, namely sedimentation of the PCMC powder towards the oil-water interface, dissolution of the PCMC powder and diffusion of the protein, and the carrier components, into the aqueous acceptor. The influence of the maximal protein concentration in the aqueous phase, the composition of the aqueous phase, variation of incubation time and temperature as well as agitation and final centrifugation on protein recovery and macroscopic appearance of the oily and the aqueous phase was investigated.

**Table 5-2: Influence of incubation conditions on protein recovery: agitation: <sup>a</sup> integrated 2 min stirring with a magnetic stirrer at 300 rpm; <sup>b</sup> continuous shaking with a frequency of 130 min<sup>-1</sup> for 24 h in a water bath; centrifugation: 30 min at 100 g**

	Incubation conditions						Protein recovery [%]
	C <sub>mAb</sub> [mg/mL]	Incubation time [h]	T [°C]	Agitation	Aqueous phase	Centrifugation	
A	0.5	24	22 ± 3	-	WFI	-	42.5 ± 1.9
B	1.0	24	22 ± 3	-	WFI	-	32.3 ± 1.8
C	0.5	24	40	-	WFI	-	62.2 ± 2.3
D	0.5	24	40	-	PBS	-	21.0 ± 0.8
E	0.5	24	40	+ <sup>a</sup>	WFI	+	99.9 ± 0.8
F	0.5	24	40	-	WFI	+	98.9 ± 1.3
G	0.5	96	40	-	WFI	-	95.2 ± 1.1
H	0.5	96	40	-	WFI	+	103.4 ± 1.1
I	0.5	24	37.5	+ <sup>b</sup>	WFI	+	84.7 ± 3.2

After incubation at 22 ± 3 °C or 40 °C for 24 h without agitation or centrifugation (A-D, Table 5-2), the aqueous acceptor medium and the upper part of the oily phase were clear. Many powder particles were detected by the naked eye in the oil close to the liquid-liquid interface. Their number was reduced in samples incubated at 40 °C for 96 h (G) or for 24 h and 96 h in combination with final centrifugation (F, H), all showing clear aqueous phases. Hence, prolonged incubation time at an elevated temperature as well as centrifugation supported the sedimentation of PCMC powder in sesame oil allowing for faster dissolution of the particles.

Applying 24 h incubation at 40 °C with 2 min of integrated horizontal stirring (E) resulted in the dispersion of the oil into numerous small droplets floating on the opalescent aqueous phase and not substantially coalescing during final centrifugation (Figure 5-2). Considering the surface-activity of proteins, the mAb fraction located at the oil-water interface was assumed to reduce the surface energy and thus to prevent the oil droplets from coalescence, as likewise described in the area of protein-silicone oil interactions [22-24]. Furthermore, proteins are widely applied for the stabilization of emulsions and foams, for example in food industry [25, 26]. Similarly to stirring, continuous shaking (I) of oily PCMC suspensions resulted in a powder-free oily phase composed of many non-coalesced droplets. As suggested by their macroscopic appearance (Figure 5-2), the microscopic analysis of the aqueous acceptors revealed the

presence of oil droplets after integrated short-term stirring, in contrast to supplementary protein particles in the case of continuous shaking (Figure 5-3).

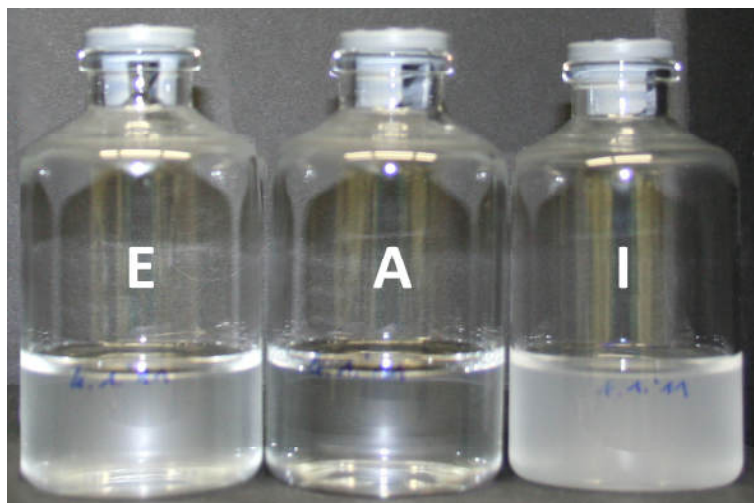


**Figure 5-2: Macroscopic appearance of aqueous acceptor after incubation with sesame oil mAb1 PCMC suspension; incubation conditions: left: 0.5 mg/mL protein, 24 h at 40 °C, WFI, integrated 2 min stirring, centrifugation (E), middle: 0.5 mg/mL protein, 24 h at 40 °C, WFI, no agitation or centrifugation (A), right: 0.5 mg/mL protein, 24 h shaking at 37.5 °C, WFI, centrifugation (I).**

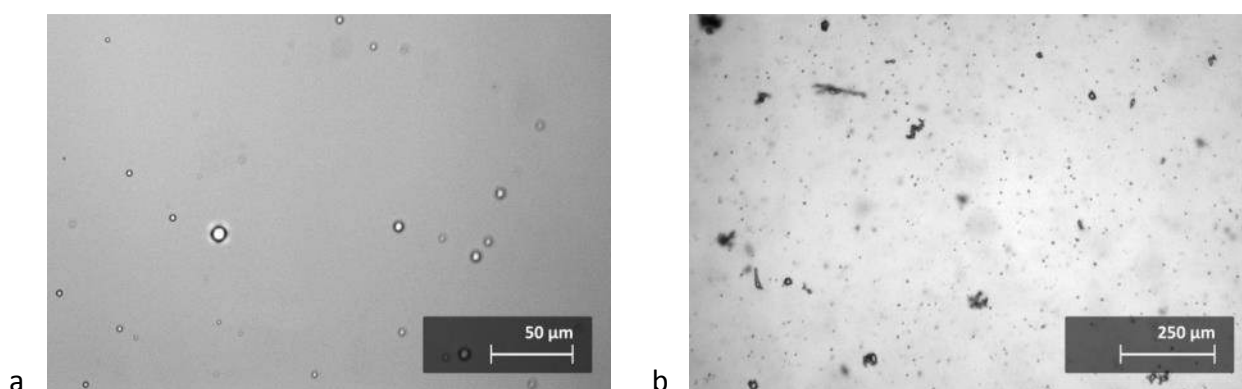


**Figure 5-3: Microscopic appearance of aqueous acceptor after incubation with sesame oil mAb1 PCMC suspension; a) oil droplets, incubation conditions: 0.5 mg/mL protein, 24 h at 40 °C, WFI, 2 min stirring, centrifugation (E); b) oil droplets and protein particles, incubation conditions: 0.5 mg/mL protein, 24 h shaking at 37.5 °C, WFI, centrifugation (I).**

In accordance with literature, the oil droplets had a circular cross section with an annular appearance [17, 18, 27], whereas the protein particles were of heterogeneous shape [18, 28]. Thus, continuous shaking led to the formation of insoluble protein aggregates, but not integrated short-term stirring. The potential destabilizing effect of silicone oil on proteins is

ambiguously discussed. For example, Li et al. as well as Ludwig et al. found that different proteins did not undergo homogenous aggregation in the presence of silicone oil [23, 28], whereas Thirumangalathu et al. observed synergistic stimulation of aggregation by a combination of silicone oil and agitation [24]. Unlike static isothermal incubation, continuous shaking at 350 rpm for several days resulted in a substantial loss of mAb monomer at both 4 °C and 37 °C [24]. In contrast, slight short-term agitation, namely shaking for 5 min at 78 rpm, had no impact on the aggregation level of albinterferon alfa-2b [17].

Table 5-2 summarizes the influence of the incubation conditions on the protein recovery in the aqueous phase. Increasing the maximal protein concentration in the aqueous acceptor from 0.5 to 1.0 mg/mL decreased the protein recovery by approx. 10 % (A: 43 % → B: 32 %). Probably, this was a simple effect of increased powder amount e.g. impeding the sedimentation and the surface contact of the individual particles. Moreover, the antibody release from the oily suspension was significantly augmented with increasing temperature (A: 43 % → B: 62 %), presumably in consequence of reduced viscosity facilitating the sedimentation of the PCMC powder towards the oil-water interface, and with prolonged incubation time (C: 62 % → G: 95 %). Centrifugation, which accelerates the transport of the powder particles to the liquid-liquid interface, further improved the protein recovery when incubation was performed for either 96 h (G: 95 % → H: 103 %) or 24 h (A: 43 % → F: 99 %). Combining final centrifugation and agitation increased the amount of protein released from the oily suspension by approx. 40 % (C: 62 % → E: 100 %) in the case of short-term stirring and by approx. 20 % when continuous shaking was performed in the water bath for 24 h (C: 62 % → I: 85 %). The incomplete protein recovery after shaking can be attributed to the formation of insoluble protein aggregates, as previously discussed.

The use of 10 mM PBS pH 7.4 instead of WFI as acceptor medium considerably decreased the protein recovery (C: 62 % → D: 21 %). A clear solution formed when mAb1 PCMC powder was simply dissolved in 10 mM PBS pH 7.4 at 1 mg/mL protein, but increasing turbidity could be noticed within 24 h at  $22 \pm 3$  °C. These observations pointed at reduced solubility of at least one mAb1 PCMC component in PBS buffer.

Overall, higher temperature, prolonged incubation time, the use of water as acceptor as well as short-term stirring and final centrifugation turned out to improve the release of the antibody. On the other hand, the use of PBS buffer resulted in reduced protein recovery and continuous shaking caused protein aggregation as indicated by an increase in turbidity. Consequently, incubation with WFI at 40 °C for 24 h with integrated short-term stirring and final centrifugation (E) was chosen as optimal incubation conditions for the subsequent investigation of the compatibility between mAb1 PCMCs and oily solvents.

### 3.2 Compatibility between mAb1 PCMCs and oily solvents

The compatibility study aimed to investigate whether the antibody could be released to 100 % from sesame oil, benzyl benzoate and MCT mAb1 PCMC suspensions without any deleterious effect, including aggregation, structural perturbation or decrease in specific binding activity. Only very few literature is available concerning the stability of protein released from oily suspensions [29], but protein instability resulting from exposure to oil-water interfaces is widely discussed in the area of protein-silicone oil interactions [17, 22-24, 27, 28, 30-33].

**Table 5-3: Turbidity and subvisible particle count in the native aqueous phase after incubation with sesame oil, benzyl benzoate and MCT mAb1 PCMC suspension; reference sample: mAb1 PCMC powder in WFI.**

	Turbidity [FNU]	Particles 1-50 $\mu\text{m}$ [ $10^3\text{ml}^{-1}$ ]	Non-oily particles 5-50 $\mu\text{m}$ [ $\text{ml}^{-1}$ ]
<b>Sesame oil</b>	18.9 $\pm$ 2.2	3441 $\pm$ 342	9865 $\pm$ 7581
<b>Benzyl benzoate</b>	5.8 $\pm$ 1.6	41 $\pm$ 13	5286 $\pm$ 1570
<b>MCT</b>	17.5 $\pm$ 1.5	4876 $\pm$ 1278	2447 $\pm$ 823
<b>Reference</b>	0.5 $\pm$ 0.1	29 $\pm$ 5	1498 $\pm$ 522

Turbidity measurements are frequently performed to detect insoluble protein aggregates of medium size [34, 35], typically  $< 1 \mu\text{m}$  [36]. Compared to the reference (0.5 FNU), the turbidity of the aqueous acceptor media after incubation with the oily PCMC suspensions was significantly higher, ranging from 6 to 19 FNU (Table 5-3), and was noticeable by the naked eye. As the particles could be removed via 0.45  $\mu\text{m}$  filtration, as indicated by turbidity values below the calibration limit of the turbidimeter (1.5 FNU) after filtration, they were assumed to be very large. Optical light microscopy revealed the presence of numerous oil droplets in all unfiltered aqueous phases (Figure 5-4). The absence of proteinaceous particles in light microscopy

indicated that the antibody formulated as PCMCs was released from the oily suspensions without forming significant amounts of insoluble aggregates, irrespective of the choice of oil. Additionally, microflow imaging was performed as orthogonal method because it may allow for differentiation between insoluble protein particles and dispersed oil droplets [18]. The total number of subvisible particles with a size of 1-50  $\mu\text{m}$  correlated well with the turbidity values (Table 5-3). As the vast majority (86-98 %) of particles were smaller than 5  $\mu\text{m}$ , an adequate aspect ratio could not be analyzed and, thus, the differentiation between these two types of particles was not feasible [18, 30]. The number of non-oily larger particles (5-50  $\mu\text{m}$ ) detected after incubation with oleaginous suspensions was not significantly higher than for the reference, except for sesame oil (Table 5-3).

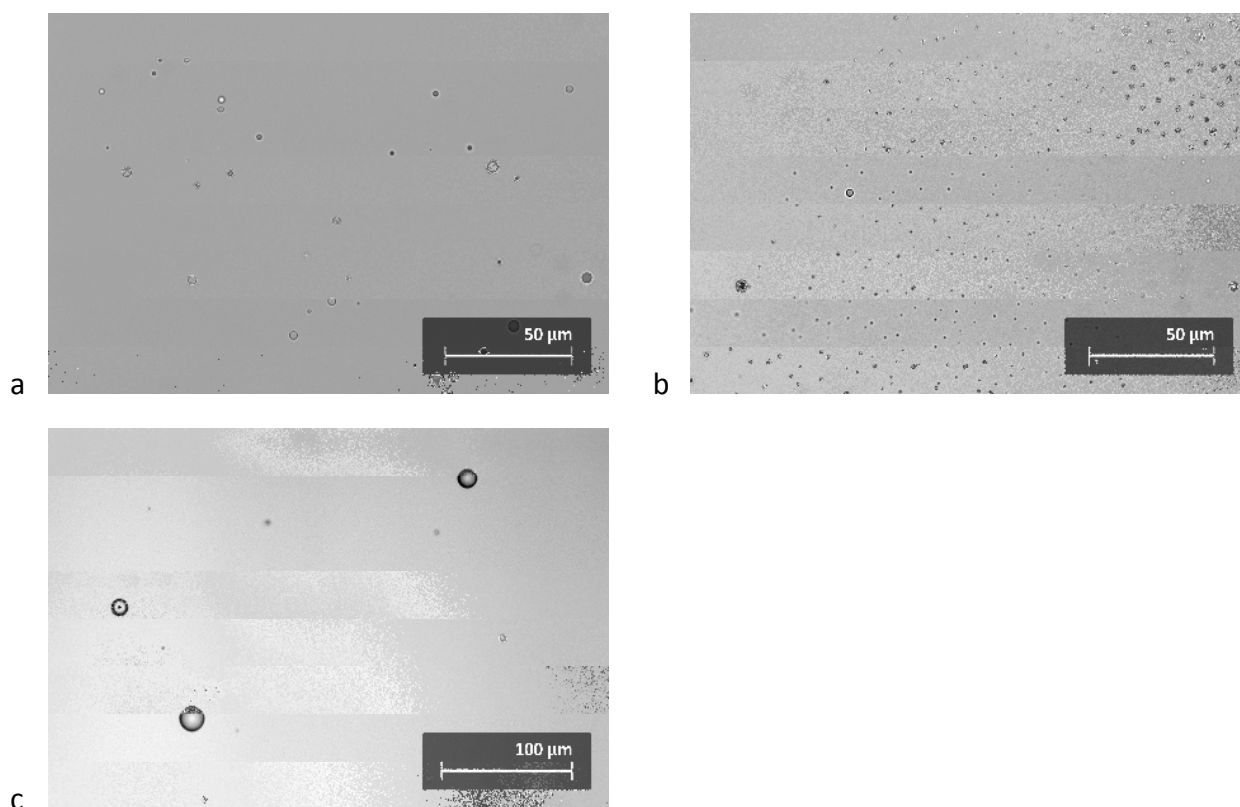


**Figure 5-4: Microscopic appearance of native aqueous acceptor after mAb1 release from a) sesame oil, b) MCT and c) benzyl benzoate PCMC suspension.**

Irrespective of the type of oil, the antibody was completely recovered in the aqueous phase with a monomer level of approx. 99 % detected via HP-SEC. Hence, the incubation with oily suspensions did not induce the formation of soluble mAb1 aggregates, at least not to a significant extent.

Similarly to the investigations on organic water-miscible solvents (chapter 4), several spectroscopic methods, namely FT-IR, intrinsic fluorescence and 2<sup>nd</sup>-derivative UV spectroscopy were used to analyze the secondary and tertiary IgG structure after release [37]. Independent of the oily solvent, the release did not change the secondary or tertiary conformational structure of the monoclonal antibody because all spectra were identical to the one recorded after incubation of mAb1 PCMCs with pure water (Figure 5-5). In FT-IR, typical intramolecular  $\beta$ -sheet bands occurred at 1692 and 1637  $\text{cm}^{-1}$  showing the predominance of  $\beta$ -sheets in IgGs [38, 39]. Well-resolved bands at frequencies of 1678 and 1662  $\text{cm}^{-1}$  represented turn structure and peaks at 1616  $\text{cm}^{-1}$  could be attributed either to more  $\beta$ -sheet structure or to side-chain effects [38, 39]. The emission maximum revealed via intrinsic fluorescence spectroscopy was located at a wavelength of  $\lambda = 327$  nm for benzyl benzoate and the reference sample and at  $\lambda = 328$  nm for sesame oil and MCT (Figure 5-5b). 2<sup>nd</sup>-derivative UV spectra of mAb1 released from oily suspensions as well as incubated with WFI (reference sample) were characterized by peak minima occurring at 271, 284 and 292 nm, while peak maxima were found at 262, 279, 289 and 297 nm (Figure 5-5c). The application of these spectroscopic methods in the development of protein formulations is described in detail in section 3.2 of chapter 4. The effect of silicone oil on the secondary and tertiary protein structure has widely been addressed [17, 23, 24, 33]. Although the structure of the proteins investigated was not substantially affected by the presence of silicone oil, the authors agree that silicone oil might nevertheless impact a small population of the particular protein, the rest remaining unaltered, and that certain biophysical methods are not sensitive enough to detect these small amounts of silicone-oil induced conformational changes.

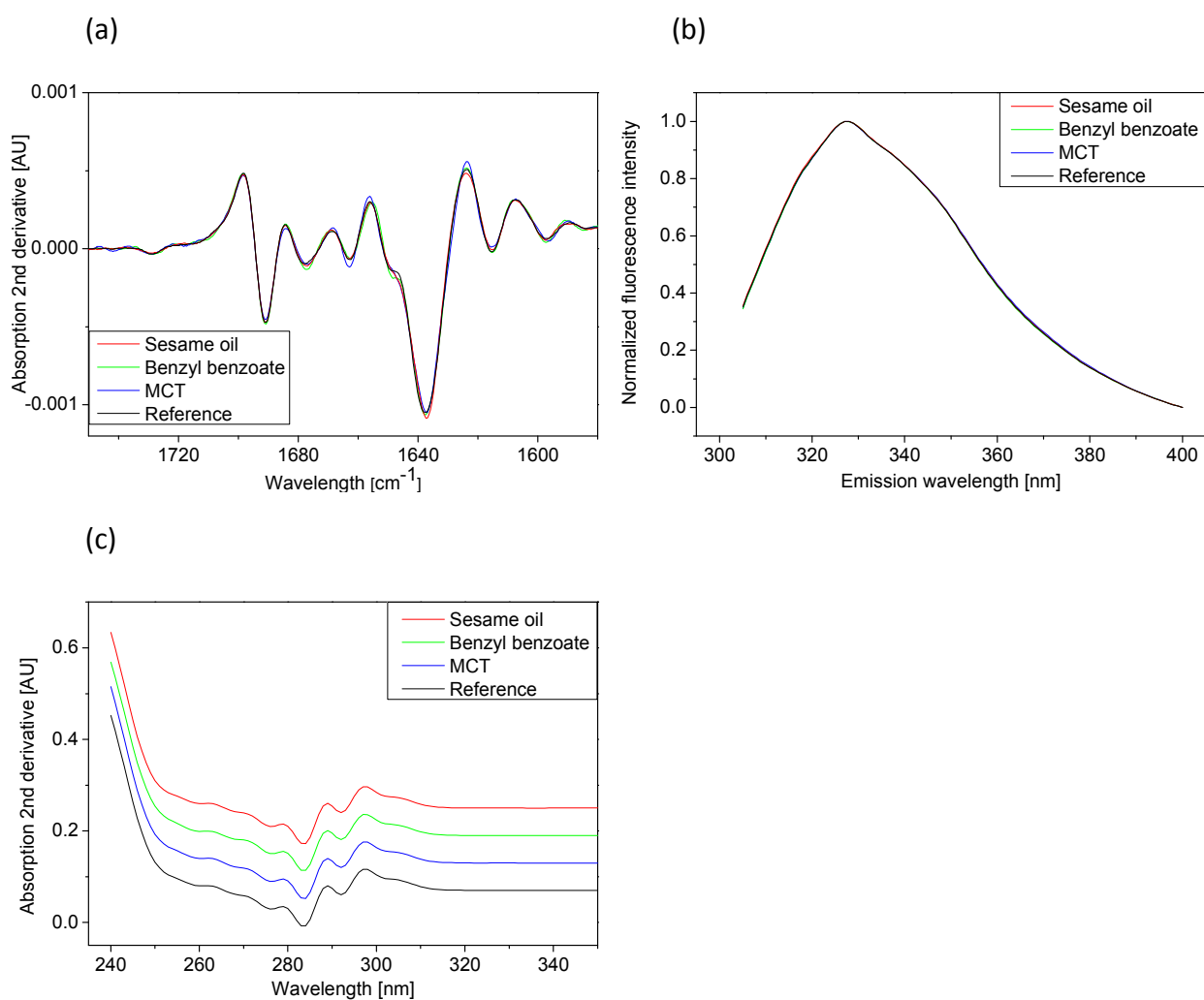


**Figure 5-5: Protein structure of mAb1 in the native aqueous phase after release from sesame oil, benzyl benzoate and MCT PCMC suspension: (a) FT-IR spectroscopy, (b) intrinsic fluorescence spectroscopy, (c) 2<sup>nd</sup>-derivative UV spectroscopy; reference sample: mAb1 PCMC powder in WFI.**

An ELISA was conducted to verify that also the specific antigen binding affinity of the antibody released from the oily PCMC suspension was not affected. Figure 5-6 visualizes that, independent of the oily vehicle, the binding activity was completely retained after release from the oily PCMC suspensions, compared to the PCMC reference sample. All values were within the specification limits of 65-130 % of the standard reference sample.

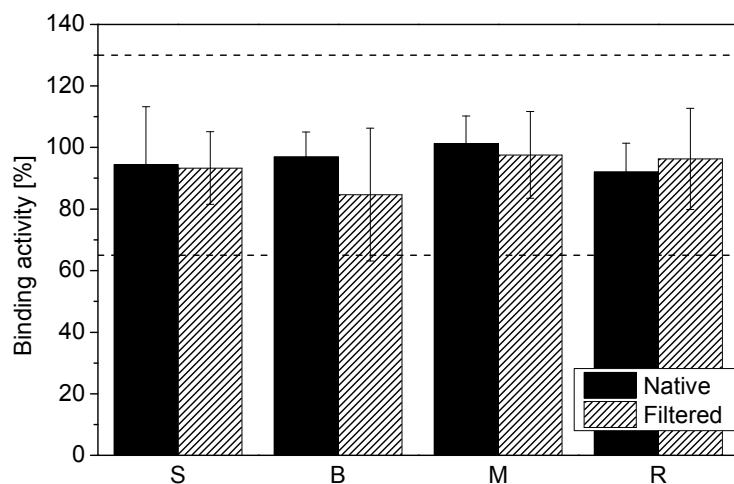


**Figure 5-6: Binding activity of mAb1 in the native and filtered aqueous phase after release from sesame oil (S), benzyl benzoate (B) and MCT (M) PCMC suspension; reference sample (R): mAb1 PCMC powder in WFI.**

Thus, neither significant protein loss nor any hint to conformational nor binding relevant changes due to protein adsorption at the oil-water interface was observed for mAb1 released from oily PCMC suspensions.

### **3.3 Injectability of oily solvents and compatibility with primary packaging material**

Although the need for functionality test procedures of pre-filled syringes and auto-injector packaged parenteral formulations is addressed in EMA and FDA guidelines, there are only very little corresponding case studies during protein product development [40, 41]. For the evaluation of oily vehicles as suspension media for PCMCs, the viscosity and the injectability of sesame oil, benzyl benzoate, MCT and mixtures made of sesame oil and benzyl benzoate were analyzed. Moreover, pre-filled syringes were stored for 6 months at room temperature to test the compatibility between the oily solvents and the primary packaging material. Swelling of stoppers and tip caps after incubation in the oils was additionally investigated.

#### **3.3.1 Viscosity and injectability of oily solvents**

The viscosity of pure sesame oil was 71.8 mPas. The addition of increasing amounts of benzyl benzoate, having a viscosity of 10.3 mPas, successively decreased the viscosity of the mixtures (Table 5-4). A viscosity of 31.1 mPas was detected for pure MCT.

**Table 5-4: Viscosity of sesame oil (S), benzyl benzoate (B), MCT and sesame oil benzyl benzoate mixtures (v/v) measured at  $\dot{\gamma}=1000\text{ s}^{-1}$ .**

Oily solvent	Viscosity [mPas]
Sesame oil	$71.8 \pm 0.9$
S:B 90:10	$56.7 \pm 0.3$
S:B 70:30	$37.4 \pm 0.5$
S:B 50:50	$25.1 \pm 0.2$
S:B 30:70	$16.6 \pm 0.1$
S:B 10:90	$12.1 \pm 0.2$
Benzyl benzoate	$10.3 \pm < 0.1$
MCT	$31.1 \pm 0.3$

Injectability tests provided force-displacement plots, exemplarily shown in Figure 5-7 for baked-on siliconized syringes. They were characterized by an initial maximum indicating the break-loose force of the stopper [10], followed by a permanent, slight increase representing the forces required to inject the oil through the needle. Amongst others, it was influenced by kinetic energy that needs to be imparted to the fluid and by friction forces of the stopper in the syringe barrel [11]. The sharp decline at approx. 29 mm depicted the end of the injectability testing.

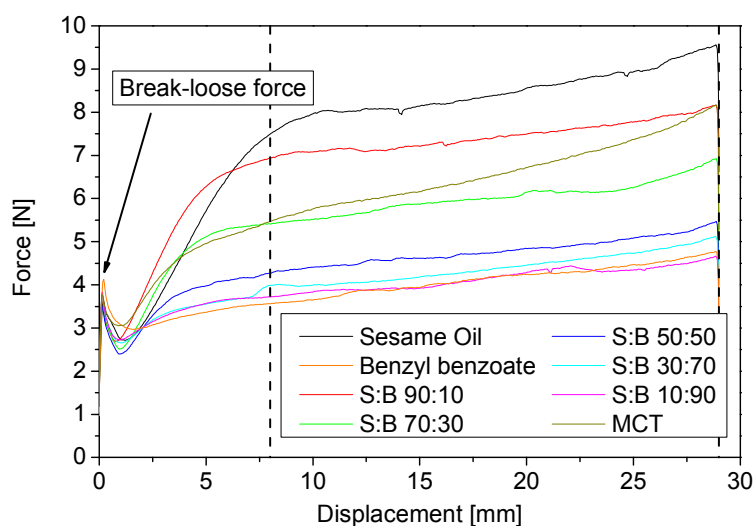


**Figure 5-7: Force-displacement curve of sesame oil (S), benzyl benzoate (B), MCT and sesame oil benzyl benzoate mixtures (v/v) expelled from baked-on siliconized syringes via 23 G 1 inch needle; vertical lines indicate the limits used for calculation of mean force.**

Without needle the mean force recorded for the injection of sesame oil, benzyl benzoate and mixtures thereof in baked-on siliconized syringes ranged from 3.3 to 3.8 N, independent of the amount of benzyl benzoate. 4.3 N were required in the case of MCT, as opposed to 4.5 N detected for syringes filled with air instead of oil. Thus, the injection force of the syringes was reduced in the presence of sesame oil and/or benzyl benzoate, acting as lubricant, but not in the presence of MCT.

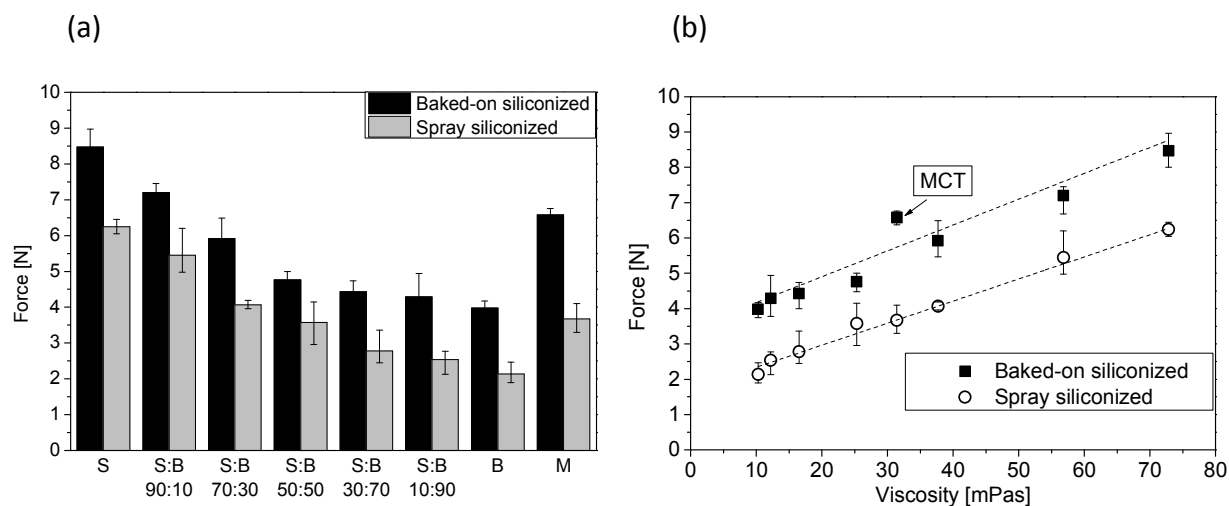


**Figure 5-8: Force required to expel sesame oil (S), benzyl benzoate (B), MCT (M) and sesame oil benzyl benzoate mixtures (v/v) from syringes through a 23 G 1 inch needle; (b) in dependence of viscosity measured at  $\dot{\gamma} = 1000 \text{ s}^{-1}$ ; linear regression  $y = 0.073x + 3.44$   $R^2 = 0.821$  (baked-on siliconized),  $y = 0.063x + 1.71$   $R^2 = 0.995$  (spray siliconized).**

For syringes equipped with a 1 inch 23 G needle significantly higher injection forces were detected (Figure 5-8a). The injection of pure sesame oil from baked-on siliconized syringes resulted in a mean force of 8.5 N. With increasing amounts of benzyl benzoate the forces decreased steadily down to a mixing ratio of 50:50 (v/v) because the viscosity of the oily mixtures continuously diminished. Further addition of benzyl benzoate did not significantly reduce the injection force because, in this range, the impact of the viscosity was overlaid by other effects, such as the gliding force of the stopper. This could also be seen in Figure 5-8b showing an overall linear correlation between the injection force and the viscosity of the oily solvents. The linear correlation corresponds to the Hagen-Poiseuille equation that describes the pressure drop ( $p_1$ ) in a fluid flowing through a cylindrical line and that can thus be applied to the injection via syringe (Equation 5-1). In Equation 5-1,  $F_1$  is the injection force and  $t$  the

injection time, while  $V$  and  $\eta$  describe the volume and the viscosity of the fluid,  $A_1$  is the internal barrel area,  $r_1$  the inner barrel radius,  $r_2$  the inner needle radius and  $l_2$  the needle length.

$$F_1 = p_1 * A_1 = \frac{8r_1^2 l_2 \eta V}{r_2^4 t} = D * \frac{\eta V}{t} \quad (5-1)$$

Hence, based on viscosity data the injection force of oily vehicles could be predicted. MCT (6.6 N) deviated from the straight line which was attributed to a less pronounced lubricating effect. The deviating behavior of MCT was also reflected in a considerably steeper force-displacement curve than for the other oils (Figure 5-7).

Furthermore, compared to baked-on siliconized syringes, significantly lower injection forces were detected when spray siliconized syringes were used (Figure 5-8), because baked-on siliconized syringes contained approx. 0.05 mg as opposed to spray siliconized syringes with  $0.8 \pm 0.2$  mg silicone oil [42], confirming the results reported by Badkar et al. [31]. However, the use of spray siliconized syringes could substantially reduce the injection force. But it has to be considered that spray siliconization is associated with a higher risk of particle formation in the subvisible range originating from silicone oil droplets with or without precipitated protein [31].

### 3.3.2 Compatibility between oily solvents and primary packaging material

Dexter and Shott observed diffusion of oil into the rubber matrix of syringe stoppers that caused the rubber to swell [10]. Swollen rubber could release higher amounts of leachables/extractables into the oily solvent which may affect protein stability, as e.g. reported by Badkar et al [31]. Therefore, the compatibility between the oils and the primary packaging material, namely stoppers and tip caps, was investigated.

The incubation of stoppers with pure sesame oil, benzyl benzoate and MCT for 24-98 h at room temperature did not affect the stoppers' height, as presented in Table 5-5. In contrast, incubated tip caps significantly increased in length which was also noticeable by the naked eye. Both components were made of bromobutyl rubber, but, as opposed to the tip caps, the stoppers were coated with a fluorocarbon film or a fluorinated polymer intended to reduce the interaction between rubber and drug product. This coating prevented the rubber from uptake of the oily vehicles. Consequently, in the development of the final application device for oily

PCMC suspensions, attention should be paid to inert coatings of rubber materials to ensure that the components in contact with the drug product do not have any detrimental effect [43].

**Table 5-5: Stoppers` and tip caps` height [mm] after storage in sesame oil, benzyl benzoate and MCT for 24 h, 48 h and 98 h.**

#### Helvoet stoppers

Oily solvent	Initial value	24 h	48 h	98 h
Sesame oil	$8.0 \pm 0.1$	$8.0 \pm < 0.1$	$8.0 \pm 0.1$	$8.0 \pm < 0.1$
Benzyl benzoate	$8.0 \pm 0.1$	$8.0 \pm 0.1$	$8.0 \pm 0.1$	$8.0 \pm < 0.1$
MCT	$8.0 \pm 0.1$	$8.0 \pm < 0.1$	$8.0 \pm 0.1$	$8.0 \pm < 0.1$

#### West stoppers

Sesame oil	$8.2 \pm 0.1$	$8.3 \pm < 0.1$	$8.3 \pm < 0.1$	$8.3 \pm 0.1$
Benzyl benzoate	$8.2 \pm 0.1$	$8.3 \pm 0.1$	$8.3 \pm 0.1$	$8.2 \pm 0.1$
MCT	$8.2 \pm 0.1$	$8.2 \pm < 0.1$	$8.2 \pm 0.1$	$8.2 \pm < 0.1$

#### Tip caps

Sesame oil	$16.3 \pm 0.1$	$16.7 \pm 0.1$	$16.8 \pm 0.1$	$17.2 \pm 0.1$
Benzyl benzoate	$16.3 \pm 0.1$	$17.0 \pm < 0.1$	$17.2 \pm < 0.1$	$17.3 \pm 0.1$
MCT	$16.3 \pm 0.1$	$16.9 \pm 0.1$	$17.3 \pm 0.1$	$17.7 \pm 0.1$

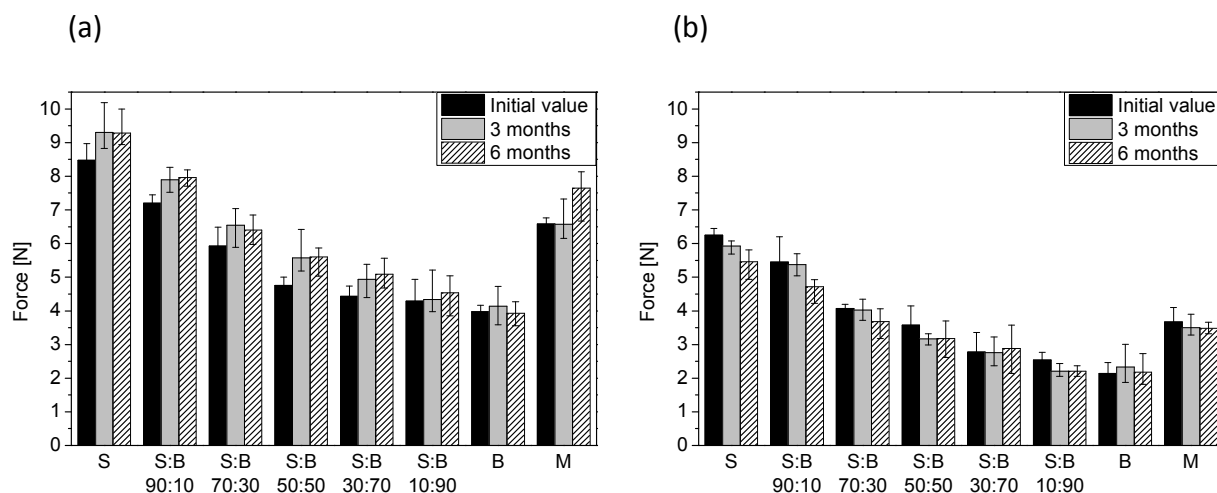


**Figure 5-9: Required force to expel sesame oil (S), benzyl benzoate (B), MCT (M) and sesame oil benzyl benzoate mixtures (v/v) from syringes after 3 and 6 months storage; (a) baked-on siliconized syringes; (b) spray siliconized syringes.**

Furthermore, incompatibility between the primary packaging material and the oily solvents could result in increasing injection forces. Therefore, injectability was tested after 3 and 6 months storage of syringes at room-temperature. Independent of the composition of the oily vehicle, the injection forces did not significantly change over storage time for baked-on and

spray siliconized syringes (Figure 5-9). Thus, apart from the tip caps, the compatibility between the syringes and the oils was proven.

### 3.4 Characterization of oily mAb1 PCMC suspensions

For the investigation of rheology and injectability of oily mAb1 PCMC suspensions, mixtures of sesame oil and benzyl benzoate with mixing ratios of 30:70 and 70:30 (v/v) as well as pure MCT were chosen as solvents. MCT and the sesame oil benzyl benzoate mixture 70:30 (v/v) were selected because they had approximately the same viscosity, whereas the viscosity of the 30:70 (v/v) mixture of sesame oil and benzyl benzoate was significantly lower (Table 5-4 in section 3.3.1). The influence of inner needle diameter on injectability was analyzed, too. Moreover, the sedimentation behavior of oily mAb1 PCMC suspensions was evaluated and injectability data was compared to the values of a corresponding liquid formulation.

#### 3.4.1 Appearance and rheology of oily mAb1 PCMC suspensions

Macroscopically even oily mAb1 PCMC suspensions were prepared up to a solid content of 316 mg/mL. Optical polarization microscopy revealed the presence of two particle fractions, birefringent needle-like crystals and fine anisotropic amorphous material (Figure 5-10). The crystals composed of  $\alpha$ -glycine, as detected via XRD analysis (Figure 5-11), were already present in the initial PCMC powder and were not a consequence of potential recrystallization of carrier material in the oily suspensions.

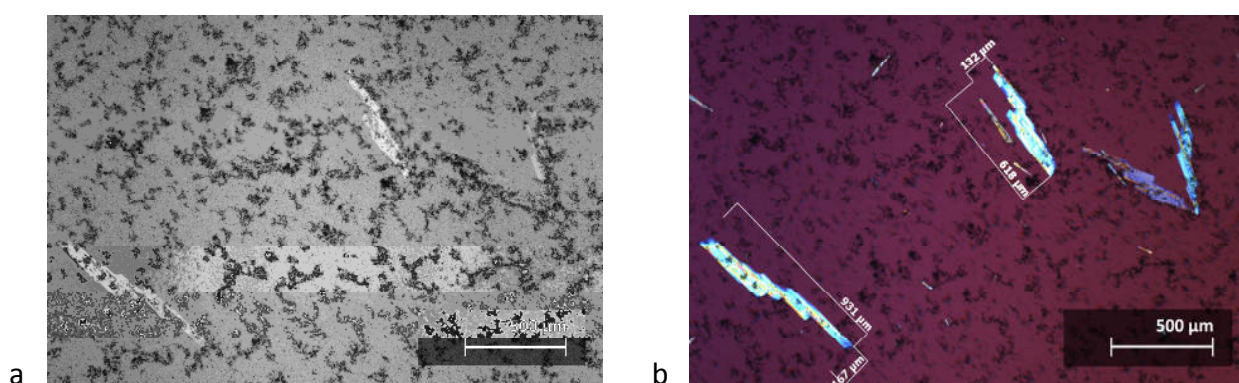


**Figure 5-10: Optical light microscopy of S:B 30:70 (v/v) PCMC suspension with a solid content of 224 mg/mL; (a) without and (b) with polarizing filters.**

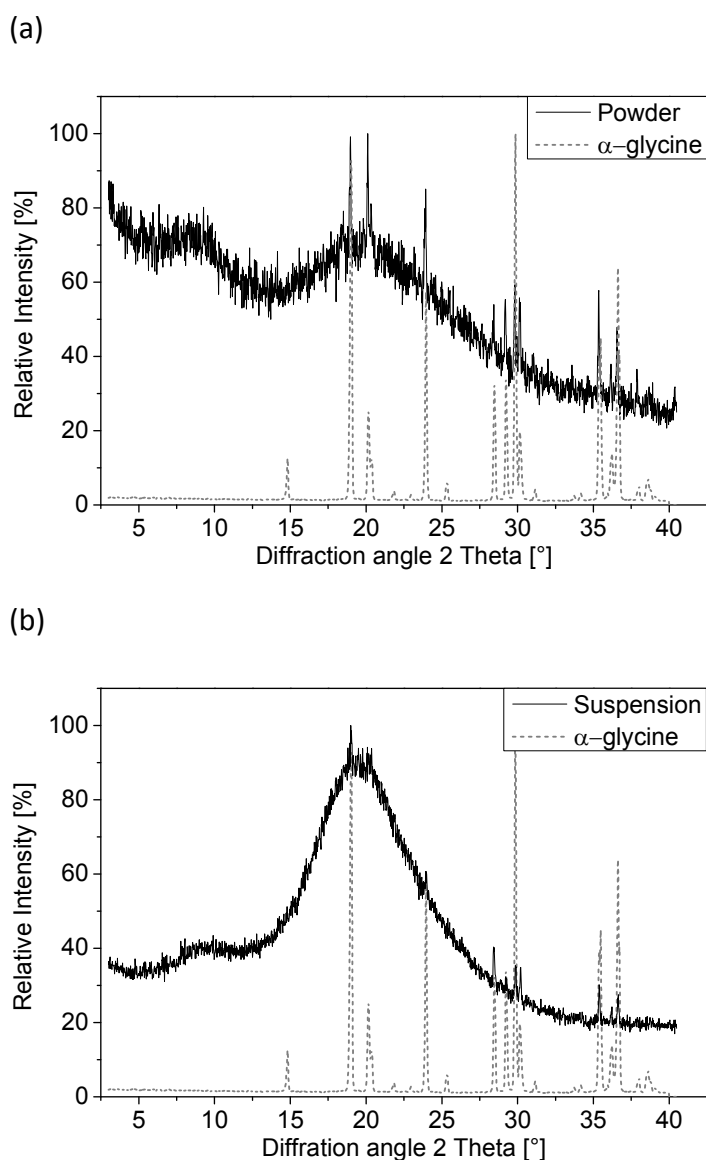


**Figure 5-11: XRD analysis of mAb1 formulated as (a) PCMC powder and (b) S:B 30:70 (v/v) PCMC suspension with a solid content of 224 mg/mL.**

The viscosity of the oily mAb1 PCMC suspensions depended on the viscosity of the pure oily media. Suspensions made of sesame oil and benzyl benzoate with a mixing ratio of 30:70 (v/v) were significantly less viscous than those containing either a 70:30 (v/v) mixture or MCT. As exemplarily presented in Figure 5-12a, the rheograms recorded for the oily mAb1 PCMC suspensions all demonstrated shear thinning or pseudoplastic flow behavior [44]. This effect was more pronounced with increasing solid content and is typical of concentrated suspensions [45]. It is widely believed that shear thinning is caused by realignment of the particles reducing the energy dissipated under shear [46]. However, based on light-scattering experiments,

Ackerson associated shear thinning to a distortion of the liquid-like structure assumed to decrease the energy dissipation [47]. Moreover, shearing at 1000 and 2000  $s^{-1}$  for several seconds resulted in continuously decreasing viscosity of the suspensions, referred to as thixotropy (Figure 5-12b). Microscopic inspection precluded at least substantial modification of suspended particles under extreme shear stress.

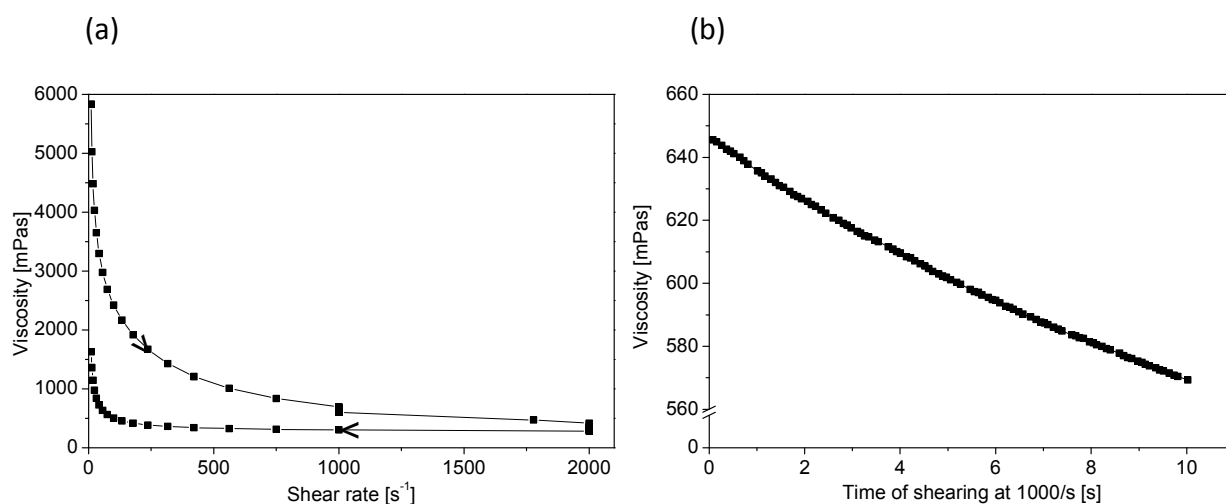


**Figure 5-12: Rheology of S:B 30:70 (v/v) mAb1 PCMC suspension with a solid content of 316 mg/mL; (a) viscosity in dependence of shear rate; (b) viscosity measured at  $\dot{\gamma} = 1000 s^{-1}$  over time.**

According to the equation of Einstein (Equation 5-2), valid for diluted suspensions with spherical particles that do not influence each other and show Newtonian flow behavior, the viscosity of the suspension ( $\eta$ ) depends on the viscosity of the suspension medium ( $\eta_0$ ) and on the volume fraction of suspended particles ( $\varphi_2$ ).

$$\eta = \eta_0 + \eta_0 * 2.5 * \varphi_2 \quad (5-2)$$

In contrast, oily mAb1 PCMC suspensions showed a nonlinear increase in viscosity with increasing volume fraction (Figure 5-13), potentially attributed to interactions between suspended particles [48].

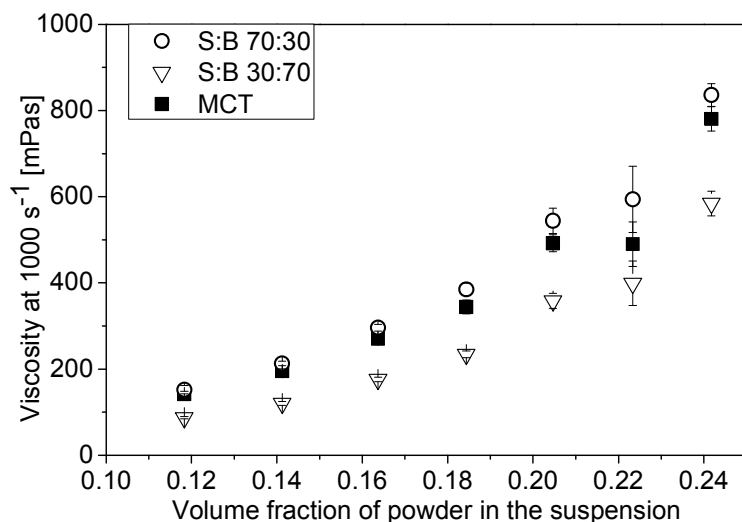


**Figure 5-13: Viscosity of oily mAb1 PCMC suspensions in dependence of the volume fraction of powder.**

### 3.4.2 Injectability of oily mAb1 PCMC suspensions

All oily mAb1 PCMC suspensions investigated were manually and mechanically injectable without any clogging phenomenon. Irrespective of the oily solvent, the injection force augmented nonlinearly with increasing solid content of the suspensions (Figure 5-14a). Due to the linear relationship between viscosity and injection force (Figure 5-14b), viscosity measurements are well suitable to predict the injectability of the oily formulations.

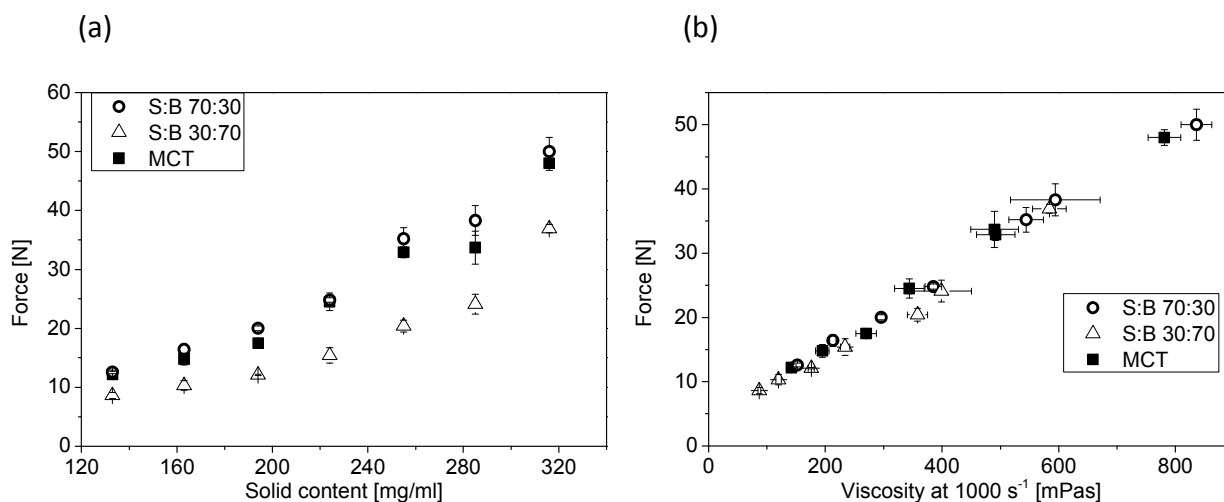


**Figure 5-14: Injection force for oily mAb1 PCMC suspensions; (a) in dependence of solid content; (b) in dependence of the viscosity measured at  $\dot{\gamma} = 1000 \text{ s}^{-1}$ , linear regression:  $y = 0.05x + 4.4$   $R^2 = 0.997$  (S:B 70:30 v/v),  $y = 0.06x + 2.1$   $R^2 = 0.982$  (S:B 30:70 v/v),  $y = 0.06x + 3.1$   $R^2 = 0.982$  (MCT).**

Moreover, the influence of the inner needle diameter on the injection force for S:B 30:70 (v/v) mAb1 PCMC suspensions with a solid content of 224 mg/mL was studied for 20 G ( $670 \pm 8 \mu\text{m}$ ), 23 G ( $416 \pm 3 \mu\text{m}$ ) and 25 G ( $328 \pm 5 \mu\text{m}$ ) needles. The inner needle diameter was measured based on SEM pictures (supplementary material). A linear relationship between the injection force and the fourth power of the inner needle diameter was revealed (Figure 5-15), in accordance to the Hagen-Poiseuille law (Equation 5-1 in section 3.3.1). Hence, the injection force could easily be calculated for needles with different inner needle diameter.

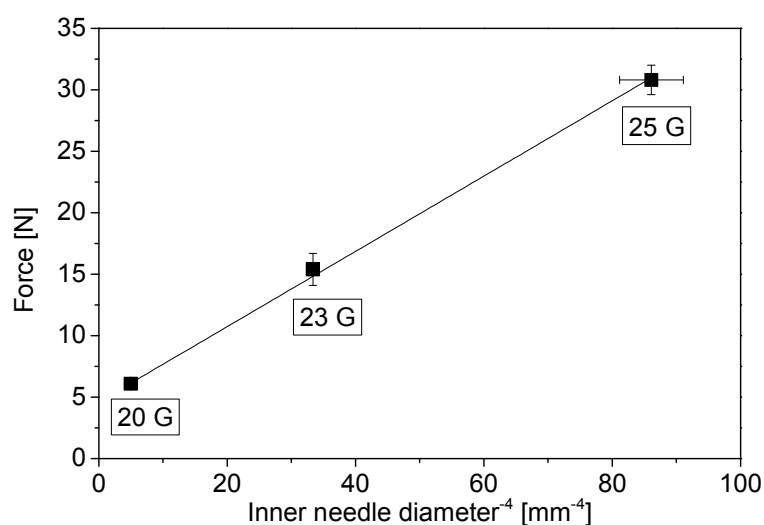


**Figure 5-15: Injection force for S:B 30:70 (v/v) mAb1 PCMC suspensions with a solid content of 224 mg/mL in dependence of inner needle diameter; linear regression:  $y = 0.31x + 4.6$   $R^2 = 0.999$ .**

Subcutaneous injectability can easily be modulated by the choice of needle and syringe, e.g. referring to inner needle diameter, needle length, plunger diameter and siliconization of the syringe. But these parameters also influence the convenience of injection for the patient. For example, the use of a needle with larger diameter is associated with increased injection pain. General recommendations of both appropriate testing procedure and maximal acceptable injection force are missing in the current Pharmacopoeias and various injectability values are reported in literature (Table 5-6). With respect to the oily PCMC suspensions, all formulations were physically injectable under the skin because the maximal injection force for the suspensions with a solid content of 316 mg/mL and a protein concentration of approx. 140 mg/mL was 50 N for MCT and the sesame oil benzyl benzoate mixture with a mixing ratio of 70:30 (v/v), as opposed to 40 N for the 30:70 (v/v) sesame oil benzyl benzoate mixture.

**Table 5-6: Injectability values reported in literature.**

Needle	Force / pressure	Description	Reference
20,22,26 G	> 45-50 N	Difficult to inject	[49]
20, 23 G	50 N		[50]
16 G	621-800 kPa	Typical adult male hand grip strength for single administration	[51]
	344-482 kPa	Typical adult male hand grip strength for multiple administration	
18 G	1193 kPa		[52]
	112 N	Maximum force of the thumb of male students generated within 3-5 s	[53]
13, 15, 17-27 G	13 N	Tolerable for an adult to maintain for 1 min	[54]
18, 20-25, 27 G	11-25 N	Easy to inject	[55]
	26-50 N	Injectable	
	51-100 N	Injectable with some difficulty	
	100-130 N	Difficult to inject	
	20 N	Easy to generate for a physician	[56]

### 3.4.3 Comparison of mAb1 formulated as oily PCMC suspension and liquid formulation

The viscosity and injection force of oily mAb1 PCMC suspensions were compared to a liquid formulation of the monoclonal antibody, containing the same excipients as the PCMCs. The viscosity of the liquid formulation and consequently also the injection force were considerably smaller than the values for the oily suspensions with the same protein concentration (Figure 5-16). Hence, formulating mAb1 as oily PCMC suspension instead of high concentration liquid formulation was not beneficial with respect to injectability. In contrast, a significant decrease of viscosity was observed by Miller et al. for nonaqueous suspensions of lysozyme based on benzyl benzoate and safflower oil, compared to a high concentration liquid formulation of the enzyme [57]. A similar finding was described by Yang et al. for subcutaneous formulations of monoclonal antibodies [58]. A suspension of infliximab in 10 % ethanol and 10 % PEG 3350 with 125 mg/mL protein had a viscosity of approx. 20 mPas, whereas the viscosity of a corresponding liquid formulation was significantly higher, with a value of approx. 85 mPas [58]. Furthermore, it has to be considered that mAb1 used in the current study on oily PCMC suspensions showed very low viscosity values, even for high protein concentrations. For

example, the viscosity at a protein concentration of approx. 120 mg/mL was only about 7 mPas. Liu al. as well as Kanai et al. found considerable higher viscosity of approx. 50 mPas for a liquid 120 mg/mL mAb1 formulation, which highly depended on pH and ionic strength of buffer and charged excipients [59, 60]. Nevertheless, the viscosity of this liquid mAb formulation was significantly lower than the values detected for oily mAb1 PCMC suspensions with comparable protein concentration. Thus, apart from limited solubility and aggregation phenomena often associated with high concentration protein solutions [61], formulating mAbs as oily PCMC suspensions could only be advantageous in the case of extremely high viscosity of the liquid injectable.

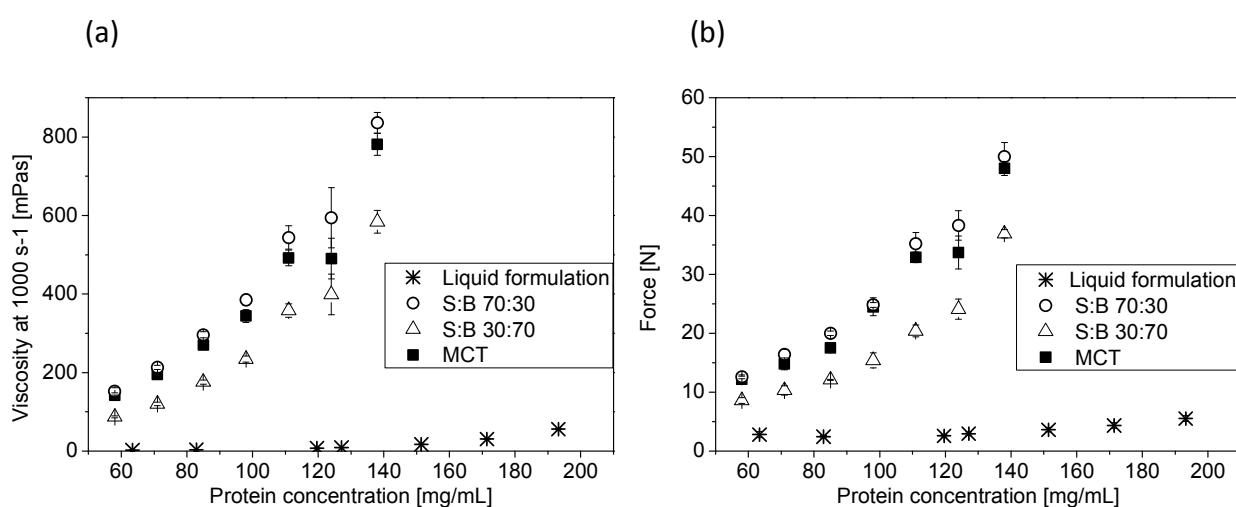


**Figure 5-16: Comparison of mAb1 formulated as oily PCMC suspension and liquid formulation with respect to (a) viscosity and (b) injection force in dependence of protein concentration.**

#### 3.4.4 Sedimentation behavior of oily mAb1 PCMC suspensions

As part of the stability testing, the sedimentation behavior of oily mAb1 PCMC suspensions based on sesame oil and benzyl benzoate mixtures with mixing ratios of 70:30 and 30:70 (v/v) as well as on MCT was monitored in vertically stored spray siliconized glass syringes over 26 d ( $t_{26d}$ ) at  $22 \pm 3$  °C. In all cases, hindered settling characterized by clear supernatants increasing with time occurred, exemplarily shown for MCT in Figure 5-17 (for S:B 70:30 and S:B 30:70 see supplementary material). With increasing solid content the volume of the clear supernatant decreased, independent of the choice of oily vehicle. Based on the height of supernatant the sedimentation rate decreased in the following order: MCT > S:B 70:30 > S:B 30:70. As no

compacted sediment formed during settling, the oily suspensions could be successfully resuspended.

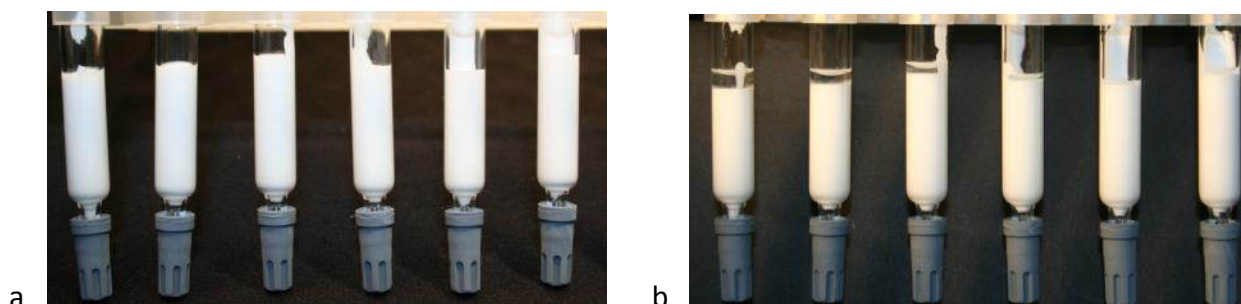


**Figure 5-17: Sedimentation behavior of MCT mAb1 PCMC suspensions at (a)  $t_0$  and (b)  $t_{26d}$ ; solid content from left to right: 133, 163, 194, 224, 255 and 285 mg/mL.**

## 4 Conclusion

The development of oily mAb1 PCMC suspensions with sesame oil, benzyl benzoate and MCT as resuspension media required the design of an appropriate *in vitro* release model. Prolonged incubation time, higher temperature, the use of water as acceptor medium as well as short-term stirring and final centrifugation ensured 100 % protein recovery after the release from oily mAb1 PCMC suspensions and enabled the analysis of protein integrity despite of considerable amounts of dispersed oil droplets in the aqueous acceptor. The analytical focus was on insoluble and soluble aggregates, protein secondary and tertiary structure as well as on binding activity of the antibody. Neither the formation of insoluble protein particles or soluble aggregates was detected nor did the spectroscopic methods indicate changes in the mAb's secondary and tertiary structure. Specific antigen binding affinity of the antibody was completely retained. As the antibody could quantitatively transfer from the oily suspensions into the aqueous phase without measurable deleterious effect, these oleaginous media represent appropriate vehicles for the suspension of mAb1 coated microcrystals.

MCT, sesame oil and benzyl benzoate as well as mixtures of the latter two could all be easily expelled from baked-on and spray siliconized glass syringes. The maximal mean injection force did not exceed 9 N. Spray siliconization of the syringes significantly reduced the injection forces because it resulted in a higher amount of the lubricant silicone oil present in the syringes. Injectability of baked-on siliconized syringes was not affected during 6 months storage at room

temperature. Coated stoppers were compatible with the oily solvents, as opposed to uncoated tip caps which swelled due to oil uptake.

Based on MCT and mixtures of sesame oil and benzyl benzoate with a mixing ratio of 70:30 and 30:70 (v/v), mAb1 PCMC suspensions were prepared up to a solid content of 316 mg/mL, corresponding to 138 mg/mL protein. The suspensions showed hindered settling, decreasing with increasing solid content, and could be resuspended without any residual compacted sediment. The rheology of the suspensions was characterized by shear thinning behavior and the viscosity increased nonlinearly with increasing solid content. Suspensions made of sesame oil and benzyl benzoate 30:70 (v/v) were significantly less viscous than MCT and S:B 30:70 (v/v) suspensions due to lower viscosity of the suspension medium. As a linear relationship between the viscosity and the injectability was revealed, the injection forces followed the same trend as the viscosity. All suspensions were injectable without any clogging phenomenon and the injection forces were in an acceptable range with a maximal mean injection force of approx. 40 N for the 316 mg/mL mAb1 PCMC suspensions in sesame oil and benzyl benzoate 30:70 (v/v) and of 50 N for MCT and S:B 30:70 (v/v). Compared to the corresponding mAb1 solutions, formulating the antibody as oily PCMC suspension was not beneficial with respect to viscosity and ease of administration by injection. As the viscosity of the oily mAb1 PCMC suspensions was also significantly higher than viscosity values of liquid high concentration mAb formulations described in literature, this dosage form would only be advantageous in the case of extremely high viscosity of protein solutions, e.g. due to gelation. However, other challenges typically associated with the development of high concentration liquid formulations, including pronounced aggregation tendency, reduced solubility and poor overall stability, might be overcome by the choice of oily PCMC suspension as promising alternative dosage form for therapeutic proteins.

## 5 References

1. Spiegel, A.J. and Noseworthy, M.M., *Use of nonaqueous solvents in parenteral products*. Journal of Pharmaceutical Sciences, 1963. **52**: p.917-927.
2. Traul, K.A., et al., *Review of the toxicologic properties of medium-chain triglycerides*. Food and Chemical Toxicology, 2000. **38**(1): p.79-98.

3. Berry, S.A., et al., *Stable non-aqueous single phase viscous vehicles and formulations utilizing such vehicles*. WO00/45790, 2000.
4. Knepp, V.M., et al., *Stability of nonaqueous suspension formulations of plasma derived factor IX and recombinant human alpha interferon at elevated temperatures*. *Pharmaceutical Research*, 1998. **15**(7): p.1090-1095.
5. Singh, S., et al., *Effect of polysorbate 80 quality on photostability of a monoclonal antibody*. *AAPS PharmSciTech*, 2012. **13**(2): p.422-430.
6. Wasylaschuk, W.R., et al., *Evaluation of hydroperoxides in common pharmaceutical excipients*. *Journal of Pharmaceutical Sciences*, 2007. **96**(1): p.106-116.
7. Goldenberg, M., et al., *Polyol/oil suspensions for the sustained release of proteins*. WO00/38652, 2005.
8. Füller, W., *Vehikel und Hilfsmittel zur Herstellung von Injektionslösungen von Steroidhormonen*. *Pharmaceutica Acta Helvetiae*, 1972. **47**: p.449-456.
9. Strickley, R., *Solubilizing excipients in oral and injectable formulations*. *Pharmaceutical Research*, 2004. **21**(2): p.201-230.
10. Dexter, M.B. and Shott, M.J., *The evaluation of the force to expel oily injection vehicles from syringes*. *Journal of Pharmacy and Pharmacology*, 1979. **31**: p.497-500.
11. Cilurzo, F., et al., *Injectability evaluation: An open issue*. *AAPS PharmSciTech*, 2011. **12**(2): p.604-609.
12. Akers, M.J., Fites, A.L., and Robinson, R.L., *Formulation design and development of parenteral suspensions*. *Journal of Parenteral Science and Technology*, 1987. **41**(3): p.88-96.
13. Ballard, B.E., *Biopharmaceutical considerations in subcutaneous and intramuscular drug administration*. *Journal of Pharmaceutical Sciences*, 1968. **57**(3): p.357-378.
14. Chien, Y.W., Przybyszewski, P., and Shami, E.G., *Syringeability of nonaqueous parenteral formulations - Development and evaluation of a testing apparatus*. *Journal of Pharmaceutical Science and Technology*, 1981. **35**(6): p.281-284.
15. Mahler, H.C., et al., *Behaviour of polysorbate 20 during dialysis, concentration and filtration using membrane separation techniques*. *Journal of Pharmaceutical Sciences*, 2008. **97**(2): p.764-774.
16. König, C., et al., *Development of a pilot-scale manufacturing process for protein-coated microcrystals (PCMC): Mixing and precipitation – Part I*. *European Journal of Pharmaceutics and Biopharmaceutics*, 2012. **80**(3): p.490-498.
17. Auge, K.B., et al., *Demonstrating the stability of albinterferon alfa-2b in the presence of silicone oil*. *Journal of Pharmaceutical Sciences*, 2011. **100**(12): p.5100-5114.

18. Sharma, D.K., Oma, P., and Krishnan, S., *Silicone microdroplets in protein formulations. Detection and enumeration*. *Pharmaceutical Technology*, 2009. **33**(4): p.74-76, 78-79.
19. Tian, F., et al., *Spectroscopic evaluation of the stabilization of humanized monoclonal antibodies in amino acid formulations*. *International Journal of Pharmaceutics*, 2007. **335**(1-2): p.20-31.
20. Meyer, J.D., et al., *Infrared spectroscopic studies of protein formulations containing glycine*. *Journal of Pharmaceutical Sciences*, 2004. **93**(5): p.1359-1366.
21. Renneker, S., et al., *Development of a competitive ELISA for detection of theileria annulata infection*. *Transboundary and Emerging Diseases*, 2008. **55**(5/6): p.249-256.
22. Dixit, N., Maloney, K.M., and Kalonia, D.S., *The effect of Tween® 20 on silicone oil–fusion protein interactions*. *International Journal of Pharmaceutics*, 2012. **429**(1–2): p.158-167.
23. Li, j., et al., *Mechanistic understanding of protein-silicone oil interactions*. *Pharmaceutical Research*, 2012. **29**(6): p.1689-1697.
24. Thirumangalathu, R., et al., *Silicone oil- and agitation-induced aggregation of a monoclonal antibody in aqueous solution*. *Journal of Pharmaceutical Sciences*, 2009. **98**(9): p.3167-3181.
25. Dickinson, E., *Adsorbed protein layers at fluid interfaces: interactions, structure and surface rheology*. *Colloids and Surfaces B: Biointerfaces*, 1999. **15**(2): p.161-176.
26. McClements, D.J., *Protein-stabilized emulsions*. *Current Opinion in Colloid & Interface Science*, 2004. **9**(5): p.305-313.
27. Liu, L., et al., *Silicone oil microdroplets and protein aggregates in repackaged Bevacizumab and Ranibizumab: Effects of long-term storage and product mishandling*. *Investigative Ophthalmology & Visual Science*, 2011. **52**(2): p.1023-1034.
28. Ludwig, D.B., et al., *Protein adsorption and excipient effects on kinetic stability of silicone oil emulsions*. *Journal of Pharmaceutical Sciences*, 2010. **99**(4): p.1721-1733.
29. Rutz, A., *Ölige Suspensionen als parenterale Depotsysteme* [dissertation]. München: Ludwig-Maximilians-Universität München, 2007.
30. Adler, M., *Challenges in the development of pre-filled syringes for biologics from a formulation scientist's point of view*. *American Pharmaceutical Review*, 2012. **15**(1): p.96, 98-101.
31. Badkar, A., et al., *Development of biotechnology products in pre-filled syringes: technical considerations and approaches*. *AAPS PharmSciTech*, 2011. **12**(2): p.564-572.
32. Kamerzell, T.J., et al., *Protein–excipient interactions: Mechanisms and biophysical characterization applied to protein formulation development*. *Advanced Drug Delivery Reviews*, 2011. **63**(13): p.1118-1159.

33. Jones, L.S., Kaufmann, A., and Middaugh, C.R., *Silicone oil induced aggregation of proteins*. Journal of Pharmaceutical Sciences, 2005. **94**(4): p.918-927.
34. Hawe, A. and Friess, W., *Stabilization of a hydrophobic recombinant cytokine by human serum albumin*. Journal of Pharmaceutical Sciences, 2007. **96**(11): p.2987-2999.
35. Mahler, H.C., et al., *Protein aggregation: Pathways, induction factors and analysis*. Journal of Pharmaceutical Sciences, 2009. **98**(9): p.2909-2934.
36. Mahler, H.-C., et al., *Induction and analysis of aggregates in a liquid IgG1-antibody formulation*. European Journal of Pharmaceutics and Biopharmaceutics, 2005. **59**(3): p.407-417.
37. Baudys, M. and Kim, S.W., *Peptide and protein characterization*, in *Pharmaceutical formulation development of peptides and proteins*, Frokjaer, S. and Hovgaard, L., editors. 2000. London: Taylor & Francis. p.41-69.
38. Andya, J., Hsu, C., and Shire, S., *Mechanisms of aggregate formation and carbohydrate excipient stabilization of lyophilized humanized monoclonal antibody formulations*. AAPS Journal, 2003. **5**(2): p.21-31.
39. Costantino, H.R., et al., *Fourier-transform infrared spectroscopic analysis of the secondary structure of recombinant humanized immunoglobulin G*. Pharmaceutical Sciences, 1997. **3**(3): p.121-128.
40. *ICH Q 6 A: Test procedures and acceptance criteria for new drug substances and new drug products: Chemical substances*, European Medicines Agency, 2010. 32 p.
41. *Guidance for industry container closure systems for packaging human drugs and biologics*, U.S. Department of Health and Human Services, et al., 1999. 56 p.
42. Reuter, B., *Siliconization of syringes* [telephone conversation], Berkenhoff, K., 2011.
43. Rathore, N. and Rajan, R.S., *Current perspectives on stability of protein drug products during formulation, fill and finish operations*. Biotechnology Progress, 2008. **24**(3): p.504-514.
44. Mewis, J. and Wagner, N.J., *Colloidal suspension rheology*. 1 ed. 2012. Cambridge: Cambridge university press. 416 p.
45. Jones, D.A.R., Leary, B., and Boger, D.V., *The rheology of a concentrated colloidal suspension of hard spheres*. Journal of Colloid Interface Science, 1991. **147**(2): p.479-95.
46. Hoffmann, R.L., *Discontinuous and dilatant viscosity behavior in concentrated suspensions. I. Observation of a flow instability*. Journal of Rheology, 1972. **16**(1): p.155-173.
47. Ackerson, B.J., *Shear induced order and shear processing of model hard sphere suspensions*. Journal of Rheology, 1990. **34**(4): p.553-590.

48. Marti, I., et al., *Rheology of concentrated suspensions containing mixtures of spheres and fibers*. *Rheologica Acta*, 2005. **44**(5): p.502-512.
49. Gao, Z.-H., et al., *Controlled release of a contraceptive steroid from biodegradable and injectable gel formulations: In vitro evaluation*. *Pharmaceutical Research*, 1995. **12**(6): p.857-863.
50. Schwach-Abdellaoui, K., et al., *Controlled delivery of metoclopramide using an injectable semi-solid poly(ortho ester) for veterinary application*. *International Journal of Pharmaceutics*, 2002. **248**(1–2): p.31-37.
51. Zingerman, J.R., et al., *Automatic injector apparatus for studying the injectability of parenteral formulations for animal health*. *International Journal of Pharmaceutics*, 1987. **36**(2–3): p.141-145.
52. Mitchell, J.W., *Prolonged release of biologically active somatotropins*. EP0177478, 1997.
53. Li, Z.-M. and Harkness Daniel, A., *Circumferential force production of the thumb*. *Medical engineering & physics*, 2004. **26**(8): p.663-70.
54. Ritschel, A. and Suzuki, K., *In vitro testing of injectability*. *Pharmazeutische Industrie*, 1979. **41**(5): p.468-475.
55. Allahham, A., et al., *Development and application of a micro-capillary rheometer for in-vitro evaluation of parenteral injectability*. *Journal of Pharmacy and Pharmacology*, 2004. **56**: p.709-716.
56. Harten, H.-U., *Physik für Mediziner*. 11 ed. 2005. Heidelberg: Springer Verlag GmbH. 367 p.
57. Miller, M.A., et al., *Low viscosity highly concentrated injectable nonaqueous suspensions of lysozyme microparticles*. *Langmuir*, 2009. **26**(2): p.1067-1074.
58. Yang, M.X., et al., *Crystalline monoclonal antibodies for subcutaneous delivery*. *Proceedings of the National Academy of Sciences of the United States of America*, 2003. **100**(12): p.6934-6939.
59. Kanai, S., et al., *Reversible self-association of a concentrated monoclonal antibody solution mediated by Fab–Fab interaction that impacts solution viscosity*. *Journal of Pharmaceutical Sciences*, 2008. **97**(10): p.4219-4227.
60. Liu, J., et al., *Reversible self-association increases the viscosity of a concentrated monoclonal antibody in aqueous solution*. *Journal of Pharmaceutical Sciences*, 2005. **94**(9): p.1928-1940.
61. Shire, S.J., Shahrokh, Z., and Liu, J., *Challenges in the development of high protein concentration formulations*. *Journal of Pharmaceutical Sciences*, 2004. **93**(6): p.1390-1402.

## 6 Appendix: supplementary material

### 6.1 Determination of inner needle diameter via SEM

The inner needle diameter of 20 G ( $670 \pm 8 \mu\text{m}$ ), 23 G ( $416 \pm 3 \mu\text{m}$ ) and 25 G ( $328 \pm 5 \mu\text{m}$ ) needles was determined via SEM, as exemplarily shown in Figure 5-18.

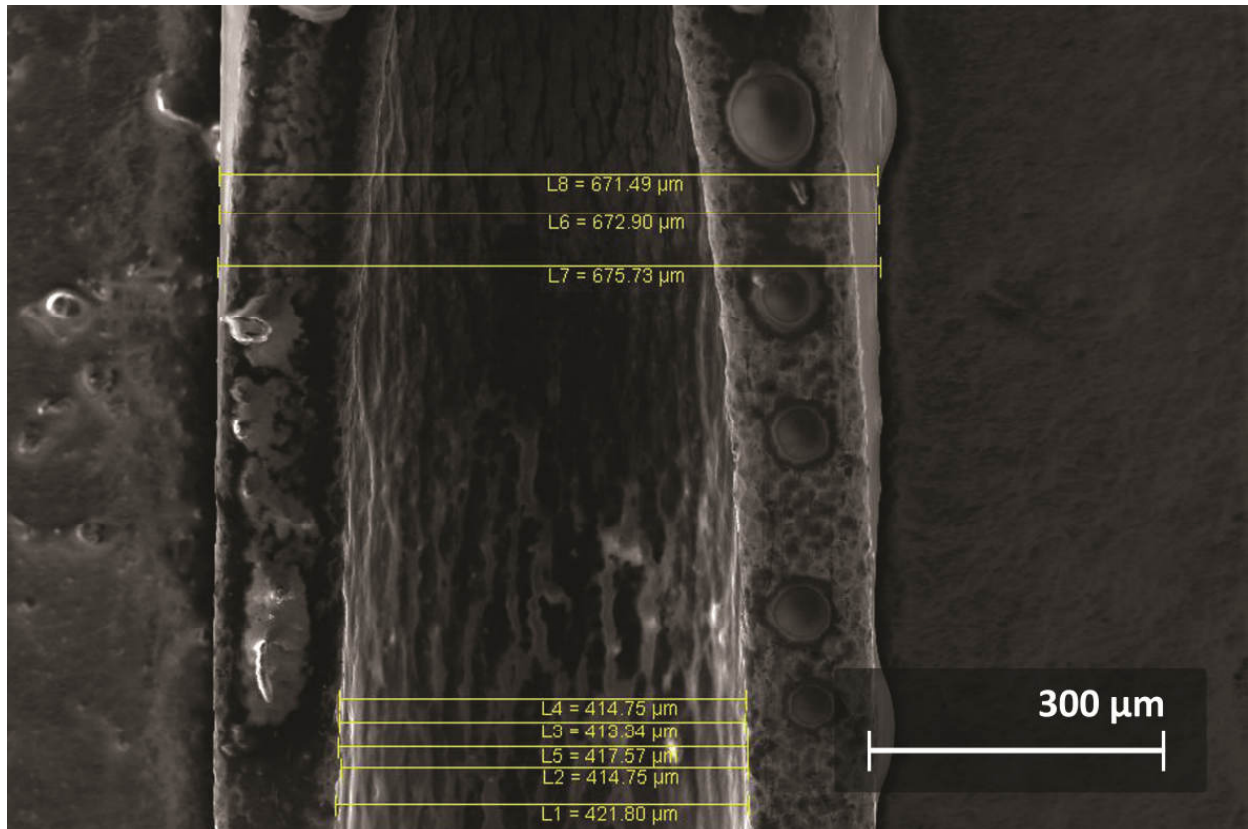


Figure 5-18: Determination of inner diameter of a 23 G needle via SEM.

## 6.2 Sedimentation behavior of S:B 70:30 and S:B 30:70 (v/v) mAb1 PCMC suspensions

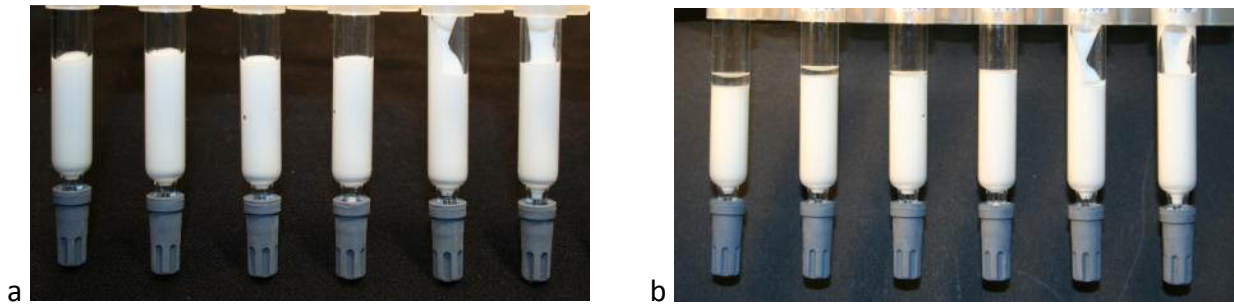


Figure 5-19: Sedimentation behavior of S:B 70:30 (v/v) mAb1 PCMC suspensions at (a)  $t_0$  and (b)  $t_{26d}$ ; solid content from left to right: 133, 163, 194, 224, 255 and 285 mg/mL.

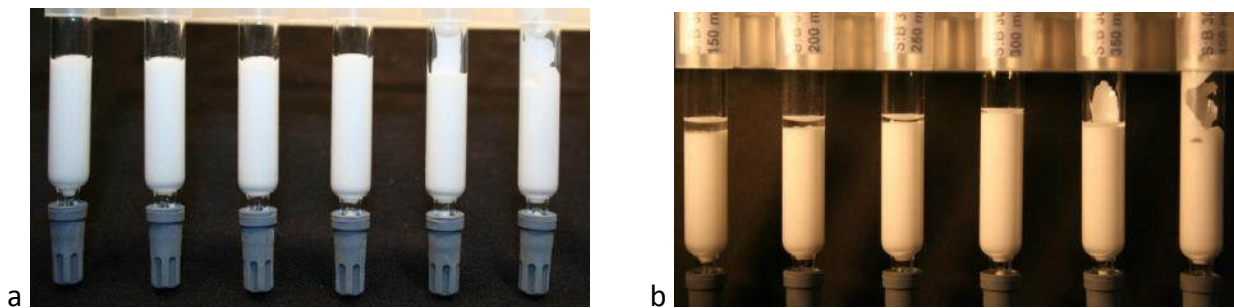


Figure 5-20: Sedimentation behavior of S:B 30:70 (v/v) mAb1 PCMC suspensions at (a)  $t_0$  and (b)  $t_{26d}$ ; solid content from left to right: 133, 163, 194, 224, 255 and 285 mg/mL.

## Chapter 6

# Mechanistic insights into the PCMC formation process

### Abstract

Although the protein-coated microcrystals (PCMC) technology has been successfully applied to a wide variety of molecules, such as peptides, proteins and DNA/RNA and the development of high concentration PCMC suspensions as final dosage form has recently advanced, the mechanism of particle formation is still unclear. Based on various studies on cytokine and mAb1 PCMCs with respect to morphology, composition and resulting stability, this chapter aimed to develop mechanistic insights in the PCMC formation process. The crystallinity/amorphy of mAb1 PCMCs, containing trehalose, glycine, NaCl, histidine, phenylalanine and EDTA as carrier components, was investigated in dependence of protein load (PL) and trehalose (tre) content. A total amount of  $\geq 85$ -90 % (m/m) protein and trehalose dihydrate, typically forming amorphous solids, was necessary to obtain a completely amorphous XRD pattern for the proteinaceous particles. The storage stability over 4 weeks at 40 °C/32 % RH of three amorphous powders with different protein loads and trehalose contents (60 % PL 30 % tre, 50 % PL 40 % tre, 40 % PL 50 % tre) and one crystalline formulation (10 % PL 30 % tre), which comprised detectable amounts of crystalline  $\alpha$ -glycine and NaCl at  $t_0$ , was analyzed with respect to insoluble and soluble protein aggregates (protein recovery, turbidity, HP-SEC, SDS-PAGE) as well as morphological and carrier stability (SEM, XRD). Except for on-going NaCl crystallization detected for crystalline mAb1 PCMCs, only marginal differences were found between the formulations, all providing good overall storage stability of the antibody. Confocal laser scanning fluorescence microscopy clearly showed homogenous mAb1 distribution within the spherical particles for the amorphous mAb1 formulations. In contrast, the crystalline formulation was characterized by non-fluorescent rod-shaped glycine crystals with amorphous proteinaceous material being attached to the crystal surface. The presence of two corresponding particle fractions, namely carrier crystals forming the core of the particles and amorphous proteinaceous material on the surface, was further proven in case of cytokine

PCMCs by powder fractionation via Andersen cascade impactor. Thus, the supramolecular structure of these particles was consistent with the initial idea of PCMCs presented by Vos [1], in contrast to the amorphous mAb1 PCMCs which did not show these two distinct material fractions, but instead a homogenous particle composition which only differed in size. Cytokine PCMCs could further be manufactured via standard one-step precipitation as well as by two-step precipitation in batch mode. Two-step precipitation comprised the separate production of carrier crystals on which the protein was precipitated in a second step. The manufacturing method did not affect the morphology or the protein process stability. Batch mode production of protein-free mAb1 PCMCs was only feasible with some limitations, but revealed the existence of an emulsion-like state, comprising dispersed droplets of an “excipient and protein rich/solvent poor” phase in a continuous “excipient and protein poor/solvent rich” phase, during the formation of these particles. Crystal growth at the liquid-liquid interface as well as inside the droplets was observed via polarization microscopy. Thus, the spinodal decomposition model was suggested to be appropriate to describe the formation process of these mAb1 PCMCs.

## **1 Introduction**

The protein-coated microcrystals technology represents an alternative method of protein stabilization in the solid state via coprecipitation of an aqueous solution of protein and carrier material induced by rapid mixing with a surplus of organic water-miscible solvent. The idea that goes back to a patent of Moore [2] has not only successfully been applied to various proteins, peptides and polypeptides, such as such as e.g. subtilisin Carlsberg protease [3], lipase [4, 5], trypsin [1, 6], BSA [6, 7], IgGs [6, 8], but also DNA and RNA [9]. König established a pilot-scale production process for PCMCs that enables a continuous production of up to 120 L suspension per hour [10]. Based on this progress, the preceding chapters of this thesis dealt with the development of cytokine (chapter 2) and mAb2 (chapter 3) PCMCs providing high process and storage stability to the protein. Additionally, organic water-miscible and oily solvents were evaluated as resuspension media for PCMCs allowing for subcutaneous application as high concentration suspensions (chapters 4 and 5). Despite these achievements, the particular mechanism how PCMC particles form via rapid dehydration of protein and carrier material

during coprecipitation is still unclear. Vos who focused on the PCMC mechanism discussed the classical nucleation and growth model as well as the model of spinodal decomposition to explain the formation of protein-coated microcrystals [1]. According to the classical nucleation theory, the free energy of a multicomponent system initially existing as a single phase is changed by modification of pressure or temperature or by homogenous mixing with a supplementary component. Consequently, phase separation, being energetically more favorable, leads to the coalescence of particles and thus to the formation of nuclei which begin to grow [11]. Spinodal decomposition describes the spontaneous rapid separation of a supersaturated, initial one-phase solution brought inside the spinodal curve, tracing the stability limit, by changing its composition without actual nucleation [11, 12]. Vos suggested that the latter model was slightly more appropriate for the description of the PCMC formation process [1]. But, it has to be considered that in most real systems the transition between the two mechanisms is gradual, as reviewed by Horn and Rieger [11].

The current chapter that comprises various studies on cytokine and mAb1 PCMCs touching their morphology, composition and resulting stability aimed to gain further mechanistic insights into the PCMC formation process. Therefore, the influence of protein load and trehalose content on the morphology and storage stability of mAb1 PCMCs was investigated. Fractionation of cytokine and mAb1 PCMC powder via Andersen cascade impactor intended to specify the chemical composition of different particle populations and ultimately the supramolecular structure of the particles. Finally, the manufacturing of cytokine and mAb1 PCMCs via one- and two-step precipitation as well as of protein-free particles was studied.

## **2 Materials and methods**

### **2.1 Materials**

L-Phenylalanine, sodium bicarbonate, dimethyl sulfoxide (DMSO), phosphate buffered saline pH 7.4 and sodium hydroxide were purchased from Sigma-Aldrich, Steinheim, D, disodium EDTA dihydrate, hydrochloric acid (1 mol/L), isobutanol (Emplura®), ethanol 95-97 % (v/v), Brij® 35, L-2-methyl-2,4-pentanediol and water free glycerin (Emprove®) from Merck, Darmstadt, D. Glycine, L-histidine and L-histidine hydrochloride monohydrate were procured

from Ajinomoto Omnicem, Louvain-la-Neuve, B. Sodium dihydrogen phosphate dihydrate was delivered by Dr. Paul Lohmann, Hungen, D, sodium chloride by Akzo Nobel, Hengelo, NL, and trehalose dihydrate by Ferro Pfanstiehl, Waukegan, IL, USA. D/L-Valine was purchased from Fluka (Buchs, CH) and trisodium citrate dihydrate and citric acid monohydrate from Jungbunzlauer (Ladenburg, D). Sucrose was obtained from Südzucker (Mannheim, D). Sodium dodecyl sulfate was from Serva, Heidelberg, D. All chemicals were utilized without further purification. The protein bulk drug substances were provided by Boehringer Ingelheim.

## **2.2 Methods**

### **2.2.1 Preparation of protein solutions**

The mAb1 bulk drug substance was composed of 20 mg/mL human IgG2 monoclonal antibody, 0.68 mg/mL L-histidine, 3.27 mg/mL L-histidine hydrochloride monohydrate, 0.1 mg/mL disodium EDTA dihydrate, 84.0 mg/mL trehalose dihydrate and 0.1 % polysorbate 80. The buffer of the bulk drug substance was exchanged via ultra- and diafiltration resulting in a protein solution that consisted of 75.1 mg/mL protein, 0.2 mg/mL L-histidine, 0.8 mg/mL L-histidine hydrochloride monohydrate, 0.03 mg/mL disodium EDTA dihydrate and approx. 0.4 mg/ml polysorbate 80 (crossflow buffer exchange and concentration unit, Boehringer Ingelheim, Biberach/Riss, D; membrane cassette Sartocon Slice, Hydrosart, 30 kd, Sartorius, Göttingen, D; Quattroflow 150 S membrane pump, Quattroflow Fluid Systems, Hardegsen, D).

The cytokine bulk drug substance contained 1.5 mg/mL hydrophobic cytokine, 50 mM sodium acetate trihydrate, 1 mM disodium EDTA dihydrate and 0.1 % sodium dodecyl sulfate (SDS). After ultra- and diafiltration (membrane cassette Sartocon Slice, Hydrosart, 5 kd, Sartorius, Göttingen, D) the protein solution comprised 18.0 mg/mL protein, 22 mM citrate and approx. 1.2 % SDS.

The surfactants polysorbate 80 or SDS were present in the final protein solutions because they cannot be removed via ultra-/diafiltration, as similarly reported by Mahler et al. for polysorbate 20 [13].

## 2.2.2 PCMC production process

The PCMC production process is divided into four main steps: preparation of protein-carrier solution, precipitation, concentration/solvent exchange, and drying.

### 2.2.2.1 Preparation of protein-carrier solutions

For the preparation of the protein-carrier solution, the carrier material was dissolved in water and the solution pH value was adjusted to 5.5 prior to the addition of the protein solution.

The composition of the protein-carrier solutions for the study on mAb1 PCMCs with varying protein load (PL) and trehalose (tre) content are presented in Table 6-1 and Table 6-2. Furthermore, a formulation with 40 % protein and 50 % trehalose was produced (Table 6-3) and additionally used for the fractionation via cascade impactor. Variation of protein load or trehalose content led to different relative amounts of the remaining carrier components (glycine, phenylalanine, sodium chloride, histidine hydrochloride monohydrate, histidine, trehalose dihydrate and Di-Na-EDTA dihydrate) to ensure a constant solid content of the protein-carrier solutions of 100 mg/mL. Depending on the protein load, the polysorbate 80 concentration ranged from approx. 0.05 to approx. 0.3 mg/mL.

Table 6-4 shows the composition of the protein-carrier solution for the production of cytokine PCMCs with a solid content of 45 mg/mL.

**Table 6-1: Composition of protein-carrier solutions with constant protein load (PL) of 50 % and varying trehalose (tre) content [% w/w].**

Excipient	50 % PL, no tre	50 % PL, 25 % tre	50 % PL, 30 % tre	50 % PL, 35 % tre	50 % PL, 40 % tre
mAb1	50.0	50.0	50.0	50.0	50.0
L-Histidine HCl monohydrate	5.0	2.5	2.0	1.5	1.0
L-Histidine	1.0	0.5	0.4	0.3	0.2
NaCl	10.0	5.0	3.9	3.0	2.0
Glycine	30.4	15.2	11.9	9.1	6.05
L-Phenylalanine	3.4	1.7	1.3	1.0	0.7
Trehalose dihydrate	--	25.0	30.4	35.0	40.0
Di-Na-EDTA dihydrate	0.2	0.1	0.1	0.1	0.05

**Table 6-2: Composition of protein-carrier solutions with constant trehalose (tre) content of 30 % and varying protein load (PL) [% w/w].**

Excipient	10 % PL 30 % tre	45 % PL 30 % tre	50 % PL, 30 % tre	55 % PL, 30 % tre	60 % PL, 30 % tre
mAb1	10.0	45.0	50.0	55.0	60.0
L-Histidine HCl monohydrate	6.0	2.5	2.0	1.5	1.0
L-Histidine	1.2	0.5	0.4	0.3	0.2
NaCl	12.0	5.0	3.9	2.9	1.9
Glycine	36.2	14.9	11.9	8.8	5.8
L-Phenylalanine	4.0	1.6	1.3	1.0	0.6
Trehalose dihydrate	30.4	30.4	30.4	30.4	30.4
Di-Na-EDTA dihydrate	0.2	0.1	0.1	0.1	0.1

**Table 6-3: Composition of protein-carrier solution with protein load (PL) of 40 % and 50 % trehalose (tre) [% w/w].**

Excipient	40 % PL 50 % tre
mAb1	40.0
L-Histidine HCl monohydrate	1.0
L-Histidine	0.2
NaCl	2.0
Glycine	6.0
L-Phenylalanine	0.7
Trehalose dihydrate	50.0
Di-Na-EDTA dihydrate	0.1

**Table 6-4: Composition of the protein-carrier solution of cytokine PCMCs [% w/w].**

Excipient	Cytokine PCMCs
Trisodium citrate dihydrate	8.6
Citric acid monohydrate	1.2
Cytokine	10.0
DL-Valine	79.2
Sucrose	1.0

### 2.2.2.2 Continuous precipitation of mAb1 and cytokine PCMCs

The continuous precipitation was carried out as described in detail by König [10]. Briefly, two equal streams of precipitating agent were mixed with one stream of protein-carrier solution in

a small double jet impingement mixer of an inner diameter of 1.5 mm (Boehringer Ingelheim, Biberach/Riss, D). The mixing ratio of the precipitating agent saturated with all carrier components, isobutanol for mAb1 PCMCs and a 1:1 mixture of isopropanol and 2-methyl-2,4-pentanediol based on volume for cytokine PCMCs, and the protein-carrier solution was set to 95 : 5 (v/v). The modular mixing platform from Ehrfeld (Bayer Technology, Wendelsheim, D) encompassed three micro gear pumps (HNP pumps m zr 11507 and 7255, Hydraulik Nord Fluidtechnik, Parchim, D), pressure sensors and temperature sensors to monitor the precipitation step. The total flow rate of 1000 mL/min was controlled by the software LabView (National Instruments, Munich, D) and Coriflow mass flow meters (Bronkhorst, Kamen, D). The final suspension volume after precipitation was 1 L for cytokine PCMCs, 2 L for mAb1 PCMCs and 0.5 L for the suspensions containing Alexa<sup>®</sup> 488 labeled mAb1.

### **2.2.2.3 Batch mode preparation of cytokine and mAb1 PCMCs via one-step and two-step precipitation**

One-step precipitation of cytokine and mAb1 PCMCs in batch mode was performed, according to Khosravani et al. and Kreiner and Parker [4, 14]. Briefly, 25.0 mL of the protein-carrier solution were added dropwise within approx. 3 min into 475 mL precipitating agent under stirring at 500 rpm (Mini MR standard IKAMAG<sup>®</sup>, IKA, Staufen, D). The precipitating agent was a 1:1 (v/v) mixture of isopropanol and 2-methyl-2,4-pentanediol saturated with all carrier components for cytokine PCMCs and pure saturated isobutanol for mAb1 PCMCs.

The preparation of PCMCs via two-step precipitation included two separate batch mode precipitation processes. First, 50.0 mL carrier solution were precipitated into 950 mL precipitating agent, as described above. After 18 h of sedimentation the supernatant was decanted and replaced by fresh precipitating agent. This procedure was repeated after another 12 h of sedimentation. Subsequently, 23.7 mL protein solution, comprising 101 mg cytokine or mAb1 in water, were added dropwise within approx. 3 min into 450 ml of the previously prepared carrier suspensions under stirring.

### **2.2.2.4 Concentration/solvent exchange**

For concentration of mAb1 PCMC suspensions, the supernatant was decanted 18 h after the precipitating step. The supernatant was replaced with fresh saturated isobutanol. After 24 h of

sedimentation the sediment, i.e. the concentrated suspension, was used for the supercritical drying process.

In the case of cytokine PCMCs, after 18 h of sedimentation, the suspension was filtered off at 600 mbar (Durapore Membrane Filter 0.45  $\mu\text{m}$  HV 47 mm, Millipore, Schwalbach, D), the filter cake was washed twice with 50 mL saturated isopropanol and finally resuspended in 50 mL saturated isopropanol.

### **2.2.2.5 Supercritical drying**

Supercritical drying (Thar SFE-500, Thar Technologies, Pittsburgh, PA, USA) was performed with carbon dioxide at 100 bar, 45 °C and a flow rate of 25 g/min. Finally, the pressure was decreased by 3 bar/min. After drying of 240 mL concentrated mAb1 PCMC suspension within 90 min, vacuum drying was conducted at 30 mbar and 40 °C for 2 h (APT.line™ VDL, Binder, Tuttlingen, D; diaphragm membrane pump MZ 2C, Vacuubrand, Wertheim, D).

For cytokine PCMCs, the resuspended filter cake was dried via supercritical drying process for 81 min. Subsequent vacuum drying was not carried out.

### **2.2.3 Binding of Alexa® 488 dye to mAb1**

Protein bulk drug substance without polysorbate 80 was dialyzed into PBS pH 7.4 within 24 h at 2-8 °C (Slide-A-Lyzer® Dialysis Cassette G2, 20,000 MWCO, 0.5 mL, Thermo Scientific, Rockford, IL, USA). After dialysis, the protein concentration was determined via UV spectroscopy, as described in detail in section 2.2.7. Alexa® 488 dye (Alexa® Fluor 488 Carboxylic Acid, Invitrogen, Darmstadt, D) was dissolved in DMSO to reach a concentration of 2 mg/mL. For coupling, 2 ml protein solution with 1 mg/mL protein was added to 200  $\mu\text{l}$  1 M sodium bicarbonate solution and 10  $\mu\text{l}$  Alexa® 488 dye solution. After incubation for 1 h at  $22 \pm 3$  °C on a horizontal shaker with 200 rpm, the sample was purified via PD-10 column (Sephadex™ G-25M, GE, Buckinghamshire, UK). Equilibration of the column and sample elution was performed with a histidine buffer containing 0.68 mg/mL L-histidine, 3.27 mg/mL L-histidine hydrochloride monohydrate, 0.1 mg/mL Di-Na-EDTA dihydrate and 56.0 mg/mL trehalose dihydrate. Fractions 4-8 out of 10-12 fractions of 500  $\mu\text{l}$  were collected, combined and dialyzed into histidine buffer within 24 h at 2-8 °C protected from light (Slide-A-Lyzer® Dialysis Cassette G2,

20,000 MWCO, 0.5 mL, Thermo Scientific, Rockford, IL, USA). The degree of labeling after dialysis was determined via UV measurement at 280 and 495 nm (Equation 6-1 and 6-2) [15].

$$[IgG] = \frac{A_{280} - 0.11 * A_{495}}{1.4286} \quad (6-1)$$

$$\text{Degree of labeling} = \frac{A_{495} * 150000}{[IgG] * 71000} \quad (6-2)$$

For the preparation of the protein-carrier solutions the ratio of labeled to unlabeled mAb1 was 1:500.

#### 2.2.4 Accelerated short-term storage stability study

For the stability study, 100 mg of the PCMC powders (10 % PL 30 % tre, 60 % PL 30 % tre, 50 % PL 40 % tre and 40 % PL 50 % tre) were filled into 2 R glass vials (Fiolax®, Schott, Mühlheim, D) and stored unstoppered at 40 °C for 4 weeks in a desiccator over saturated MgCl<sub>2</sub> solution providing relative humidity of approx. 32 % [16]. Analysis of the PCMC powder (protein content, turbidity, HP-SEC, SDS-PAGE) was performed after one and four weeks of storage. Investigations via x-ray diffractometry, scanning electron microscopy and Karl-Fischer titration were limited to t<sub>4wk</sub>.

#### 2.2.5 Powder fractionation via cascade impactor

Fractionation of PCMC powders was performed via Andersen Cascade Impactor (eight stage non-viable sample series 20-800, Thermo Andersen, Smyrna, GA, USA) at a flow rate of 39 L/min (corresponding to a pressure drop of 4 kPa with the HandiHaler®), as described in detail by Claus et al. [17]. Within 6.15 s a total air volume of 4 L passed through the device and the PCMC powder encapsulated into polyethylene capsules was inserted into the induction port of the cascade impactor. The baffle plates were uncoated to allow easy harvesting of the powder suitable for further analysis via HPLC. On the contrary, the fixation of SEM patches (Leitfähige Haftaufkleber Ø 12 mm, Plano, Wetzlar, D) for morphological analysis of the powder required the coating of the plates with a mixture made of 83 % glycerin, 14 % ethanol 95-97 % (v/v) and 3 % Brij® 35.

### 2.2.6 X-ray powder diffraction (XRD)

The crystallinity of mAb1 PCMCs was analyzed with XRD in transmission mode from  $3^{\circ}$ - $40^{\circ}$   $2\theta$ ,  $0.5^{\circ}$  steps and 20 s/step based on  $1.5406 \text{ \AA}$  CuK $\alpha$ -radiation at 40 kV and 40 mA (Stoe, Darmstadt, D). Samples were fixed in the sample holder between two Ultraphan foils (cellulose diacetate) with a thickness of 0.014 mm (Stoe, Darmstadt, D).

### 2.2.7 Protein content via UV measurement

MAb1 PCMC powder was dissolved in deionized water to give a concentration of approx. 0.4 mg/mL and ensure absorption within the linear range of the spectrometer (0.3 to 0.8 AU). 30 min after reconstitution, absorption in Halfmicro Plastibrand<sup>®</sup> cuvettes (Brand, Wertheim, D) was measured at 279 nm based on an extinction coefficient of 1.43 with a Lambda 20 spectrometer (PerkinElmer, Rodgau-Jügesheim, D) and deionized water serving as blank (n=3).

30 mg of cytokine PCMC powder were dissolved in 11.5 mM NaCl pH 2 and filtered through a  $0.45 \mu\text{m}$  syringe filter (Rotilabo-Spritzenfilter steril  $0.45 \mu\text{m}$  PVDF, Carl Roth, Karlsruhe, D) 30 min after reconstitution. UV measurement was carried out at 280 nm, corrected against buffer, based on an extinction coefficient of 1.70 (n=3) [18, 19].

### 2.2.8 Turbidimetry

After dissolution of mAb1 PCMC powder with deionized water, turbidity was measured at a protein concentration of 1 mg/mL by  $90^{\circ}$  light scattering at  $\lambda = 633 \text{ nm}$  30 min after reconstitution (UH turbidimeter, Boehringer Ingelheim, self-construction) and expressed in formazine nephelometric units (FNU) (n=3).

### 2.2.9 High performance size exclusion chromatography (HP-SEC)

30 min after reconstitution of mAb1 PCMC powder in deionized water, the solution was filtered through a  $0.45 \mu\text{m}$  syringe filter (Rotilabo-Spritzenfilter steril  $0.45 \mu\text{m}$  PVDF, Carl Roth, Karlsruhe, D) and 25  $\mu\text{l}$  samples of 2.0 mg/mL protein were injected in duplicate. Soluble protein aggregates, monomers and fragments were separated on an Äkta micro (GE Healthcare, Uppsala, S) with a TSKGel G3000 SWXL column (7.8 mm ID x 30.0 cm L, Tosoh, Stuttgart, D), equipped with a 40 x 6.0 mm TSKgel SWXL Guardcol precolumn, using filtered ( $0.22 \mu\text{m}$ ) and degassed mobile phase of 60 mM sodium chloride and 5 mM sodium dihydrogen phosphate pH 7.0 in deionized water at 1.0 mL/min flow rate and UV detection at 280 nm. Aggregation

and fragmentation in percent was calculated based on the ratio of the area under the curve (AUC) of soluble aggregates and fragments to the total AUC of aggregates, monomer and fragments (n=2). Furthermore, changes in the AUC were considered.

According to Hawe and Friess, for HP-SEC analysis of cytokine PCMCs a TSKgel G3000SW column (7.8 mm ID x 60.0 cm L) and a TSKgel SWXL Guardcol precolumn (Tosoh Bioscience, Stuttgart, D) were used on an Äkta micro with 200 mM sodium dihydrogen phosphate and 0.1 % SDS [18]. 25 µl samples of 0.6 mg/mL protein were injected in duplicate and protein elution was monitored via UV-detection at 210 nm (n=2).

### **2.2.10 Sodium dodecyl sulfate polyacrylamide gel electrophoresis (SDS-PAGE)**

SDS-PAGE of mAb1 PCMC powders was conducted at 200 V with Power Ease 500 and XCell Sure Lock in combination with 12 % Bis-Tris gels (NuPAGE®, 1 mm, 15 wells, Invitrogen, Darmstadt, D) and NuPAGE® MOPS SDS running buffer. Samples were mixed 8:2 with NuPAGE® LDS sample buffer, and 7:2:1 with NuPAGE® LDS sample buffer and 0.5 M dithiothreitol for the reducing SDS-PAGE. After heating up to 95 °C for 5 min, 5 µl of the samples and the marker (Precision Plus Protein Standard, Bio-Rad, Hercules, CA, USA), representing 1 µg protein, were loaded to each well. Furthermore, 2 ng BSA were loaded to one well for the purpose of sensitivity control. The gels were stained with SilverXpress® Silver Staining Kit. All equipment was from Invitrogen (Darmstadt, D).

### **2.2.11 Particle morphology via scanning electron microscopy (SEM)**

Particle morphology of PCMC powder was analyzed by the use of a scanning electron microscope (Model Tescan Vega II SBH, Tescan, Brno, CZ). Samples were prepared on an aluminum stub and coated with gold/palladium (Model Cressington 108auto/SE Cool Sputter Coater, Cressington, Watford, GB).

### **2.2.12 Water content via Karl-Fischer titration**

For water content quantification, two aliquots of 100 mg mAb1 PCMC powder per sample were filled into 2R vials and flanged either immediately after the drying process or after storage for 4 weeks at 40 °C/32 % RH. After dissolution in methanol (Mallinckrodt Baker, Phillipsburg, NY, USA), titration was performed using Hydranal® Coulomat-AG reagent (Fluka, Buchs, CH) and a 756 KF-Coulometer (Methrom, Sofingen, CH) for endpoint detection (n=2).

### **2.2.13 Confocal laser scanning fluorescence microscopy (CLSM)**

CLSM of mAb1 PCMCs containing Alexa<sup>®</sup> 488 labeled protein was performed via inverted fluorescence microscope (Leica DM IRBE) equipped with a confocal scanner (Leica TCS SP2), a multiline argon laser with an excitation wavelength of 488 nm and oil immersion objectives (Leica HC PL APO 10x 0.4 IMM and HC PL APO 10x 0.7 IMM/CORR). Leica Confocal Software, version 2.61, was used for taking and evaluation of pictures. All equipment was from Leica (Heidelberg, D).

### **2.2.14 Quantification of the cytokine by reverse-phase high performance liquid chromatography (RP-HPLC)**

The amount of cytokine after powder fractionation via cascade impactor was analyzed by RP-HPLC (Alliance 2695, Waters, Milford, MA, USA) with a Zorbax 300SB-CN column (4.6 x 150 mm, Agilent, Böblingen, D) as stationary phase at 40 °C, as developed by BI. The mobile phase was composed of phase A (100 % water with 0.1 % trifluoroacetic acid (TFA)) and phase B (84 % acetonitrile, 16 % water, 0.084 % TFA). The volume fraction of phase B was increased from 40 % to 55 % (9 min), 60 % (15 min) and 80 % (20 min) and finally reduced back to 40 % (21 min). Cytokine PCMC powder was reconstituted in 11.5 mM NaCl pH 2 within 15 min. A duplicate of samples with 0.04-0.25 mg/mL protein was injected at a flow rate of 0.7 mL/min and detected at 214 nm (UV). Based on the AUC, the cytokine content was calculated using the linear calibration curve (n=2).

### **2.2.15 Quantification of valine by gas chromatography (GC)**

For quantification of valine in cytokine PCMCs via BI internal method, the powder was dissolved in 1 mL NaCl/Na<sub>2</sub>CO<sub>3</sub> buffer (62 mmol/L and 28 mmol/L, respectively) and valine was derivatized via EZ: faast™ kit (GC-FID Physiological, Amino Acid Analysis Kit, Phenomenex, Torrance, CA, USA) (n=2). An Agilent 6890N Network GC equipped with a ZB-AAA column (10 m x 0.25 mm, 0.25 μm film thickness, Phenomenex, Torrance, CA, USA) and a flame-ionization detector was used at a column flow of 1.5 mL He/min. The column oven temperature was raised by 38 °C/min from 110 to 320 °C and the FID detector temperature was 320 °C. A duplicate of 2 μl samples was injected at 250 °C and a split level of 1:15 (n=2). L-Norleucine (Sigma-Aldrich, Steinheim, D) was used as internal standard amino acid.

### **2.2.16 Quantification of trehalose by high performance liquid chromatography (HPLC)**

Lower molecular substances, such as trehalose and the amino acids, were separated from protein via centrifugation (Heraeus® Biofuge® primo, Carl Roth, Karlsruhe, D). The filtration units (Amicon® Ultra-0.5 Ultracel-10k, Millipore, Schwalbach, D) were rinsed with 0.5 mL 0.1 N NaOH and subsequently equilibrated with dissolved PCMCs containing 2 mg/mL mAb1 in deionized water at 12000 g for 10 min. 0.5 mL samples of dissolved PCMCs with 2 mg/mL protein were subsequently separated at 12000 g for 10 min. The filtrate was checked for protein residues via UV absorption and analyzed (2 x 40 µl) by HPLC using a Rezex RCM Monosaccharide Ca<sup>2+</sup> 300 x 7.80 mm column with guard column (SecurityGuard Cartridges Carbo-Ca 4 x 3.0 mm, Phenomenex, Torrance, CA, USA) at 85 °C. Filtered HPLC-water (Chromasolv® plus, Sigma-Aldrich, Steinheim, D) was used for elution at a flow rate of 0.6 mL/min. Detection was performed via changes in refractive index (RI). The trehalose RI signal between 5.5 and 6.9 mL was integrated and trehalose content was calculated using the linear calibration curve for concentrations from 0.25 to 0.8 mg/mL (n=3).

### **2.2.17 Bioactivity assay**

The bioassay of cytokine PCMCs was based on lung cancer indicator cells A549 [20]. Briefly, preincubated with different concentrations of the cytokine, the cells were infected with encephalomyocarditis virus and thus a cytopathic effect was evoked leading to cell lysis. The number of viable cells was analyzed by an MTT (3-(4,5-Dimethylthiazol-2-yl)-2,5-diphenyltetrazolium bromide) assay. The concentration of the cytokine that led to the lysis of 50 % of the cells (ED<sub>50</sub>) was referred to cytokine standard. The biological activity of the samples was determined based on three independent batches of each sample. Each batch consisted of two plates with the sample in triplicates.

### 3 Results and discussion

#### 3.1 Investigation of mAb1 PCMCs with varying protein load and trehalose content

To investigate the role of the crystallizing carrier components of mAb1 PCMCs as well as of the amorphous excipient fraction and to gain insight into the supramolecular structure of the particles, first, the crystallinity of mAb1 PCMCs was studied in dependence of protein load (10-60 %) and trehalose level (0-40 %). Four formulations were subsequently chosen and stored at 40 °C/32 % RH for 4 weeks to study the influence of the composition on protein storage stability with respect to aggregation (protein content, turbidity, HP-SEC and SDS-PAGE) and on carrier and morphology stability (XRD and SEM). Confocal laser scanning microscopy was performed to analyze the localization of the protein within the microcrystals.

##### 3.1.1 Crystallinity of mAb1 PCMCs in dependence of protein load and trehalose content

For mAb1 PCMCs that contained 50 % protein and trehalose ranging from 0-40 %, the crystallinity/amorphy of the microcrystals depended on the level of the disaccharide. In the absence of trehalose, mainly crystalline  $\alpha$ -glycine and NaCl were detected via XRD (Figure 6-1a). Furthermore, peaks associated with  $\beta$ -glycine were identified in the spectrum. Increasing amounts of trehalose reduced the crystallization tendency of both NaCl and glycine. In the sample prepared with 50 % mAb1 and 25 % trehalose crystalline signals were limited to  $\alpha$ -glycine and were clearly less pronounced than in the sample without trehalose. The degree of crystallinity of  $\alpha$ -glycine further decreased in the presence of 30 % trehalose. Higher amounts of the disaccharide led to completely amorphous PCMCs. Hence, an increasing amount of trehalose prevented NaCl and glycine from crystallization during the manufacturing of the particles. As discussed in detail in chapter 3, trehalose played a key role in the stabilization of mAb2 formulated as PCMCs via formation of a glassy matrix. In accordance with the current findings on mAb1 PCMCs, the absence of trehalose resulted in the crystallization of  $\alpha$ -glycine. These at least partially crystalline mAb2 PCMCs provided less stabilization against aggregation of the monoclonal antibody during production as well as storage, compared to completely amorphous formulations. As opposed to the corresponding mAb1 formulation, no crystalline

signal was observed in the XRD spectrum for mAb2 PCMCs with a protein load of 50 % and a trehalose level of 30 % (see chapter 3 section 3.1.1). This PCMC composition thus represented the borderline between partially crystalline and predominantly amorphous mAb microcrystals. Moreover, it has to be considered that the mAb1 and mAb2 bulk drug substances slightly differed in the EDTA concentration and the polysorbate amount and type. Inhibition of glycine crystallization in the presence of trehalose was also observed during lyophilization by Chatterjee et al. [21]. In that case, the prevention of glycine crystallization required a mass ratio of glycine to trehalose dihydrate below 1. For mAb1 PCMCs, the mass ratio of glycine to trehalose dihydrate was 1.2 for the formulation containing crystalline glycine and 0.12-0.19 for the amorphous ones, being in line with the results of Chatterjee et al.

With respect to the mAb1 PCMC formulations with a constant trehalose content of 30 % and varying protein load in the range of 10-60 %, the degree of crystallinity decreased with increasing protein load (Figure 6-1b). The spectrum of the sample that comprised 10 % protein and 30 % trehalose showed peaks that were attributed to crystalline  $\alpha$ -glycine and NaCl. The use of 45, 50 and 55 % mAb1 resulted in PCMC powder that only contained crystalline  $\alpha$ -glycine, at decreasing levels, whereas all the other components were amorphous. MAb1 PCMCs composed of 60 % protein and 30 % trehalose did not manifest any crystalline signal in the XRD spectrum and were thus assumed to be completely amorphous. Hence, increasing amounts of monoclonal antibody impeded crystallization of NaCl and glycine, which corresponds to literature [22-25]. However, it also has to be taken into consideration that, in parallel with the augmenting level of mAb1 in the formulations, the amount of the potentially crystallizing components NaCl and glycine decreased and gradually approached the detection limit of the analytical technique. The additional formulation containing 40 % mAb1 and 50 % trehalose was also amorphous in XRD. In summary, the sum of trehalose dihydrate and mAb1, typically forming amorphous solids, was essential for the overall physical state of the mAb1 PCMC formulations.

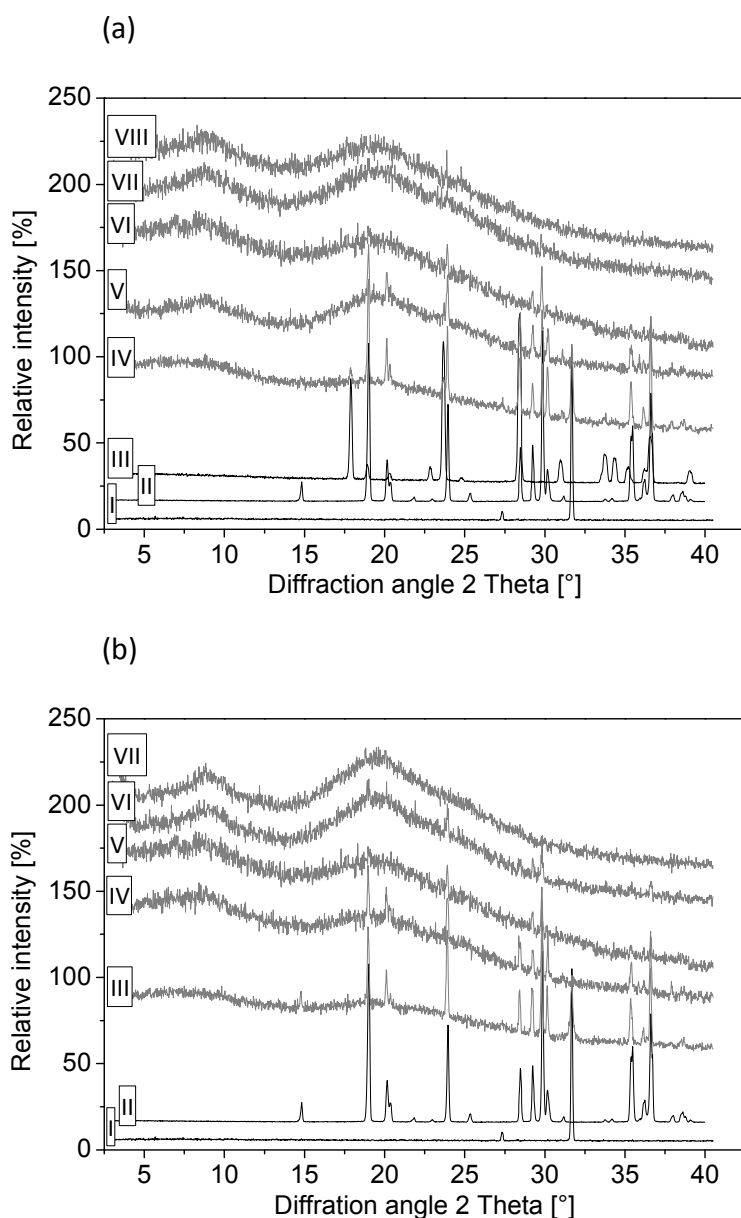


**Figure 6-1: XRD analysis of mAb1 PCMCs with (a) varying trehalose content and (b) varying protein load; spectrum assignment: (a) I: NaCl, II:  $\alpha$ -glycine; III:  $\beta$ -glycine; IV: 50 % PL no tre; V: 50 % PL 25 % tre; VI: 50 % PL 30 % tre; VII: 50 % PL 35 % tre; VIII: 50 % PL 40 % tre; (b) I: NaCl, II:  $\alpha$ -glycine; III: 10 % PL 30 % tre; IV: 45 % PL 30 % tre, V: 50 % PL 30 % tre; VI: 55 % PL 30 % tre; VII: 60 % PL 30 % tre; arbitrary offset for better comparison.**

### 3.1.2 Accelerated short-term stability study

For 4 weeks storage at 40 °C/32 % RH, one crystalline (10 % PL 30 % tre) and three amorphous mAb1 PCMC formulations (60 % PL 30 % tre, 50 % PL 40 % tre, 40 % PL 50 % tre) were chosen. The study aimed to investigate whether a crystalline or a completely amorphous matrix could provide best storage stability of the monoclonal antibody. With respect to the overall

crystalline formulation, the question was if the amount of amorphous excipient fraction was sufficient for adequate protein stabilization. Referring to the amorphous formulations, the impact of trehalose content and protein load, and thus of the molar ratio of amorphous excipient to protein, was further investigated.

Karl-Fischer titration revealed that the initial water content of the crystalline formulation (10 % PL 30 % tre) with a value of 1.7 % was significantly lower than for the amorphous formulations which ranged from 2.5 to 3.6 % (Table 6-5). After 4 weeks of storage, the water content of the amorphous formulations amounted to approx. 6 %, as opposed to 3.8 % detected for the crystalline formulation. Thus, the amorphous powders were more hygroscopic than the crystalline one, being consistent with literature [23, 26]. Ahlneck and Zografis found that in combinations of amorphous and crystalline material, absorption of water vapor preferentially occurred into the amorphous structure [27], thus rendering a higher water content and greater plasticizing effect in the amorphous fraction. Hygroscopicity of amorphous spray-dried and lyophilized powders bearing the risk of recrystallization and consequently instability during storage was also described for protein formulations, e.g. by Hawe and Friess [23] as well as by Hino et al. [28].

**Table 6-5: Water content [% m/m] of mAb1 PCMCs with varying protein load and trehalose content stored at 40 °C/32 % RH for 4 weeks.**

Formulation	$t_0$	$t_{4wk}$
10 % PL 30 % tre	1.7 ± 0.08	3.8 ± 0.02
60 % PL 30 % tre	3.6 ± 0.24	6.1 ± 0.04
50 % PL 40 % tre	3.1 ± 0.19	6.0 ± < 0.01
40 % PL 50 % tre	2.5 ± 0.04	6.0 ± 0.05

Turbidity measurement is frequently applied in the formulation development and purification of therapeutic proteins to detect insoluble protein aggregates [29, 30]. Independent of protein load and trehalose content, it revealed very low and constant turbidity values ranging from 0.4 to 1.7 FNU for the amorphous formulations (60 % PL 30 % tre, 50 % PL 40 % tre, 40 % PL 50 % tre) (Figure 6-2a). In contrast, the turbidity of the crystalline mAb1 PCMC sample (10 % PL 30 % tre) was higher with 3.0-6.5 FNU and a slight, but statistically significant increase was found within 4 weeks of storage ( $p < 0.05$ ). Hence, the protection against insoluble

proteinaceous particle formation throughout the PCMC production process as well as storage was better in an amorphous carrier matrix than in a crystalline one. This difference between the PCMC formulations selected for the accelerated short-term stability study was too low to be reflected in the protein content that did not change significantly within 4 weeks of storage, irrespective of the PCMC composition (Figure 6-2b).

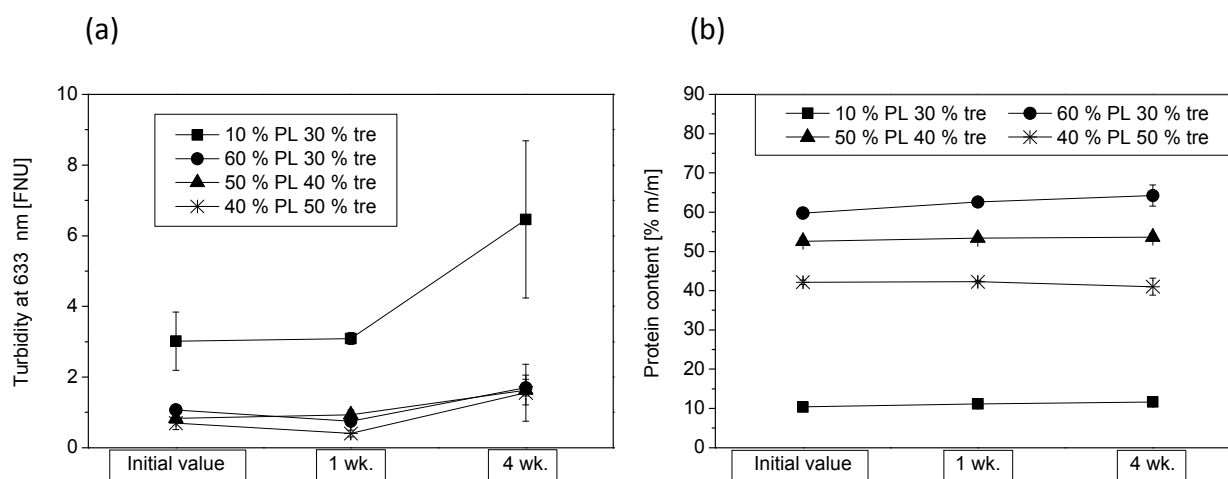


**Figure 6-2: Turbidity (a) and protein content (b) of mAb1 PCMCs with varying protein load and trehalose content stored at 40 °C/32 % RH for 4 weeks.**

Soluble protein particles are most commonly assessed via HP-SEC [31, 32]. After 4 weeks storage, all mAb1 PCMC formulations showed a faint decrease of the monomer content (Figure 6-3) and only minor differences were found between the formulations. The smallest decline, by only 0.5 %, was detected for the crystalline formulation (30 % PL 10 % tre), whereas this formulation displayed the smallest initial monomer level of all formulations analyzed. The amorphous formulations with a protein load of 60 and 50 % lost 2.3 and 2.4 % of the initial monomer level, respectively, whereas the monomer content of the amorphous formulation containing 40 % mAb1 was only reduced by 0.9 %. The latter formulation also had the highest initial monomer content, compared to the other mAb1 PCMC formulations. This outcome indicated that a protein load of 60 and 50 % was probably too high to be optimally stabilized via PCMC technology, which is consistent with the findings on mAb2 PCMCs discussed in chapter 3. Independent of the formulation, the decrease of the monomer content was ascribed to the formation of soluble protein aggregates because fragmentation of mAb1 formulated as PCMCs was not observed during the accelerated short-term stability study. Moreover, irrespective of

the formulation, the AUC in HP-SEC did not change significantly over time. Thus, all samples were free of considerable amounts of large protein particles typically prone to accumulate in the precolumn or at the column top [32].

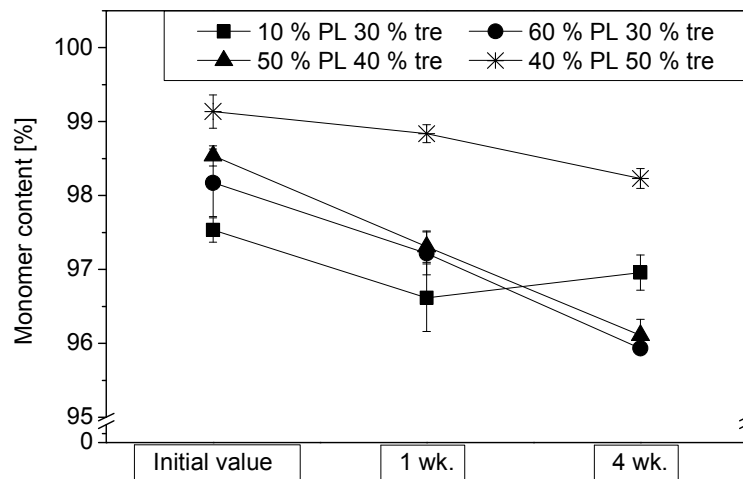
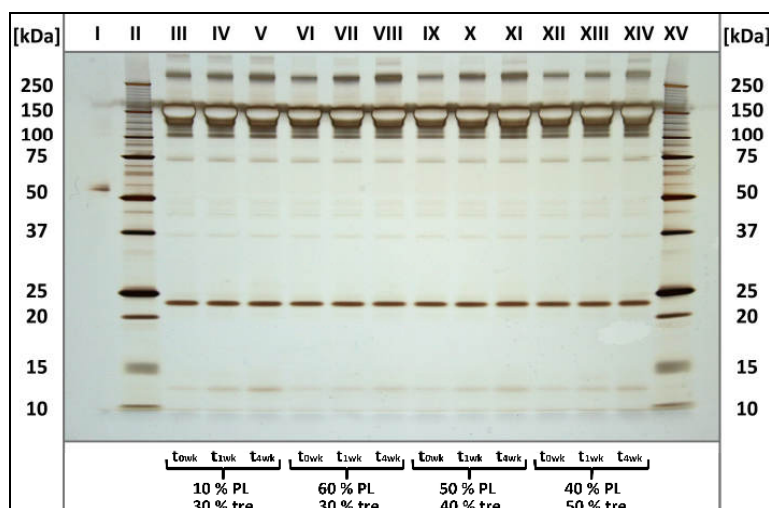


**Figure 6-3: Monomer content of mAb1 PCMCs with varying protein load and trehalose content stored at 40 °C/32 % RH for 4 weeks.**

SDS-PAGE, representing an orthogonal method for the analysis of soluble protein aggregates [31], confirmed the HP-SEC results with an obvious increase in aggregates for all mAb1 PCMC formulations investigated (Figure 6-4). The broad aggregate band above 250 kDa under non-reducing conditions (gel a) was more pronounced in lanes V, VIII, XI and XIV compared to all other lanes. Likewise, the bands at about 100 kDa, 75 kDa and 37 kDa under reducing conditions (gel b) were slightly darker in those lanes. But generally, as silver stained bands cannot be quantified reliably, interpretation should mainly be restricted to qualitative evaluation [31]. A faint extra band above 250 kDa indicating mAb1 aggregation with prolonged storage time was detected for all amorphous formulations (lanes VIII, XI and XIV) at  $t_{4wk}$ . For the crystalline formulation (10 % PL, 30 % tre), this band was already present at  $t_0$  and  $t_{1wk}$ , in accordance with the higher initial aggregate level detected via HP-SEC. Additional faint bands found above 10 kDa in the lanes IV, V, VIII, XI and XIV under non-reducing as well as reducing conditions were attributed to mAb1 fragments formed during storage of the PCMC powders. Fragments were not detected during HP-SEC analysis and therefore fragment levels were assumed to be very low (< 0.1 %). No further differences between the samples with varying

protein load and trehalose content were observed within 4 weeks of storage. Non-reducible aggregates were not detected because no aggregate band persisted under reducing conditions. In summary, SDS-PAGE indicated only negligible formation of covalent soluble aggregates.

(a)



(b)

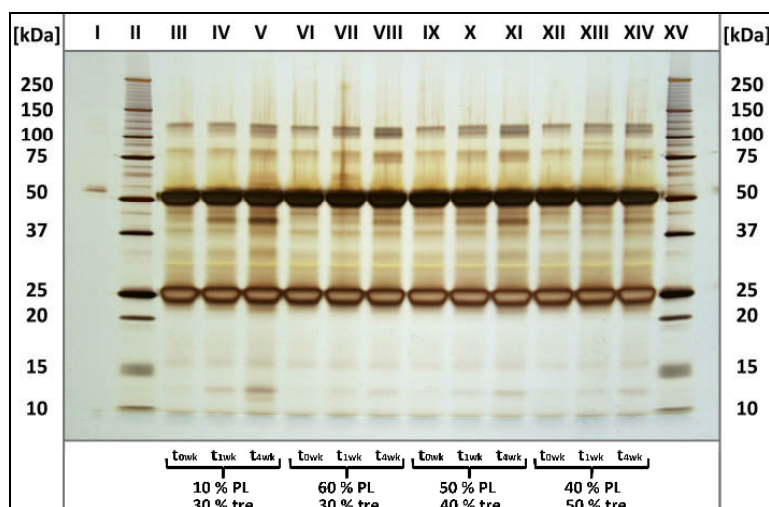


**Figure 6-4: SDS-PAGE of mAb1 PCMCs with varying protein load and trehalose content stored at 40 °C/32 % RH for 4 weeks; (a) non-reducing and (b) reducing conditions; lane assignment: I: BSA control; II: Precision Plus Protein Standard; III-V: reconstituted mAb1 PCMC samples with 10 % PL 30 % tre ; VI-VIII: reconstituted mAb1 PCMC samples with 60 % PL 30 % tre ; IX-XI: reconstituted mAb1 PCMC samples with 50 % PL 40 % tre ; XII-XIV: reconstituted mAb1 PCMC samples with 40 % PL 50 % tre; XV: Precision Plus Protein Standard.**

Overall, only minor differences were revealed between the 4 formulations with respect to protein storage stability. The turbidity of the crystalline sample (10 % PL 30 % tre) was slightly

higher than of the amorphous ones (60 % PL 30 % tre, 50 % PL 40 % tre, 40 % PL 50 % tre) and increased with prolonged storage time. However, the formation of soluble protein particles analyzed via HP-SEC was slightly less pronounced in the presence of an at least partially crystalline carrier matrix, compared to completely amorphous particles. Thus, based on these results of the accelerated short-term stability study, the physical state of the mAb1 PCMCs had no tremendous effect on the degree of stabilization of the monoclonal antibody during storage and all formulations investigated provided good protein stability. The amorphous state in comparison to the crystalline state is defined by a lack of long-range order of molecular packing or well-defined molecular conformation if the constituent molecules are conformationally flexible as it is the case for proteins [33, 34]. In general, amorphous solids are supposed to be less stable physically and chemically [34]. Nevertheless, the effect of the physical state of the solid on the stabilization of proteins is ambiguously discussed in literature. Crystalline glucose oxidase and lipase [35] as well as lysozyme [36] and amylase [37] were reported to be more stable than their amorphous counterparts. However, Pikal and Rigsbee who studied the stability of pure insulin in crystalline and amorphous solids revealed a greater stability for the amorphous form, although the mechanism involved could not successfully be clarified [38, 39]. Nevertheless, one aims to achieve a fully amorphous product during freeze-drying processes as successful interaction between excipient and protein is thought to be more likely if both interaction partners are within the same amorphous phase [40, 41]. Therefore, crystallization is inhibited by the addition of 'impurities' such as other excipients as well as by the protein it-self [34, 42].

Furthermore, the molar ratio of trehalose dihydrate to protein, being approx. 200 (60 % PL 30 % tre), 320 (50 % PL 40 % tre) and 500 (40 % PL 50 % tre), influenced the storage stability of the amorphous mAb1 PCMC formulations. As the decrease of the monomer content was less pronounced for mAb1 PCMCs with 40 % PL and 50 % tre, the literature recommendation of a molar sugar to protein ratio of  $\geq 360$  for adequate protein stabilization in lyophilisates [43-45] could be successfully applied to these microcrystals.

Apart from protein stability, the carrier and its morphology stability need to be investigated during PCMC storage studies because they are often associated with each other, as described in

chapter 2 section 4.3.2. Referring to the mAb1 microcrystals with varying protein load and trehalose content, carrier and morphology stability was assessed via XRD and SEM. X-ray spectra of all amorphous samples (60 % PL 30 % tre, 50 % PL 40 % tre, 40 % PL 50 % tre) recorded after 4 weeks of storage did not differ from the initial pattern (Figure 6-5a). This indicated the absence of recrystallization processes of the amorphous carrier components. For the crystalline sample containing 10 % mAb1 and 30 % trehalose, the signals at  $27.2^\circ$  and  $31.6^\circ$   $2\theta$  that were attributed to NaCl increased within 4 weeks storage (Figure 6-5b). Thus, NaCl further crystallized under the storage conditions selected for the accelerated short-term stability study. Excipient crystallization during storage of solid protein formulations was reported to cause protein destabilization, e.g. by Kreilgaard et al. as well as by Izutsu et al. [46, 47]. The authors speculated, amongst others, that the maintenance of an amorphous protein-excipient phase allowing for extensive molecular interactions between these two formulation components was essential for long-term storage stability. However, sucrose crystallization taking place during storage of partially collapsed freeze-dried cakes of LDH did not significantly reduce the activity of the protein since a sucrose amount sufficient for LDH stabilization remained in the amorphous state [48]. This explanation could also be applied to the recent findings on mAb1 PCMCs. Despite continuing NaCl crystallization during the accelerated short-term stability study, the integrity of the antibody was not affected. As NaCl represented only 12 % of the total solid in the protein powder, the other components forming a glassy matrix, such as trehalose, were suggested to provide sufficient protein storage stability.

Ongoing NaCl crystallization of mAb1 PCMCs with 10 % PL and 30 % trehalose was not noticeable in SEM (Figure 6-6a and b). The pictures taken at  $t_{4wk}$  did not differ from those of the initial PCMC powder and showed rod-shaped crystals partially coated with a less compact crumbly material. In accordance with the observations made on cytokine-coated microcrystals, described in detail in chapter 2, the latter powder fraction was assumed to be made of amorphous carrier components, mainly trehalose and antibody. The stabilization mechanism of the disaccharide as well as its use in solid protein formulations is discussed in detail in section 3.1.1. The rod-shape of PCMCs that contained glycine as main carrier component was also reported by König [6] and is consistent with the description of glycine crystals by Lahav and Leiserowitz [49]. The amorphous mAb1 PCMC formulations (Figure 6-6c-h) were characterized

by spherical particles similar to those obtained after spray-drying [24, 50, 51]. Moreover, SEM pictures did not provide any indication of excipient recrystallization or collapse either, proving high excipient and morphology stability of the amorphous PCMCs. Though, it has to be taken into consideration that the mAb1 PCMCs were not exposed to high moisture levels during storage.

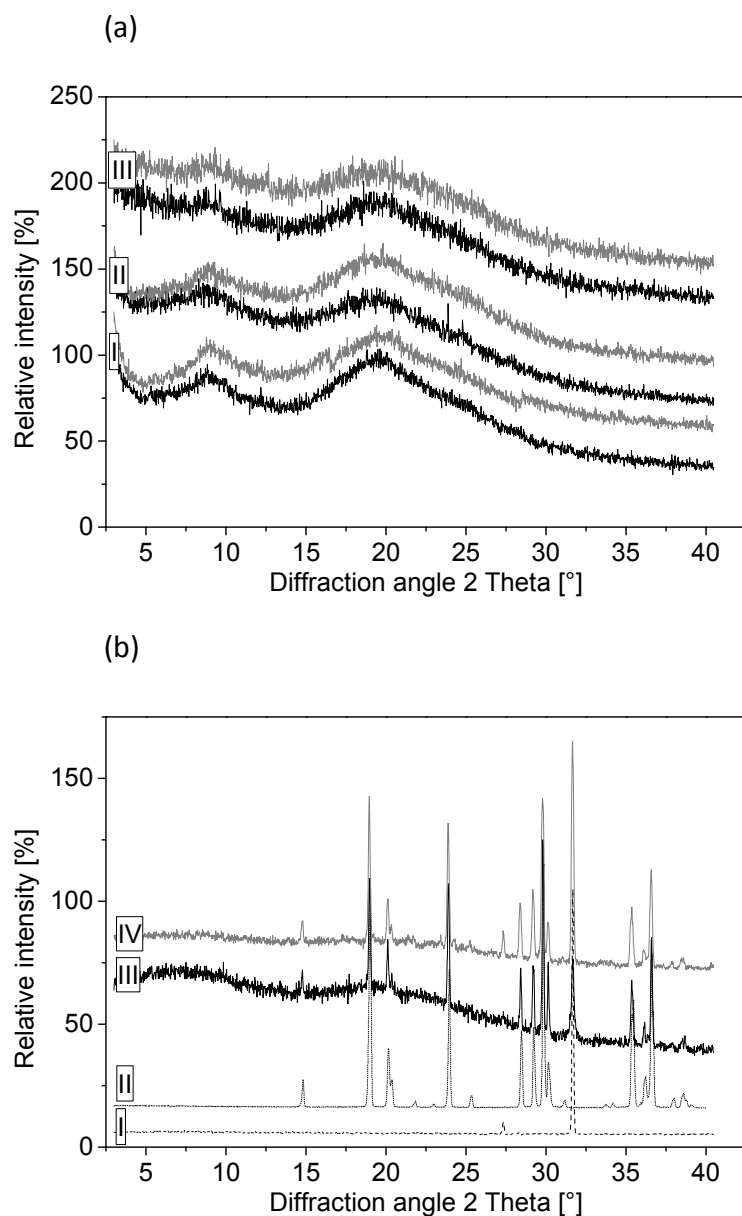


**Figure 6-5: XRD of mAb1 PCMCs with varying protein load and trehalose content stored at 40 °C/32 % RH for 4 weeks; (a) spectrum assignment: I: 60 % PL 30 % tre; II: 50 % PL 40 % tre; III: 40 % PL 50 % tre; black:  $t_0$ , grey:  $t_{4wk}$ ; (b) spectrum assignment: I: NaCl, II:  $\alpha$ -glycine; III: 10 % PL 30 % tre  $t_0$ ; 10 % PL 30 % tre  $t_{4wk}$ .**

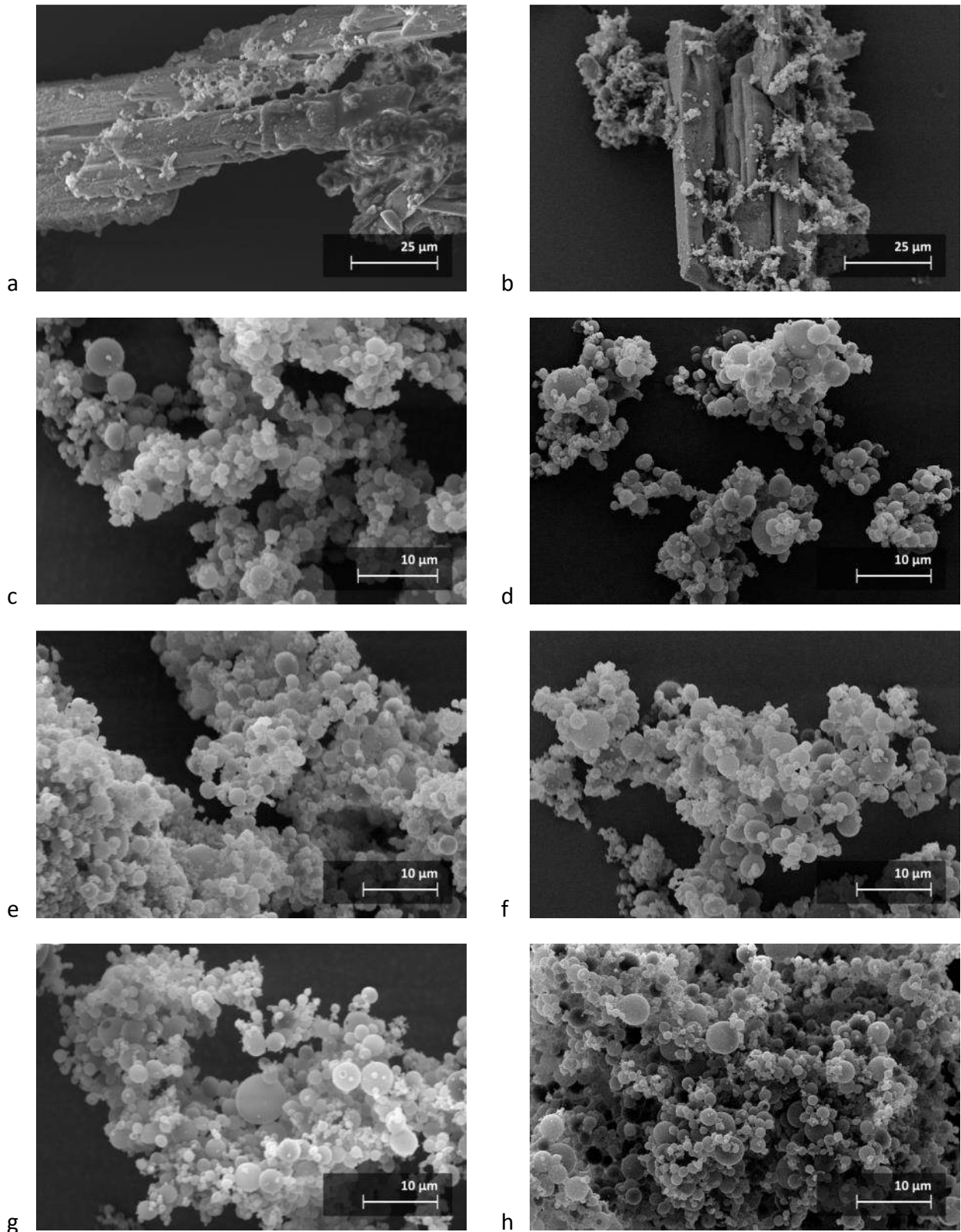


**Figure 6-6: SEM pictures of mAb1 PCMCs with varying protein load and trehalose content at  $t_0$  (left) and stored at 40 °C/32 % RH for 4 weeks (right); a)/b) 10 % PL 30 % tre; c)/d) 60 % PL 30 % tre; e)/f) 50 % PL 40 % tre; g)/h) 40 % PL 50 % tre.**

### 3.1.3 Confocal laser scanning fluorescence microscopy of mAb1 PCMC powders

Confocal laser scanning fluorescence microscopy of mAb1 PCMC formulations selected for the accelerated short-term stability study was applied to investigate the protein distribution within these particles. Scanning through different layers of the microcrystals, this technique allowed also assessing the interior structure of the particles, as opposed to SEM. Widely, CLSFM has successfully been used in numerous applications of cellular biology, as reviewed by Földes-Papp et al. as well as by Halbhuber and König [52, 53]. Furthermore, there is considerable interest in the use of this technique in pharmacologic and therapeutic areas.

In accordance with the SEM analysis of the powders (section 3.1.2), the morphology of the crystalline microcrystals (10 % PL 30 % tre) detected via CLSFM differed from the microscopic appearance of the amorphous formulations (60 % PL 30 % tre, 50 % PL 40 % tre and 40 % PL 50 % tre). In the crystalline mAb1 PCMC powder, the silhouettes of large rod-shaped crystals were clearly visible (Figure 6-7). These structures also observed in SEM and associated with glycine crystals were further characterized by low fluorescence intensity, indicating that they were essentially free of labeled protein. Besides these crystalline structures, material attached to the glycine crystal surface without distinct outlines exhibiting high fluorescence intensity was observed. The fluorescence intensity of this material increased when scanning from the outside to the inside of the particles. Thus, labeled protein was present throughout all layers of this material.

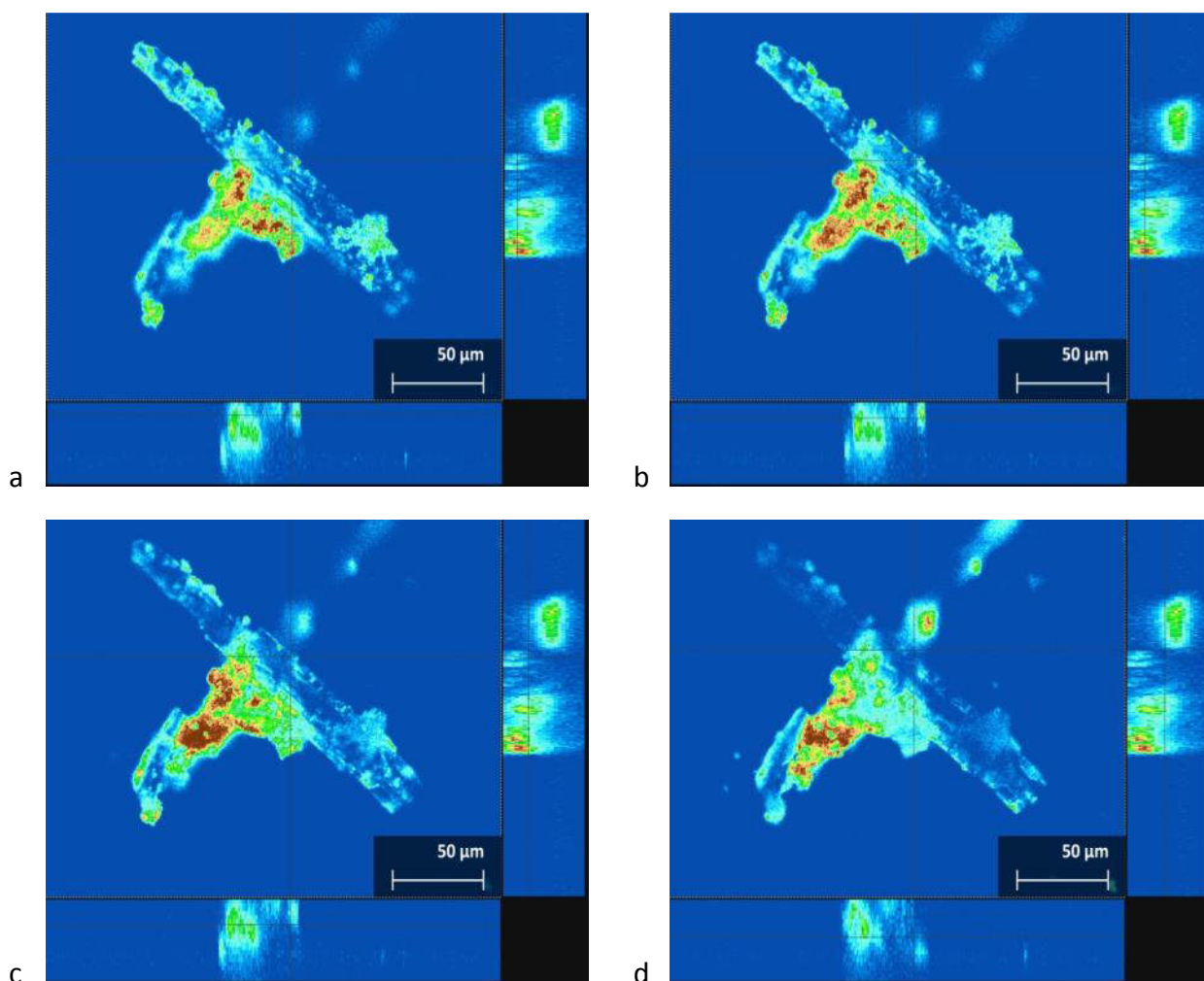


**Figure 6-7: CLSM of mAb1 PCMCs with 10 % protein load and 30 % trehalose; the lower and right sections represent the cross-sections of the particles; fluorescence intensity: blue < cyan < green < yellow < brown.**

These morphological observations were consistent with the general idea of the PCMC technology including a crystalline core of carrier and amorphous protein coated onto the surface of these crystals, as presented in Figure 6-8 modified from Vos [1]. The author's theory was derived from several experiments on PCMCs, including atomic force microscopy (AFM), zeta potential measurements and dynamic light scattering (DLS) as analytical techniques. AFM analysis revealed the presence of protein clusters on the crystal surface, showing clear step-contours, for valine subtilisin Carlsberg PCMCs. Zeta potential measurements of uncoated and coated microcrystal particles further revealed a shift of the particles' surface charge when protein was coprecipitated with the carrier material. Moreover, Ostwald ripening was detected via DLS for uncoated microcrystals, as opposed to particles coated with protein. The complete

inhibition of this phenomenon in the presence of albumin was associated with the formation of a protein coating on the excipient surface. During the desorption experiment albumin valine PCMCs were resuspended in a saturated aqueous valine solution, impeding the dissolution of the microcrystals. The vast majority of the protein was afterwards recovered in the supernatant. With respect to the cytokine PCMCs, the amorphous fraction attached to the crystal surface was further assumed to be not only composed of pure protein, but additionally of carrier excipients tending towards the formation of an amorphous structure, such as trehalose (see section 3.1.1).

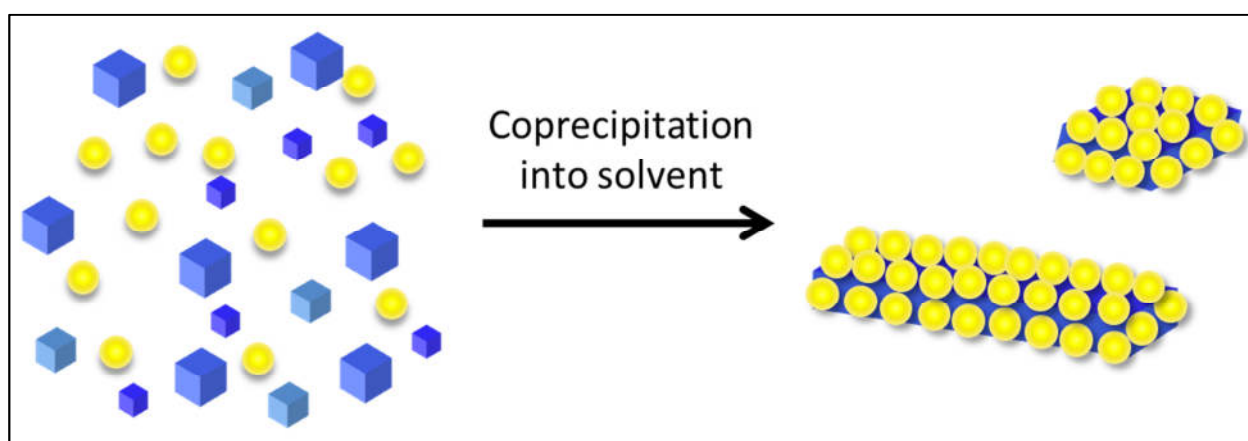


**Figure 6-8: Formation of PCMCs modified from Vos [1]; protein (yellow spheres) and excipient (blue cubes) are preblended/dissolved in water and coprecipitated into non-solvent, resulting in the self-assembly of PCMCs with protein located on the surface of the excipient crystals.**

Independent of the exact composition of the particles, the CLSFM appearance of all amorphous mAb1 PCMC formulations, exemplarily shown in Figure 6-9 for the sample containing 60 % protein and 30 % trehalose, was similar. Being in line with the XRD and SEM results (section 3.1.1 and 3.1.2), the amorphous powders were free of any crystalline structures and were composed of one homogenous particle fraction. Within these particles the labeled antibody was evenly distributed as indicated by the fluorescence intensity changing from blue/green over yellow and brown back to blue/green while scanning through the PCMCs. The cross-section further revealed a spherical shape of the single particles forming larger powder agglomerates, as also observed via SEM analysis.

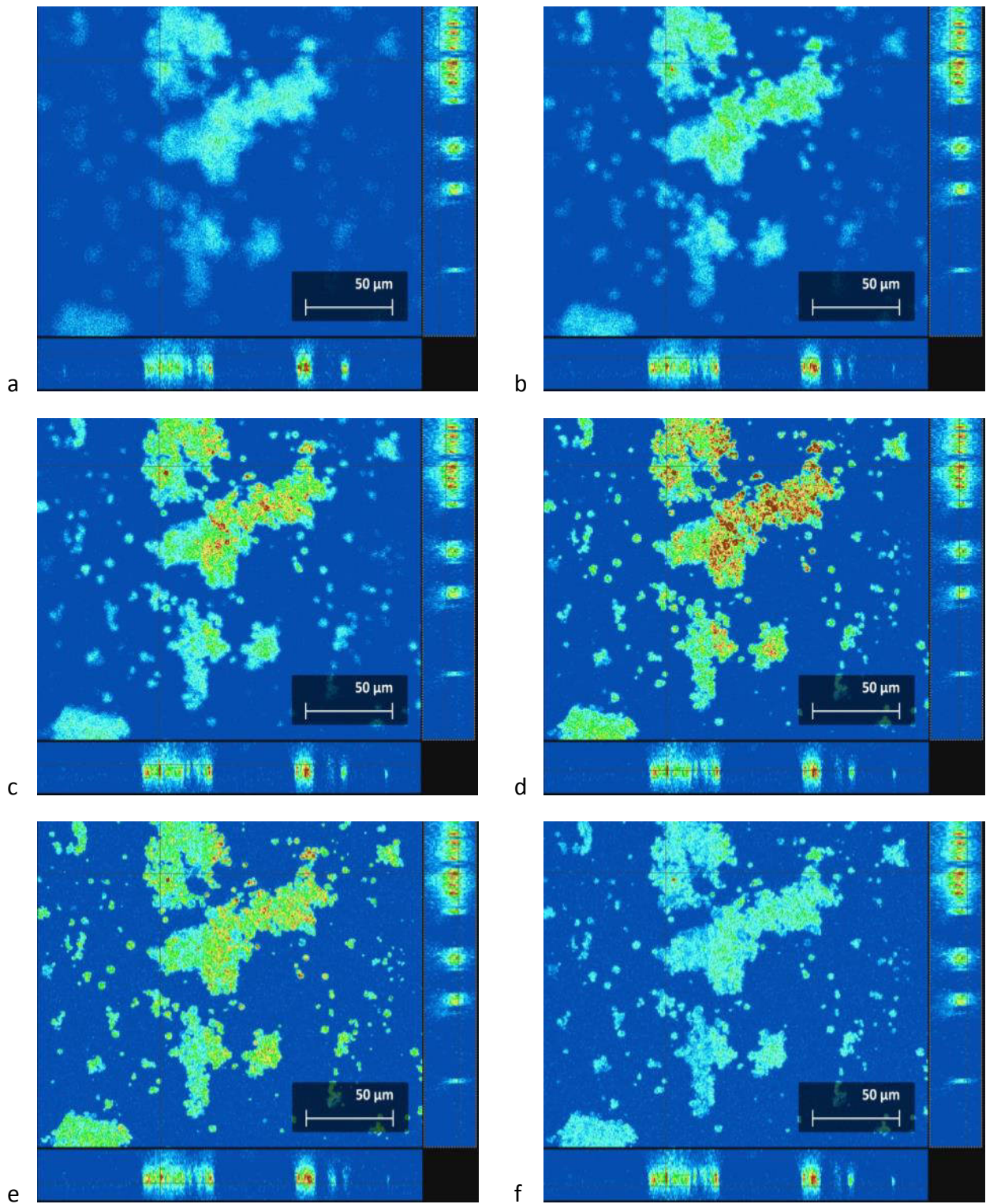
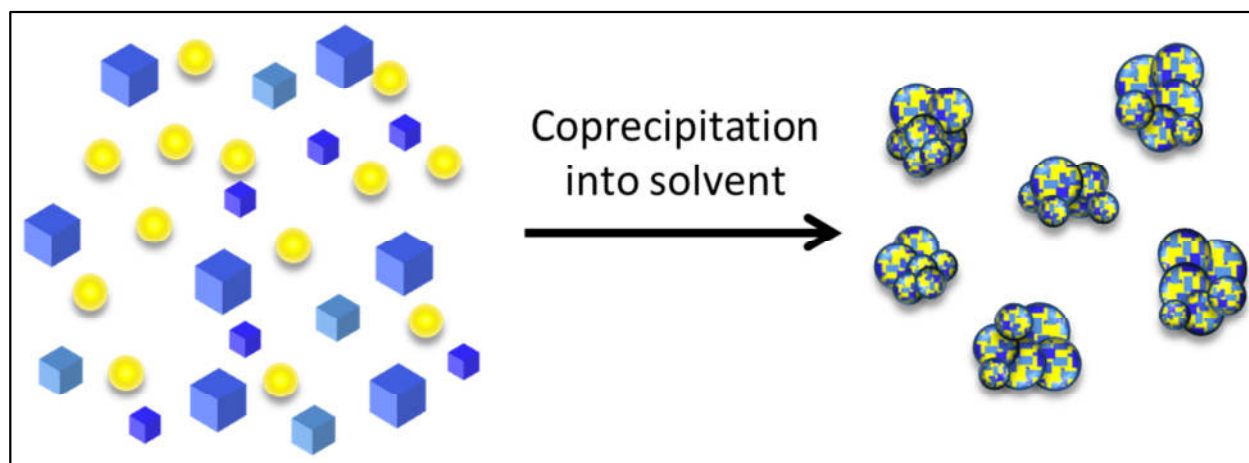


Figure 6-9: CLSM of mAb1 PCMCs with 60 % protein load and 30 % trehalose; the lower and right sections represent the cross-sections of the particles; fluorescence intensity: blue < cyan < green < yellow < brown.

Hence, the structure of these particles did neither correspond to the conception of Vos presented in Figure 6-8 nor to the term “protein-coated microcrystals”, because carrier excipients and protein did not form two morphologically and chemically different fractions, but amorphous, uniform spherical particles. Therefore, the idea offered in Figure 6-10 seemed to be more suitable for the graphical description of these particles.



**Figure 6-10: Proposed formation process of mAb1 PCMCs; the coprecipitation of protein (yellow spheres) and excipient (blue cubes) results in the self-assembly of homogeneous, amorphous “PCMCs”.**

### **3.2 Fractionation of cytokine PCMCs and mAb1 PCMCs via cascade impactor**

SEM analysis of crystalline cytokine PCMCs with 10 % protein load (chapter 2 section 3.2), and amorphous mAb1 PCMCs with a protein level of 40-60 % and 50-30 % trehalose (section 3.1.2 of the current chapter), suggested fundamentally different morphologies of these particles. The former, which contained valine as main carrier component as well as citrate/citric acid and sucrose, were composed of two particle fractions, a compact crystalline one forming rosettes and another less compact crumbly one (Figure 6-11a). Some of the less compact crumbly material was coated on the surface of the compact crystalline fraction, another part existed separate from the crystals. Amorphous mAb1 PCMCs, with trehalose, glycine, NaCl, histidine and phenylalanine as carrier excipients, however, were characterized by homogenous spherical material (Figure 6-11b). For more detailed characterization of the powders, an attempt was made to separate different size fractions of the powders via Andersen Cascade Impactor.

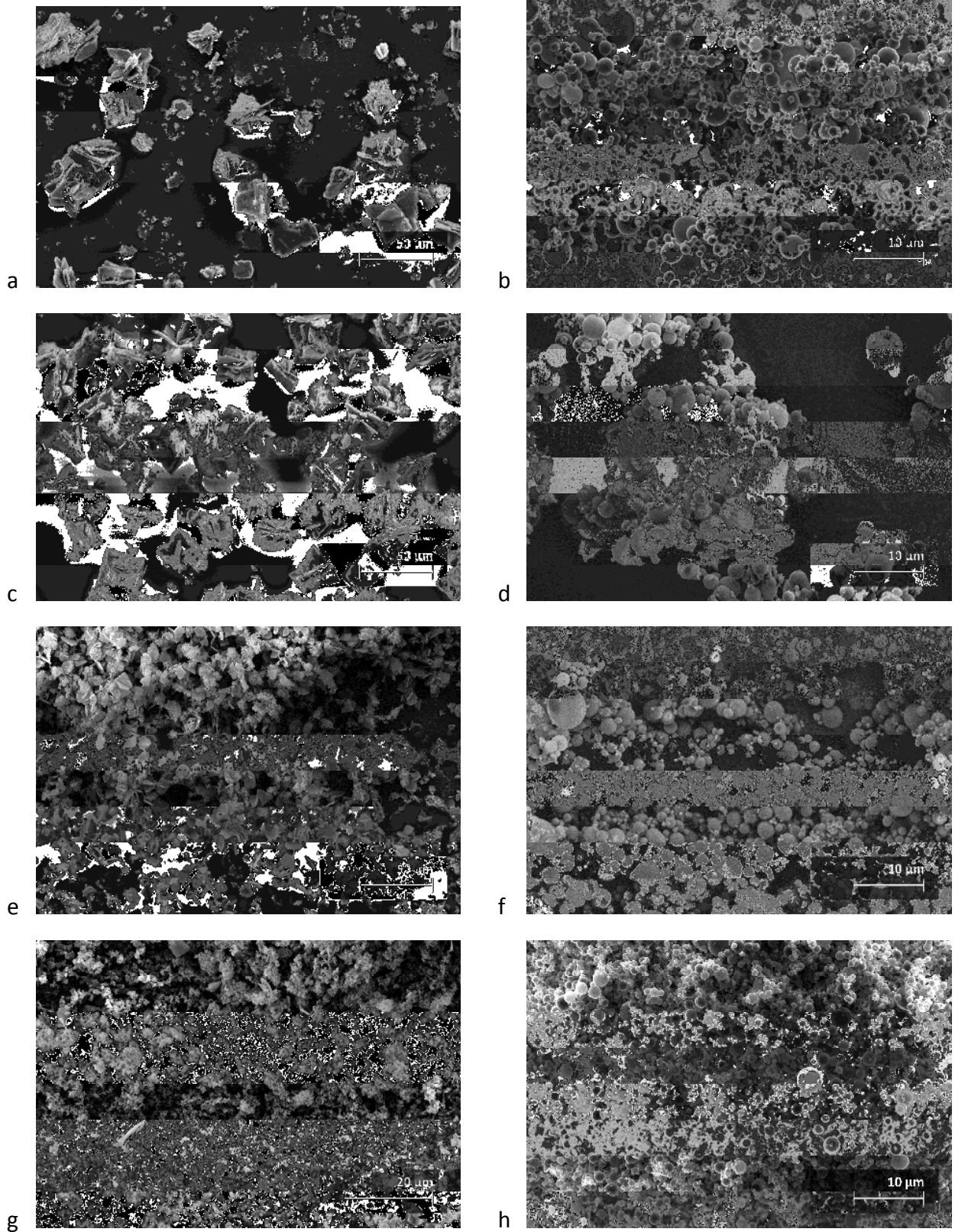


**Figure 6-11 : Cytokine PCMCs (left) and mAb1 PCMCs (40 % PL 50 % tre) (right) separated via Andersen Cascade Impactor; picture alignment: a)/b) initial PCMC powder, powder harvested from c)/d) stage 0, e)/f) stage 3, g)/h) stage 5.**

The cytokine PCMC powder collected from plate 0 of the cascade impactor resembled the initial powder inserted into the device (Figure 6-11c). The powder harvested from plate 1, however, only contained few intact rosette-shaped crystals. Furthermore, platelets representing fragments of the rosettes were visible and considerably more crumbly material was present, compared to the initial powder. The number of rosettes further decreased from plate 1 to plate 2. Powder deposited on plate 3, 4 and 5 was free from larger crystals, whereas the amount of crumbly material increased (Figure 6-11e). Plates 6 and 7 only contained very little amounts of powder insufficient for SEM analysis. Thus, the cascade impactor successfully divided the cytokine PCMCs into these two particle fractions based on a smaller aerodynamic diameter of the crumbly material compared to the large valine crystals.

In case of mAb1 PCMC powder with a protein load of 40 % and 50 % trehalose, the material deposited on plate 0 of the cascade impactor was composed of many spherical particles different in size (Figure 6-11d). It seemed as if the amount of larger particles was slightly increased at the expense of smaller ones, compared to the initial mAb1 PCMCs (Figure 6-11b and d). With increasing plate number the quantity of larger particles decreased and the average particle size decreased (Figure 6-11f and h).

The composition of the powder fractions gained via cascade impactor was analyzed with respect to the protein content, i.e. cytokine and mAb1, and the content of valine and trehalose dihydrate representing the main carrier components of the PCMCs selected. For the cytokine PCMCs, the protein content increased with increasing plate number, whereas the amount of valine in the powder fractions decreased (Figure 6-12a). This increase of the cytokine content with increasing plate number corresponded to an augmented level of fluffy and crumbly material. Hence, the cytokine was primarily located in this particle fraction, as opposed to the crystalline material, being in line with the hypothesis presented in chapter 2 section 4.1. Since proteins and peptides in the solid state usually exist in the amorphous form [22], this particle fraction was further assumed to be amorphous, being consistent with its loose microscopic appearance. As sucrose and citrate, representing additional carrier components of the cytokine formulation besides valine, are prone to form amorphous solids [24, 54-57], the loose and crumbly material certainly does not only incorporate the hydrophobic cytokine, but at least

some parts of those carriers (see chapter 2 section 4.1). This could also explain the high process and storage stability of the cytokine PCMCs because interactions between excipients and proteins are supposed to be most successful if both partners exist in the same amorphous phase (see section 3.1.2). On the contrary, the crystalline rosette-shaped powder fraction essentially consisted of the main carrier component valine. Consequently, the morphology and composition of these cytokine PCMCs was well in accordance with the original idea of this technology [1, 2, 58].

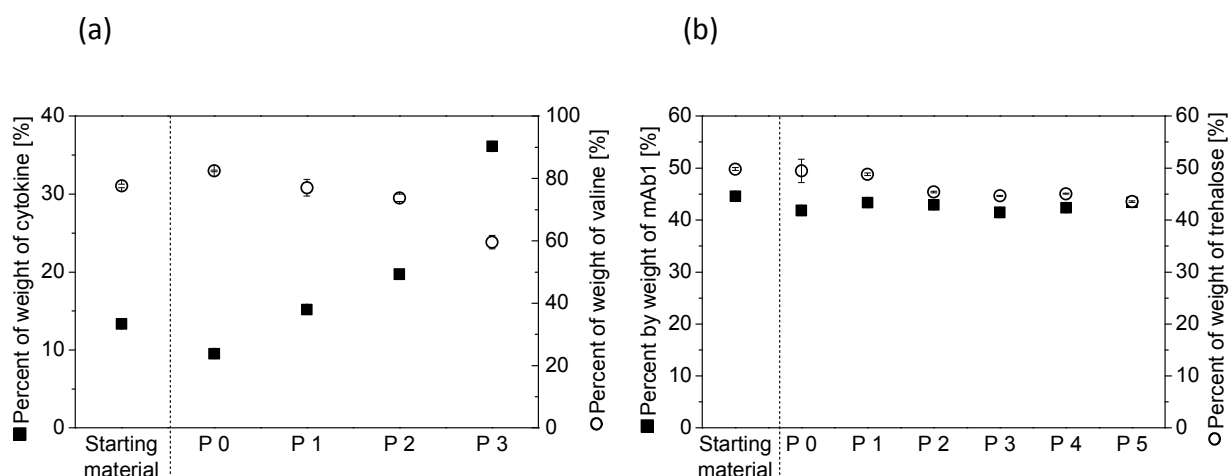


**Figure 6-12: Composition of (a) cytokine PCMC and (b) mAb1 PCMC (40 % PL 50 % tre) fractions separated via Andersen Cascade Impactor with respect to protein content, valine content and trehalose dihydrate content in dependence of the plate (P) number; the amount of powder collected from plates 4-7 (cytokine PCMCs) and 6+7 (mAb1 PCMCs), respectively, was too small to be analyzed.**

The powder fractions of mAb1 PCMCs collected from plate 0 to plate 5 neither differed in the protein nor in the trehalose content (Figure 6-12b). Thus, in accordance with the SEM pictures, these PCMCs did not include one protein-rich fraction and one fraction that was dominated by the presence of carrier material, unlike cytokine PCMCs. Instead, mAb1 PCMCs were proposed to comprise a mixed phase homogeneously unifying mAb1 and carrier excipients as spherical particles of different size. Hence, the powder did not correspond to the PCMCs' definition. Therefore, a new name seems to be required to adequately describe these particles originating from formulation variations of the initial PCMC technology. The term "coprecipitated amorphous protein particles" (CAPPs) would only be applicable to predominantly amorphous PCMC formulations, as opposed to "solvent precipitated protein powder" (SP3s) which does

not specify the overall physical state of the precipitated protein carrier particles. However, the latter is evocative of the well-known ethanol protein precipitation used for plasma fractionation for decades, which was first described in detail by Cohn et al [59]. Finally, as the morphology of the amorphous mAb1 formulations was similar to typical spray-dried protein formulations, as discussed in section 3.1.2, a new term is not mandatory.

### 3.3 Preparation of cytokine and mAb1 PCMCs via one-step and two-step precipitation in batch mode

In this study cytokine and mAb1 PCMCs, intended to be prepared via one-step and two-step precipitation, were compared with respect to particle morphology (SEM) and protein process stability (HP-SEC, bioassay). The one-step precipitation represented a simultaneous coprecipitation of carrier material and protein, usually applied for the manufacturing of PCMCs. On the contrary, the two-step precipitation process consisted of separate precipitation of pure crystalline excipients, followed by subsequent protein precipitation on these carrier particles.

#### 3.3.1 Precipitation of protein-free carrier solutions

Precipitation of pure carrier material of the cytokine PCMC formulation resulted in the formation of rosette-shaped crystals (Figure 6-13), being consistent with the crystal shape observed in the corresponding cytokine formulation (chapter 2 section 4.1). Likewise, the precipitation was slightly decelerated and the product was not yet turbid at the outlet of the mixer, but turbidity immediately built up in the container used for harvesting. Thus, the presence of the protein was not prerequisite for the precipitation process.

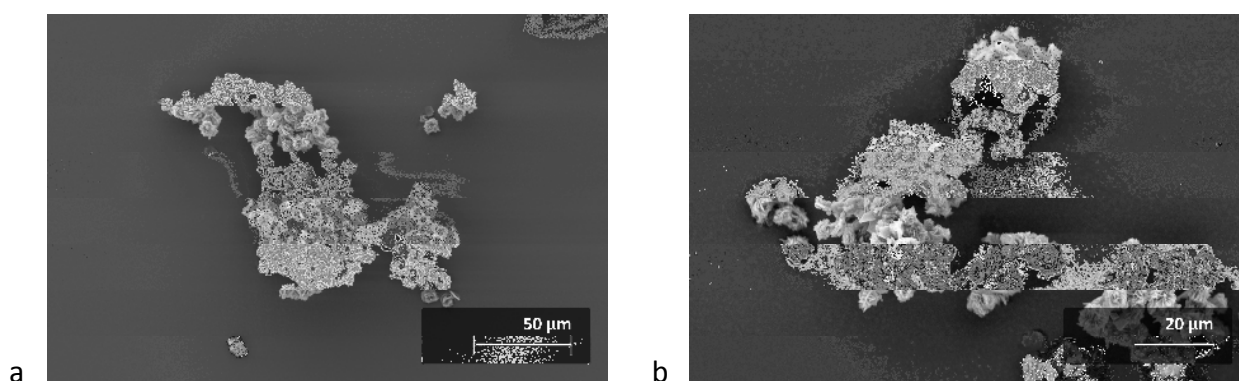
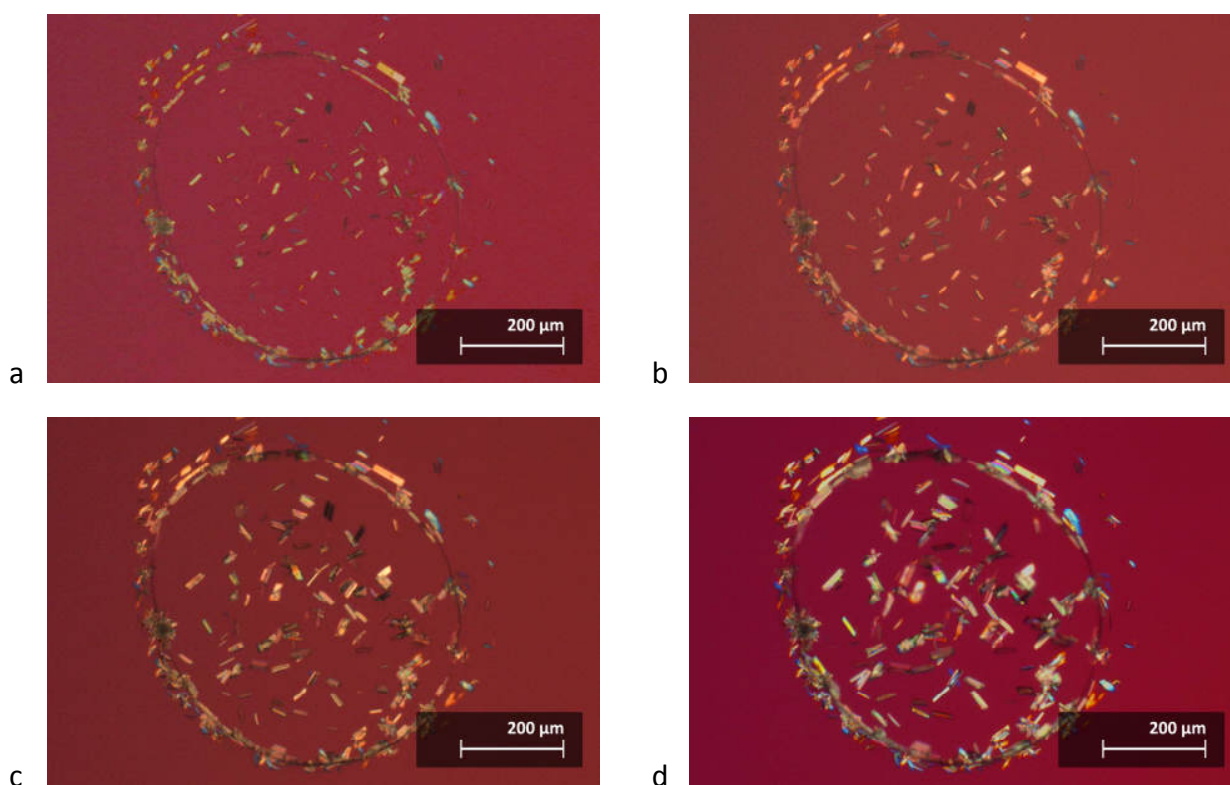


Figure 6-13: SEM of separately precipitated carrier crystals of cytokine PCMCs.



**Figure 6-14: Polarization microscopy of separately precipitated carrier material of corresponding mAb1 PCMCs; a) immediately, b) approx. 2 min, c) approx. 3 min and d) approx. 5 min after precipitation.**

As opposed to cytokine-free valine PCMCs, the precipitation of pure carrier material of the standard mAb1 formulation was not possible. The dropwise addition of the aqueous carrier solution to the precipitating agent immediately caused turbidity associated with particle formation, but the product could not be harvested. Macroscopically droplets deposited and finally stuck to the bottom of the device despite continuous stirring. Microscopic investigation of the supernatant revealed the presence of dispersed droplets in a continuous phase (Figure 6-14). The droplets contained birefringent crystals mainly aligned at the liquid-liquid interphase, but also inside. The crystalline structures significantly grew within a few minutes after precipitation. These observations were evocative of the ouzo effect derived from the alcoholic beverage and described in detail by Vitale and Katz who studied the formation of liquid droplet dispersions by homogenous liquid-liquid nucleation [12]. This physical effect that occurs in liquid systems comprising three or more components describes the formation of dispersed oil droplets in water in consequence of the rapid addition of water to a solution of oil dissolved in a solvent. As the oil supersaturates, it then nucleates into small relatively stable

droplets. In his review on recent developments and applications of the ouzo effect, Botet further specified that the ouzo region only represents a particular part of the area between the binodal and spinodal line (Figure 6-15) [60].

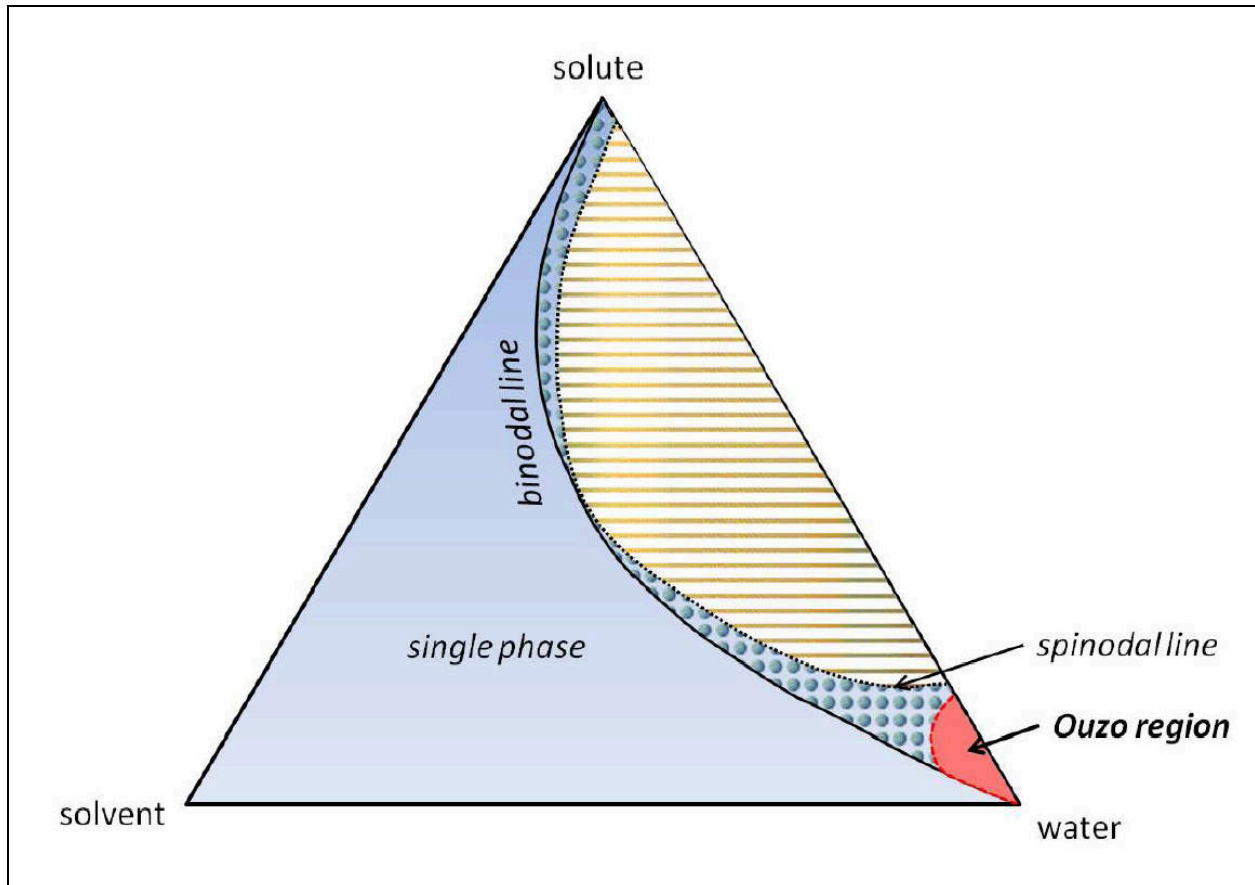


**Figure 6-15: Ternary phase diagrams with ouzo region at constant temperature and pressure according to Botet [60]; the ouzo effect occurs when a three-component solution is rapidly brought into the ouzo region in the metastable area between the binodal (miscibility-limit curve) and spinodal (stability-limit curve) curves by the addition of solvent.**

However, as opposed to the PCMC precipitation, the ouzo effect occurs spontaneously without the use of mechanical agitation, surfactants or dispersing agents and corresponding emulsions appeared to be stable for months [12, 60]. Therefore, according to Vos [1], spinodal decomposition representing the rapid separation of an initial one-phase solution brought inside the spinodal curve by changing its compositions [12] seemed to be more suitable for characterizing the PCMC formation process. As the large surplus of organic solvent strips out the water molecules, protein and excipient partition into small, dense precursor droplets resembling oils or melts of excipient and protein. These droplets coalesce and the protein is

transported to the outer periphery of the droplet. As soon as the oily excipient core reaches saturation, nucleation and growth of the crystalline core is highly favorable and solid PCMCs form. In a secondary process, the excluded protein assembles at the surface of the excipient core to form a continuous network, being attached via hydrogen bonding and van der Waals interactions. Vos' hypothesis was derived from DLS and simultaneous laser obscuration measurements of in-situ prepared PCMC samples [1]. The observation that the particle formation process was typically completed after approx. 100 s in combination with calculations on the time taken for dense pre-cursor particles to aggregate by shear forces as well as by Brownian motion was in line with the spinodal decomposition model. The particle formation process by nucleation and growth, however, was expected to take in the order of minutes, not seconds, and in that case particles were assumed to exhibit significantly more Ostwald ripening effects. Therefore, spinodal decomposition appeared to be more appropriate for the description of the PCMC formation process.

The recent observation of dispersed droplets containing crystallizing excipients, mainly at the liquid-liquid interface, after the precipitation of a mAb1 carrier solution was well in line with the spinodal decomposition model. Therefore, the rapid introduction of excessive solvent was proposed to result in the formation of two phases, one "excipient and protein rich/solvent poor" phase and one "excipient and protein poor/solvent rich" phase, via spinodal decomposition (Figure 6-16). Diffusion of water molecules out of the inner "excipient and protein rich/solvent poor" phase in the continuous second phase and of solvent in the opposite direction was suggested to lead to supersaturation of excipients and protein finally resulting in precipitation. At this stage excipient crystallization could be avoided by the choice of formulation composition, as discussed in previous sections of this chapter (section 3.1.2) as well as in chapter 3 (sections 3.1.1 and 3.2.1). The amount of protein and excipients tending towards the formation of amorphous solids significantly influences the overall physical state of the particles formed via coprecipitation. At last, the continuous phase is removed via supercritical fluid extraction. The overall spherical particle form revealed for amorphous mAb1 PCMC formulations via SEM (chapter 3 and 6) supported the hypothesis of spinodal decomposition. Based on confocal laser scanning fluorescence microscopy (section 3.1.3) proposing homogenous distribution of the protein within the amorphous mAb1 PCMCs, the

protein is not expected to be transported to the periphery of the droplets during the particle formation process, as opposed to the conception of Vos [1].

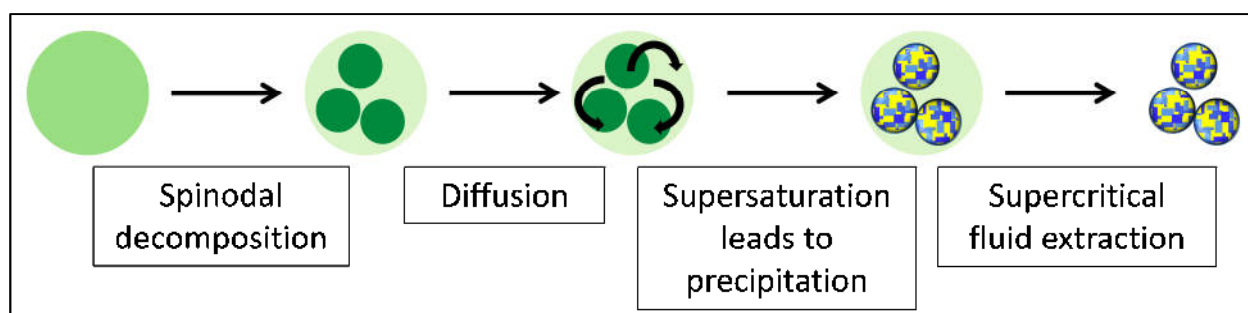


**Figure 6-16: Particle formation process proposed for amorphous mAb PCMCs via spinodal decomposition model; color assignment: green: homogenous phase of aqueous protein-carrier solution and solvent immediately after addition of the solvent; light green: “excipient and protein poor/solvent rich” phase; dark green: “excipient and protein rich/solvent poor” phase; yellow: precipitated protein; blue: precipitated carrier material.**

Probably, this proposed particle formation process was only applicable for amorphous mAb PCMC formulations and not for cytokine-coated microcrystals, as discussed in the following section, because an emulsion-like intermediate was not detected during the production of both proteinaceous and protein-free cytokine PCMC formulations.

### 3.3.2 Precipitation of cytokine on separately prepared carrier crystals in comparison to standard one-step precipitation

As protein-free particles corresponding to standard mAb1 formulation could not be produced, this study was limited to cytokine PCMCs. The cytokine PCMCs manufactured via two-step precipitation did not morphologically differ from those particles produced via coprecipitation of carrier material and protein (Figure 6-17). Moreover, no significant differences between the PCMCs produced via one-step and two-step precipitation were revealed with regard to protein content, monomer content, AUC in HP-SEC and biological activity (Table 6-6). The results were comparable to the values found for the bulk drug substance of the cytokine. Hence, irrespective of the type of preparation, the PCMC technology provided good overall process stability to the cytokine.

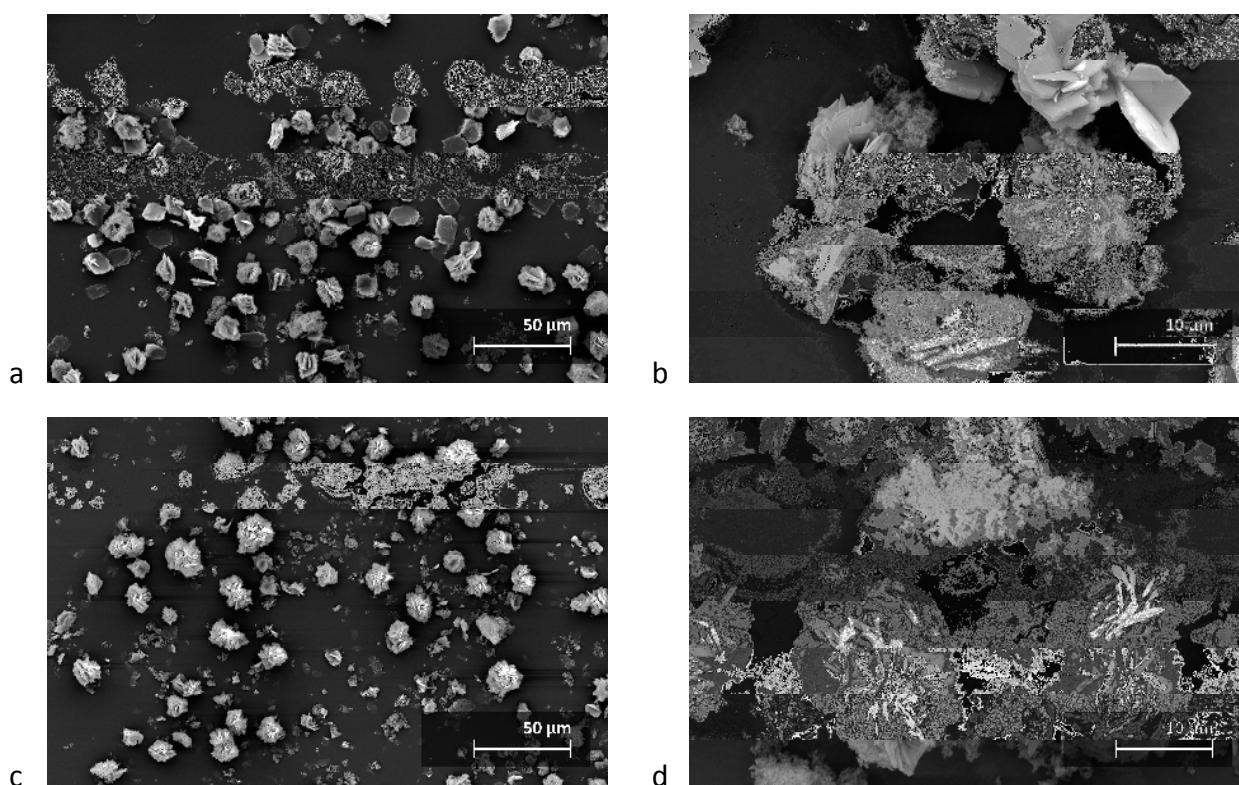


**Figure 6-17: Cytokine PCMCs produced via a)/b) one-step and c)/d) two-step precipitation.**

These observations suggested that the so-called one-step precipitation might be subdivided into two separate processes, the parallel precipitation of crystalline “carrier rich/protein poor” material and amorphous “carrier poor/protein rich” solid subsequently attaching to the surface of the crystalline structures in a second step, thus leading to the formation of protein-coated microcrystals. If the cytokine was involved into the early precipitation step of the carrier material, one-step precipitation and two-step precipitation would probably affect the particle morphology as well as the protein process stability. A secondary protein coating step was also proposed by Vos based on his DLS and laser obscuration measurements [1]. The author hypothesized that the carrier crystals primarily formed via spinodal decomposition (see above). However, no observations supporting the latter hypothesis were made during the current study on cytokine PCMCs, as opposed to mAb1 PCMCs. Therefore, it is also possible that the formation of carrier crystals was based on the classical nucleation and growth model. However, in most real systems the transition of the two mechanisms is known to be gradual [11]. Thus, further detailed investigations on the PCMC formation process are indispensable to answer this question. According to Horn and Rieger, to understand the stages through which the formation

of colloidal particles pass it is necessary to experimentally record the particle formation process by time resolution from the timepoint when supersaturation is achieved [11]. As this procedure is not trivial at all, the description of the particle formation process is often still limited to a retrospective derivation from the particle structure formed. Correspondingly, there are no doubts that mechanistic differences exist in the formation of cytokine PCMCs, on the one hand, and mAb1 PCMCs, on the other hand, as also reflected by their supramolecular structure.

**Table 6-6: Protein process stability of cytokine PCMCs produced via one-step and two-step precipitation with respect to protein content, monomer content (HP-SEC), AUC in HP-SEC and biological activity; cytokine bulk drug substance contained  $98.9 \pm < 0.1$  % monomer and resulted in an AUC of  $315 \pm 1$  mAU\*mL.**

	One-step precipitation	Two-step precipitation
Protein content [%]	$12.7 \pm 0.1$	$11.7 \pm < 0.1$
Monomer content [%]	$98.8 \pm 0.1$	$98.6 \pm 0.1$
AUC in SEC [mAU*mL]	$296 \pm 16$	$293 \pm 3$
Biological activity [IU/mg protein]	$(2.2 \pm 0.4) \times 10^7$	$(2.4 \pm 0.3) \times 10^7$

### 3.3.3 Precipitation of cytokine in the absence of carrier material

This study aimed to investigate whether the cytokine could be successfully precipitated via standard PCMC process from a pure aqueous protein solution that did not contain any carrier material. When a mixture made of 2-methyl-2,4-pentanediol and isopropanol (1:1 v/v), saturated with all carrier components, was used as precipitating agent, the precipitation process resulted in the formation of a gel that could neither be further processed nor analyzed. Gel formation due to protein aggregation has been reported several times, as reviewed by Wang [61]. For example, Renard et al. studied the gelation and aggregation properties of  $\beta$ -lactoglobulin in ethanol/water solutions [62]. In the presence of pure saturated isopropanol, as opposed to unsaturated solvent, cytokine precipitation was detected, but the small amount of powder harvested did not allow for analysis of protein integrity. Thus, the saturation of isopropanol with all carrier excipients was prerequisite for the precipitation of the protein. After saturation of the solvent, residual carrier crystals were removed via filtration through a 0.22  $\mu$ m membrane filter (Stericup-GV, 47mm, PVDF, Sartorius, Göttingen, D). However, small

carrier particles passing the filter were assumed to act as heterogeneous nuclei indispensable for the precipitation of the cytokine.

## 4 Conclusion

Based on various studies on cytokine and mAb1 PCMCs focusing on the morphology, composition and stability of the particles, this chapter aimed to gain mechanistic insights into the PCMC formation process. The initial PCMC conception presented by Vos comprised a crystalline particle core made of carrier excipients that was coated by a protein layer. Confocal laser scanning fluorescence microscopy revealed such a supramolecular structure for crystalline mAb1 PCMCs containing 10 % antibody and 30 % trehalose. An equivalent assembly was also proposed for cytokine PCMCs with a protein load of 10 % that could successfully be separated into a crystalline rosette-shaped carrier fraction and a less dense amorphous fraction dominated by protein via Andersen Cascade Impactor in combination with SEM analysis. Furthermore, cytokine PCMCs could be manufactured via standard one-step precipitation, but also via two-step precipitation describing the protein precipitation on previously prepared carrier crystals. The precipitation type neither affected the morphology nor the protein process stability of the cytokine PCMCs. In contrast, two-step precipitation was not possible for amorphous mAb1 PCMCs because the carrier could not be processed in the absence of protein in batch mode. However, the presence of an emulsion-like state of the protein-free mAb1 PCMC formulation was detected in this study via polarization microscopy. Transferred to proteinaceous mAb1 PCMCs, the inner dispersed phase was assumed to be made of much carrier material and protein but a small amount of solvent, as opposed to the outer continuous “excipient and protein poor/solvent rich” phase. Crystal growth was observed at the boundary and inside the dispersed droplets. Hence, the spinodal decomposition model seemed to be suitable to describe the mAb1 PCMC formation mechanism. After addition of a surplus of organic water-miscible solvent to the aqueous protein-carrier solution, phase separation of the homogenous phase was proposed to occur via spinodal decomposition resulting in one continuous “excipient and protein poor/solvent rich” and one dispersed “excipient and protein rich/solvent poor” phase. Diffusion of the solvent from the outer into the inner phase and from water in the opposite direction probably leads to supersaturation and finally precipitation of

protein and carriers in the inner phase. Spherical particles containing homogeneously distributed protein and carrier material were suggested to form in this way, while the outer “excipient and protein poor/solvent rich” is removed via supercritical fluid extraction. This formation process was also in line with the particle morphology and supramolecular structure of mAb1 PCMCs representing uniform spherical particles of different size in which the protein was homogeneously distributed instead of being bound to the surface. Thus, these particles could only be fractionated by size via Andersen Cascade Impactor.

The question whether this particle formation process might also be applied to cytokine PCMCs and crystalline mAb1 formulations could not be answered yet because an emulsion-like state was not observed in these cases. Therefore, additional mechanistic investigations are necessary to clarify the PCMC formation mechanism. Depending on the sum of protein and trehalose dihydrate in the formulation, both typically forming amorphous solids, crystalline or amorphous particles were formed. A completely amorphous state of mAb1 PCMCs could be achieved in the case of  $\geq 85\text{-}90\%$  (m/m) mAb1 and trehalose dihydrate. Despite the structural differences between crystalline and amorphous mAb1 PCMC formulations, only marginal differences with respect to protein storage stability, namely turbidity values and monomer content, were revealed after storage at  $40\text{ }^{\circ}\text{C}/32\%$  RH for 4 weeks. All formulations provided good overall stability to the antibody. Hence, in all cases, the amount of amorphous excipient fraction was sufficient for adequate protein stabilization.

## 5 References

1. Vos, J., *Understanding the formation mechanism of protein coated microcrystals* [dissertation]. Glasgow: University of Strathclyde, 2006.
2. Moore, B.D., et al., *Rapid dehydration of proteins*. WO00/69887, 2000.
3. Kreiner, M.M., Moore, B.D., and Parker, M.C., *Enzyme-coated micro-crystals: A 1-step method for high activity biocatalyst preparation*. Chemical Communications, 2001: p.1096-1097.
4. Kreiner, M. and Parker, M.C., *Protein-coated microcrystals for use in organic solvents: Application to oxidoreductases*. Biotechnology Letters, 2005. **27**(20): p.1571-1577.
5. Kreiner, M.M., et al., *Stability of protein-coated microcrystals in organic solvents*. Journal of Molecular Catalysis B: Enzymatic, 2005. **33**: p.65-72.

6. König, C., *Entwicklung eines Prozesses in Pilotgröße zur Herstellung von Protein-coated Microcrystals* [dissertation]. Bonn: Universität Bonn, 2010.
7. Partridge, J., Lyle, C., and Moore, B.D., *Protein coated microcrystals dry powder formulations with payloads of 30 % w/w to 0.01 % w/w*. AAPS National Biotechnology Conference. 2007. San Diego, CA, USA.
8. Partridge, J., et al., *Stabilization of proteins in dry state without sugars*. AAPS National Biotechnology Conference. 2005. Nashville, TN, USA.
9. Kreiner, M., et al., *DNA-coated microcrystals*. Chemical Communications, 2005(21): p.2675-2676.
10. König, C., et al., *Development of a pilot-scale manufacturing process for protein-coated microcrystals (PCMC): Mixing and precipitation – Part I*. European Journal of Pharmaceutics and Biopharmaceutics, 2012. **80**(3): p.490-498.
11. Horn, D. and Rieger, J., *Organic nanoparticles in the aqueous phase—Theory, experiment, and use*. Angewandte Chemie-International Edition, 2001. **40**(23): p.4330-4361.
12. Vitale, S.A. and Katz, J.L., *Liquid droplet dispersions formed by homogeneous liquid-liquid nucleation: “The ouzo effect”*. Langmuir, 2003. **19**(10): p.4105-4110.
13. Mahler, H.C., et al., *Behaviour of polysorbate 20 during dialysis, concentration and filtration using membrane separation techniques*. Journal of Pharmaceutical Sciences, 2008. **97**(2): p.764-774.
14. Khosravani, A., et al., *Formulation of the adenylate cyclase toxin of Bordetella pertussis as protein-coated microcrystals*. Vaccine, 2007. **25**(22): p.4361-4367.
15. *Amine-reactive probe labeling protocol*. Life Technologies GmbH, accessed January 11, 2013. Available from: <http://de-de.invitrogen.com/site/de/de/home/References/protocols/cell-and-tissue-analysis/Labeling-Chemistry-Protocols/Amine-Reactive-Probe-Labeling-Protocol.html#>.
16. Hong Tran, D., et al., *Saturated salt solutions for humidity control and the survival of dry powder and oil formulations of Beauveria bassiana conidia*. Journal of invertebrate pathology, 2005. **89**(2): p.136-43.
17. Claus, S., et al., *Novel dry powder inhalation system based on dispersion of lyophilisates*. European Journal of Pharmaceutical Sciences, 2011. **43**(1–2): p.32-40.
18. Hawe, A. and Friess, W., *Development of HSA-free formulations for a hydrophobic cytokine with improved stability*. European Journal of Pharmaceutics and Biopharmaceutics, 2008. **68**(2): p.169-182.
19. Meager, A. and Das, R.G., *Biological standardization of human interferon beta: Establishment of a replacement world health organization international biological*

- standard for human glycosylated interferon beta*. Journal of Immunological Methods, 2005. **306**(1–2): p.1-15.
20. Runkel, L., et al., *Structural and functional differences between glycosylated and non-glycosylated forms of human interferon- $\beta$  (IFN- $\beta$ )*. Pharmaceutical Research, 1998. **15**(4): p.641-649.
  21. Chatterjee, K., Shalaev, E.Y., and Suryanarayanan, R., *Partially crystalline systems in lyophilization: I. Use of ternary state diagrams to determine extent of crystallization of bulking agent*. Journal of Pharmaceutical Sciences, 2005. **94**(4): p.798-808.
  22. Forbes, R.T., et al., *Water vapor sorption studies on the physical stability of a series of spray-dried protein/sugar powders for inhalation*. Journal of Pharmaceutical Sciences, 1998. **87**(11): p.1316-1321.
  23. Hawe, A. and Friess, W., *Physico-chemical lyophilization behavior of mannitol, human serum albumin formulations*. European Journal of Pharmaceutical Sciences, 2006. **28**(3): p.224-232.
  24. Schüle, S., et al., *Stabilization of IgG1 in spray-dried powders for inhalation*. European Journal of Pharmaceutics and Biopharmaceutics, 2008. **69**(3): p.793-807.
  25. Wang, W., *Lyophilization and development of solid protein pharmaceuticals*. International Journal of Pharmaceutics, 2000. **203**(1-2): p.1-60.
  26. Naini, V., Byron, P.R., and Phillips, E.M., *Physicochemical stability of crystalline sugars and their spray-dried forms: Dependence upon relative humidity and suitability for use in powder inhalers*. Drug Development and Industrial Pharmacy, 1998. **24**(10): p.895-909.
  27. Ahlneck, C. and Zografi, G., *The molecular basis of moisture effects on the physical and chemical stability of drugs in the solid state*. International Journal of Pharmaceutics, 1990. **62**(2–3): p.87-95.
  28. Hino, T., Tanimoto, M., and Shimabayashi, S., *Change in secondary structure of silk fibroin during preparation of its microspheres by spray-drying and exposure to humid atmosphere*. Journal of Colloid and Interface Science, 2003. **266**(1): p.68-73.
  29. Bondos, S.E. and Bicknell, A., *Detection and prevention of protein aggregation before, during, and after purification*. Analytical Biochemistry, 2003. **316**(2): p.223-231.
  30. Mahler, H.-C., et al., *Induction and analysis of aggregates in a liquid IgG1-antibody formulation*. European Journal of Pharmaceutics and Biopharmaceutics, 2005. **59**(3): p.407-417.
  31. Mahler, H.C., et al., *Protein aggregation: Pathways, induction factors and analysis*. Journal of Pharmaceutical Sciences, 2009. **98**(9): p.2909-2934.
  32. Zölls, S., et al., *Particles in therapeutic protein formulations, Part 1: Overview of analytical methods*. Journal of Pharmaceutical Sciences, 2012. **101**(3): p.914-935.

33. Lai, M.C. and Topp, E.M., *Solid-state chemical stability of proteins and peptides*. Journal of Pharmaceutical Sciences, 1999. **88**(5): p.489-500.
34. Yu, L., *Amorphous pharmaceutical solids: preparation, characterization and stabilization*. Advanced Drug Delivery Reviews, 2001. **48**(1): p.27-42.
35. Shenoy, B., et al., *Stability of crystalline proteins*. Biotechnology and Bioengineering, 2001. **73**(5): p.358-369.
36. Elkordy, A.A., Forbes, R.T., and Barry, B.W., *Stability of crystallised and spray-dried lysozyme*. International Journal of Pharmaceutics, 2004. **278**(2): p.209-219.
37. Pechenov, S., et al., *Injectable controlled release formulations incorporating protein crystals*. Journal of Controlled Release, 2004. **96**(1): p.149-158.
38. Pikal, M.J. and Rigsbee, D.R., *The stability of insulin in crystalline and amorphous solids: observation of greater stability for the amorphous form*. Pharmaceutical Research, 1997. **14**(10): p.1379-1387.
39. Pikal, M.J. and Rigsbee, D.R., *The stability of insulin in crystalline and amorphous solids: observation of greater stability for the amorphous form*. [Erratum to document cited in CA128:7258]. Pharmaceutical Research, 1998. **15**(2): p.362-363.
40. Ohtake, S., Kita, Y., and Arakawa, T., *Interactions of formulation excipients with proteins in solution and in the dried state*. Advanced Drug Delivery Reviews, 2011. **63**(13): p.1053-1073.
41. Wang, W., et al., *Antibody structure, instability, and formulation*. Journal of Pharmaceutical Sciences, 2007. **96**(1): p.1-26.
42. Pyne, A., Chatterjee, K., and Suryanarayanan, R., *Solute crystallization in mannitol-glycine systems—implications on protein stabilization in freeze-dried formulations*. Journal of Pharmaceutical Sciences, 2003. **92**(11): p.2272-2283.
43. Andya, J., Hsu, C., and Shire, S., *Mechanisms of aggregate formation and carbohydrate excipient stabilization of lyophilized humanized monoclonal antibody formulations*. AAPS Journal, 2003. **5**(2): p.21-31.
44. Chang, L., et al., *Mechanism of protein stabilization by sugars during freeze-drying and storage: Native structure preservation, specific interaction, and/or immobilization in a glassy matrix?* Journal of Pharmaceutical Sciences, 2005. **94**(7): p.1427-1444.
45. Cleland, J.L., et al., *A specific molar ratio of stabilizer to protein is required for storage stability of a lyophilized monoclonal antibody*. Journal of Pharmaceutical Sciences, 2001. **90**(3): p.310-321.
46. Kreilgaard, L., et al., *Effects of additives on the stability of recombinant human factor XIII during freeze-drying and storage in the dried solid*. Archives of Biochemistry and Biophysics, 1998. **360**(1): p.121-134.

47. Izutsu, K.-i., Yoshioka, S., and Kojima, S., *Physical stability and protein stability of freeze-dried cakes during storage at elevated temperatures*. *Pharmaceutical Research*, 1994. **11**(7): p.995-999.
48. Schersch, K., et al., *Systematic investigation of the effect of lyophilizate collapse on pharmaceutically relevant proteins, part 2: Stability during storage at elevated temperatures*. *Journal of Pharmaceutical Sciences*, 2012. **101**(7): p.2288-2306.
49. Lahav, M. and Leiserowitz, L., *The effect of solvent on crystal growth and morphology*. *Chemical Engineering Science*, 2001. **56**(7): p.2245-2253.
50. Maa, Y.-F. and Prestrelski, S.J., *Biopharmaceutical powders: Particle formation and formulation considerations*. *Current Pharmaceutical Biotechnology*, 2000. **1**(3): p.283-302.
51. Ógáin, O.N., et al., *Particle engineering of materials for oral inhalation by dry powder inhalers. I—Particles of sugar excipients (trehalose and raffinose) for protein delivery*. *International Journal of Pharmaceutics*, 2011. **405**(1–2): p.23-35.
52. Halbhuber, K.-J. and König, K., *Modern laser scanning microscopy in biology, biotechnology and medicine*. *Annals of Anatomy - Anatomischer Anzeiger*, 2003. **185**(1): p.1-20.
53. Földes-Papp, Z., Demel, U., and Tiliz, G.P., *Laser scanning confocal fluorescence microscopy: an overview*. *International Immunopharmacology*, 2003. **3**(13–14): p.1715-1729.
54. Dani, B., Platz, R., and Tzannis, S.T., *High concentration formulation feasibility of human immunoglobulin G for subcutaneous administration*. *Journal of Pharmaceutical Sciences*, 2007. **96**(6): p.1504-1517.
55. Izutsu, K.-i., et al., *Stabilization of protein structure in freeze-dried amorphous organic acid buffer salts*. *Chemical and Pharmaceutical Bulletin*, 2009. **57**(11): p.1231-1236.
56. Jovanović, N., et al., *Stable sugar-based protein formulations by supercritical fluid drying*. *International Journal of Pharmaceutics*, 2008. **346**(1-2): p.102-108.
57. Lueckel, B., et al., *Effects of formulation and process variables on the aggregation of freeze-dried interleukin-6 (IL-6) after lyophilization and on storage*. *Pharmaceutical Development and Technology*, 1998. **3**(3): p.337-346.
58. Moore, B.D., et al., *Pharmaceutical composition*. US2006/0292224, 2006.
59. Cohn, E.J., et al., *Preparation and properties of serum and plasma proteins. IV. A system for the separation into fractions of the protein and lipoprotein components of biological tissues and fluids*. *Journal of the American Chemical Society*, 1946. **68**: p.459-75.
60. Botet, R., *The "ouzo effect", recent developments and application to therapeutic drug carrying*. *Journal of Physics: Conference Series*, 2012. **352**(012047).

61. Wang, W., *Protein aggregation and its inhibition in biopharmaceutics*. International Journal of Pharmaceutics, 2005. **289**(1–2): p.1-30.
62. Renard, D., et al., *Structural investigation of  $\beta$ -lactoglobulin gelation in ethanol/water solutions*. International Journal of Biological Macromolecules, 1999. **26**(1): p.35-44.

## Chapter 7

# Final summary

The focus of the thesis was on pharmaceutical applications of the protein-coated microcrystals (PCMC) technology. As described in detail in chapter 1, the PCMCs represent an alternative method for the stabilization of protein in the solid state via coprecipitation of protein and carrier material. Apart from mechanistic investigations, the thesis included formulation considerations of cytokine and mAb2 PCMCs as well as the evaluation of concentrated PCMC suspensions for s.c. administration as final dosage form.

Chapter 2 aimed to develop a stable HSA-free formulation of a hydrophobic cytokine. A formulation screening that focused on protein process stability as well as on PCMC formation and particle structure was conducted to optimize the PCMC composition with respect to amino acid, sugar and salt. As only minor differences were revealed between the formulations during this study, a promising one comprising valine and sucrose as carriers was selected for detailed investigation of protein bioactivity and long-term stability over one year at  $5 \pm 3$  °C and  $22 \pm 3$  °C. These cytokine PCMCs completely retained their bioactivity during the PCMC production process. The amount of aggregated species monitored via HP-SEC and SDS-PAGE as well as the oxidation level of the protein only augmented slightly over storage time in dependence of the temperature. Stored at  $5 \pm 3$  °C, the PCMCs provided high overall stability to the cytokine over one year. In comparison to long-term stability studies of marketed lyophilized cytokine formulations, the stability as PCMCs was slightly superior.

Similarly to the preceding section of the thesis, chapter 3 dealt with the formulation of a therapeutic monoclonal antibody (mAb2). The formulation screening aimed to reduce the number of carrier excipients and thus investigated the influence of each carrier component, namely sodium chloride, glycine, histidine, phenylalanine and trehalose, on the protein process stability. Apart from positive effects on the manufacturability of PCMCs, the use of sodium chloride inhibited the formation of considerable amounts of insoluble protein aggregates. Glycine, histidine and trehalose elicited positive effects on the monomer content. Trehalose

further prevented glycine from crystallization and thus ensured the formation of a homogenous amorphous product. Phenylalanine had no positive effects on the PCMC product quality and was thus eliminated in the lead formulation to reduce the complexity of the system. Based on an accelerated short-term stability study conducted at 40 °C over 4-8 weeks, an optimum protein loading of approx. 50-62.5 % was revealed for the lead formulation. Higher protein load led to increased amounts of soluble protein particles detected via HP-SEC and SDS-PAGE, but no alterations of tertiary protein structure were noticeable in 2<sup>nd</sup>-derivative UV and intrinsic fluorescence spectra. Thus, mAb2 formulated as PCMCs provided good overall storage stability, not only compared to corresponding liquid formulations that were prone to both aggregation and fragmentation phenomena.

The development of PCMC suspensions for subcutaneous administration required physiologically acceptable solvents that show good protein compatibility and that do not, at least substantially, dissolve the PCMC powder prior to application. Besides organic water-miscible solvents, namely glycerol, NMP, propylene glycol and PEG 400 (chapter 4), oily vehicles, sesame oil, benzyl benzoate and MCT (chapter 5), were studied for the resuspension of mAb1 PCMC powder. Among the organic water-miscible solvents, glycerol and PEG 400 were found to be overall compatible with mAb1 PCMCs with respect to protein aggregation (turbidimetry, HP-SEC), protein structure (FT-IR, intrinsic fluorescence and 2<sup>nd</sup>-derivative UV spectroscopy) and specific binding capacity of the antibody, irrespective of the solvent content ranging from 10 to 100 % (v/v). Macroscopically acceptable suspensions were formed in the presence of  $\geq 50$  % solvent. In the case of propylene glycol, at least 90 % solvent was necessary for the formation of a suspension. However, these high propylene glycol concentrations induced the formation of considerable amounts of insoluble and soluble protein aggregates and perturbation of secondary and tertiary protein structure. For NMP, a PCMC suspension was obtained in the presence of the pure solvent leading to a significant level of aggregated antibody. Reduction of the solvent concentration either led to complete dissolution of the PCMC powder (90 and 70 % NMP) or protein instability in terms of aggregate formation or/and conformational changes ( $\leq 50$  % NMP). Consequently, glycerol and PEG 400 are suggested to be used for further development of PCMC suspensions in water-miscible organic solvents for subcutaneous delivery.

Besides the analysis of the compatibility between protein and solvent, the evaluation of the oily components as resuspension media included the development of an appropriate in vitro release model, the investigation of protein integrity after release from oily suspensions, the compatibility between the oily solvents and primary packaging material as well as the characterization of rheology and injectability of the suspensions. A 24 h incubation at 40 °C in water with integrated short-term stirring and final centrifugation at 100 g for 30 min ensured 100 % recovery of mAb1. Irrespective of the choice of oily solvent, the integrity of mAb1 was completely retained with respect to aggregation, secondary and tertiary protein structure and specific antigen binding affinity after release from oily PCMC suspensions. The injection forces for the oily solvents that depended on the siliconization process of the glass syringes were not impacted by 6 months storage at  $22 \pm 3$  °C proving compatibility with the primary packaging material. The maximal solid content achieved for oily suspensions based on MCT and 70:30 and 30:70 (v/v) mixtures of sesame oil and benzyl benzoate was 316 mg/mL, corresponding to 138 mg/mL protein. In dependence of the viscosity of the pure oils, the viscosity of the suspensions, showing shear thinning behavior, augmented with increasing solid content. The relationship between viscosity and injectability of the suspensions was found to be linear. Maximal injection forces were approx. 40 N for a 30:70 (v/v) sesame oil benzyl benzoate suspension with a solid content of 316 mg/mL, opposed to 50 N for the inverse mixture and MCT. Thus, the formulation of mAb1 as oily PCMC suspension was feasible, but it was not beneficial with respect to viscosity and injectability compared to a corresponding mAb1 solution.

Based on various studies on cytokine and mAb1 PCMCs with respect to morphology, composition and resulting stability, chapter 6 aimed to gain mechanistic insights in the PCMC formation process. The crystallinity/amorphicity of mAb1 PCMCs depended on the protein load (PL) and trehalose (tre) content of the formulation. A combination of either a protein load of 50 % with a trehalose content of  $\geq 35$  % or a trehalose content of 30 % with a protein load of  $\geq 60$  % were required to obtain completely amorphous mAb1 PCMCs according to the XRD spectra. The storage stability over 4 weeks at 40 °C/32 % RH of three amorphous formulations (60 % PL 30 % tre, 50 % PL 40 % tre, 40 % PL 50 % tre) and one crystalline powder (10 % PL 30 % tre) was analyzed with respect to insoluble and soluble protein aggregates

(protein recovery, turbidity, HP-SEC, SDS-PAGE) as well as morphological and carrier stability (SEM, XRD). Apart from ongoing NaCl crystallization detected for crystalline mAb1 PCMCs, no crucial differences were found between the formulations all providing good overall storage stability to the antibody. Homogenous mAb1 distribution within the spherical particles for the amorphous mAb1 formulations, as opposed to the crystalline one, was detected via confocal laser scanning fluorescence microscopy. The crystalline formulation was characterized by non-fluorescent rod-shaped glycine crystals with amorphous proteinaceous material deposited on the crystal surface. Powder fractionation via Andersen cascade impactor confirmed the presence of corresponding particle fractions in cytokine PCMCs, namely crystalline carriers forming the core of the particles and amorphous proteinaceous material being attached on the surface. The overall structure of these particles was hence in line with the initial idea of PCMCs, unlike amorphous mAb1 PCMCs that could only be separated depending on the size of the spherical, homogeneously composed particles. The manufacturing of cytokine PCMCs was further feasible via standard one-step precipitation as well as by two-step precipitation in batch mode. Two-step precipitation included the separate production of carrier crystals on which the protein was coated in a second step. The production method did not influence the morphology or the protein process stability. Batch mode production of protein-free mAb1 PCMCs was only feasible with some limitations. The existence of an emulsion-like state characterized by dispersed droplets of an “excipient and protein rich/solvent poor” phase in a continuous “excipient and protein poor/solvent rich” phase was observed during the formation of these particles. Crystal growth at the liquid-liquid interface as well as inside the droplets was detected via polarization microscopy. Hence, the spinodal decomposition model was suggested to be appropriate to describe the formation process of these mAb1 PCMCs. Overall, the physical state, morphology and supramolecular structure of the PCMCs that were found to strongly depend on the formulation composition including protein type (cytokine vs. mAb1) and load as well as choice and amount of carrier excipients, suggested that the formation mechanisms of these particles differed to some extent.

Thus, although further investigations on the PCMC formation process are still necessary to explain the self-assembly of the particles in detail, the studies provided an extensive characterization of cytokine and mAb PCMCs, not only with respect to formulation

considerations but also regarding mechanistic questions. Organic water-miscible as well as oily solvents were shown to be compatible with mAb1 PCMCs allowing for subcutaneous administration as PCMC suspension. This final dosage form, especially in combination with a dual chamber device enabling resuspension immediately before administration, could be an alternative to liquid protein formulations in the case of reduced solubility or poor overall stability.



---

# Appendix

## List of abbreviations

AFM	atomic force microscopy
Arg	arginine
Asp	aspartic acid
AUC	area under the curve
BI	Boehringer Ingelheim
BSA	bovine serum albumin
CD	circular dichroism
CLSM	confocal laser scanning fluorescence microscopy
CO <sub>2</sub>	carbon dioxide
CSP	cell surface protein
DLS	dynamic light scattering
DMSO	dimethyl sulfoxide
DSC	differential scanning calorimetry
EDTA	ethylenediaminetetraacetic acid
ELISA	enzyme-linked immunoassay
EMA	European Medicines Agency
FDA	US Food and Drug Administration
FNU	formazine nephelometric units
FT-IR	fourier transform infrared spectroscopy
GC	gas chromatography
Glu	glutamic acid
Gly	glycine
HCl	hydrochloride, hydrochloride acid
His	histidine
HP-SEC	high pressure size exclusion chromatography
HSA	human serum albumin

---

ID	inner diameter
IFN	interferon
Ig	immunoglobulin
IgG	immunoglobulin class G
IgG1	immunoglobulin G subclass 1
IgG2	immunoglobulin G subclass 2
kDa	kilodalton
K <sub>2</sub> SO <sub>4</sub>	potassium sulfate
L	length
mAb	monoclonal antibody
MCT	medium-chain triglycerides
MFI	microflow-imaging
MOPS	3-(N-morpholino)-1-propanesulfonic acid
MTT	3-(4,5-dimethylthiazol-2-yl)-2,5-diphenyltetrazolium bromide
Na <sub>2</sub> CO <sub>3</sub>	sodium carbonate
NaCl	sodium chloride
NaHCO <sub>3</sub>	sodium bicarbonate
NaOH	sodium hydroxide
NMP	N-methyl-pyrrolidone
NTU	nephelometric turbidity unit
PBS	phosphate buffered saline
PCMC	protein-coated microcrystals
PEG	polyethylene glycol
Ph.Eur.	European Pharmacopoeia
Phe	phenylalanine
pI	isoelectric point
PL	protein load
rpm	rounds per minute
RH	relative humidity
RI	refractive index

---

RP-HPLC	reversed phase high pressure liquid chromatography
s.c.	subcutaneous
SCF	supercritical fluid
SDS	sodium dodecyl sulfate
SDS-PAGE	sodium dodecyl sulfate polyacrylamide gel electrophoresis
SEM	scanning electron microscopy
Suc	sucrose
TFA	trifluoroacetic acid
T <sub>g</sub>	glass transition temperature
Tre	trehalose
UV	ultraviolet
Val	valine
VIS	visible
WFI	water for injection
XRD	x-ray powder diffraction

## **Presentations and publications associated with this thesis**

### **Publications (in preparation)**

K. Berkenhoff, K. Bechtold-Peters, V. Christ, S. Bassarab, W. Friess, HSA-free formulation of a hydrophobic cytokine as protein-coated microcrystals.

K. Berkenhoff, V. Saller, V. Christ, S. Bassarab, K. Bechtold-Peters, W. Friess, Formulation of a therapeutic monoclonal antibody via PCMC technology.

K. Berkenhoff, V. Christ, S. Bassarab, W. Friess, Development of oily mAb PCMC suspensions for subcutaneous administration.

### **Oral presentations**

K. Berkenhoff, Stabilization of biopharmaceuticals for high concentrated suspensions by coprecipitation, International Pharmaceutics Meeting 2011, Heidelberg, Germany, October 4-6, 2011.

### **Posters**

K. Berkenhoff, V. Christ, S. Bassarab, W. Friess, Compatibility between an IgG stabilized by PCMC technology and oily suspension media, International Pharmaceutics Meeting 2011, Heidelberg, Germany, October 4-6, 2011.

K. Berkenhoff, V. Christ, S. Bassarab, W. Friess, Integrity and conformational structure of an IgG upon release from oily PCMC suspensions, Protein Stability Conference, Breckenridge, CO, USA, July 19-21, 2011, poster award (1st prize).

K. Berkenhoff, K. Bechtold-Peters, S. Bassarab, W. Friess, Bioactivity and conformational studies on cytokine-coated microcrystals, Jahrestagung 2010 der Deutschen Pharmazeutischen Gesellschaft, Braunschweig, Germany, October 4-7, 2010.

K. Berkenhoff, V. Baum, K. Bechtold-Peters, S. Bassarab, H. Hoffmann, W. Friess, Conversion of a therapeutic cytokine into protein-coated microcrystals enabling powder-based dosage forms of a biopharmaceutical, 7th World Meeting on Pharmaceutics, Biopharmaceutics and Pharmaceutical Technology, Valletta, Malta, March 8-11, 2010.